Design and optimization of (chemo-)enzymatic processes for the synthesis of hydroxynitriles and their derivatives

Von der Fakultät für Lebenswissenschaften

der Technischen Universität Carolo-Wilhelmina zu Braunschweig

zur Erlangung des Grades einer

Doktorin der Naturwissenschaften

(Dr. rer. nat.)

genehmigte

D i s s e r t a t i o n

von Laura Leemans Martin
aus Arrecife

1. Referentin: Professorin Dr. Anett Schallmey
2. Referent: Professor Dr. Marc Walter
eingereicht am: 27.11.2019
mündliche Prüfung (Disputation) am: 03.06.2020

Druckjahr 2020

Vorveröffentlichungen der Dissertation

Teilergebnisse aus dieser Arbeit wurden mit Genehmigung der Fakultät für Lebenswissenschaften, vertreten durch die Mentorin der Arbeit,
in folgenden Beiträgen vorab veröffentlicht:

Publikationen

Leemans, L.; Walter, M. D.; Hollmann, F.; Schallmey, A.; van Langen, L. Multi-catalytic Route for the Synthesis of (*S*)-Tembamide. Catalysts 9: 822 (2019)

Leemans, L.; van Langen, L.; Hollmann, F.; Schallmey, A. Bienzymatic Cascade for the Synthesis of an Optically Active *O*-benzoyl Cyanohydrin. Catalysts 9: 522 (2019),

Tagungsbeiträge

Leemans, L.; van Langen, L.; Schallmey, A.: Bi-enzymatic cascade to optically active *O*-acyl cyanohydrins. (Vortrag). Gordon Research Conference (GRC) on Biocatalysis, Biddeford, ME, US (2018).

Posterbeiträge

Leemans, L.; Walter, M. D.; Hollmann, F.; Schallmey, A.; van Langen, L. Novel multi-catalytic route for the synthesis of an *N*-acyl-β-aminoalcohol (Poster). 14th International Symposium on Biocatalysis and Biotransformations, Groningen, The Netherlands (2019).

Leemans, L.; van Langen, L.; Schallmey, A.: Bi-enzymatic cascade to optically active *O*-acyl cyanohydrins. (Poster). Gordon Research Conference (GRC) and Gordon Research Seminar (GRS) on Biocatalysis, Biddeford, ME, US (2018).

Leemans, L.; van Langen, L.; Schallmey, A.: Bi-enzymatic cascade to optically active *O*-acyl cyanohydrins. (Poster). 8th International Cebitec Research Conference, Bielefeld, Germany (2018).

Leemans, L.; van Langen, L.; Schallmey, A.: Towards a cascade synthesis of enantiopure tembamide (Poster). 13th International Symposium on Biocatalysis and Biotransformations, Budapest, Hungary (2017).

Leemans, L.; Hollmann, F.; van Langen, L.: A novel chemo-enzymatic route towards *(R)*-tembamide. International Congress on Biocatalysis, Hamburg, Germany (2016).

Leemans, L.; Hollmann, F.; van Langen, L.: Towards a cascade synthesis of *N*-acylated β-amino alcohols (Poster). XVII Netherlands' Catalysis and Chemistry Conference (NCCC), Noordwijkerhout, The Netherlands (2016).

Leemans, L.; Hollmann, F.; van Langen, L.: Towards a cascade synthesis of *N*-acylated β-amino alcohols (Poster). Chemistry as Innovating Science (CHAINS), Veldhoven, The Netherlands (2016).

Abstract

In recent years, the development of enzymatic cascades for the production of valuable chemical products has received special attention. These approaches offer potential economic and environmental benefits, for they avoid the isolation of intermediates and enable the synthesis of chemically complex molecules. They are of special interest for the synthesis of active pharmaceutical ingredients (APIs), which often require high enantiopurity and are traditionally synthesized *via* long and cumbersome synthetic pathways that usually involve several protecting and deprotecting steps.

Enantiopure β-amino alcohols constitute one of the most significant building blocks for the synthesis of APIs. Despite the availability of a range of chiral β-amino alcohols from a chiral pool, there is a growing demand for new enantioselective synthetic routes to vicinal amino alcohols and their derivatives. In this thesis, an asymmetric 2-step chemo-enzymatic cascade that converts 4-anisaldehyde into a β-amino alcohol derivative with antiviral activity, (*S*)-tembamide, with excellent enantiopurity (98% enantiomeric excess) has been developed. The first step of the developed strategy consists in a concurrent bi-enzymatic synthesis of (*S*)-4-methoxymandelonitrile benzoate ((*S*)-**3**), using immobilized *Manihot esculenta* hydroxynitrile lyase (*Me*HNL) and *Candida antarctica* lipase A (CALA) as catalysts. To accomplish this, each biocatalytic step was studied separately in search for a window of compatibility and potential cross-interactions between the two reactions were identified. In a second step, the nitrile group is catalytically reduced to give (*S*)-tembamide, *via* an acyl transfer of the amino ester formed upon hydrogenation. To achieve hydrogenation of the nitrile moiety with highest chemoselectivity and enantioretention, various parameters such as nature of the catalyst, reaction temperature and hydrogen pressure were studied. Finally, after optimization of the chemo-enzymatic cascade, a preparative synthesis of (*S*)-tembamide was performed. The optimized enzymatic cascade afforded intermediate **3** in 80% yield and 99% e.e.. However, due to the low chemoselectivity of the hydrogenation reaction, the total isolated yield of tembamide was 15%, albeit with excellent enantiopurity (98% e.e.). The developed strategy might be transferrable to the synthesis of other *N*-acyl-β-amino alcohols with potential biomedical properties. Furthermore, this is the first reported example of a successful combination of an HNL and a lipase in concurrent fashion.

Additionally, using site-saturation mutagenesis, it was attempted to improve the cyanolytic activity of halohydrin dehalogenase from *Ilumatobacter coccineus* YM16-304 (HheG) in order to enable the preparative synthesis of β-cyanohydrins starting from cyclic epoxides and acyclic disubstituted epoxides.

Table of contents

1. Introduction

1.1. Biocatalysis

Biocatalysis is often defined as the use of enzymes or microorganisms as catalysts for chemical transformations [1]. This field can be subdivided into fermentation processes, which involve a growing cell culture with *in situ* enzyme production – exploiting the cellular metabolism – and require a carbon source; or biotransformations in which the catalytic reaction takes place after the enzyme production phase [2,3]. The latter may be further classified based on whether whole cells, cell-free extract or isolated enzymes are used. For thousands of years, fermentation processes have been used by humans for food processing and preservation (e.g. production of cheese, beer, vinegar and wine) [4]. In the nineteenth century, biocatalysis began to further develop aided by the contributions of numerous scientists, such as Louis Pasteur's pioneering work on the enzyme-catalyzed resolution of ammonium tartrate optical isomers [5] and Emil Fischer's lock and key hypothesis of stereoselective enzyme catalysis [6]. However, it was not until the second half of last century that enzymes gained importance as catalysts in synthetic organic chemistry for the production of unnatural products. In the late 1970s, hydrolases and oxidoreductases became interesting catalysts for the synthesis of chiral building blocks in the pharmaceutical industry, where stereoselectivity was a key issue [1]. In addition, the discovery in the 1980s that certain enzymes, such as lipases, could work in organic solvents under low-water conditions and at elevated temperature [7,8], broadened the substrate scope towards non-polar compounds and established the eligibility of enzymes as an alternative to classical chemical catalysts in organic chemistry. Since then, several advances have contributed to the great diversification of enzymes available for synthetic organic chemistry and allow for the use of enzymes as biocatalysts in many industrial processes, together with their modification and optimization for the design of new synthetic routes [1,9]. Firstly, the development of gene and recombinant technologies for cloning, expressing and manipulating genes allows for the nearly unlimited production of enzymes in suitable microorganisms, eliminating the need for wild-type crude cell extracts. Furthermore, the development of bioinformatics and protein engineering methods such as directed evolution, together with high-throughput screening tools enabled the optimization of enzymes' properties for their use in biocatalytic processes by improving their stability, catalytic activity, selectivity and substrate tolerance. Additionally, the performance, recovery and recycling of enzymes could be optimized thanks to the development of enzyme immobilization methods [10]. Finally, the discovery of new enzymes was facilitated by the technological advances that contributed to broadening the range of available sequenced genomes.

Biocatalysis has now become an industrially attractive technology for the manufacture of chiral pharmaceutical intermediates and precursors in the synthesis of fine chemicals, as well as a tool for a wide range of analytical purposes, such as diagnostics [9,11,12]. The collection of organic reactions that can be catalyzed by enzymes is constantly growing, steered by the aforementioned improved methods for enzyme discovery, screening and engineering. Biocatalysis offers a number of advantages over traditional synthesis methodologies, that can contribute to more sustainable manufacturing processes [1].

As a result of their complex three-dimensional structures, enzymes generally exhibit high chemo- regio- and stereoselectivity. Their chemoselectivity may contribute to decreasing the number of steps in a synthetic route by avoiding the use of protecting groups. Likewise, due to their high regioselectivity, extra steps to distinguish between identical functional groups are often unnecessary and yields may be increased by avoiding the formation of regioisomeric products. However, in terms of selectivity, the most valuable advantage of enzymatic reactions over conventional synthetic methods is the enantio- or diastereoselectivity that enzymes often exhibit. Products can be obtained with high stereoisomeric purity, which is reflected in higher yields and, again, eliminates extra steps for the separation of stereoisomers. This is especially interesting for the pharmaceutical industry, where active ingredients often show different activities depending on their stereochemistry [11,13].

Biocatalysis, however, also presents certain limitations [1,14]. The high selectivity of enzymes means that they often catalyze a given reaction only on a narrow selection of substrates. Moreover, the process of interest might require harsh conditions that may not be tolerated by the enzymes, since most of them have evolved to work under mild conditions. In addition, the enzyme might exhibit poor or inverse regio- or stereoselectivity for the selected substrate. Finally, enzymes may suffer from substrate or product inhibition and many classes of enzymes require a cofactor, which can be expensive. Some of these limitations, however, can be overcome by protein engineering as mentioned before and some issues may be tackled by careful optimization of the reaction variables [14].

1.1.1. Enzymatic cascades

In recent years, considerable progress has been made in developing enzymatic cascades for the production of valuable chemical products, motivated by their potential economic and environmental benefits [15–18]. These are biocatalytic processes that combine two or more transformations in a single reaction vessel and can be performed in a concurrent or sequential mode, circumventing the isolation of intermediates and enabling the synthesis of chemically complex molecules [19,20].

While biocatalytic cascades may be classified according to different parameters [19], a generally accepted classification attends to the reaction design (*i.e.* the number of steps, substrates and products and how they relate) [19,20]. As depicted in Figure 1A, cascades may be linear if one single substrate is converted into the product of interest in one or more reaction steps in a one-pot fashion. If the main transformation is coupled with one or more secondary reactions – which may have the purpose of by-product removal but are sometimes used for cofactor or co-substrate regeneration – the cascade is classified as orthogonal (Figure 1B). Closely related are parallel cascades (Figure 1C), in which enzymes catalyze the transformation of two substrates into two products of interest, in reactions that require complementary cofactors or co-substrates, thereby achieving the regeneration of the cofactor or co-substrate while obtaining two valuable products. In cyclic cascades (Figure 1D), one substrate out of a starting mixture (usually isomers) is selectively converted into an intermediate that is further transformed back to the starting substrate mixture. This results in the enrichment of the unreacted substrate in the starting mixture (S_2 in the depicted example) and usually is applied in deracemization reactions.

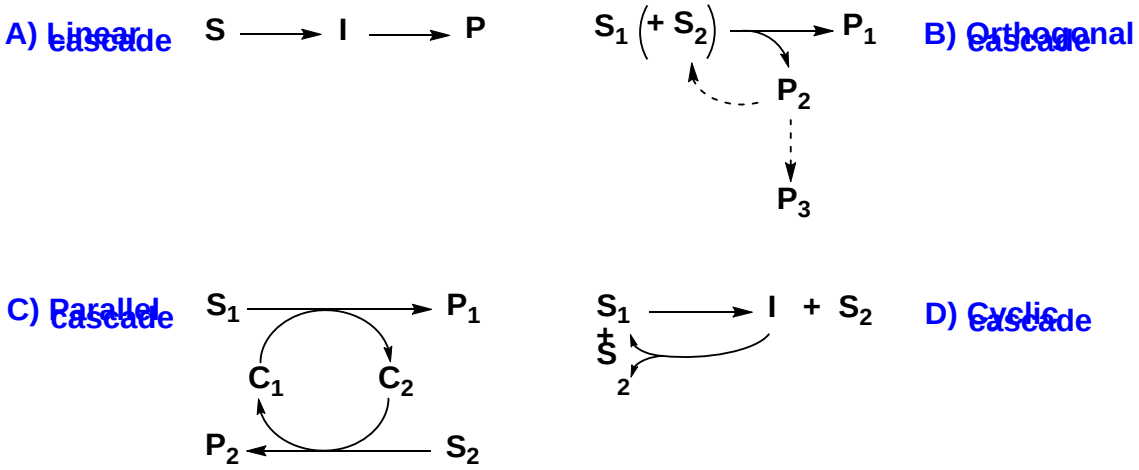

Figure 1. Four main designs of enzymatic cascades. In Figure 1C, C1 and C2 may be cofactors or co-substrates. Adapted from Schrittwieser et al. [19] and Ricca et al. [20].

Additionally, enzyme-catalyzed reactions may be combined with traditional organic chemistry transformations, resulting in chemo-enzymatic cascades [17,18]. The orthogonality of the merged fields further widens the range of possible synthetic routes, affording molecules of higher complexity. Given the major challenge of finding compatible reaction conditions for both chemical processes (usually performed in organic solvents using harsh temperatures) and enzymatic transformations (traditionally carried out in aqueous media under mild temperatures), this is a relatively new concept. The first example of a successful chemo-enzymatic cascade was developed by the van Bekkum group in 1980, which combined an enzymatic isomerization of D-glucose into D-fructose with an *in situ* platinum-catalyzed hydrogenation of D-fructose allowing

for the synthesis of the preferred product D-mannitol in 46% [21]. According to Gröger *et al.* [18], chemo-enzymatic one-pot processes may be subdivided into two main approaches. The case reported by the van Bekkum group corresponds to the first one, which consists in the coupling of an isomerization reaction (generally catalyzed by a chemical catalyst, although in the mentioned example it is catalyzed by glucose isomerase) with the catalytic transformation of one of the isomers (usually a biocatalytic reaction, but may also be chemo-catalytic, as in the case reported by van Bekkum where platinum catalyzes the hydrogenation of D-fructose). The other approach consists in coupling a substrate synthesis (not an isomerization reaction) with a subsequent transformation of the substrate in a linear cascade approach. Here, the enzymatic reaction may be integrated as first or second step depending on the route design and often one or both reactions are asymmetric [18].

The combination of individual reaction steps in a one-pot process has several advantages in terms of process efficiency and sustainability, since the solvent consumption and waste generation is generally decreased due to the lower number of work-up steps [17]. Furthermore, the coupling of reactions generally increases space-time yields and has the potential to drive thermodynamically unfavored equilibria towards the desired products, hence, reducing the excess of required reagents [22,23]. Additionally, cascade reactions may facilitate the handling of unstable or toxic intermediates [19,24]. There are, however, some limitations associated with the design of enzymatic cascades. Nature is the best example of how enzymes are capable of efficiently catalyzing a great variety of cascade reactions within the same reaction medium, the cytoplasm. However, while these enzymes have evolved to work in coordination in the same bioreactor through millions of years, synthetic enzymatic cascades designed by organic chemists often involve enzymes that were not evolved to function under the same conditions. Therefore, when multiple reactions are run in one pot, it is often impossible to work under the optimal conditions for all reactions in terms of reaction rate and stability. Furthermore, enzymes (and chemical catalysts, in the case of chemo-enzymatic cascades) may experience inhibition caused by certain reagents or reaction intermediates. Inhibition of a catalyst by a compound involved in a later step may be addressed by performing the cascade in a sequential mode. If, however, the inhibition is caused by a substrate or product of a previous step, aside from applying a sequential mode, the problem can be circumvented by controlling the substrate feed when working in a concurrent mode [20,25]. In contrast, in cases when inhibition is caused by the reaction product, the process may actually benefit from a concurrent approach if this product is consumed in a subsequent reaction [19].

1.2. Vicinal amino alcohols

1,2-amino alcohols (also known as vicinal or β-amino alcohols) are a common moiety found in natural products. Given their broad range of biological activity, it is not surprising that amino alcohols and their derivatives constitute one of the most significant building blocks used for the synthesis of active pharmaceutical ingredients (APIs), chiral subunits and ligands. In Figure 2, several examples of amino alcohol-containing molecules found in the human body (adrenaline, sphingosine, serine and threonine), natural products with medicinal properties (quinine and ephedrine) and active pharmaceutical ingredients from top marketed drugs (Salbutamol, Metoprolol and Fingolimod) are displayed.

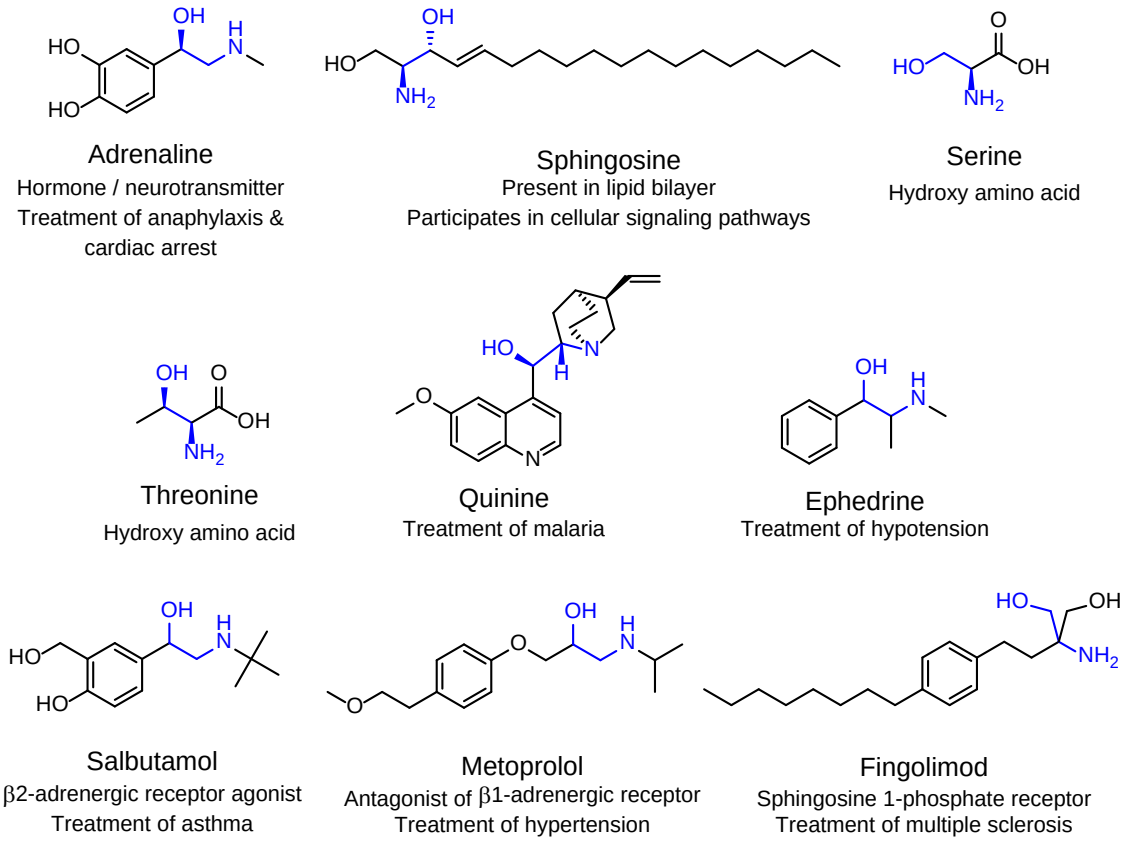

Figure 2. Biologically active natural (first two rows) and synthetic (third row) molecules carrying the amino alcohol motif.

Enantiopure vicinal amino alcohols have traditionally been synthesized through derivatization of the limited chiral pool of amino acids [26]. In view of their high potential for the synthesis of APIs, considerable efforts have been directed towards the development of new asymmetric synthetic routes to vicinal amino alcohols [27–34]. These synthetic strategies can be divided into two approaches [35]:

1) Introduction of the β-amino alcohol moiety on a pre-existing carbon skeleton

2) Formation of a carbon–carbon bond between two fragments containing the oxygen and nitrogen functionalities, forming one or two of the vicinal stereocenters in one step.

1.2.1. Tembamide

Tembamide is a natural amino alcohol derivative that can be isolated from various members of the *Rutaceae* family [36,37]. Extracts from *Aegle marmelos Correa* containing tembamide were used in traditional Indian medicine because of its hypoglycemic activity [38]. This amino alcohol derivative also shows adrenaline-like activity, mild insecticidal properties [39] and, furthermore, (*S*)-tembamide has been reported to exhibit anti-HIV activity [40]. The *N*-acyl-β-amino alcohol moiety that characterizes tembamide is found in various biologically active natural and synthetic compounds, as shown in Figure 3.

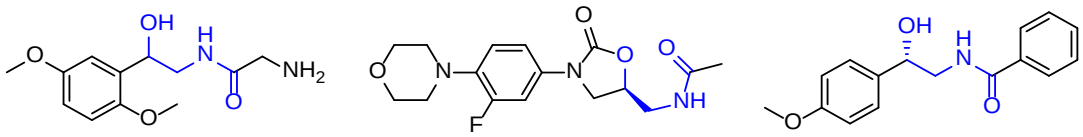

Figure 3. Biologically active natural (tembamide) and synthetic (midodrine, linezolid) molecules carrying the *N*-acyl-β-amino alcohol motif.

Although tembamide possesses a chiral center, it has only been isolated from natural sources as a racemate or with low enantiomeric excess (e.e.) [41], prompting scientists to develop chiral synthetic routes towards both enantiomers [42,43,52–55,44–51]. These synthetic routes can be classified within the two above mentioned synthetic strategies:

1) Asymmetric synthesis of tembamide from a pre-existing carbon skeleton

Schrittwieser *et al.* developed a biocatalytic one-pot, four-step synthesis consisting in an initial azidolysis of haloketone **A** followed by the *Codexis* ketoreductase KRED-NADH-110-catalyzed reduction of the carbonyl group in one pot (see Figure 4) [42]. The subsequent hydrogenation of the azide group in compound (*S*)-**C** catalyzed by palladium nanoparticles and a final chemical benzoylation of the resulting amino alcohol afforded (*S*)-tembamide. A similar approach was published by Yadav *et al*., where the reduction of the keto group is catalyzed by enzymes present in carrot root (*Daucus carota*) [43]. The resulting (*R*)-**C** is then subjected to a palladium on carbon-catalyzed hydrogenation of the azide and a chemical benzoylation of (*R*)-**D** to yield (*R*)-tembamide. Another biocatalytic approach was reported by Kamal *et al.* where the ketone **B** was reduced with sodium borohydride to yield (±)-**C** [44]. A kinetic resolution of the azido alcohol *via* a *Pseudomonas cepacia* lipase-catalyzed acetylation afforded (*S*)-**F** and (*R*)-**C**,

which can be isolated using column chromatography. (*S*)-**C** is obtained treating (*S*)-**F** with anhydrous potassium carbonate in methanol. Hydrogenation of the azide group of either (*R*)-**C** or (*S*)-**C** catalyzed by palladium on carbon, followed by a chemical benzoylation affords (*R*)-**E** and (*S*)-**E**, respectively. Recently, Liardo *et al.* reported a route involving a chemo-enzymatic cascade [45]. The conversion of β-ketonitrile **G** into optically active β-hydroxyamide (*R*)-**H** is catalyzed by a dual ruthenium/ketoreductase system. A Hofmann rearrangement of (*R*)-**H** with iodobenzene diacetate affords oxazolidinone (*S*)-**I**, which is then hydrolyzed and subsequently treated with benzoyl chloride to yield (*S*)-tembamide.

Buchanan *et al.* developed a route where the chirality was introduced *via* a highly diastereoselective oxy-Michael addition of (*S*)-6-methyl-δ-lactol to the nitro olefin **K**, which is synthetized through condensation of 4-anisaldehyde (**J**) with nitromethane (see Figure 5) [46]. The acidic methanolysis of **L** and subsequent hydrogenation of the nitro group catalyzed by palladium on carbon yielded (*R*)-**D**. Again, (*R*)-tembamide was obtained after a chemical benzoylation of the amino alcohol. The route reported by Sadyandy *et al.* is based on the Sharpless asymmetric dihydroxylation of 4-methoxystyrene (**N**), which affords the diol (*R*)-**O** with high enantiopurity [47]. Conversion of the primary hydroxyl group into tosylate and posterior azidolysis yields (*R*)-**C**, which is further converted into (*R*)-tembamide after hydrogenation and benzoylation.

The remaining routes under this classification use a chemical catalyst to selectively reduce the keto group to yield the hydroxyl group with *R*-configuration. Cortez *et al.* described the benzoylation of 2-amino-1-(4-methoxyphenyl)ethanone (**Q**), followed by the asymmetric transfer hydrogenation of the keto group catalyzed by a rhodium complex to yield (*R*)-tembamide [48]. Cho *et al.* [49] and Lee *et al.* [50] reported very similar routes which only differed in the catalyst used for the hydrogenation reaction. Their approach starts with the tosyloxylation of 1-(4-methoxyphenyl)ethanone (**S**) and a subsequent hydrogenation catalyzed by an oxazaborolidine in the case of Cho *et al.* and a chiral Rhodium complex in the case of Lee *et al.*. The resulting (*R*)-**P** is then further reacted in the same way as described by Sadyandy to yield (*R*)-tembamide.

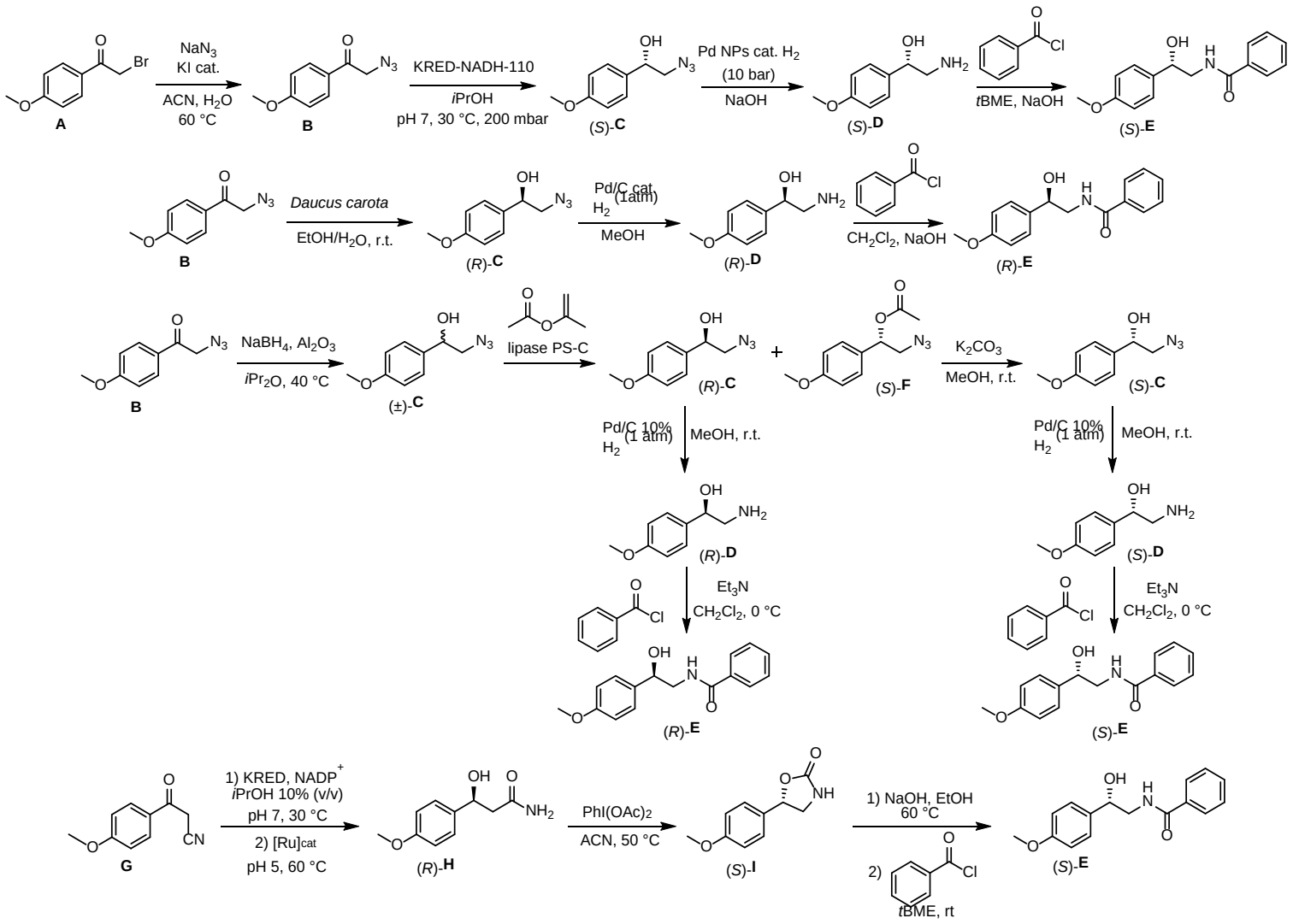

Figure 4. Reported asymmetric chemo-enzymatic routes for the synthesis of tembamide starting from a pre-existing carbon skeleton.

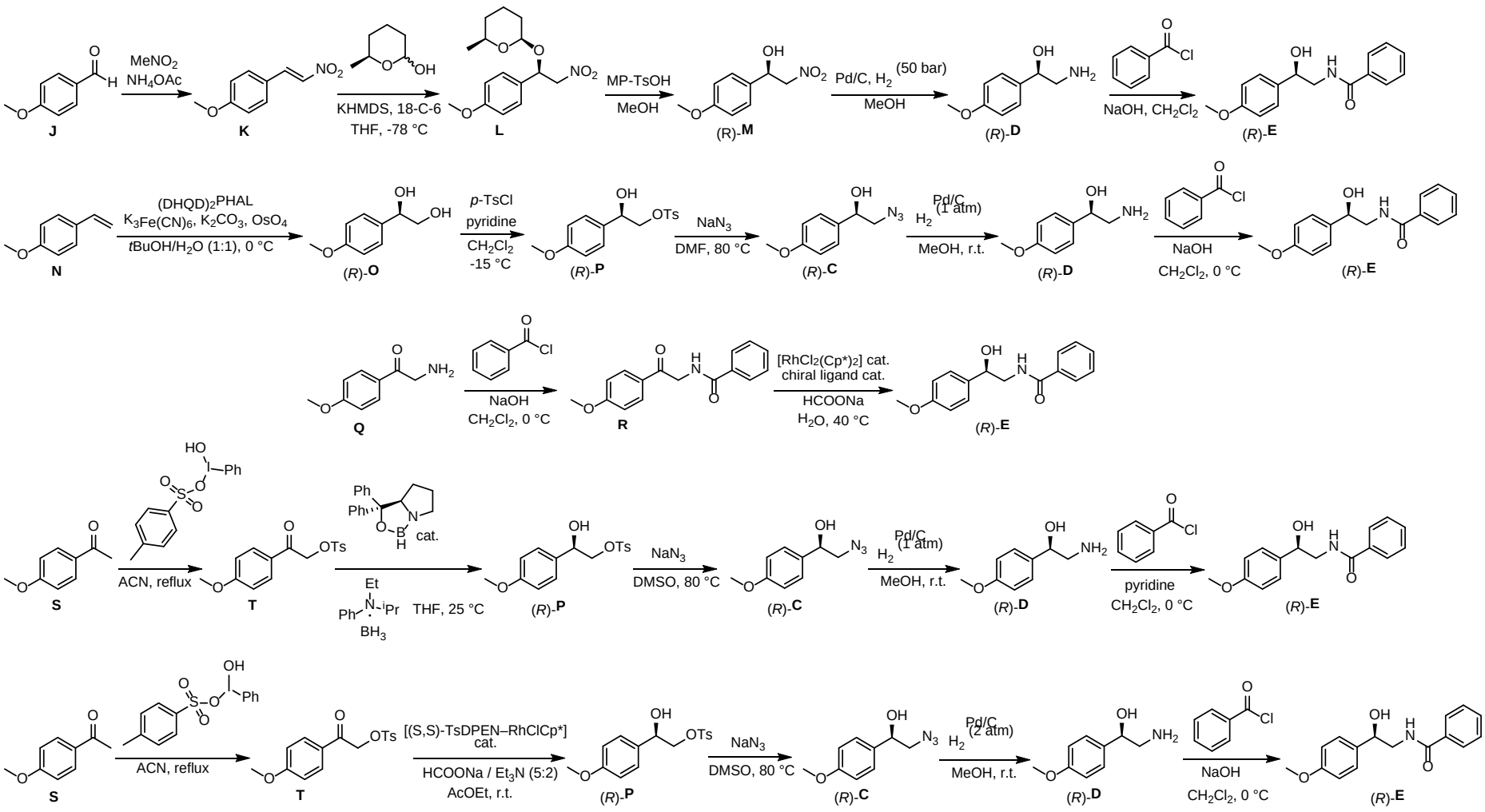

Figure 5. Reported non-enzymatic asymmetric routes for the synthesis of tembamide starting from a pre-existing carbon skeleton.

2) Asymmetric synthesis of tembamide from C–C bond forming reactions

All synthetic pathways that involve a concomitant formation of a C–C bond between two molecules containing the oxygen and nitrogen functionalities and the stereogenic center in one step start from 4-anisaldehyde, as shown in Figure 6.

Zhu *et al.* developed an asymmetric route towards (*R*)- and (*S*)-tembamide consisting in a cyanation of the aldehyde using trimethylsilyl cyanide (TMSCN), catalyzed by a chiral cadmium metal-organic framework (MOF) [51]. Catalysis using (*S*)-Cd-MOF yields (*R*)-**U**, whereas (*R*)-Cd-MOF catalyzes the formation of (*S*)-**U**. An acetylation reaction followed by the reduction of the ester and nitrile functionalities with $LiAlH_4$ afforded the amino alcohols (*R*)-**D** and (*S*)-**D**, which were finally acylated with benzoyl chloride to synthetize (*R*)- and (*S*)-tembamide. A similar route was described by Aguirre *et al.* where the cyanation is catalyzed by a titanium complex with a chiral ligand that affords (*R*)-**U** [52]. After removal of the TMS group, the nitrile was reduced using borane dimethylsulfide and the resulting amino alcohol was finally benzoylated to form (*R*)-tembamide.

An interesting approach developed by Brown *et al.* consists in the enantioselective hydrocyanation of 4-anisaldehyde catalyzed by the dipeptide (*S,S*)-cyclo(phenylalanylhistidyl), followed by the reduction of the isolated cyanohydrin (*R*)-**W** using $LiAlH_4$ and, finally, the formation of (*R*)-tembamide using benzoyl chloride [53]. Another route, involving the enantioselective cyanophosphorylation of **J** catalyzed by a Lewis acid-(*S*)-BINOLAM complex, was reported by Baeza *et al*. [54]. The nitrile moiety of *O*-phosphorylated cyanohydrin (*R*)-**X** is then reduced with $LiAlH_4$ and (*R*)-tembamide is obtained after reaction with benzoyl chloride.

Finally, Das *et al.* developed the synthesis of (*R*)-tembamide *via* an asymmetric Henry reaction of 4-anisaldehyde catalyzed by a copper complex bearing a chiral ligand [55]. The posterior hydrogenation of the nitro alcohol (*R*)-**M** and final reaction with benzoyl chloride afforded the target product.

It must be noted that all reported pathways achieve the formation of the amide bond by acylating the amine precursor with benzoyl chloride. Furthermore, most of the routes starting from inexpensive substrates involve at least four steps, with the exception of the 3-step syntheses reported by Brown *et al.* [53], Baeza *et al*. [54] and Das *et al.* [55].

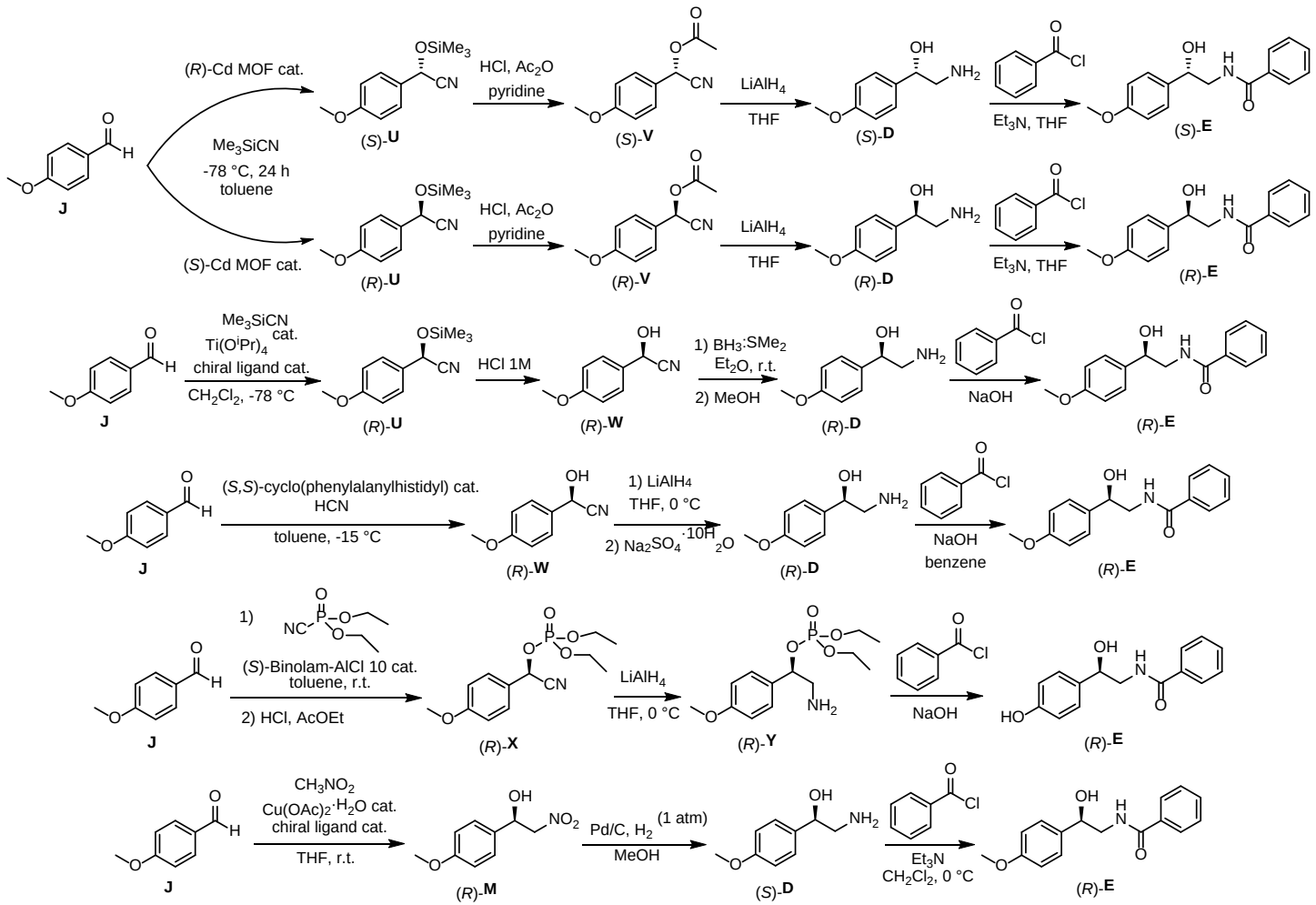

Figure 6. Reported asymmetric routes for the synthesis of tembamide *via* C–C forming reactions catalyzed by synthetic catalysts.

1.3. Hydroxy nitriles

α- and β-hydroxy nitriles are not only precursors of β- and γ-amino alcohols, but also constitute important building blocks for the synthesis of both fine and bulk chemicals – such as APIs, fragrances, agrochemicals and flavors – owing to the synthetic versatility of the two functional groups [56]. The nitrile group may be hydrolyzed (yielding amides or carboxylic acids), reduced (leading to amines, imines or aldehydes) or subject to a nucleophilic attack. As for the hydroxyl group, it may be protected, oxidized or substituted by a wide range of nucleophiles after activation (e.g. sulfonylation) [56,57]. To illustrate the versatility of these type of compounds, Figure 7 shows a collection of possible follow-up reactions of optically pure α-hydroxy nitriles or α-cyanohydrins [56–58].

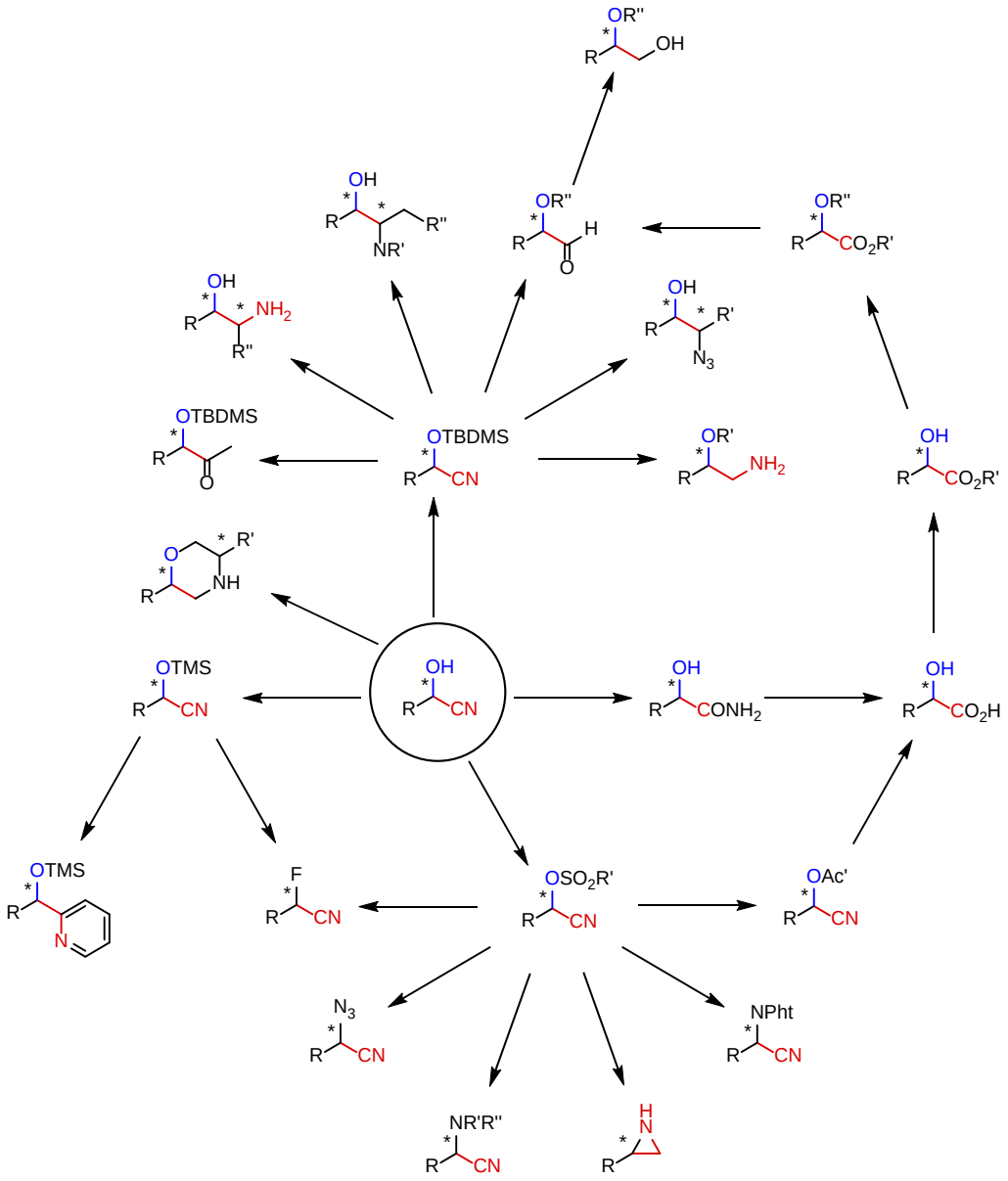

Figure 7. Follow-up chemistry of α-cyanohydrins. Adapted from Bracco *et al.* [56], Gruber-Khadjawi *et al.* [58] and Holt *et al.* [57].

Biocatalysis allows for the synthesis of α- and β-hydroxy nitriles with high enantioselectivity, which is of central importance for the synthesis of pharmaceutical ingredients. Examples of chiral compounds with pharmaceutical applications derived from α- and β-hydroxy nitriles are depicted in Figure 8.

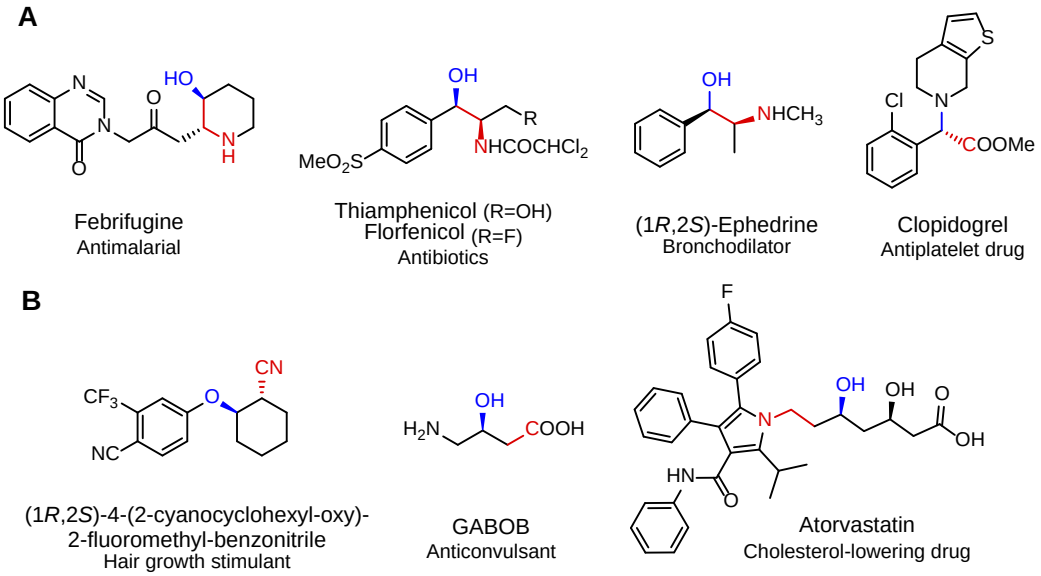

Figure 8. Molecules with pharmaceutical applications containing moieties derived from α-hydroxy nitriles (A) and β-hydroxy nitriles (B).

Although there are several biocatalytic approaches for the asymmetric synthesis of α- and β-hydroxy nitriles, such as the stereoselective reduction of α- or β-ketonitriles [59,60], nitrilase-catalyzed resolution of α- or β-hydroxy nitriles [61] or lipase-catalyzed resolution of α- or β-hydroxy nitriles and their acetates [62,63], the synthesis *via* C–C bond formation is of especial interest since asymmetric C–C bond-forming reactions are challenging in classic organic chemistry [64–68]. On the one hand, the hydrocyanation of aldehydes or ketones catalyzed by hydroxynitrile lyases yields α-hydroxy nitriles. The synthesis of β-hydroxy nitriles, on the other hand, may be achieved by cyanide-mediated epoxide ring-opening catalyzed by halohydrin dehalogenases.

1.3.1. Enzymatic synthesis of α-hydroxynitriles catalyzed by hydroxynitrile lyases

The synthesis of enantiopure α-cyanohydrins *via* C–C bond formation is achieved *via* the nucleophilic addition of cyanide to a prochiral carbonyl compound, a reaction catalyzed by *R*- or *S*-selective hydroxynitrile lyases (HNLs). HNLs (EC 4.1.2.X, X = 10, 11, 46, 47) are a group of C–C lyases that catalyze the cleavage of cyanohydrins, releasing HCN and the corresponding carbonyl compounds. Given the reversibility of this reaction, the synthetic value of HNLs derives from their capability to catalyze the formation of α-cyanohydrins.

The first HNL-catalyzed reaction was described in 1837, when Wöhler and Liebig reported the generation of HCN by decomposition of a cyanohydrin catalyzed by bitter almond extract [69]. However, it was not until 1908 when the first enantioselective synthesis of an α-cyanohydrin, mandelonitrile, was reported [70]. The portfolio of HNLs discovered since then offers a broad substrate scope, allowing for the synthesis of a wide range of unnatural cyanohydrins bearing multiple functional groups [56,57,71,72]. Furthermore, HNLs generally offer high reaction rates and excellent selectivities for either (*R*)- or (*S*)- enantiomers [56].

The cyanide required for the reaction may be obtained from inorganic salts or generated *in situ* (e.g. from acetone cyanohydrin [73]). Although it is a highly toxic compound, the handling of HCN in industry is not an issue, and the use of HNLs is well-established in the industrial sector [74–78]. The prochiral carbonyl substrate may be an aldehyde, in which case the equilibrium generally lies on the product side, or a ketone, often characterized by an unfavorable equilibrium due to steric constraints and lower electrophilicity [57]. To overcome low product yields in cases where the balance lies on the substrate side, changing the thermodynamic conditions can help to drive the reaction towards the cyanohydrin formation. This may be achieved, for example, by using an excess of cyanide, by *in situ* product removal or by lowering the reaction temperature [57,74,79–83].

Although HNLs generally catalyze hydrocyanation reactions with high enantioselectivity, the enantiopurity of the product is also determined by the competitive base-catalyzed chemical hydrocyanation. This is a non-stereoselective equilibrium reaction that must be suppressed in order to guarantee the highest product enantiopurity. Therefore, reactions are normally performed under acidic pH, always within the enzyme's activity range. Researchers have found that the addition of water-miscible solvents to increase substrate solubility has a negative impact on the enzymes [84]. However, performing the reaction in a biphasic system can greatly improve the process. While the enzymatic hydrocyanation takes place in the aqueous phase, the substrate and product mainly remain in the organic solvent, which limits the base-catalyzed hydrocyanation. Furthermore, HNLs may also be applied in pure organic solvents, further suppressing the non-selective hydrocyanation [73,74,81]. In this context, hydrophilic solvents generally lead to lower activities than hydrophobic solvents, since they are more effective at stripping the necessary enzyme-bound water [73,81,85,86]. As a general rule, solvents with a log $P < 1.5$ usually deactivate enzymes, whereas the effect of solvents with $1.5 < \log P < 2$ is difficult to predict and solvents with $\log P > 2$ often ensure high retention of enzymatic activity [87]. However, this is not always the case, as shown by Paravidino *et al.* in their study on the activity and enantioselectivity of *Manihot esculenta* HNL (*Me*HNL) in dry organic solvents [73]. Replacing

tert-butyl methyl ether (log *P* = 0.94) for toluene (log *P* = 2.73) actually led to slightly poorer enzyme performance. Often, immobilized HNLs are used in water- or buffer-saturated solvents such as diisopropyl ether (*i*Pr$_2$O), *tert*-butyl methyl ether (*t*BME) or alkanes, which typically allow for high substrate solubility [56,74]. The immobilization of HNLs is often required for their optimal performance and to enable their recovery and reuse, which is of special interest for industrial applications [74,75,88]. The application of immobilized HNLs in pure organic solvents or biphasic systems has afforded shorter reaction times and higher enantioselectivity values in industry [89].

HNLs show several types of unrelated structural features and are, therefore, an example of non-homologous isofunctional enzymes resulting from convergent evolution [71]. The HNLs discovered up to date have been classified within six protein superfamilies according to protein sequence alignment and crystal structure (see Figure 9). These are FAD-dependent HNLs from the glucose-methanol-choline (GMC) oxidoreductases superfamily [90,91] and non-FAD-containing HNLs belonging to the esterase-lipase [92–96], medium-chain-dehydrogenase/reductase (MDR) [97], carboxypeptidase [98], cupin [99–101] and Bet-v1 [102] superfamilies.

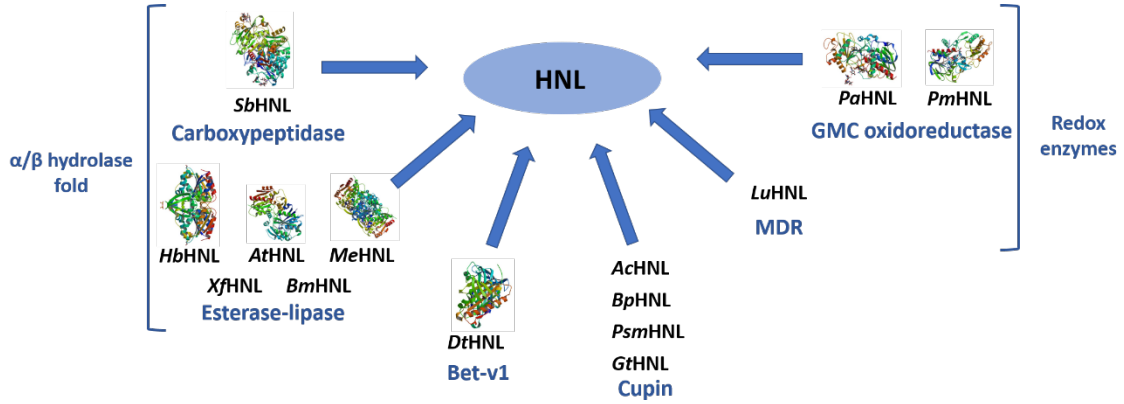

Figure 9. Convergent evolution of HNLs. *Sorghum bicolor Sb*HNL has an α/β hydrolase fold and belongs to the serine carboxypeptidase superfamily. *Hevea brasiliensis Hb*HNL, *Manihot esculenta Me*HNL, *Arabidopsis thaliana At*HNL, *Xylella fastidiosa Xf*HNL and *Baliospermum montanum Bm*HNL belong to the esterase-lipase superfamily, which also holds an α/β hydrolase fold. The recently discovered *Davallia tyermannii Dt*HNL exhibits a Bet v1-like fold. *Acidobacterium capsulatum Ac*HNL, *Burkholderia phytofirmans Bp*HNL, *Pseudomonas mephitica Psm*HNL and *Granulicella tundricola Gt*HNL belong to the cupin superfamily. The Zn-dependent *Linum usitatissimum Lu*HNL belongs to the MDR superfamily. FAD-dependent HNLs *Prunus amygdalus Pa*HNL and *Prunus mume Pm*HNL belong to the GMC oxidoreductase superfamily. The Protein Data Bank IDs of the X-ray structures are 1GXS (*Sb*HNL), 3C6X (*Hb*HNL), 3DQZ (*At*HNL), 1EB9 (*Me*HNL), 5E4D (*Dt*HNL), 3GDN (*Pa*HNL) and 3RED (*Pm*HNL). Adapted from Hanefeld [74].

Among the HNLs used in preparative scale, *Prunus amygdalus* HNL (*Pa*HNL) is the most widely applied enzyme for the synthesis of (*R*)-cyanohydrins thanks to its outstanding robustness and wide substrate scope [58]. It is a glycosylated enzyme from the GMC oxidoreductase superfamily that may be isolated from almonds, but can also be heterologously expressed in *Pichia pastoris*, ensuring large-scale availability [103]. *Manihot esculenta* HNL (*Me*HNL), an *S*-

selective enzyme from the α/β-hydrolase superfamily is also used in preparative scale [71]. It presents a broad substrate scope and is available in large quantities, being overexpressed in *Escherichia coli* [89]. The structure of *Me*HNL is one of the most extensively studied and X-ray crystallography of *Me*HNL and *Hb*HNL, in combination with mutagenesis data and enzyme kinetics has allowed for the elucidation of the cyanogenesis (*i.e.* the breakdown of a cyanohydrin into cyanide and the corresponding carbonyl compound) reaction mechanism, which is identical for these two enzymes [104]. As shown in Figure 10 for *Hb*HNL, during the resting state, a water molecule forms hydrogen bonds with residues His235 and Lys236. This water molecule is then replaced by the cyanohydrin molecule, which is connected *via* H bonds to Ser80, Thr11 and Lys236. His235 also forms a H bond with Ser80, allowing for the serine to abstract the proton from the cyanohydrin, with simultaneous deprotonation of this residue accomplished by His235. The positive charge of Lys236 facilitates the cleavage of the C–C bond, stabilizing the cyanide ion, which also forms a H bond with the protonated His235. Cyanide is then protonated by His235, released and replaced with a water molecule. The carbonyl O atom forms H bonds with Thr11 and Ser80, which polarize it, activating the carbonyl C atom towards nucleophilic attack in the reverse reaction. Finally, the carbonyl compound is released and the active site is reconstituted.

Regarding *Pa*HNL, the reaction mechanism does not involve FAD, although it is generally accepted that this cofactor is essential to maintain the catalytic activity [105,106]. Based on the crystal structure of *Pa*HNL1 isoform, complexed with its natural product benzaldehyde, Dreveny and coworkers proposed the reversible cyanogenesis reaction mechanism depicted in Figure 11. In the resting state, several water molecules are found forming hydrogen bonds within the active site. These are replaced by the cyanohydrin, which forms H bonds with His459 His 497, Cys328 and Tyr457. His497, which is likely bound to Ser496 *via* H bond, acts as a base deprotonating the cyanohydrin. The cleavage of the C–C bond is facilitated due to the stabilization of cyanide by the overall positive electrostatic potential in the active site region. After the cyanogenesis reaction takes place, cyanide and, lastly, benzaldehyde leave the active site, according to the mechanism suggested by Jorns [107].

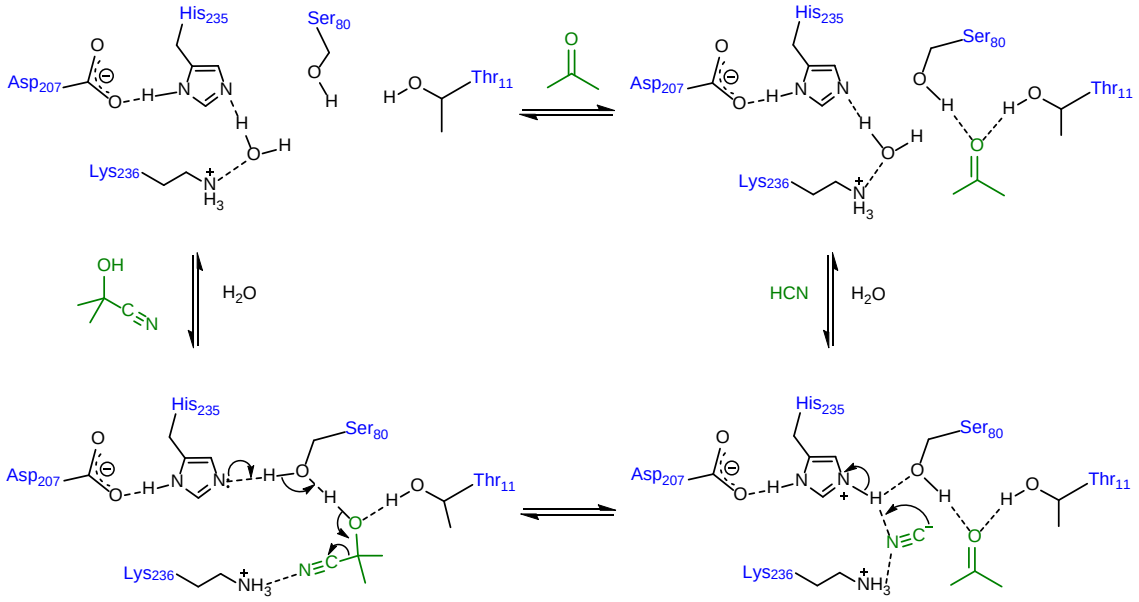

Figure 10. Anti-clockwise: proposed mechanism for the reversible cyanogenesis reaction catalyzed by *Hb*HNL, modified from Gruber *et al*. [104].

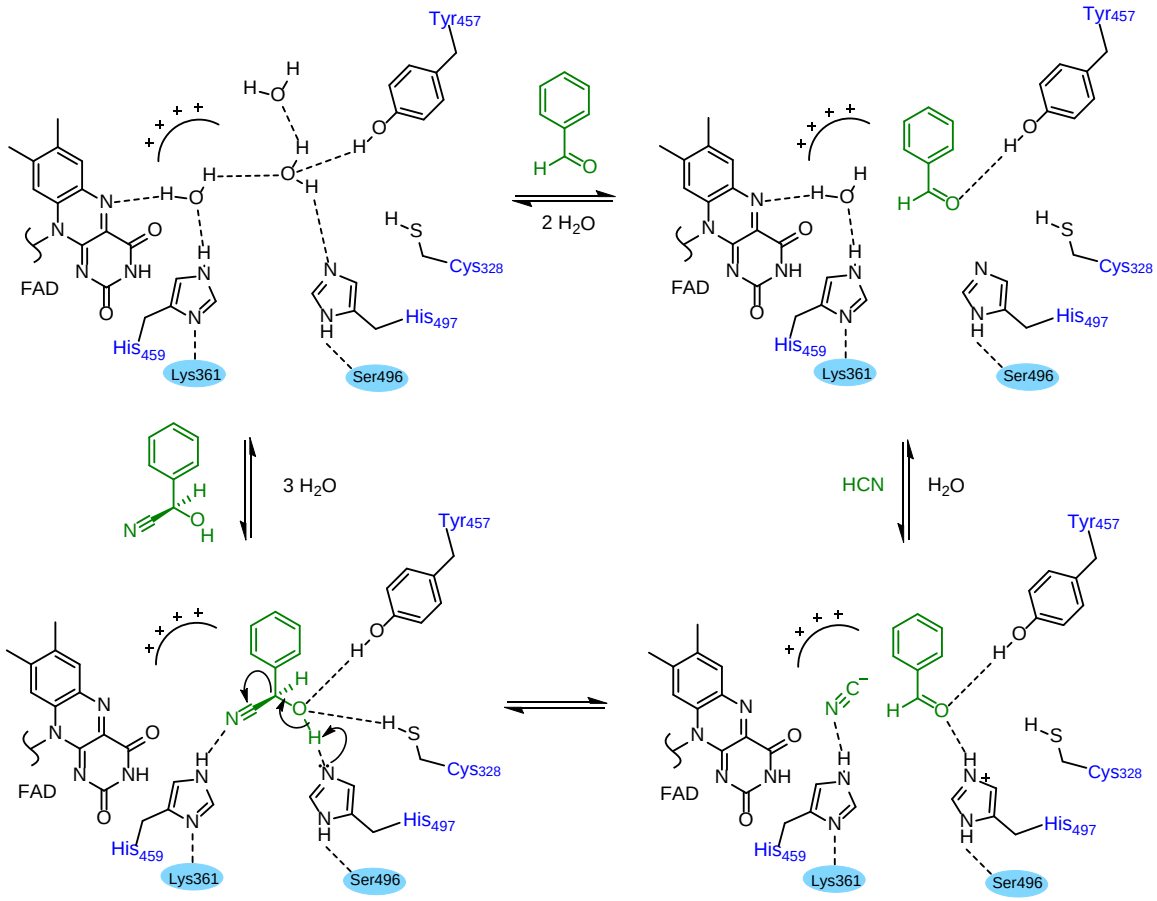

Figure 11. Anti-clockwise: proposed mechanism for the reversible cyanogenesis reaction catalyzed by *Pa*HNL1, modified from Dreveny *et al*. [106].

1.3.2. Enzymatic synthesis of β-hydroxynitriles catalyzed by halohydrin dehalogenases

Halohydrin dehalogenases (HHDH, EC 4.5.1.X) are a class of enzymes capable of synthetizing β-hydroxynitriles, also called β-cyanohydrins, *via* a cyanide-mediated epoxide ring-opening. These enzymes belong to the carbon-halide lyases, since their natural reaction is the dehalogenation of vicinal haloalcohols, leading to the formation of epoxides [108–111]. However, they can also catalyze the reverse reaction – the epoxide ring-opening – and accept a wide variety of anionic nucleophiles besides halides, such as azide, cyanide, nitrite, cyanate, thiocyanate and formate. This is of great synthetic relevance, since it enables the formation of C–C, C–N, C–O and C–S bonds, leading to a wide range of β-substituted alcohols, as shown in Figure 12. While enzymes displaying catalytic promiscuity often show low activity and selectivity, in the case of HHDHs, synthetically useful activity was observed for all accepted nucleophiles and excellent enantioselectivities were observed in numerous cases [112–114].

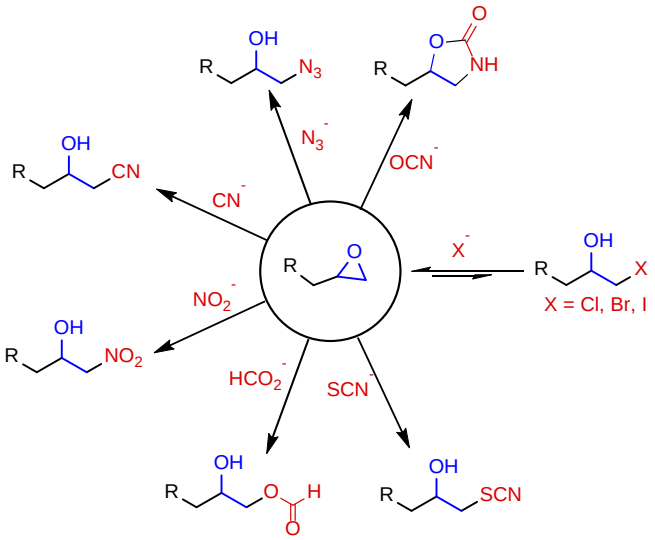

Figure 12. HHDHs can catalyze the opening of an epoxide ring using a variety of anionic nucleophiles. Simplified from Schallmey *et al.* [113].

Furthermore, the nucleophilic attack of terminal epoxides generally takes place regioselectively at the terminal carbon – with the exception of G-type HHDHs – and may also be stereoselective depending on the substrate and enzyme [114–116]. Among the different accepted nucleophiles, cyanide – the only one leading to the formation of C–C bonds – is especially interesting, given the challenging task of achieving asymmetric C–C bond formation using synthetic catalysts [67]. However, the k_{cat} values for the HHDH-catalyzed cyanolysis of epoxides are generally much lower than those for the azidolysis [112,114] and, thus, there is great interest in improving the cyanolytic activity of these enzymes [117–119]. As it occurs with HNL-catalyzed hydrocyanations, the HHDH-catalyzed cyanolysis of epoxides also competes with a non-

enzymatic nucleophilic substitution, given the strong nucleophilic character of cyanide [112]. This background reaction may be controlled, for example, by *in situ* generation of the epoxide *via* dehalogenation of a halohydrin precursor [112].

HHDHs are related to the short-chain dehydrogenase/reductase (SDR) superfamily both structurally and mechanistically. Their tertiary structure resembles a Rossman-fold – characteristic of the SDR superfamily – and their quaternary structure is also composed of four subunits (homotetramer) [120]. Moreover, the catalytic triad in HHDHs (Ser-Tyr-Arg) is similar to that of SDR enzymes (Ser-Tyr-Lys), where the tyrosine acts abstracting or donating a proton from/to the substrate. However, while SDR enzymes possess a nicotinamide cofactor binding site, HHDHs lack this feature, and show a nucleophile binding pocket instead [121]. The catalytic triad and nucleophile binding site are depicted in Figure 13, which shows the mechanism of the dehalogenation and epoxide ring-opening reactions. In the case of the dehalogenation reaction, the haloalcohol is positioned within the active site by formation of an H bond between its hydroxyl group and the serine. The arginine forms H bonds with the tyrosine, lowering its pKa and, thus, the deprotonated tyrosine abstracts the proton from the substrate's hydroxyl group. In the epoxide ring-opening reaction, the nucleophile attacks one of the carbons forming the epoxide and the resulting oxygen anion receives a proton from the tyrosine.

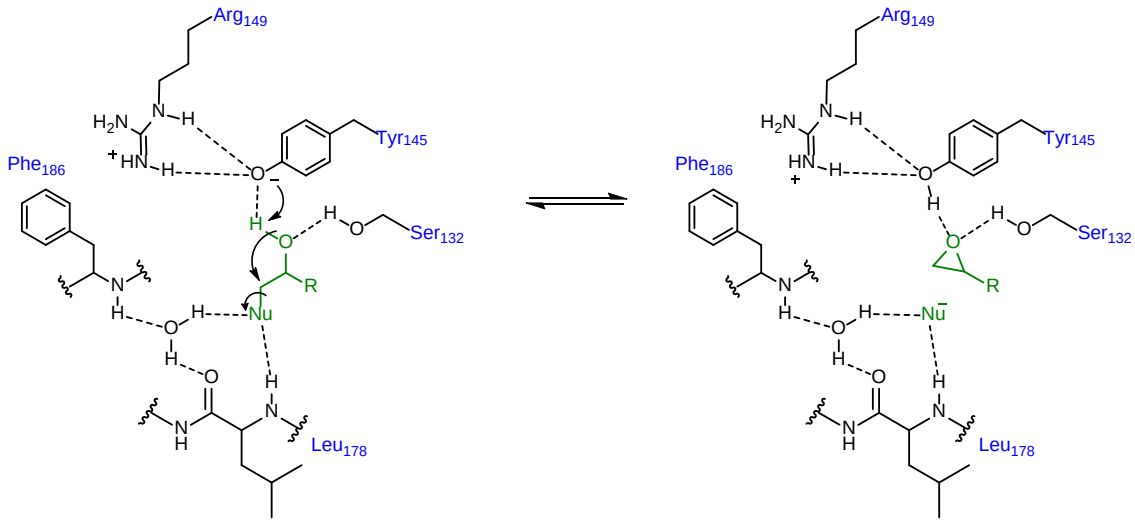

Figure 13. Mechanism of the dehalogenation (from left to right when Nu = halide) and epoxide ring-opening (from right to left) reactions catalyzed by HHDHs. Residue numbers correspond to HheC and bond-forming or bond-cleaving arrows correspond to the dehalogenation reaction. Adapted from Schallmey *et al.* [113].

According to phylogenetic analyses, all HHDHs identified so far have been divided into 6 subtypes including HHDH A to G [122]. This classification was further supported by the biochemical and biocatalytic characterization of 17 of the newly identified HHDHs [123]. Among the HHDHs identified so far, HheG is of special synthetic interest since it accepts cyclic epoxides,

as well as a range of acyclic disubstituted epoxides [115]. This broader substrate scope is probably due to the different architecture of its active site, as shown by Koopmeiners *et al.* [112]. Whereas most HHDHs have relatively narrow substrate tunnels that lead to the active site and influence the activity and selectivity of the enzyme [124–126], HheG's active site is placed in an open cleft as shown in Figure 14 [112].

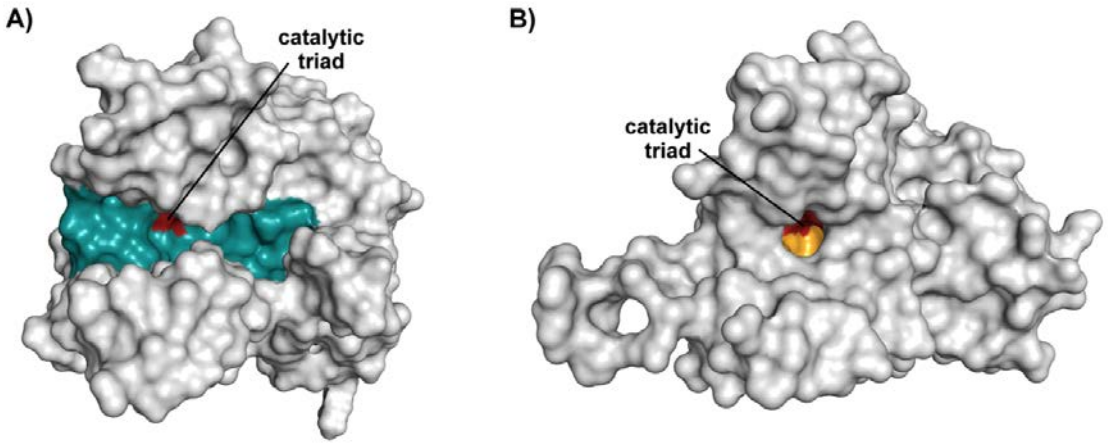

Figure 14. Surface representation of A) HheG from *Ilumatobacter coccineus* (PDB entry: 5O30) and B) HheC mutant from *Agrobacterium tumefaciens* (PDB entry: 3ZN2). For both enzymes, the active site harboring the catalytic triad is highlighted in red, and the open cleft of HheG is shown in turquoise, while the narrow tunnel in HheC is colored yellow. Taken from Koopmeiners *et al.* [112].

1.4. Acyl cyanohydrins

As discussed in section 1.3, the hydrocyanation of carbonyl compounds is a reversible reaction and when starting from ketones or aldehydes with low electrophilicity, the equilibrium lies on the substrate side [57]. In these cases, the equilibrium may be shifted towards the product side by using a larger excess of cyanide, performing the reaction at lower temperature or, more effectively, by constant product removal. Therefore, *in situ* concurrent acylation of the synthesized cyanohydrin – catalyzed by a hydrolase – is an interesting approach and has been intensely studied during the past decades [25,127–131]. The hydrolase-catalyzed acylation of enantioenriched cyanohydrins can, moreover, contribute to increasing the enantiomeric excess of the final product when an appropriate hydrolase is used. Acylated cyanohydrins can be used as building blocks, but also have direct applications in industry as potent insecticides, for example [132,133]. Furthermore, they can be converted into chiral β-amino alcohols and other derivatives with a broad range of applications in the fine chemicals and pharma industry.

1.4.1. Enzymatic acylation of cyanohydrins

The enzymatic synthesis of acyl cyanohydrins is achieved *via* a hydrolase-catalyzed transesterification using an acyl donor. Hydrolases are enzymes that catalyze the cleavage of a chemical bond by the addition of water. Within this class, lipases (E.C. 3.1.1.3) naturally catalyze the hydrolysis of triacylglycerols into glycerol and the corresponding fatty acids in water. However, they can also perform esterification or transesterification reactions using other nucleophiles instead of water, thereby catalyzing the formation of esters or amides when alcohols or amines are used, respectively. Owing to their versatility, ability of working in organic solvents and often high regio- and stereoselectivity, lipases are one of the most popular enzymes in the industrial sector [134,135].

Hydrolases are often used in hydrophobic solvents – such as *t*BME, iPr$_2$O and alkanes – in which they are generally more active, these being less effective at stripping the often essential enzyme-bound water than hydrophilic solvents [136]. When performing transesterification reactions, hydrolysis must be suppressed, since it lowers the process yield [136,137]. To minimize hydrolysis, reactions are often performed in water-free solvents, where the water activity (a_w) may be additionally controlled by adding salt hydrates [25,138,139].

Lipases belong to the serine hydrolases and share an α/β-hydrolase fold often found in this superfamily [92]. A common feature to these enzymes is the role of a serine residue in the active site, which acts as a nucleophile attacking the substrate. This serine, together with a histidine and either glutamate or aspartate form the catalytic triad that characterizes lipases [140]. Many of them possess a polypeptide lid or flap rich in hydrophobic residues, which blocks the active site in the closed conformation. Upon contact with a hydrophobic phase, the lid opens and thereby activates the enzyme by exposing the large hydrophobic pocket containing the active site [140].

The lipase-catalyzed hydrolysis, alcoholysis or amidolysis of esters follows a mechanism which involves two substrates and two products, as depicted in Figure 15 for *Candida antarctica* lipase A [141,142]. Within the catalytic triad, Ser184 forms a hydrogen bond with His366, which further shares a hydrogen with the acid anion residue Asp334. This way, the serine becomes a better nucleophile. When an ester (S_1) enters the active site, it is attacked by the deprotonated serine, forming a tetrahedral intermediate (I-1), which is stabilized forming H bonds with Asp95, Gly185 and His366. The alcohol moiety is subsequently cleaved and released (P_1) and the nucleophilic second substrate (S_2) attacks the acyl-enzyme complex, forming a second tetrahedral intermediate (I-2) characterized by the same H bonding as I-1. The serine-substrate bond is finally cleaved, releasing the second product (P_2) and the free enzyme, completing the catalytic cycle.

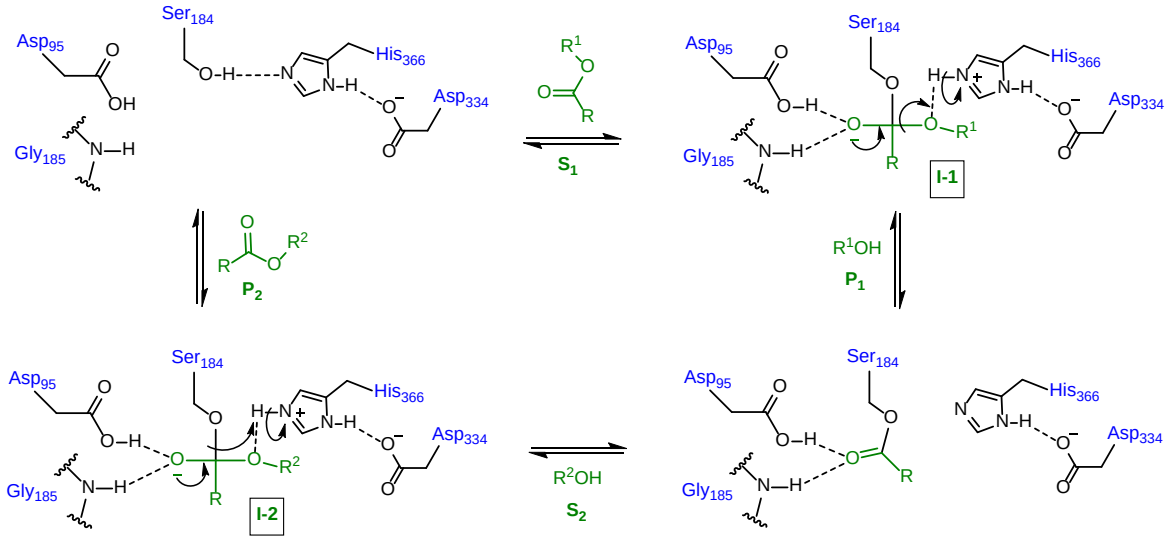

Figure 15. Clockwise: mechanism of the reversible hydrolysis (R^2 = H) or alcoholysis of ester **S_1** catalyzed by *Candida antarctica* lipase A (CALA) as proposed by Ericsson [141].

The major enantiomer resulting from a lipase-catalyzed reaction can be predicted by an empirical model known as the Kazlauskas rule (see Figure 16) [143,144]. According to this model, (*R*)-alcohols or (*R*)-esters will react faster than their complementary enantiomers, provided that the larger group (L) of the corresponding secondary alcohol has higher priority than the smaller substituent (M), according to the Cahn-Ingold-Prelog classification. Proteases, such as subtilisin, often prefer the opposite enantiomer [145], although their enantiopreference depends on the reaction medium and can change or even reverse depending on the different hydrophobicity of the substituents and the solvent's capacity for solvating each of them. Although there can be exceptions [146,147], lipases and proteases tend to follow the Kazlauskas model, enabling the synthesis of virtually any (*S*)- and (*R*)-cyanohydrin, as long as they are accepted by the enzymes.

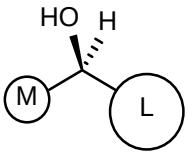

Figure 16. The Kazlauskas rule predicts that the faster reacting secondary alcohol enantiomer in a lipase-catalyzed reaction is the (*R*)-enantiomer, provided that L has higher priority than M according to Cahn-Ingold-Prelog rules. L = large substituent; M = medium substituent. Modified from [144].

The acylation of cyanohydrins (and, generally, of alcohols and amines) is an equilibrium reaction and, in order to reach the highest yields, chemists may adopt several measures. A straightforward solution is to add one of the reagents in excess, although this obviously leads to lower process yields. Alternatively, the removal of water – which may come from the enzyme preparation, for example – *via* distillation can benefit the reaction. However, increasing the

reaction temperature may not only lead to cleavage of the cyanohydrin, but can also affect the chirality of the product. The influence of temperature on the enantioselectivity of enzymatic reactions can be explained by a simple theoretical model [148]. Depending on whether the reaction takes place below or above the so-called racemic temperature, a decrease in temperature will increase or decrease the enantioselectivity, respectively. A more efficient approach to shift the acylation equilibrium towards the desired product is the use of activated acyl donors [136,149]. These may be reversible, such as oxime esters, esters from alcohols with poor nucleophilicity (e.g. naphtol, phenol or trifluoroethanol) or thioesters; or irreversible, such as anhydrides or enol esters, the latter having a leaving group that immediately tautomerizes to the keto form [136].

The yeast *Candida antarctica* produces two lipases, A and B, which exhibit high thermostability. Lipase B (CALB) is probably the most popular of all lipases and its applications range from the resolution of racemic mixtures to the production of biodiesel and the production or degradation of polymers [150–152]. Although lipase A (CALA) has found less applications in industry, it displays several interesting features [153]. Along with an outstanding thermostability and good performance in organic solvents, the presence of large cavities around the active site confers it the ability to accept bulky substrates [153–155]. Furthermore, it possesses acyltransferase activity and, thus, is able to synthesize alcohol esters of fatty acids even in aqueous medium, albeit with competition of hydrolysis [156,157].

1.4.2. Biocatalytic one-pot concurrent synthesis of acyl cyanohydrins from carbonyl compounds

A current challenge in the field of enzymatic cascades is the coupling of a hydroxynitrile lyase-catalyzed cyanohydrin synthesis with an acylation catalyzed by a lipase. This is an interesting process, given the above-mentioned advantage of immediately acylating the formed cyanohydrin to prevent the back reaction from taking place, yielding a chemically more stable product with potentially higher enantiomeric excess.

However, the one-pot one-step combination of the two enzymes is not trivial, for they have very different requirements. While water acts as a competing nucleophile in lipase-catalyzed transesterification reactions, HNLs require a relatively high water content when working in organic solvents [73,85,158]. Due to these different water content requirements, the cascade synthesis of acylated cyanohydrins catalyzed by an HNL and a lipase is a challenging task. Hanefeld *et al.* attempted to couple the hydrocyanation of benzaldehyde with the acetylation of the formed mandelonitrile in order to shift the equilibrium of the first reaction, as shown in Figure 17

[25]. The reactions were catalyzed by *Hb*HNL and CALB, respectively, using acetone cyanohydrin as cyanide donor and isopropenyl acetate as acyl donor. However, they encountered problems due to hydrolysis of the acyl donor, resulting in complete deactivation of the *Hb*HNL caused by the released acetic acid. Nevertheless, it has been shown that under certain conditions HNLs can work at low water content [159–161], opening the possibility for combining the two mentioned enantioselective enzymatic steps by better controlling the water activity of the medium.

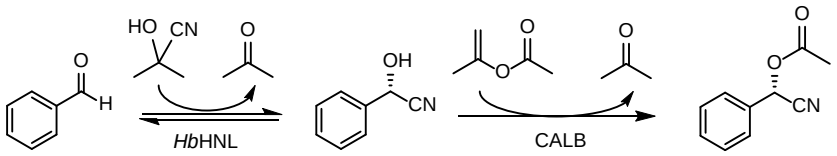

Figure 17. Concurrent cascade proposed by Hanefeld and coworkers for the enzymatic formation and esterification of (*S*)-mandelonitrile [25].

As an alternative to the bi-enzymatic synthesis of acylated cyanohydrins, researchers have studied kinetic resolutions of cyanohydrins or acyl cyanohydrins and dynamic kinetic resolution approaches combining an unselective hydrocyanation with an enantioselective transesterification [127–131,162–164]. An interesting alternative concurrent and enantioselective synthesis of acyl cyanohydrins developed by Purkarthofer *et al*. consisted in the *Pa*HNL-catalyzed hydrocyanation of benzaldehyde using ethyl cyanoformate as both cyanide source and acylating agent (see Figure 18, scheme I) [165]. The HNL was immobilized on Celite for this approach and it was found that the enzyme carrier catalyzed the acylation of the cyanohydrin, yielding the corresponding carbonate. Similarly, Baeza *et al.* reported the cyanobenzoylation of aldehydes catalyzed by an enantioselective Ti(IV) complex with Lewis acid and Brönsted base character (see Figure 18, scheme II) [166]. However, Purkarthofer *et al.* only achieved a maximum of 46% yield when reactions were performed in organic solvent to ensure highest enantioselectivity (99% e.e.), whereas Baeza's procedure afforded products of low enantiopurity (≤ 68% e.e.). An approach based on the latter was further developed to reach 97% yield and excellent enantiopurity by means of a combined enantioselective acylcyanation of aldehydes – catalyzed by a Lewis base (LB) and Ti complex Lewis acid (LA) – with simultaneous recycling of the minor enantiomer *via* CALB-catalyzed hydrolysis, as reported by Wingstrand *et al.* (see Figure 18, scheme III) [147].

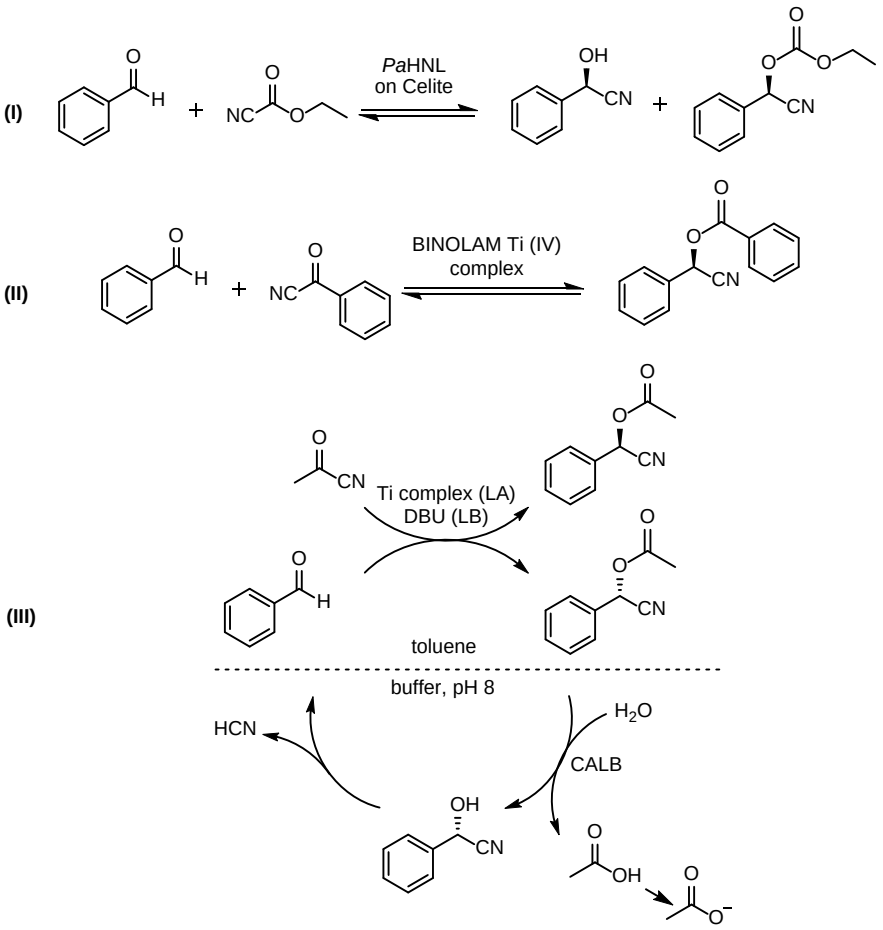

Figure 18. Examples of concurrent enantioselective synthesis of protected mandelonitrile starting from benzaldehyde. Adapted from [165] (I), [166] (II) and [147] (III).

1.5. Catalytic hydrogenation of nitriles to primary amines

Amines are one of the most relevant intermediates in the synthesis of pharmaceuticals, agrochemicals and polymers [167,168]. Among these, primary amines play a key role as they are versatile precursors in organic chemistry. However, their high reactivity makes the synthesis of primary amines a challenging task [169,170]. Their synthesis *via* reduction of nitriles constitutes an approach with high atom economy, there being a multitude of examples of efficient reduction of nitriles to primary amines with optimal selectivity [169]. However, the high redox potential of nitriles, the low C-CN dissociation energy – which may lead to reductive decyanation – and the reactivity of the imine intermediates has resulted in this pathway being less investigated [169].

The reduction of nitriles is usually achieved either by using stoichiometric amounts of metal hydrides [171–173] or *via* catalytic hydrogenation using heterogeneous transition metal catalysts [174–179]. When using metal hydrides, compatibility with other functional groups must be assessed, since the commonly used $LiAlH_4$ also reduces esters, amides and carboxylic acids, for example [180]. Alternatively, less reactive metal hydrides – such as $NaBH_4$ – may also be used in

combination with a heterogeneous metal catalyst, which in certain cases affords higher functional group compatibility [181–183]. Nevertheless, while metal hydrides are generally effective, their use results in the co-production of stoichiometric amounts of metal salts, which may cause elaborate work-up procedures and require special waste disposal. The alternative catalytic hydrogenation typically yields secondary and tertiary amines as side products, due to the condensation reactions that take place between the reduction intermediate imines (II) with the formed amines (III and VI) (see Figure 19) [184–186]. Notwithstanding, the hydrogenation of nitriles catalyzed by heterogeneous catalysts is the preferred method for the synthesis of primary amines in industry [186].

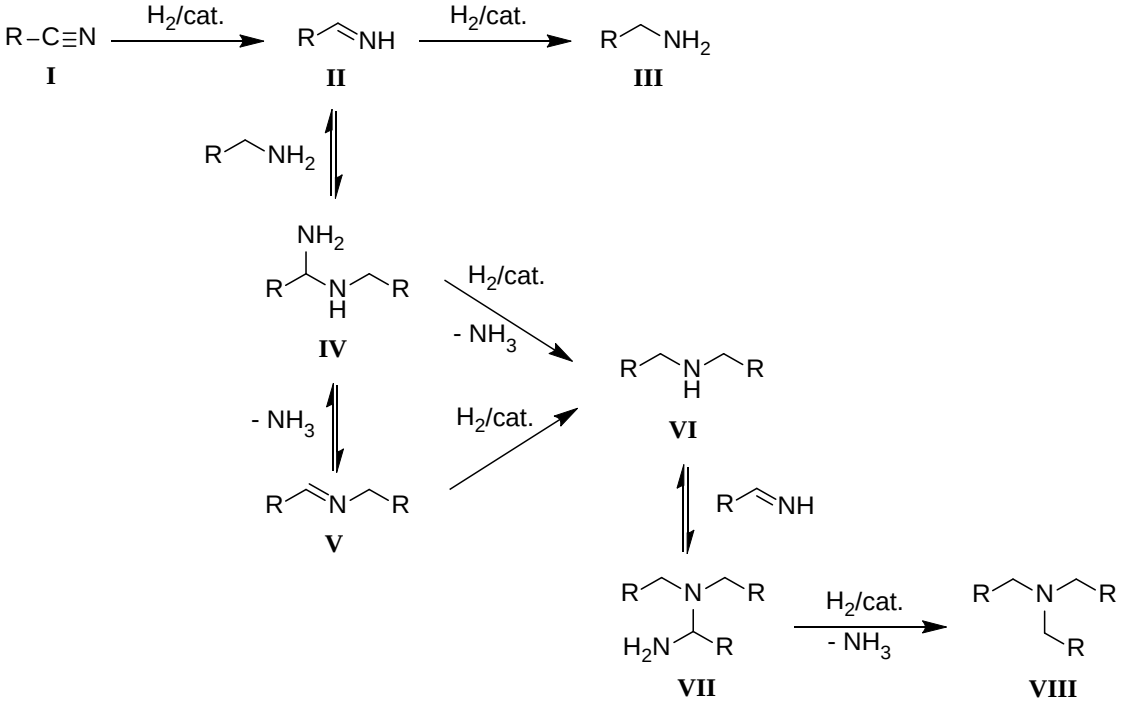

Figure 19. Mechanism for the formation of primary, secondary and tertiary amines in the catalytic hydrogenation of nitriles as proposed by Braun [187] and modified by Greenfield [188].

Besides the aforementioned intrinsic side reactions, selectivity must also be considered in terms of functional group compatibility. The formation of undesired side products can significantly reduce the efficiency of the process and, thus, the reaction parameters must be optimized to enhance its selectivity. The chemoselectivity of the catalytic hydrogenation of nitriles depends on the substrate structure, the nature and loading of catalyst, the reaction temperature, the hydrogen pressure, the selected solvent and the presence of additives such as ammonia [184–186]. Furthermore, the hydrogenation conditions may affect the chiral center of the reactant resulting in partial or total racemization [174,189]. Among the different parameters affecting the reaction selectivity, the nature of the catalyst appears to be the most crucial factor [184–186,190]. In order to enhance the selectivity towards primary amines, suppressing the

formation of secondary and tertiary amines, there are two main strategies. These consist in either keeping a low concentration of imine intermediate (Figure 19, compound II) or shifting the equilibrium between imine II and secondary or tertiary amines VI and VIII by addition of ammonia or an appropriate base [169]. However, the addition of ammonia or bases, such as NaOH, LiOH or Na_2CO_3, has proven to exert beneficial effects only in certain cases and can also lead to other undesired reactions [174,186].

Catalytic hydrogenation of nitriles has been successfully achieved for a wide selection of substrates – aliphatic, aromatic and heteroaromatic – with varying functional group tolerance. Catalysts may be homogeneous – generally limited by poor stability and hampered recycling – or heterogeneous, which are generally more cost-efficient. Among the latter, the most frequently used metals are nickel, cobalt, ruthenium, palladium and platinum, although catalysts based on copper, rhodium, manganese, iron and iridium have also been applied for the reduction of nitriles [169,186]. As mentioned before, the nature of the catalyst has a decisive influence on the conversion and selectivity. An evaluation of different silica-supported metals, Co, Ni, Pt, Pd, Cu, Ru, on the hydrogenation of butyronitrile was performed by Segobia *et al.* [177]. The highest activity and selectivity towards n-butylamine was achieved with Ni > Co > Ru, whereas Pd, Pt and Cu produced dibutylamine primarily, with lower conversions. Although the order observed by Segobia is not universal, there is indeed a trend whereby Ni and Co catalysts often offer high activity and selectivity towards primary amines, whereas Pd and Pt are often used for the synthesis of secondary or tertiary amines [184].

Given the harsh conditions often required by metal-catalyzed nitrile hydrogenations and the numerous side reactions that decrease the yields and lead to cumbersome product purification procedures, a biocatalytic alternative – performed under mild conditions and with high selectivity – is highly desirable. Nitrile reductases constitute a new class of NADPH-dependent oxidoreductases that catalyze the selective reduction of a nitrile ($PreQ_0$) to yield a primary amine ($PreQ_1$) in the biosynthesis of the tRNA modified nucleoside queuosine, which is considered to play an important role in the fidelity of translation (see Figure 20) [191]. However, nitrile reductases have only been shown to effectively catalyze the reduction of $PreQ_0$, showing negligible or very poor activity with other substrates [192–194]. Furthermore, although Zhou and co-workers recently achieved a 50% increase of the activity of a nitrile reductase *via* protein engineering [191], the catalytic efficiency of these enzymes is very low and thus must be further improved before these enzymes can be applied on an industrial scale.

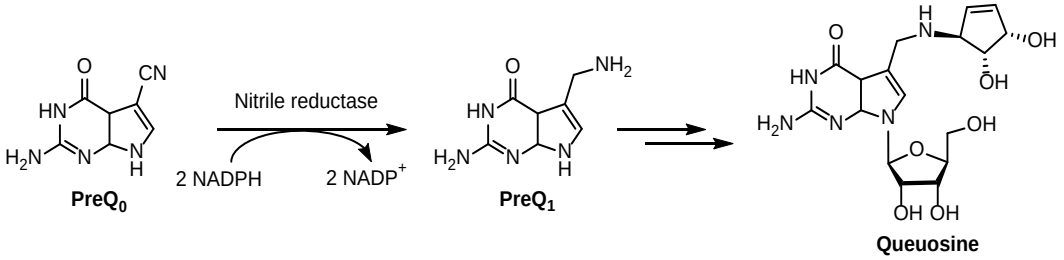

Figure 20. Reduction of the nitrile moiety in $PreQ_0$ catalyzed by nitrile reductases in the queuosine pathway.

1.6. Enzyme engineering

Natural selection has driven the evolution of enzymes through billions of years. Enzymes have, thereby, evolved to catalyze often very specific reactions with varying efficiency [195] and are usually not fitted for their application in industrial processes, where normally higher (non-natural) substrate concentrations and harsh conditions are used [196]. However, enzyme superfamilies show tremendous functional diversity [197] and HNLs are an example of how nature has the power of evolving completely unrelated enzymes to catalyze the same reaction (see section 1.3.1). Inspired by the potential of natural evolution, scientists have developed numerous technologies for the engineering of enzymes in order to broaden their substrate scopes [198], increase or invert selectivity [199], improve enzyme activity or stability [200,201] or harness enzyme promiscuity [202], for example. Enzyme engineering can be achieved by means of two different approaches: directed evolution and rational design.

Directed evolution aims at mimicking the process of natural evolution by which all natural enzymes were developed, using random mutations at an increased frequency and selecting variants with improved properties. The earliest examples of laboratory enzyme evolution focused on this approach, since it requires no structural or mechanistic information of the enzyme to be engineered. This strategy aims at introducing mutations over the whole gene sequence encoding the protein of interest [203,204] and is effective for a wide range of applications, such as improving enzyme activity or stability [200] or modifying its enantioselectivity [199]. Within this approach, random mutagenesis is applied to generate genetic diversity by means of DNA recombination or non-recombining methods (see Figure 21), which often use DNA polymerases (e.g. error-prone PCR) [204,205], but may also employ chemical mutagens or mutator strains [206]. To maximize the chances of finding variants with improved characteristics, large libraries are generated and, thus, a high throughput screening method is crucial. Additionally, this approach often requires several rounds of evolution before obtaining a variant with the desired properties.

The rational design of enzymes using targeted mutagenesis is especially useful when aiming at dramatically altering the enzyme's specificity or regioselectivity, which may require multiple mutations in or near the active site [203]. When using random mutagenesis, libraries with a small number of mutations per gene often contain very few multiple active site mutations, whereas libraries containing a large number of mutations tend to produce inactive mutants. Therefore, to increase the chances of success, a selection of the positions likely to deliver improved variants upon mutagenesis is required, which strongly relies on biochemical and structural information. In addition to protein structure elucidation techniques (X-ray crystallography, cryo-electron microscopy and protein NMR), protein molecular modelling tools (e.g. PyMol, Yasara or Rosetta) have greatly contributed to the development of new enzyme mutants *via* rational design. A comparison between random and targeted mutagenesis performed by Kazlauskas *et al.* aiming at improving the enantioselectivity of an esterase showed that, although improved variants were identified with both approaches, focusing mutations to the substrate binding site was more effective [207].

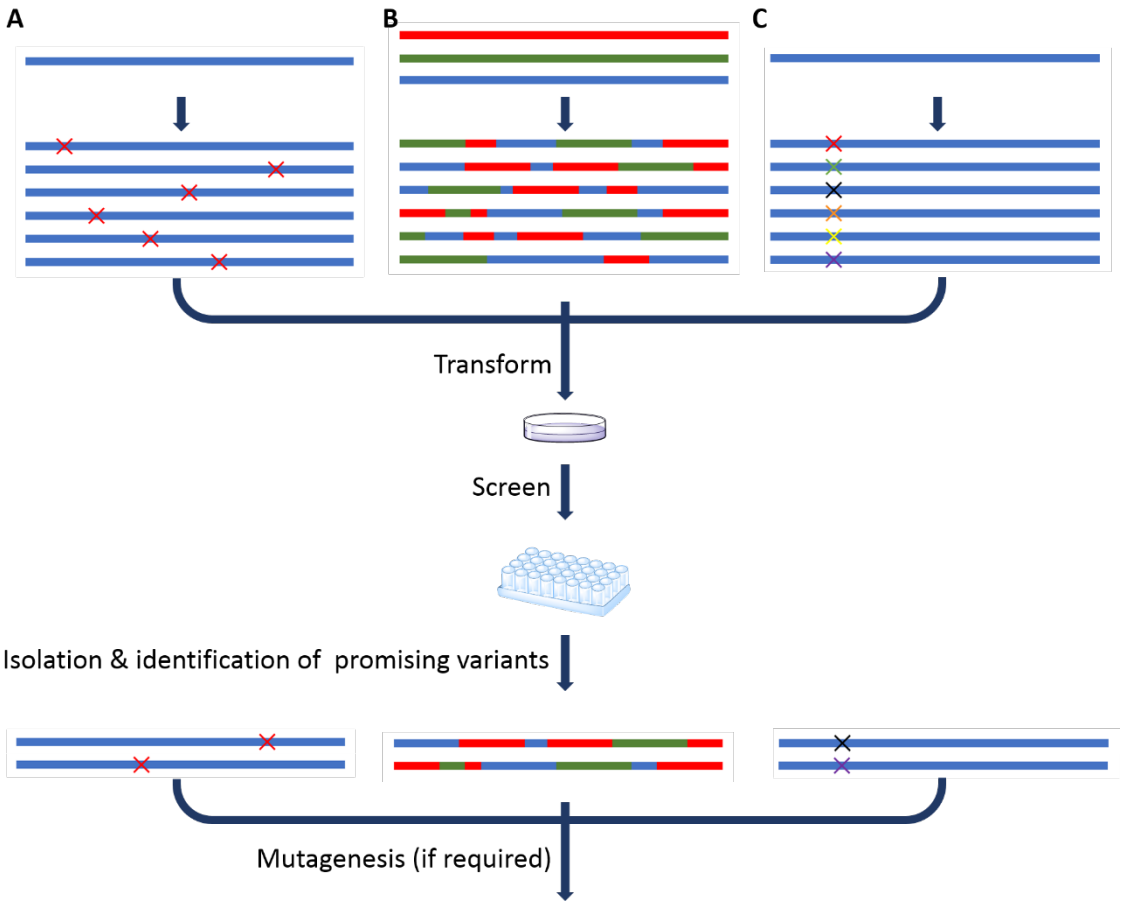

Figure 21. Schematic representation of the three main strategies for generating genetic diversity in the laboratory. A) Non-recombining random mutagenesis methods; B) DNA Recombination; C) Targeted mutagenesis.

Semi-rational design combines the advantages of random mutagenesis and rational design, creating smaller libraries than random mutagenesis approaches, but with larger mutant variety than in targeted mutagenesis [208]. Here, site-saturation mutagenesis (SSM) of rationally selected positions is generally used. SSM consists in replacing one or more specific amino acids with all other 19 canonical amino acids, thereby increasing the possibility of identifying variants with the desired characteristics. Due to the degeneracy of the genetic code, the distribution of amino acids in the generated library is unbalanced when NNN-codons (N: Ade/Cyt/Gua/Thy) are used. Furthermore, in order to achieve 95% coverage of all possible substitutions in a single residue SSM library, 192 variants must be screened (= *oversampling factor* × (*number of possible bases* ^ *number of positions at codon*) = 3×4^3) [209], while this number increases exponentially when multiple sites are saturated. To overcome this problem, a popular solution is the use of specific degenerated codons that notably reduce the required library size to be screened to maintain a 95% coverage. Examples are NNS (S: Cyt/Gua) or NNK (K: Gua/Thy), which also encode for all 20 amino acids, but reduce the number of covered codons from 64 to 32. Other degeneracies, such as NDT (D: Ade/Gua/Thy; T: Thy) or NRT (R: Ade/Gua), further decrease the screening effort by introducing only 12 and 8 codons, respectively, as well as eliminating all stop codons, although they do not encode for all 20 amino acids [209].

1.6.1. Engineering of HHDHs for improved cyanolytic activity

As mentioned in section 1.3.2., among the different reactions that HHDHs can catalyze, the cyanolysis of epoxides is of special interest, since it allows for the selective formation of C–C bonds, enabling the synthesis of β-cyanohydrins. However, the k_{cat} values for the HHDH-catalyzed cyanolysis of epoxides are generally much lower than those for the azidolysis [112,114] and, thus, there is great interest in improving their cyanolytic activity [117–119] to enable the synthesis of β-cyanohydrins in preparative scale. HheC from *Agrobacterium radiobacter* is one of the first HHDHs to be ever identified and, owing to its remarkable enantioselecivity and the availability of its crystal structure, it is the most studied HHDH [113]. Aiming at enhancing the activity of HheC in the synthesis of hydroxynitriles, Schallmey *et al.* demonstrated an influence of residue Thr134 on the cyanolytic activity of this enzyme. Mutation of this residue, which is located close to the catalytic triad forming a hydrogen bond with Ser132, was shown to improve its catalytic efficiency (k_{cat}/K_M) in the cyanide-mediated epoxide ring-opening when threonine is substituted by an alanine [118]. Furthermore, the dehalogenase activity was also improved for several substrates, although a loss of enantioselectivity was generally observed both in the dehalogenation and cyanolysis reactions. Based on a structural alignment of HheG and HheC, Julia Koopmeiners

identified residue Thr154 in HheG as structurally homologous to residue Thr134 in HheC [117]. The exchange of this residue to alanine, however, did not render an HheG mutant with higher cyanolytic activity and, furthermore, the mutation had a negative effect on the activity in the dehalogenation of chlorocyclohexanol.

Previous studies on HheC have demonstrated the influence of residues P175 and N176 on its enantioselectivity, resulting in increased enantioselectivity upon single site-directed mutagenesis of P175 [124], and achieving enantioselectivity enhancement as well as inversion after multiple site-directed mutagenesis involving residues N176 and P175 among others [119,210]. Residues P175 and N176 are found in proximity to the nucleophile-binding region and to the O-site, respectively [119], which makes them interesting targets for the manipulation of HheC activity and selectivity. Based on a structural alignment of HheG and HheC, Julia Koopmeiners identified residues T195 and N196 in HheG as structurally homologous to residues P175 and N176 in HheC [117]. Aiming at generating variants with higher activity and selectivity in the dehalogenation reaction, she randomized both residues simultaneously using SSM. However, no variant was found which could afford higher conversion than the wild-type control in the dehalogenation of 2-chlorocyclohexanol.

Given the great difference between the structures of HheC and HheG regarding the entrance to the active site – HheG features a large open cleft, whereas HheC presents a narrow substrate tunnel [112] –, Elia Calderini applied a different approach for the improvement of the enantioselectivity of HheG by using Rosetta protein design [211]. First, the crystal structure of HheG (PDB-ID: 5O30) was aligned with available crystal structures of HheC in complex with (*R*)-4-cyano-3-hydroxybutyrate or styrene oxide and chloride in the active site (PDB-ID: 4IXT and 1ZMT, respectively) and, subsequently, cyclohexene oxide and 2-cyanocyclohexanol were docked as substrates in the active site of HheG. Excluding the catalytic triad, residues of HheG within 5 Å from the substrates were selected and randomly mutated *in silico*. When using 2-cyanocyclohexanol as substrate, the Rosetta result revealed a high variability at positions 195 and 196, suggesting that threonine and asparagine, respectively, are not the best residues for optimal substrate binding in this case. This indicates that mutagenesis at these sites could lead to several putatively more enantioselective variants and might also lead to mutants with higher activity. Therefore, site-directed mutagenesis was performed on positions 195 and 196, exchanging the amino acids for those suggested by Rosetta. However, none of the mutants exhibited enhanced enantioselectivity in the cyanolysis of cyclohexene oxide. Mutant HheG-N196M exhibited increased cyanolytic activity, albeit with lower enantioselectivity when compared to HheG WT. In order to maximize the possibility of finding variants with increased activity and selectivity, given

the relevance and flexibility of positions T195 and N196, site-saturation mutagenesis was performed by Janine Mayer (Master thesis, 2017) [212] on each position independently. The library at position N196 was screened by Janine Mayer in the cyanide-mediated epoxide ring-opening of cyclohexene oxide using whole-cell biocatalysis starting directly from the epoxide or *via* a cascade reaction starting from 2-chlorocyclohexanol (see Figure 22). Four colonies exhibited a 4-fold to 6-fold higher conversion compared to the HheG wild-type controls, although sequencing showed that three of them were, in fact, wild-type HheG. Also, several colonies showed higher enantioselectivity. In the case of the library at position T195, only a cyanolysis test *via* a cascade reaction starting from 2-chlorocyclohexanol was performed, where 14 colonies displayed up to 4-fold increased conversion compared to HheG wild-type.

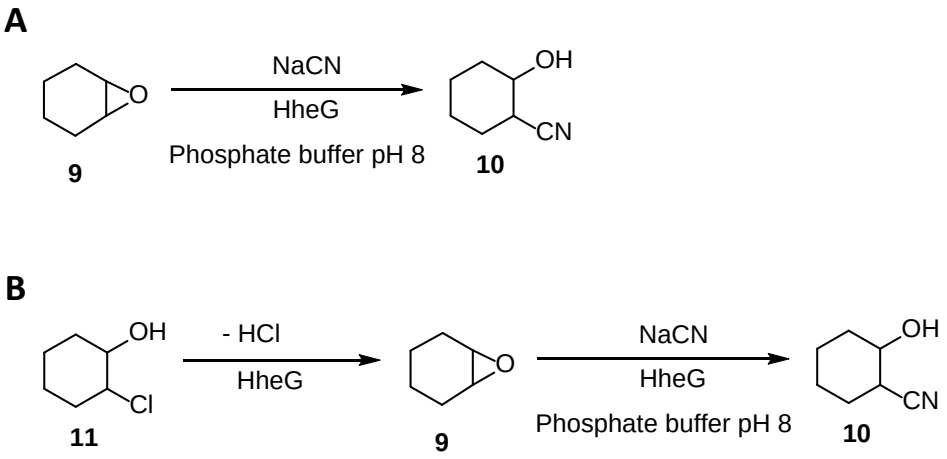

Figure 22. Alternative cyanolysis screening experiments used for the HheG T195-NNS and N196-NNS libraries. Method A starts directly from the cyanolysis substrate cyclohexene oxide, whereas in method B, the substrate is gradually generated *via* dehalogenation of 2-chlorocyclohexanol catalyzed also by HheG.

1.7. Aim of the project

The main objective of this project was the design and optimization of an enantioselective chemo-enzymatic cascade for the synthesis of the vicinal amino alcohol derivative tembamide. With this, we aimed at contributing to the synthetic toolbox for the asymmetric preparation of amino alcohol derivatives, given their high potential for the synthesis of APIs and the importance of enantiopurity that usually characterizes the pharmaceutical industry. We envisioned a pathway involving a concurrent bi-enzymatic synthesis of tembamide precursor 4-methoxymandelonitrile benzoate (**3**), and the subsequent reduction of the nitrile moiety to yield tembamide (**4**), as shown in Figure 23. To achieve this, both the enzymatic cascade and the reduction step had to be investigated and optimized independently and in parallel.

The enzymatic step consisted in a concurrent approach involving an HNL-catalyzed hydrocyanation of 4-anisaldehyde in combination with a hydrolase-catalyzed benzoylation of the cyanohydrin **2**. By performing the two enzymatic reactions in a concurrent fashion, we expected to observe an equilibrium-shifting effect on the unfavorable hydrocyanation reaction thanks to the constant product removal catalyzed by the hydrolase. To ensure successful combination of the two enzymes, an initial goal was their immobilization, followed by a systematic study of the relevant reaction variables for each enzymatic step. The results of this investigation are presented in chapter 3.1.

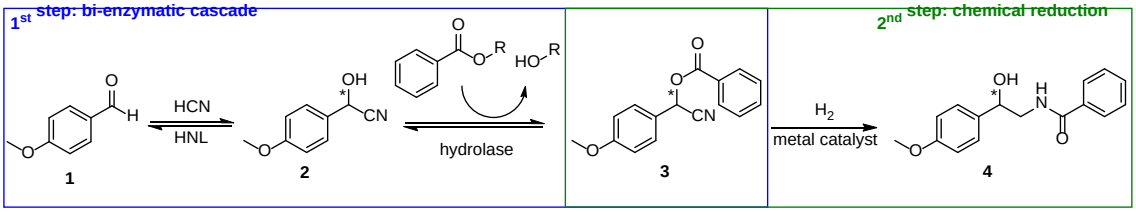

Figure 23. Proposed 2-step synthesis of enantiopure tembamide (**4**). By combining an *S*-selective or an *R*-selective HNL with a suitable hydrolase, we expected to achieve the synthesis of (*S*)-**4** and (*R*)-**4**, respectively, provided that the reduction step proceeded with enantioretention.

For the reduction of the nitrile moiety a catalytic hydrogenation reaction was planned, aiming at a fully catalytic route for the synthesis of tembamide. The catalytic hydrogenation of acylated cyanohydrins initially forms an amino-ester intermediate that spontaneously undergoes acyl transfer to yield the corresponding *N*-acyl-β-amino alcohol. To achieve this reaction with the highest chemoselectivity and enantioretention, a proper catalyst had to be selected and the hydrogenation conditions, optimized. Once the enzymatic cascade and the catalytic hydrogenation had been optimized, a final milestone was to perform the preparative scale synthesis of tembamide following the developed chemo-enzymatic cascade as a proof of concept. These results are presented in chapter 3.2.

Furthermore, in our aim to expand the portfolio of biocatalytic reactions for the synthesis of chiral amino alcohols and their derivatives in a preparative scale, an additional goal was to investigate the engineering of HheG in order to improve its activity in cyanide-mediated epoxide ring-opening reactions for the synthesis of β-hydroxynitriles. To this end, position T154 was selected as a target for site-saturation mutagenesis and subsequent screening of the generated library in search of variants with improved cyanolytic activity. These results can be found in chapter 3.3.

2. Materials and Methods

2.1. Materials

2.1.1. Chemicals

Unless otherwise indicated, reagents and organic solvents were purchased from either Fisher Scientific (Schwerte, Germany), TCI Europe N.V. (Zwijndrecht, Belgium), Merck KGaA (Darmstadt, Germany), VWR International GmbH (Darmstadt, Germany) or Acros Organics (Geel, Belgium) and were of the highest purity available.

Celite R-633 was a gift from Imerys S.A. (Paris, France); Relizyme EXE309 was kindly provided by Resindion S.r.l. (Binasco, Italy), and SYLOID silicas were a gift from former Grace Davison, Inc. (Grace GmbH & Co., Worms, Germany). Raney® Cobalt was kindly provided by Dr. Klaas van Gorp from Grace Catalysts Technologies, Grace GmbH & Co (Worms, Germany). *(S)*-Tembamide used for construction of HPLC calibration curves had been previously synthetized by Joerg Schrittwieser at Frank Hollmann's group [42].

Media components for bacterial cell growth were purchased from Carl Roth (Karlsruhe, Germany) or Fisher Scientific (Schwerte, Germany).

2.1.1.1. Preparation of hydrocyanic acid solutions

For the preparation of hydrogen cyanide solution, potassium cyanide (26 g, 0.4 mol) was dissolved in a stirred mixture of distilled water (200 mL) and the desired organic solvent (100 mL). The solution was cooled in an ice-water bath and 1.33 M citric acid (100 mL, 0.13 mol, 1 equivalent) was slowly added. The aqueous layer was extracted twice with 50 mL of the organic solvent. The combined organic phases were stored in a dark bottle containing 1 M citrate buffer pH 5.5 (10 mL). The HCN concentration was determined by measuring the absorption of the $[Ni(CN)_4]^{2-}$ complex ion at 267 nm. HCN solution (20 µL) was added to 3.5 mM $NiSO_4 \cdot 6H_2O$ in 1 M NH_3 (4 mL) [118]. After vigorous mixing, the solution was further diluted 50 times with 1 M NH_3 in a cuvette. The absorption was measured and the resulting HCN concentration was calculated based on a calibration curve.

2.1.1.2. Synthesis of (±)-4-methoxymandelonitrile, (±)-2

(±)-4-Methoxymandelonitrile was synthetized *via* chemical hydrocyanation of 4-anisaldehyde following a modified literature procedure [213]. In a 100 mL round-bottom flask, NaCN (4.4 g, 90 mmol) was dissolved in water (30 mL) and $NaHSO_3$ (9.4 g, 90 mmol) was slowly

added. 4-Anisaldehyde (2.4 g, 18 mmol) was dissolved in ethyl acetate (20 mL) and added to the reaction mixture. After 4 hours 45 minutes of vigorous stirring, the flask was introduced in an ice-water bath and stirred for another 4 hours. The reaction was followed by HPLC until it reached plateau at 92% conversion. Distilled water (30 mL) was added to dissolve the salts and the aqueous phase was extracted with ethyl acetate (2 × 10 mL). The combined organic phase was washed with brine, dried over anhydrous $MgSO_4$, and concentrated on a rotary evaporator using a 10 °C bath, whereupon crystallization occurred. The crystals were washed with a 2:1 mixture of cold heptane and ethyl acetate, and stored at 5 °C. HPLC analysis showed that the (±)-4-methoxymandelonitrile crystals contained 3% 4-anisaldehyde impurity.

2.1.1.3. Synthesis of (±)-4-methoxymandelonitrile benzoate, (±)-3

The racemic cyanohydrin ester was synthesized *via* chemical benzoylation of (±)-**2** (97.0%). A sealed 50 mL round-bottom flask containing (±)-4-methoxymandelonitrile (2.02 g, 12 mmol) and benzoyl chloride (1.5 mL, 13.2 mmol) in dry dichloromethane (20 mL) under N_2 atmosphere, was introduced in an ice-water bath and anhydrous pyridine (10.7 mL, 13.2 mmol) was added dropwise with a syringe. The reaction mixture was vigorously stirred for 2 h. The mixture was then transferred to a 100 mL separatory funnel and washed with demineralized water (2 × 20 mL), citrate 0.2 M pH 4 (2 × 20 mL) and phosphate buffer pH 8 (0.2 M, 2 × 20 mL). The organic phase was then dried over anhydrous $MgSO_4$ and concentrated in a rotary evaporator. Recrystallization (1:4 mixture of dichloromethane and diethyl ether) afforded (±)-4-methoxymandelonitrile benzoate (1.90 g, 58% isolated yield).

2.1.1.4. Synthesis of (R)-4-methoxymandelonitrile benzoate, (R)-3

The same procedure as described for (±)-**3** was followed using commercially available *(R)*-4-methoxymandelonitrile benzoate (0.50 g, 98.0%, 3 mmol), affording white crystals of (*R*)-4-methoxymandelonitrile benzoate in 60% yield.

2.1.2. Enzymes

2.1.2.1. Commercial enzymes

Table 1: Commercial enzymes used in this project.

Enzyme	Organism of origin	Supplier
Candida antarctica lipase A (Novozym CALA L)	*Candida antarctica*	Novozymes A/S (Bagsværd, Denmark)
*Pfu*Turbo DNA polymerase	*Pyrococcus furiosus*	Agilent Technologies (Santa Clara, CA, USA)
NdeI	*Neisseria denitrificans*	New England BioLabs GmbH (Frankfurt am Main, Germany)
DpnI	*Diplococcus pneumoniae* G41	New England BioLabs GmbH (Frankfurt am Main, Germany)

2.1.2.2. Recombinantly expressed enzymes

Mutant L1Q/A111G of isoenzyme 5 from *Prunus amygdalus* hydroxynitrile lyase was kindly provided by Martin Schürmann (InnoSyn B.V., Geleen, The Netherlands) as unpurified fermentation supernatant from heterologous expression in *Pichia pastoris* [103].

Hydroxynitrile lyase from *Manihot esculenta* was heterologously expressed in *E. coli* K12 Top 10F' harboring the pSE420-MeHNL plasmid, which was kindly provided by the Austrian Centre of Industrial Biotechnology (ACIB GmbH, Graz, Austria). The procedure is described in section 2.2.2.1.

Halohydrin dehalogenase from *Ilumatobacter coccineus* YM16-304 (HheG), as well as the SSM library mutants were heterologously expressed in *E. coli.* BL21 (DE3) Gold cells. The procedure is described in section 2.2.2.1.

2.1.3. Kits

Table 2: Kits used in this project.

Kit	Supplier
E.Z.N.A.® Plasmid Mini Kit I	Omega Bio-tek (Norcross, GA, USA)
PfuUltra II Hotstart PCR Master Mix	Agilent Technologies (Santa Clara, CA, USA)

2.1.4. Strains, vectors and oligonucleotides

The *Escherichia coli* DH5α strain (Invitrogen, Carlsbad, CA, USA) was used for plasmid amplification and DNA manipulation, whereas wild-type HheG and HheG mutants were expressed in *E. coli* BL21 (DE3) Gold (Novagen, EMD Biosciences, San Diego, CA, USA).

E. coli K12 Top 10F' (Invitrogen, Carlsbad, CA, USA) was used for heterologous expression of *Me*HNL.

The vector pET-28a(+)-hheG (HheG gene cloned with *NdeI* and *HindIII* in pET-28a(+) with hexa-histidine-tag fusion at the N-5'-end and kanamycin resistance) was available from previous projects [112,123]. Vector pET-28a(+)-hheG(NNS-T154) was prepared using QuikChange PCR.

The vector pSE420-MeHNL (*Me*HNL gene cloned in pSE420 carrying ampicillin resistance), transformed into *E. coli* K12 Top 10F' cells, was provided by the ACIB.

Table 3: List of oligonucleotides used for gene amplification and sequencing. The table shows the sequences, as well as the length (in base pairs) and melting temperature (T_m).

Name	Sequence (5´→3´)	Length (bp)	T_m (°C)
NNS-T154-1-fwd	TTTTTACCAGCGCGNNSGGTGGTCGTCCG	29	81.2
NNS-T154-1-rev	GGACGACCACCSNNCGCGCTGGTAAAAAC	29	78.2
NNS-T154-2-fwd	TTGTTTTTACCAGCGCGNNSGGTGGTCGTCCGGATC	36	84.6
NNS-T154-2-rev	ATCCGGACGACCACCSNNCGCGCTGGTAAAAACAAC	36	83.4
T7 term	CTAGTTATTGCTCAGCGGT	19	54.5

2.2. Methods

2.2.1. Molecular and microbiological methods

2.2.1.1. Bacterial cell growth

Escherichia coli cells were grown in 2×YT (16 g/L tryptone, 10 g/L yeast extract, 5 g/L NaCl), LB (10 g/L tryptone 5g/L, 5 g/L yeast extract,10 g/L NaCl) or TB medium (4 mL/L glycerol, 12 g/L peptone, 24 g/L yeast extract, K_2HPO_4 0.072 M, KH_2PO_4 0.019 M). After sterilization of the culture media by autoclaving, antibiotics were added (50 mg/L kanamycin for cells expressing HheG, or 100 mg/L ampicillin in the case of cells expressing *Me*HNL). Agar plates were prepared adding agar-agar (15 g/L) to the medium before autoclaving.

2.2.1.2. Transformation of chemically competent *E. coli* cells

Chemically competent *E. coli* DH5α and BL21 (DE3) Gold cells were prepared according to the method described by Hanahan [214]. 50 µL aliquots of chemically competent cells were transformed adding 50-100 ng of vector DNA. After incubating the mixture on ice for 30 minutes, heat shock was performed for 60 s at 42 °C, followed by a 2-minute incubation in ice. 1 mL SOC medium (10 g/L tryptone, 5 g/L yeast extract, 2 g/L KCl, 2 g/L NaCl, 10 mM $MgCl_2$, 10 mM $MgSO_4$, 20 mM glucose) was subsequently added and the mixture was incubated for 1 h at 37 °C for cell recovery. Finally, in the case of *E. coli* DH5α cells, 900 µL of the cell culture was centrifuged (900 g, 4 °C, 5 minutes, Heraeus Fresco 21 Microcentrifuge, Fisher Scientific), flipped over to discard

the supernatant and the pellet was gently resuspended in the remaining supernatant before plating it onto an LB agar plate containing 50 mg/L kanamycin, using sterile glass beads. In the case of *E. coli* BL21 (DE3) Gold cells, 50 µL of the culture was diluted 10× with sterile Milli-Q® water and 100 µL was plated onto an LB agar plate containing 50 mg/L kanamycin, using sterile glass beads.

2.2.1.3. Polymerase chain reaction (PCR) – Preparation of SSM library of HheG

The PCR is an essential molecular biology technique that allows for rapid amplification of selected DNA sequences. Depending on the primers used and the composition of the reaction buffer, this technique has different applications [215,216]. In this project, PCR was used to perform site-saturation mutagenesis at residue Thr154 of HheG, using the QuikChange PCR method. The SSM library was prepared using *PfuUltra* II Hotstart PCR Master Mix from Agilent Technologies. 20 µL of parental pET-28a(+)-HheG template DNA solution (1 ng/µL) and each 2.5 µL of the respective forward and reverse primers (NNS-T154-1-fwd and NNS-T154-1-rev or NNS-T154-2-fwd and NNS-T154-2-rev) solutions (10 µM) were added to 25 µL *PfuUltra* II Hotstart Master Mix. Table 4 lists the used temperature program.

Table 4: Temperature program used in the thermocycler for the QuikChange PCR.

Step	Temperature (°C)	Time (min)	Cycles
1	95	2	1
2	95	0.5	25
3	55	1	
4	68	9 (1.5 min/kb)	
5	68	10	1

Afterwards, 1 µL *DpnI* (20 U) was added and the mixture was incubated for 1 h at 37 °C to digest the parental DNA. An agarose gel was run with the PCR product to confirm the presence of one single band from the desired PCR product. Chemically competent *E. coli* DH5α cells were transformed with 5 µL of the PCR mixture and plated on LB agar plates containing kanamycin as described in section 2.2.1.2. After picking four single colonies for sequencing, all colonies were resuspended in LB medium containing 5 mg/L kanamycin using a sterile glass hook spatula and transferred to a sterile tube for overnight culture in a total of 5 mL kanamycin-containing LB medium. After plasmid isolation, the quality of the library was confirmed by sequencing (Eurofins Genomics LLC, Ebersberg, Germany). The DNA concentration was determined using a NanoPhotometer NP80 (Implen GmbH, Munich, Germany). Chemically competent *E. coli* BL21 (DE3) Gold cells were then transformed with the isolated plasmid DNA and plated on LB agar plates containing kanamycin as described in section 2.2.1.2. Finally, single colonies were picked

and transferred to a microtiter plate (MTP) containing 150 µL of LB medium complemented with 50 mg/L kanamycin per well. As controls, *E. coli* BL21 (DE3) Gold clones containing the wild-type HheG gene were transferred to wells A1 and D7 and clones containing empty vector (EV) were transferred to wells E6 and H12. Cells were incubated at 37 °C, 800 rpm overnight in an MTP shaker. A master plate was prepared by adding 28 µL of 60% glycerol solution to each well (final concentration of glycerol is 10%) after overnight incubation, and the plate was stored at -80 °C.

2.2.1.4. Agarose gel electrophoresis

Agarose gel electrophoresis is a common molecular biology technique for separation and visualization of DNA fragments by applying an electric field. Agarose gel electrophoresis was employed for visualization of the PCR product after *DpnI* digestion (see section 2.2.1.3.). For the preparation of the gel, 0.8% agarose was dissolved in TAE buffer (40 mM Tris-HCl, 2 mM acetic acid, 1 mM EDTA at pH 8.5) by microwave heating. Midori Green Direct (Nippon Genetics EUROPE GmbH, Düren, Germany) was diluted 10× with 6× DNA Gel Loading Dye (Fisher Scientific). DNA samples, as well as the marker (GeneRuler 1kb DKA Ladder from Fisher Scientific) were mixed 5:1 with the diluted Midori Green Direct and 6 µL were loaded on the gel. DNA fragments were separated based on molecular weight applying an electric field of 105 V for 40 minutes, using TAE as running buffer.

2.2.2. Biochemical methods

2.2.2.1. Heterologous expression of proteins in E. coli

*Me*HNL expression in shake flasks

Hydroxynitrile lyase from *Manihot esculenta* was heterologously expressed in *E. coli.* K12 Top 10F' harboring the pSE420-MeHNL plasmid. 2×YT medium (100 mL, containing 100 µg/mL ampicillin) was inoculated from a glycerol stock (10 µL) and the culture was incubated overnight at 37 °C, 200 rpm. A 5 mL aliquot of this preculture (OD_{600} = 4.4) was used to inoculate 2×YT medium (500 mL, containing 100 µg/mL ampicillin), and the new culture was grown at 37 °C, 200 rpm. At an optical density at 600 nm (OD_{600}) of 0.8, IPTG was added to a final concentration of 0.1 mM and the culture was further incubated at 18 °C, 160 rpm for 48 h. To follow the protein expression, samples were taken 0.5, 24 and 48 hours after induction and their OD_{600} was measured in a Cary 60 UV-Vis Spectrophotometer (Agilent Technologies). Samples corresponding to an OD_{600} = 2 were centrifuged and the pellets were stored at -20 °C.

48 h after induction, cells were harvested by centrifugation at 4000 g, 4 °C for 10 minutes (Heraeus Multifuge X3R Centrifuge, Fisher Scientific), washed with sodium acetate buffer pH 5.8

(25 mM), and centrifuged again (4000 g, 4 °C for 30 minutes). Cell pellets were resuspended in sodium acetate buffer pH 5.8 (25 mM) (4 mL per g of wet cells), and 10 mL aliquots were sonicated at 4 °C using a Fisherbrand™ Model 120 Sonic Dismembrator (Fisher Scientific) at 60% amplitude, 2 s pulse, 5 s pause for 7 minutes. The resulting crude extract was centrifuged to remove cell debris (18500 g, 4 °C for 45 minutes) and the obtained cell-free extract was stored at −20 °C. Concentration of cell-free extract was performed in an Amicon Ultra Filter Device (Merck KGaA) with 10 kDa cut-off at 4 °C.

HheG expression in deep-well plates

Both wild-type HheG and the SSM library mutants of HheG were heterologously expressed in *E. coli.* BL21 (DE3) Gold harboring pET-28a(+)-hheG or pET-28a(+)-hheG(NNS-T154) vectors, respectively. 2 mL polypropylene deep-well plates (DWP) (HJ-BIOANALYTIK GmbH, Erkelenz, Germany) containing each 100 µL of TB medium (50 mg/L kanamycin) per well were inoculated from the master plate and incubated overnight at 37 °C and 800 rpm, covered with a breathable seal. Expression was induced by addition of 1.2 mL of TB containing kanamycin (50 mg/L) and 0.2 mM IPTG per well. The DWP was incubated at 22 °C for 24 h. For the expression test, samples were taken 3.5, 7, 24 and 48 hours after induction and their OD_{600} was measured in a Cary 60 UV-Vis Spectrophotometer (Agilent Technologies). Samples corresponding to an OD_{600} = 2 were centrifuged (Heraeus Fresco 21 Microcentrifuge) and the pellets were stored at -20 °C.

2.2.2.2. SDS-PAGE

Sodium dodecyl sulfate polyacrylamide gel electrophoresis allows for the separation of proteins depending on their molecular weight by applying an electric current in a gel under denaturing conditions [217]. SDS denatures the proteins and acts as a surfactant, homogenizing the charges around the protein and, thus, allowing for it to be separated according to its molecular weight. The gel is composed of an initial stacking gel with low acrylamide content (6% v/v) and low pH, which allows for the concentration of the proteins in a narrow front, so that they are later separated in the resolving gel, containing a higher amount of acrylamide (12% v/v) and higher pH (see detailed composition in Table 5). Evaluation of the protein expression of *Me*HNL and WT HheG was performed by SDS-PAGE. Cell pellet-containing samples taken at different time points during expression (normalized to an OD_{600} = 1 or OD_{600} = 2) were lysed by incubating the pellets for 15 minutes at room temperature after addition of 20 µL or 40 µL of B-PER™ Bacterial Protein Extraction Reagent (Fisher Scientific). After centrifugation (21100 g, 4 °C for 5 minutes in Heraeus Fresco 21 Microcentrifuge), the supernatant was separated and both pellet and cell-free extract were analysed on SDS-PAGE. Pellets were resuspended in 40 µL of Milli-Q® water and both

CFE and pellet were diluted 4×. Diluted samples (15 µL) were mixed with 5 µL of loading dye (50 mM Tris HCl pH 6.8, 10 % (v/v) glycerol, 4 % (w/v) SDS, 0.03 % (w/v) bromophenol blue and 15 mg/mL DTT) and incubated at 95 °C for 10 minutes. 7 µL samples were loaded on each well and the gel was run in a Mini PROTEAN® Electrophoresis System (Bio-Rad, Feldkirchen, Germany). For molecular weight determination Unstained Protein Molecular Weight Marker (Fisher Scientific) was loaded on one well. Initially, a field of 80 V was used to stack the proteins, followed by 120 V for separation. Finally, the gels were stained with staining solution (500 mL/L methanol, 100 mL/L acetic acid, 400 mL/L Milli-Q® water, 1 g/L Coomassie Brilliant Blue R-250) for 1 h and destained with protein destaining solution (300 mL/L ethanol, 100 mL/L acetic acid, 600 mL/L Milli-Q® water) overnight.

Table 5: Composition of stacking and resolving gel used for SDS-PAGE in this project. Amounts are given in mL.

Component	Stacking gel (6% acrylamide)	Resolving gel (12% acrylamide)
Milli-Q® water	1.5	2.25
Acrylamide (40%)	0.375	1.5
1.5 M Tris-HCl (pH 8.8) 0.4% SDS	-	1.25
1.5 M Tris-HCl (pH 6.8) 0.4% SDS	0.625	-
10% APS	0.025	0.05
TEMED	0.0025	0.005

2.2.2.3. Screening of SSM libraries

For the screening of the SSM libraries of HheG at position T154 and at position T195, pre-cultures in deep-well plates, containing 100 µL of TB medium supplemented with 50 mg/L kanamycin per well, were inoculated from the frozen master plates (see section 2.2.1.3. for library at T154; master plate for SSM library at position T195 was prepared by Janine Mayer during her master thesis). Expression was carried out as described in section 2.2.2.1., 24 hours after induction the plates were centrifuged at 2770 g, 4 °C for 10 minutes, and the pellets were stored at -20 °C overnight. The substrate solution was prepared freshly before the reaction by mixing cyclohexene oxide (1M) in DMSO (220 µL), NaCN (2 M) in aqueous NaOH (1 mM, 220 µL) and phosphate buffer pH 8.0 (50 mM, 21.56 mL). The cell pellets were thawed and resuspended in each 200 µL of substrate solution by covering the DWP with an aluminum foil seal and quickly vortexing inside the fumehood. The plates were incubated at room temperature, 800 rpm for 5 h 30 min. After the reaction, 400 µL of *t*BME containing 0.1% of n-octanol as internal standard was added to each well. The DWP was covered with a PTFE-coated silicone cover mat, tightly secured by placing an MTP on top and holding everything with tape to avoid the silicone mat from detaching due to the pressure build-up. Then the DWP was vortexed in order to extract the

remaining cyclohexene oxide and formed 2-cyanohexanol into the organic phase. After centrifugation at 2770 g, 4 °C for 2 minutes for phase separation, the organic phase of each well was transferred to a new MTP plate and dried over anhydrous $MgSO_4$, and roughly 150 µL was transferred to a GC vial with insert.

2.2.2.4. Enzyme activity determination

The enzymatic activities of free *Me*HNL and free *Pa*HNL5-L1Q/A111G were measured following the cleavage of racemic mandelonitrile into benzaldehyde and HCN, according to a literature procedure [218]. Samples were prepared by diluting the *Me*HNL cell-free extract or the *Pa*HNL5-L1Q/A111G supernatant in phosphate buffer pH 6.5 (5 mM). The enzymatic activity of immobilized *Me*HNL was determined following the hydrocyanation of 4-anisaldehyde (100 mM) using 6.5 equivalents of HCN in diisopropyl ether at 20 °C, 800 rpm. A negative control was performed using the enzyme support instead. Samples were analyzed by chiral HPLC.

The enzymatic activity of CALA was measured according to a modified literature procedure following the hydrolysis of tributyrin in phosphate buffer at pH 7 [219]. The resulting butyric acid was titrated with sodium hydroxide (0.1 M), and the consumption of the latter was recorded as a function of time. The enzymatic activity of immobilized CALA was determined following the hydrolysis of 4-nitrophenyl butyrate (1.67 mM) in a 1:5 mixture of acetonitrile and phosphate buffer pH 7.4 (50 mM). A calibration curve of the product 4-nitrophenol was used to calculate the reaction rate based on the absorbance of the reaction mixture at 410 nm.

2.2.3. Enzyme immobilization

General procedure for *Me*HNL: In a 5 mL glass vial containing a magnetic stirring bar and the carrier (100 mg), *Me*HNL-containing cell-free extract previously adjusted to pH 5 (40 µL) was added dropwise while stirring. The mixture was stirred for 30 minutes and was then dried at room temperature under high vacuum for 48 hours.

Immobilization of CALA: CALA (30 g, 880 U), Relizyme EXE309 (30 g), and demineralized water (30 mL) were mixed in a 100 mL bottle. The pH was adjusted to 6 with a solution of sodium hydroxide (2 M) and the mixture was incubated overnight at room temperature in an orbital shaker. After filtering the solution, the activity of the supernatant was measured and compared to the initial activity of the enzyme solution before immobilization, giving an immobilization yield of 84%. The immobilized enzyme was washed several times with demineralized water and dried at room temperature under high vacuum for 48 hours.

CALA-D122L (50 mg, 12U), Relizyme EXE309 (300 mg), and demineralized water (600 µL) were mixed in a 5 mL glass vial. The same procedure as for WT CALA was followed, resulting in an immobilization yield of 89%.

2.2.4. Optimization of the enzymatic hydrocyanation and benzoylation reactions and their combination in a concurrent cascade

Unless otherwise noted, all reactions catalyzed by *Pa*HNL5-L1Q/A111G, *Me*HNL and/or CALA were performed in 1.5 mL glass vials in an orbital shaker at 800 rpm and 20 °C.

2.2.4.1. Solvent selection for MeHNL- and *Pa*HNL5-L1Q/A111G-catalyzed reactions

4-Anisaldehyde (530 mM) in diisopropyl ether or *tert*-butyl methyl ether (150 µL), HCN (800 mM) in diisopropyl ether or *tert*-butyl methyl ether (650 µL), citrate buffer pH 4 (500 mM, 200 µL), and *Me*HNL-containing cell-free extract (33.2 µL, 5 U) or *Pa*HNL5-L1Q/A111G-containing supernatant (36.8 µL, 5 U) were incubated at 20 °C. Samples (20 µL) were taken from the upper organic phase after 4 and 18 h and analyzed by HPLC.

2.2.4.2. pH effect on MeHNL and *Pa*HNL5-L1Q/A111G – general procedure

4-Anisaldehyde (530 mM) in diisopropyl ether (188 µL), HCN (800 mM) in diisopropyl ether (812 µL), citrate buffer pH 3.5 – 5.5 (500 mM, 200 µL), and *Me*HNL-containing cell-free extract (33.2 µL, 5 U) or *Pa*HNL5-L1Q/A111G-containing supernatant (36.8 µL, 5 U) were incubated at 20 °C. Reactions were performed in duplicate. Additionally, non-enzymatic hydrocyanation reactions were performed following the same procedure, without addition of the enzymes, using buffer at pH 4, 4.5, 5 and 5.5. Samples (20 µL) were taken from the upper organic phase at different time points and analyzed by HPLC.

2.2.4.3. Screening of free hydrolases – hydrolysis test

A total of 41 hydrolase preparations were evaluated in a hydrolysis test. In a 10 mL glass vial containing (±)-4-methoxymandelonitrile benzoate (20 mM) in diisopropyl ether (1 mL) and potassium phosphate buffer pH 7 (100 mM, 1 mL), 50 mg or 50 µL of enzyme was added. The reaction mixture was incubated at room temperature, 800 rpm for 18 h. Samples (20 µL) were analyzed in chiral HPLC.

2.2.4.4. Screening of immobilized hydrolases – DKR test

To a 10 mL glass vial containing 1 g of 3 Å molecular sieves, a solution of 4-anisaldehyde (100 mM) and HCN (1 M) in diisopropyl ether (4 mL) was added. The reaction was stirred at room

temperature, 800 rpm for 20 h. Afterwards, the immobilized lipase (100 mg) was added, together with vinyl benzoate (150 µL, 1.1 mmol) and the mixture was stirred for 4 hours. Samples (20 µL) were analyzed in chiral HPLC.

2.2.4.5. Benzoyl donor screening

To a vial containing immobilized CALA (4.2 mg, 0.46 U), racemic 4-methoxymandelonitrile (200 mM) in diisopropyl ether (250 µL) and benzoyl donor (300 mM) in diisopropyl ether (500 µL) was added. Reactions were performed in duplicate and were incubated at 25 °C. Samples (20 µL) were taken after 4, 20, and 27.5 hours and analyzed by HPLC. The enantioselectivity of the enzyme was calculated according to the method of Chen *et al.* for conversion values between 5 and 20% [220]. The same procedure was followed for the benzoyl donor screening of CALA-D122L.

2.2.4.6. Temperature effect on MeHNL

4-Anisaldehyde (530 mM) in diisopropyl ether (188 µL), HCN (800 mM) in diisopropyl ether (812 µL), citrate buffer pH 5 (500 mM, 125 µL), and *Me*HNL-containing cell-free extract (33.2 µL, 5 U) were incubated at 5, 10, and 20 °C. Reactions were performed in duplicate and a negative control reaction was performed for each temperature value, where no enzyme was added. Samples (20 µL) were taken from the upper organic phase after 6, 22, and 75 h and analyzed by HPLC.

2.2.4.7. Temperature effect on CALA

To a vial containing CALA on Relizyme EXE309 (2 mg, 0.22 U), (±)-4-methoxymandelonitrile (195 mM) in diisopropyl ether (125 µL) and phenyl benzoate (300 mM) in diisopropyl ether (250 µL) was added. The mixture was incubated at 5, 10, and 25 °C. Reactions were performed in duplicate. Samples (20 µL) were taken after 3, 7, 21, and 46 hours and analyzed by HPLC. The same procedure was followed for the benzoyl donor screening of CALA-D122L.

2.2.4.8. Comparison of WT CALA and CALA-D122L – Evaluation of chemoselectivity

To a vial containing CALA on Relizyme EXE309 (2 mg) or CALA-D122L on Relizyme EXE309 (4 mg), (±)-4-methoxymandelonitrile (195 mM) in diisopropyl ether (125 µL) and phenyl benzoate (300 mM) in diisopropyl ether (250 µL) was added. The mixture was incubated at 25 °C. Reactions were performed in duplicate. Samples (20 µL) were taken after 1, 2, 4, 7 and 23 hours and analyzed by HPLC.

2.2.4.9. Evaluation of the MeHNL immobilisates

To a vial containing *Me*HNL immobilisate (15 mg) and $Na_2HPO_4 \cdot 2H_2O$ (30 mg, 0.17 mmol), a solution of 4-anisaldehyde (100 mM) and HCN (650 mM) in diisopropyl ether (500 µL) was added. Negative controls for the silica- and Celite-supported enzyme were performed in parallel adding 15 mg of the carrier instead of the immobilized *Me*HNL. The reactions were incubated at 20 °C in an orbital shaker at 800 rpm. Samples (20 µL) were analyzed by HPLC.

2.2.4.10. Effect of Na_2HPO_4 salt hydrates on chemical hydrocyanation

To a solution of 4-anisaldehyde (100 mM) and HCN (650 mM) in diisopropyl ether (1 mL), anhydrous Na_2HPO_4 (70 mg, 0.5 mmol), $Na_2HPO_4 \cdot 2H_2O$ (85 mg, 0.5 mmol), or $Na_2HPO_4 \cdot 7H_2O$ (134 mg, 0.5 mmol) was added. Reactions were performed in duplicate and a control reaction without salt was run in parallel. The amount of salt added is based on the maximum solubility of water in diisopropyl ether (0.55 wt%) [221] and the water capacity of the $Na_2HPO_4/Na_2HPO_4 \cdot 2H_2O$ salt pair (11.2 mmol/g) [222]. Reactions were stopped after 24 hours and analyzed by HPLC.

2.2.4.11. Effect of a_w on MeHNL

To a vial containing *Me*HNL immobilized on Celite R-633 (12 mg, 0.36 U), a solution of 4-anisaldehyde (90 mM) and HCN (590 mM) in diisopropyl ether (550 µL) was added, together with either anhydrous Na_2HPO_4 (35 mg, 0.25 mmol), $Na_2HPO_4 \cdot 2H_2O$ (42 mg, 0.25 mmol) or $Na_2HPO_4 \cdot 7H_2O$ (67 mg, 0.25 mmol). Reactions were performed in duplicate. Samples (20 µL) were taken after 5 and 24 hours and analyzed by HPLC.

2.2.4.12. Effect of a_w on CALA

To a vial containing CALA immobilized on Relizyme EXE309 (4 mg, 0.44 U), a solution of (±)-4-methoxymandelonitrile (100 mM) and vinyl benzoate (300 mM) in diisopropyl ether (500 µL) was added, together with either anhydrous Na_2HPO_4 (35 mg, 0.25 mmol), $Na_2HPO_4 \cdot 2H_2O$ (42 mg, 0.25 mmol), or $Na_2HPO_4 \cdot 7H_2O$ (67 mg, 0.25 mmol). Samples (20 µL) were taken after 6, 22, and 30 hours and analyzed by HPLC.

2.2.4.13. Effect of phenol and phenyl benzoate on MeHNL

To a solution of 4-anisaldehyde (100 mM) and HCN (600 mM) in diisopropyl ether (670 µL), *Me*HNL on Celite R-633 (8 mg, 0.24 U) and either phenol (18.8 mg, 200 µmol) or phenyl benzoate (39.6 mg, 200 µmol) were added. A control was performed without addition of phenol or phenyl benzoate. Samples (20 µL) were taken after 17 and 22 hours and analyzed by HPLC.

2.2.4.14. Effect of 4-anisaldehyde and HCN on CALA

To a solution of (±)-4-methoxymandelonitrile (65 mM) and phenyl benzoate (200 mM) in diisopropyl ether (375 µL), CALA on Relizyme EXE309 (2 mg, 0.22 U) and either 4-anisaldehyde (200 mM) in diisopropyl ether (160 µL) or HCN (700 mM) in diisopropyl ether (160 µL) were added. Reactions were performed in duplicate and a control was performed adding diisopropyl ether (160 µL) instead of the hydrocyanation reagents. The reactions were incubated at 25 °C. Samples (20 µL) were taken after 3, 7, 21, 29, and 46 hours and analyzed by HPLC.

2.2.4.15. Effect of benzoic acid on MeHNL

To a vial containing *Me*HNL on Celite R-633 (15 mg, 0.45 U) and benzoic acid (1.5 mg, 12 µmol; 3 mg, 25 µmol; or 6 mg, 50 µmol), a solution of 4-anisaldehyde (100 mM), HCN (650 mM), and mesitylene (100 mM) (internal standard) in diisopropyl ether (500 µL) was added. A control was performed without addition of benzoic acid. Samples (20 µL) were analyzed by HPLC.

2.2.4.16. Effect of benzoic acid on CALA

To a solution of (±)-4-methoxymandelonitrile (100 mM), phenyl benzoate (300 mM) and mesitylene (100 mM) (internal standard) in diisopropyl ether (350 µL), CALA on Relizyme EXE309 (2 mg, 0.22 U), and $Na_2HPO_4 \cdot 2H_2O$ (30 mg, 0.17 mmol), benzoic acid (70 mM) in diisopropyl ether (150 µL, 1 equivalent) were added. A control was performed adding diisopropyl ether (150 µL) instead of benzoic acid solution. Samples (20 µL) were analyzed by HPLC.

2.2.4.17. Effect of HCN equivalents on immobilized MeHNL

To a vial containing *Me*HNL immobilized on Celite R-633 (4.3 mg, 6 U), a solution of 4-anisaldehyde (187 mM) and mesitylene (100 mM) in diisopropyl ether (267 µL) was added. To this mixture, HCN (1.4 M) in diisopropyl ether (107, 143, 178 or 233 µL) and diisopropyl ether (126, 90, 55 or 0 µL) was added respectively, for a total number of HCN equivalents of 3, 4, 5 or 6.5, and the reactions were incubated at 20 °C, 800 rpm. Reactions were performed in duplicate. Samples (20 µL) were taken after 5 and 24 hours and analyzed by HPLC.

2.2.4.18. Effect of HCN equivalents on non-immobilized MeHNL

4-Anisaldehyde (303 mM) in diisopropyl ether (165 µL), citrate buffer pH 5 (500 mM, 30 µL), and *Me*HNL-containing cell-free extract (30 µL, 7.5 U) were added to a vial. To this mixture, HCN (970 mM) in diisopropyl ether (103, 155, 206 or 258 µL) and diisopropyl ether (232, 180, 129 or 77 µL) was added respectively, for a total number of HCN equivalents of 2, 3, 4 or 5, and the

reactions were incubated at 20 °C, 800 rpm. Samples (20 µL) were taken from the upper organic phase after 1, 2, 4, 8.5 and 27 hours and analyzed by HPLC.

2.2.4.19. General procedure for the cascade synthesis of (S)-4-methoxymandelonitrile benzoate

To a vial containing *Me*HNL on Celite R-633 and CALA on Relizyme EXE309, $Na_2HPO_4 \cdot 2H_2O$ (30 mg, for experiments 1-3, Table 9) was added. A solution of 4-anisaldehyde (360 mM) and mesitylene (360 mM) (internal standard) in diisopropyl ether (140 µL) and HCN (900 mM) in diisopropyl ether (360 µL) was subsequently added. To this mixture, phenyl benzoate (2-4 equivalents) was added (in case of experiments 7 and 8 from Table 9, 1 equivalent was added each time at t = 0, after 24 hours and after 46 hours) and the reactions were incubated at 10, 20, or 25 °C. Negative control reactions without enzyme addition were performed in parallel. Reactions were performed in duplicate and 20 µL samples were analyzed by HPLC.

2.2.5. Hydrogenation reactions

2.2.5.1. Pretreatment of catalysts

When mentioned, Ni@Al_2O_3/SiO_2 65% and Rh@Al_2O_3 5% were preactivated overnight at 120 °C under 10 bar of H_2 in diisopropyl ether. Unless otherwise noted, Raney catalysts were washed 2× with Milli-Q® water, then 2× with ethanol and finally 2× with the reaction solvent.

2.2.5.2. General procedure for the hydrogenation of (±)-3 at room temperature under 1 bar of H_2 - Initial catalyst screening

In a 4 mL glass vial with septum cap containing a magnetic stirring bar, the catalyst was weighed. A solution (2 mL) containing 19 mM (±)-4-methoxymandelonitrile benzoate, **3,** (38 µmol) and 20 mM mesitylene (40 µmol, internal standard) in dioxane or diisopropyl ether was added and, after flushing with N_2, the gas was replaced with H_2 using a balloon. Finally, the balloon was refilled with H_2 and the reactions were stirred at 350 rpm at room temperature (25 °C) for 24 h. Samples (20 µL) were analyzed by HPLC.

2.2.5.3. Hydrogenation of 3 in an autoclave reactor

General procedure for the hydrogenation of (±)-3

To a stainless-steel reactor (Büchi tinyclave) provided with a Teflon vessel with 10 mL maximum capacity and a magnetic stirring bar, a solution (3.5 mL) containing 21.7 mM (±)-**3** (76 µmol) and 22.9 mM mesitylene (80 µmol, internal standard) in diisopropyl ether was added. The

pretreated catalyst was subsequently added, together with diisopropyl ether (0.5 mL). The autoclave was then tightly closed and flushed with four cycles of N_2-vacuum. Finally, it was pressurized with 5 or 10 bar of H_2, introduced in a preheated oil bath and stirring was set to 600 rpm. After the selected reaction time, the autoclave was removed from the oil bath and allowed to cool for 20 minutes. The reactor was then de-pressurized and dioxane was added to dissolve all species, since formation of crystals was observed. Samples (20 µL) were analyzed by HPLC.

Hydrogenation of (R)-3

To a stainless-steel reactor (Büchi tinyclave) provided with a Teflon vessel with 10 mL maximum capacity and a magnetic stirring bar, a solution (3.5 mL) containing 21.7 mM (*R*)-**3** (76 µmol) and 22.9 mM mesitylene (80 µmol) in dioxane was added. Pretreated Raney Ni was subsequently added, together with dioxane (0.5 mL). The autoclave was then tightly closed and flushed with four cycles of N_2-vacuum. Finally, it was pressurized with 5 bar of H_2, introduced in an oil bath preheated to 100 °C and stirring was set to 600 rpm. After 2.5 h, the autoclave was removed from the oil bath and allowed to cool for 20 minutes. The reactor was then de-pressurized and dioxane was added to dissolve all species. Samples (20 µL) were analyzed by HPLC.

2.2.5.4. Stability of tembamide under hydrogenating conditions in an autoclave reactor

To a stainless-steel reactor (Büchi tinyclave) provided with a Teflon vessel with 10 mL maximum capacity and a magnetic stirring bar, a solution (3.5 mL) containing 4.6 mM (±)-tembamide (16 µmol) and 22.9 mM mesitylene (80 µmol) in diisopropyl ether was added. (±)-Tembamide was prepared before, following the procedure described in section 2.2.5.3. for the hydrogenation of (±)-**3** at 100 °C, under 5 bar H_2 using pretreated Raney Ni as catalyst, and further purified using column chromatography (ethyl acetate/n-heptane). Pretreated Ni@Al_2O_3/SiO_2 65% (5 mg) was subsequently added, together with diisopropyl ether (0.5 mL). For the control reaction, only diisopropyl ether (0.5 mL) was added. The autoclave was then tightly closed and flushed with four cycles of N_2-vacuum. Finally, it was pressurized with 5 bar of H_2, introduced in an oil bath preheated to 100 °C and stirring was set to 600 rpm. After 2 h, the autoclave was removed from the oil bath and allowed to cool for 20 minutes. The reactor was then de-pressurized and dioxane was added to dissolve all species. Samples (20 µL) were analyzed by HPLC.

2.2.5.5. Evaluation of the effect of HCN on the hydrogenation of (±)-3 in an autoclave reactor

In a 25 mL glass reactor (Büchi tinyclave) provided with a magnetic stirring bar, a solution (4 mL) containing 23.8 mM (±)-**3** (95 µmol) and 25.0 mM mesitylene (100 µmol) in diisopropyl ether was added. Pretreated Raney Ni was subsequently added, together with diisopropyl ether (0.5 mL) and, finally, 1.2 M HCN in diisopropyl ether (0.5 mL, 0.6 mmol) was added. For the control reaction, diisopropyl ether (0.5 mL) was added instead of the HCN solution. The autoclave was then tightly closed and flushed with four cycles of N_2-vacuum. Finally, it was pressurized with 5 bar of H_2, introduced in a steel cage and in an oil bath preheated to 70 °C and stirring was set to 600 rpm. After 1 h, the autoclave was removed from the oil bath and allowed to cool for 20 minutes. The reactor was then de-pressurized and dioxane was added to dissolve all species. Samples (20 µL) were analyzed by HPLC.

2.2.6. Preparative synthesis of (S)-tembamide

In a 100 mL round-bottomed flask provided with a magnetic stir bar, immobilized *Me*HNL (190 mg, 0.03 U/mg) and immobilized CALA (137 mg, 0.11 U/mg) were weighed. Subsequently, a solution (22 mL) containing 100 mM 4-anisaldehyde (2.2 mmol), 650 mM HCN (14.3 mmol) and 50 mM mesitylene (1.1 mmol, internal standard) was added. Finally, phenyl benzoate (440 mg, 2.2 mmol, 1 equivalent) was added at the beginning of the reaction, after 24 h and after 48 h (total of 3 equivalents). The mixture was stirred at 300 rpm and room temperature. The reaction was followed by HPLC and was stopped after 136 h, affording (*S*)-4-methoxymandelonitrile benzoate in 80% HPLC yield and 99% e.e. The mixture was then centrifuged (4000 g, 4 °C for 15 minutes) and the volatiles of the clear solution were evaporated using a rotary evaporator.

The crude reaction mixture from the biocatalytic step was re-dissolved in diisopropyl ether (93 mL) and introduced in a stainless-steel reactor (Büchi miniclave) provided with a Teflon vessel with 300 mL maximum capacity, containing a magnetic stirring bar. Raney Ni slurry (1 mL) was centrifuged and the aqueous phase was removed. After adjusting the moist weight, the catalyst (224 mg) was added together with diisopropyl ether (1 mL) to the reactor. The autoclave was then tightly closed and flushed with four cycles of N_2-vacuum. Finally, it was pressurized with 5 bar of H_2, introduced in an oil bath preheated to 100 °C and stirring was set to 600 rpm. After 1.5 h, the autoclave was removed from the oil bath and allowed to cool for 20 minutes. The reactor was then de-pressurized and dioxane was added to dissolve all species. A sample (20 µL) analyzed by HPLC showed that (*S*)-tembamide was synthetized with 32% yield and 98% e.e. The solvents were then evaporated using a rotary evaporator. Column chromatography purification using an eluent

mixture of ethyl acetate and n-heptane (gradient starting with 1:2 ratio and finishing with 1:1 ratio) followed by recrystallization of the enriched fractions (1:9 mixture of ethyl acetate and n-heptane) afforded 91 mg of pure colorless (*S*)-tembamide crystals (isolated overall yield of 15%). The purity of the crystals was confirmed using ^{1}-H and ^{13}C-NMR (300 MHz, crystals dissolved in deuterated DMSO).

^{1}H NMR (300 MHz, DMSO-d_6): δ [ppm] = 3.25–3.34 (1H, m, CH_2), 3.40–3.49 (1H, m, CH_2), 3.73 (3H, s, OCH_3), 4.72 (1H, dt, J = 7.5 Hz, 4.8 Hz, CH-OH), 5.41 (1H, d, J = 4.5 Hz, OH), 6.89 (2H, d, J = 8.7 Hz, Ar-m), 7.28 (2H, d, J = 8.7 Hz, Ar-o), 7.45 (2H, t, J = 6.9 Hz, Ar-m'), 7.51 (1H, tt, J = 6.9 Hz, 1.5 Hz, Ar-p'), 7.83 (2H, dd, J = 6.9 Hz, 1.5 Hz, Ar-o'), 8.47 (1H, t, J = 5.4 Hz, NH). ^{13}C-NMR (300 MHz, DMSO-d_6): δ [ppm] = 47.6, 54.9, 70.6, 113.3, 127.0, 127.1, 128.1, 130.9, 134.5, 135.7, 158.2, 166.2.

2.2.7. Analytical methods

2.2.7.1. HPLC analysis

The quantification of 4-anisaldehyde, (*S*)- and (*R*)-4-methoxymandelonitrile, (*S*)- and (*R*)-4-methoxymandelonitrile benzoate, (*S*)- and (*R*)-tembamide and benzoic acid was achieved using chiral normal phase HPLC. Samples were diluted to a final mesitylene concentration of 1 mM with an 8:2 v/v mixture of n-heptane and isopropanol, and dried over anhydrous $MgSO_4$. Analysis was performed using a Hitachi Elite LaChrom HPLC system, consisting of a VWR Hitachi L-2130 pump, L-2200 auto-sampler, L-2350 column oven, L-2400 UV detector using a D_2 lamp, coupled to a Hitachi organizer module. Separation was achieved on a Chiralpak AD-H column (250 mm × 4.6 mm × 5 µm; Daicel, Japan), using n-heptane/isopropanol 82:18 v/v at a flow rate of 0.65 mL/min. The column oven temperature was set at 35 °C and a detection wavelength of 225 nm was chosen. Under these conditions, the compounds were separated with the following retention times: mesitylene (internal standard) 5.0 min, benzoic acid 6.7 min, phenol 7.0 min, phenyl benzoate 7.3 min, 4-anisaldehyde (**1**) 8.3 min, (*S*)-4-methoxymandelonitrile {(*S*)-**2**} 9.6 min, (*R*)-4-methoxymandelonitrile {(*R*)-**2**} 10.5 min, (*S*)-4-methoxymandelonitrile benzoate {(*S*)-**3**} 13.1 min, (*R*)-4-methoxymandelonitrile benzoate {(*R*)-**3**} 13.9 min, (*S*)-tembamide {(*S*)-**4**} 16.4 min and (*R*)-tembamide {(*R*)-**4**} 17.4 min.

In samples were quantification of benzoic acid was not possible due to the nearness of the phenol peak (usually all except for hydrogenation reactions), benzoic acid was quantified using achiral reverse phase HPLC. Samples from reaction mixtures were diluted 50× with acetonitrile/water 1:1 v/v. Analysis was performed using a Shimadzu Nexera XR HPLC system equipped with a DGU-20A5R degassing unit, coupled to two LC-20AD solvent delivery units, a SIL-

20AC Autosampler, a CTO-20A column oven, an SPD-20A UV/VIS detector using a D_2 lamp, and a CBM-20A system controller. Separation was achieved on a Nucleoshell RP 18 column (150 mm × 3 mm × 2.7 µm; Macherey-Nagel, Düren, Germany) at 30 °C, 0.7 mL/min flow rate using Milli-Q® water containing 0.1% trifluoroacetic acid (solvent A) and acetonitrile (solvent B) as mobile phase and UV detection at 225 nm. The following eluent program was used; 10% solvent B for 0.5 min, followed by a linear gradient to 45% solvent B in 5.5 min, 45% solvent B for 10 min, another linear gradient to 100% solvent B in 5 minutes, 100% solvent B for 3 minutes, and finally a linear gradient to 10% solvent B in 3 minutes followed by 10% solvent B for 3 minutes. Under these conditions, the compounds were separated with the following retention times: phenol 4.3 min, benzoic acid 4.9 min, (±)-4-methoxymandelonitrile (**2**) 5.2 min, 4-anisaldehyde (**1**) 5.9 min, phenyl benzoate 14.8 min, (±)-4-methoxymandelonitrile benzoate (**3**) 16.1 min, and mesitylene (internal standard) 19.3 min.

Calibration curves were prepared using commercial 4-anisaldehyde (>99.0%), (*R*)-4-methoxymandelonitrile (98.0%) and benzoic acid (>99.5%) as well as chemically synthesized (±)-4-methoxymandelonitrile benzoate (99%) and (*S*)-tembamide (99%).

2.2.7.2. GC analysis

Analysis of the cyanolysis of cyclohexene oxide was performed on a GC2010 plus gas chromatograph (Shimadzu, Duisburg, Germany) with FID detection. Samples were prepared as described in section 2.2.2.3. Separation was achieved on an OPTIMA 5 MS column (Macherey Nagel) with a length of 30 m, an inner diameter of 0.25 mm, and a film thickness of 0.25 µm. The injection volume was 1 µL and the split ratio was set to 1:50. Temperature program: 110 °C (7.5 min), 100 °C/min to 335 °C (2.25 min). The hydrogen carrier gas was set to 1.0 mL/min flow rate (constant flow mode). Substrate cyclohexene oxide (**9**) eluted with a retention time of 1.04 min, the internal standard n-octanol eluted at 1.85 min and product 2-cyanocyclohexanol (**10**) at 3.00 min.

2.2.7.3. High resolution GC-MS analysis

The crude reaction mixture obtained after evaporating the volatiles from a Raney Ni-catalyzed hydrogenation of (±)-4-methoxymandelonitrile benzoate was re-dissolved in acetone and analyzed using high resolution gas chromatography coupled to mass spectrometry (GC-MS).

GC conditions: An Agilent 6890 gas chromatograph was equipped with a 30 m analytical column (Phenomenex ZB1-MS, 30 m x 0.25 mm ID, tf=0.25 µm). A split injection port at 270°C was used for sample introduction and the split ratio was set to 10:1. Temperature program: 50 °C

(3 min), 10 °C/min to 310 °C (3 min). The helium carrier gas was set to 1.0 mL/min flow rate (constant flow mode).

MS conditions: A JMS-T100GC (GCAccuTOF, JEOL, Japan) time of flight mass spectrometer in electron ionization (EI) mode at 70 eV and JEOL MassCenter™ workstation software was used. The source and transfer line temperature were set at 200 °C and 290 °C respectively. The detector voltage was set at 2050 V. The acquisition range was from m/z 41 to 600 with spectrum recording interval of 0.4 s. The system was tuned with PFK to achieve a resolution of 6,000 (FWHM) at m/z 292.9824. 1-Iodonaphtalene was used as internal standard.

2.2.7.4. NMR analysis

The structure of side product **8** was elucidated using ^{1}H NMR, ^{13}C NMR and DEPT-135 NMR analysis. The purity of (*S*)-tembamide crystals prepared in this project was confirmed using ^{1}H NMR and ^{13}C NMR analysis. The spectra were recorded on a Bruker Avance II 300 MHz spectrometer (Bruker, Billerica, MA, USA). Samples were prepared in deuterated DMSO.

3. Results

The results of this thesis are divided into three sections. Section 3.1 describes the design and optimization of a bi-enzymatic cascade synthesis of 4-methoxymandelonitrile benzoate (**3**) *via* a hydroxynitrile lyase-catalyzed hydrocyanation of 4-anisaldehyde (**1**) combined with a hydrolase-catalyzed benzoylation of the formed cyanohydrin (**2**). The catalytic hydrogenation of the enzymatic cascade product **3** to yield enantiopure tembamide is studied in section 3.2., focusing on the catalyst screening for the selective hydrogenation of the nitrile moiety and the optimization of the reaction parameters. An alternative biocatalytic reaction for the formation of amino alcohols is the halohydrin dehalogenase (HHDH)-catalyzed epoxide ring-opening using azide or cyanide as nucleophiles, which, after reduction, leads to β- or γ-amino alcohols, respectively. Section 3.3 describes the protein engineering *via* site-saturation mutagenesis (SSM) of HheG – an HHDH that accepts cyclic epoxides – in order to enhance its activity in cyanide-mediated epoxide ring-opening reactions.

3.1. Bi-enzymatic cascade for the synthesis of an optically active *O*-benzoyl cyanohydrin

3.1.1. Design of an enzymatic chiral route towards 4-methoxymandelonitrile benzoate from 4-anisaldehyde

Compared to other benzaldehydes, the hydrocyanation of 4-anisaldehyde requires a particularly high excess of HCN to drive the equilibrium towards the cyanohydrin [213,223,224], which is attributed to the positive mesomeric effect of the *para*-methoxy substituent. Therefore, the direct benzoylation of the cyanohydrin was envisioned as a possible solution to avoid isolating this instable product (see Figure 24).

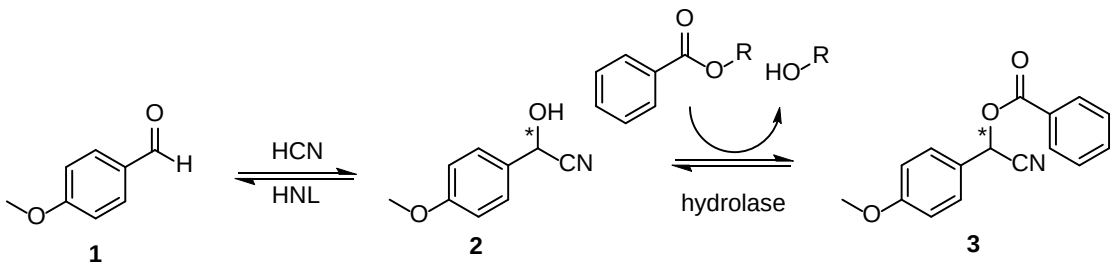

Figure 24. Proposed cascade synthesis of enantiopure 4-methoxymandelonitrile benzoate. Depending on whether an *S*-selective or an *R*-selective HNL are used together with a suitable hydrolase, (*S*)-**3** or (*R*)-**3** will be synthetized.

In this work, *Manihot esculenta* hydroxynitrile lyase (*Me*HNL) and mutant L1Q/A111G of isoenzyme 5 from *Prunus amygdalus* hydroxynitrile lyase (*Pa*HNL5-L1Q/A111G) were studied for the enantioselective hydrocyanation of 4-anisaldehyde to yield (*S*)- and (*R*)-4-methoxymandelonitrile, respectively. In order to select suitable hydrolases for the benzoylation step, a screening of over 40 hydrolases was planned.

For a successful combination of the HNL-hydrolase pair in the cascade synthesis of enantiopure 4-methoxymandelonitrile benzoate, it was required to subject the enzymatic hydrocyanation and transesterification reactions to a systematic study of the relevant reaction variables. For example, evaluating the effects of temperature and water activity on both reactions, as well as the potential cross interactions between the reactions' enzymes, substrates, byproducts and side products, was of great importance to ensure the optimal performance of the cascade.

In the designed cascade, a low-water organic solvent system was envisioned, for which the immobilization of both enzymes would be required. In organic solvents, free lipases generally express low catalytic activity and they tend to form aggregates which can lead to mass transfer limitations [225]. A simple and generally effective immobilization method when working in organic solvents is physical adsorption. Adsorption is believed to enhance the catalytic activity of most lipases due to hydrophobic interactions between the support and part of the enzyme, yielding the active enzyme conformation by opening the lid [226]. Similarly, immobilization of hydroxynitrile lyases can improve their activity and stability towards organic solvents [74] and may lead to higher enantioselectivity [160]. Therefore, the immobilization of the HNL and the hydrolase was considered a key step prior to their combination in a concurrent fashion.

3.1.2. Non-enzymatic hydrocyanation of 4-anisaldehyde and benzoylation of 4-methoxymandelonitrile benzoate

Prior to studying the enzymatic hydrocyanation of 4-anisaldehyde and benzoylation of 4-methoxymandelonitrile, the chemical hydrocyanation and benzoylation reactions were carried out. The goal was to synthetize (±)-4-methoxymandelonitrile benzoate, which would be used as a substrate in hydrolase screening experiments and for the study of the nitrile hydrogenation (see section 3.2.).

The hydrocyanation of 4-methoxymandelonitrile was achieved following an adapted literature procedure [213]. During the reaction optimization it was observed that when using 6 cyanide equivalents, a maximum conversion of 85% was reached when performing the reaction at room temperature. However, cooling the mixture in an ice-water bath could shift the

equilibrium further to 92% conversion (see Figure 25). This indicates that the reaction is exothermic, which is in accordance with literature reports on the formation of cyanohydrins [227,228]. After the reaction workup, the solution was concentrated in a rotary evaporator in a cooled water bath to minimize the decomposition of the cyanohydrin. The first attempts to isolate (±)-**2** proved unsuccessful due to its instability leading to an increased concentration of 4-anisaldehyde in the mixture, which hampered the crystallization of the cyanohydrin given its oily consistency. (±)-**2** was finally successfully isolated as light yellow crystals – containing 3% of 4-anisaldehyde impurity –, which were formed during the controlled evaporation of the volatiles at -10 °C, and were subsequently washed with cold heptane/ethyl acetate (2:1) before being stored at -5 °C.

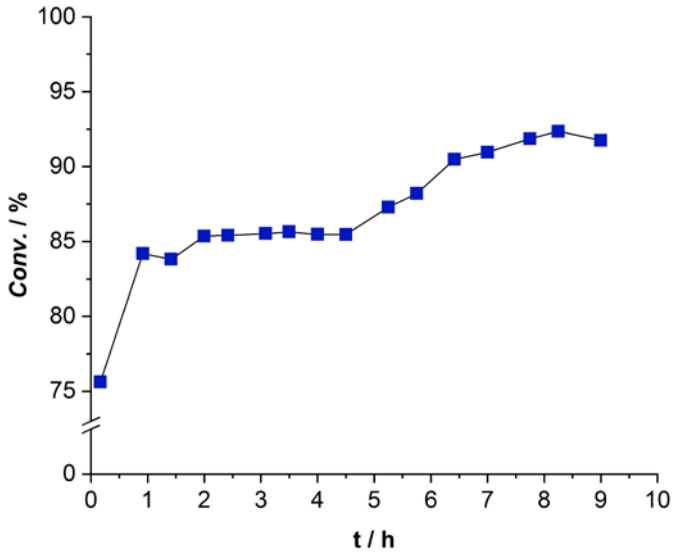

Figure 25. Hydrocyanation of 4-anisaldehyde using NaCN and $NaHSO_3$ in water/AcOEt (3/2). The reaction was initially performed at room temperature and, after 4.75 hours, the flask was introduced in an ice-water bath and the reaction continued until it reached 92% conversion.

The chemically synthetized (±)-4-methoxymandelonitrile was benzoylated using benzoyl chloride and pyridine dichloromethane. This reaction was performed using the concentrated crude mixture of the hydrocyanation reaction. The same procedure was followed for the preparative synthesis of (*R*)- and (*S*)-methoxymandelonitrile benzoate, using (*R*)- and (*S*)-methoxymandelonitrile resulting from the *Pa*HNL5-L1Q/A111G- and *Me*HNL-catalyzed hydrocyanation of 4-anisaldehyde, respectively.

3.1.3. Enzymatic hydrocyanation of 4-anisaldehyde

The initial idea was to develop the concurrent cascade synthesis of both (*R*)- and (*S*)-4-methoxymandelonitrile benzoate. To this end, mutant L1Q/A111G of isoenzyme 5 from the *R*-

selective *Prunus amygdalus* hydroxynitrile lyase and the *S*-selective *Manihot esculenta* hydroxynitrile lyase were selected for the first reaction step based on their availability.

Regarding the solvent of choice, relatively polar solvents such as diisopropyl ether (*i*Pr_2O, log *P* = 1.52) and *tert*-butyl methyl ether (*t*BME, log *P* = 0.94) have shown to be among the most suitable for hydroxynitrile lyases [229–232]. A test in which both solvents were evaluated in the *Pa*HNL5-L1Q/A111G- and *Me*HNL-catalyzed hydrocyanation of 4-anisaldehyde in a biphasic system containing citrate buffer at pH 4 and the ether showed that both enzymes maintained much higher activity in the presence of *i*Pr_2O, compared to when *t*BME was used (see Figure 26).

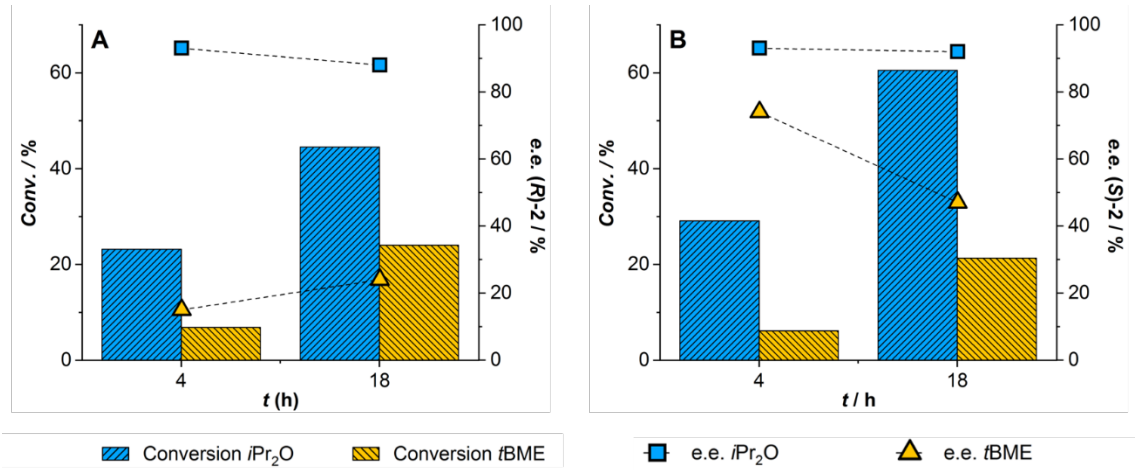

Figure 26. Effect of diisopropyl ether and *tert*-butyl methyl ether on the hydrocyanation of 4-anisaldehyde catalysed by *Pa*HNL5-L1Q/A111G (A) and *Me*HNL (B) in a 1:4 mixture of citrate buffer, pH 4 and ether.

The competing non-enzymatic hydrocyanation reaction is favored at high pH and, thus, in order to suppress this reaction for a higher enantioselectivity of the process, one must work at the lowest pH possible. Therefore, a series of experiments were performed to determine the optimal pH for each reaction. The *Pa*HNL5-L1Q/A111G- and *Me*HNL-catalyzed hydrocyanation of 4-anisaldehyde was studied under a range of different pH values in a biphasic system (see Figure 27).

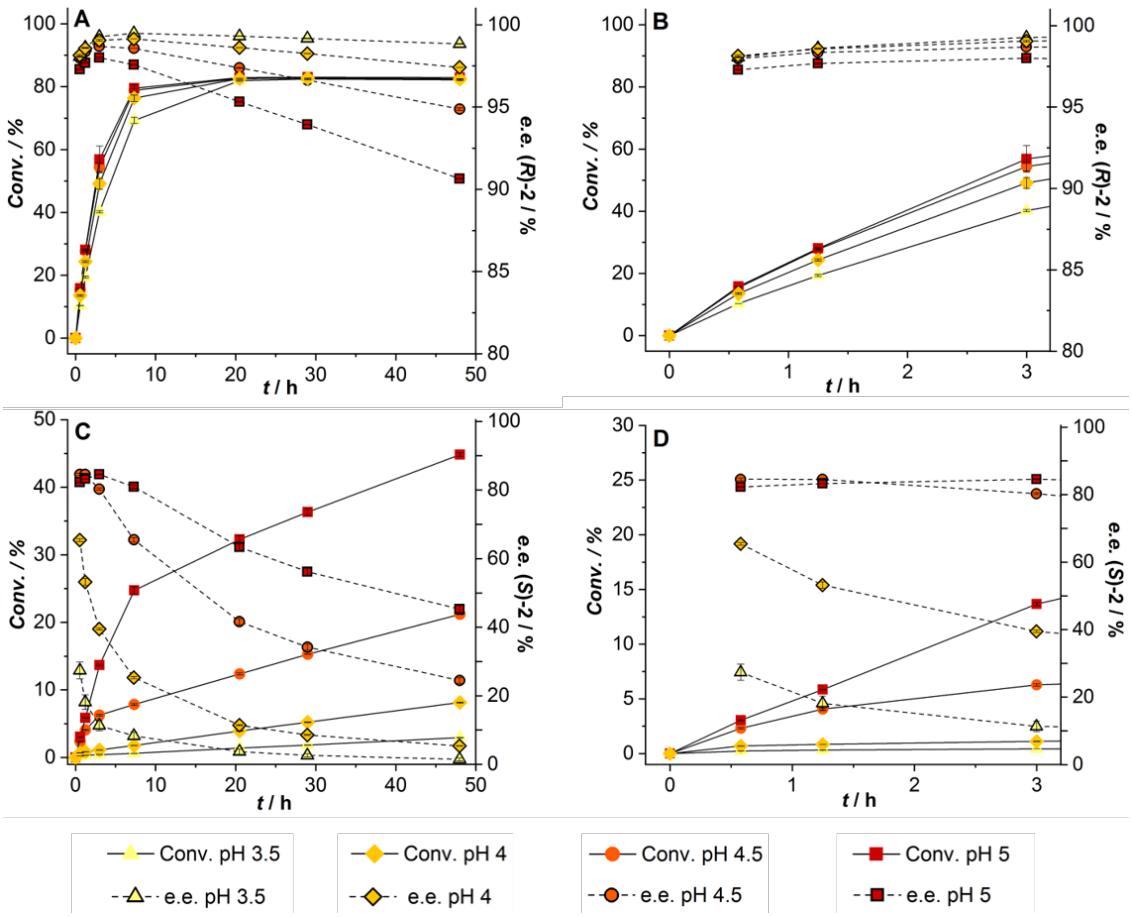

Figure 27. Effect of pH on the hydrocyanation of 4-anisaldehyde catalyzed by *Pa*HNL5-L1Q/A111G (A and B) and *Me*HNL (C and D) in a 1:5 mixture of 500 mM citrate buffer and *i*Pr_2O.

Figures 27A and 26B show that in the case of *Pa*HNL5-L1Q/A111G an optimal reaction rate is reached between pH 4.5 and 5. Since the positive effect of an increase from pH 4.5 to 5 on the initial rate is negligible (see Figure 27B), and given the detrimental effect of this pH increase on the reaction enantioselectivity due to an increase in the non-enzymatic hydrocyanation rate (see Figure 28), pH 4.5 was selected for the *Pa*HNL5-L1Q/A111G-catalyzed hydrocyanation of 4-anisaldehyde. Regarding *Me*HNL, the lower pH values tested had a pronounced negative effect on the enzymatic activity (see Figures 27C and 27D). Given the difference in reaction rate and e.e. values observed in this case between pH 4.5 and pH 5, a second experiment was performed for *Me*HNL in the range of pH 4 to pH 5.5. Figure 29 shows that pH 5 remained the best condition for this enzyme, since further increasing the pH greatly enhances the rate of the non-enzymatic hydrocyanation, as established in Figure 28.

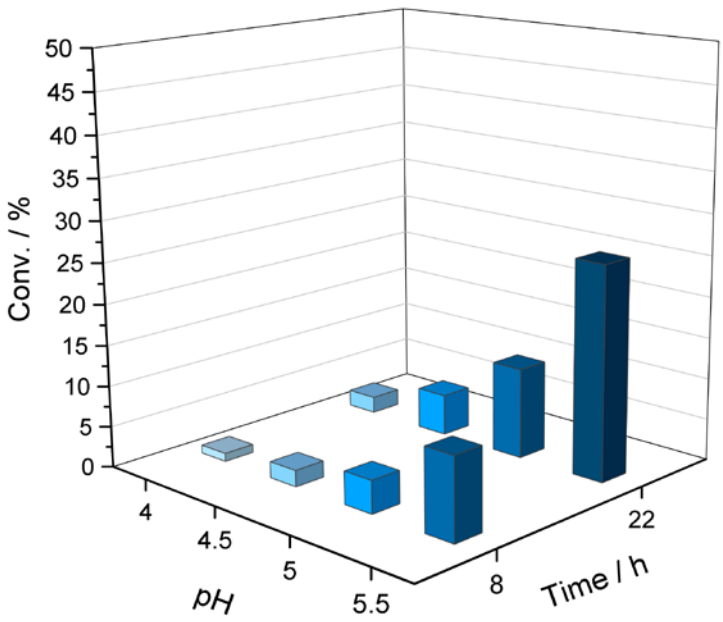

Figure 28. Effect of pH on the non-enzymatic hydrocyanation of 4-anisaldehyde in a 1:5 mixture of 500 mM citrate buffer and *i*Pr$_2$O.

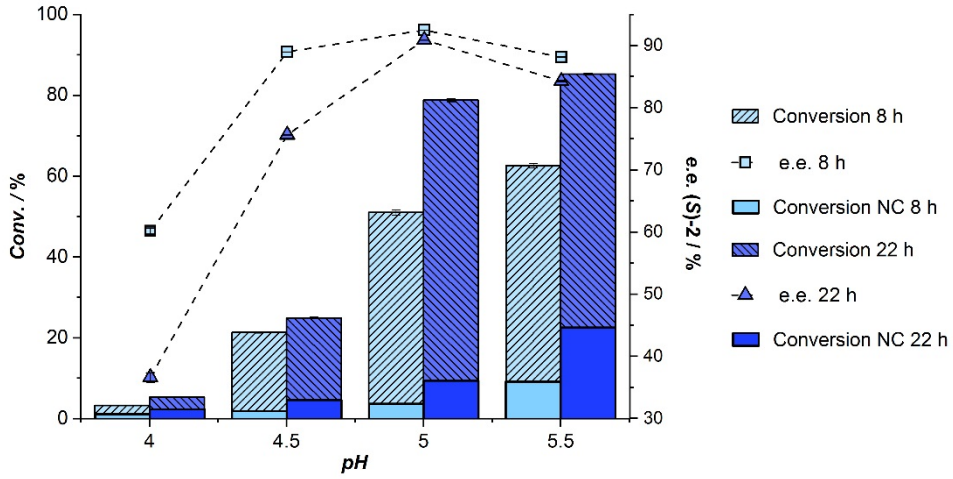

Figure 29. Effect of pH on the hydrocyanation of 4-anisaldehyde catalyzed by *Me*HNL in the range of pH 4 to 5.5, using a 1:5 mixture of 500 mM citrate buffer and *i*Pr$_2$O. NC is negative control.

The optimized pH values for both enzymatic reactions were used in the preparative synthesis of (*R*)- and (*S*)-methoxymandelonitrile. Also, given that enzymes have been reported to present a memory effect, tending to keep the conformation and ionization state that they had when being immobilized [86,233], the selected optimal pH value was used during immobilization of *Me*HNL as well.

3.1.4. Screening of hydrolases

A total of 41 non-immobilized hydrolase preparations were evaluated in a hydrolysis test using (±)-4-methoxymandelonitrile benzoate as a substrate (see Table 6). The aim was to select hydrolases with affinity for both (*R*)- and (*S*)-4-methoxymandelonitrile benzoate in order to combine them with either *Pa*HNL5-L1Q/A111G or *Me*HNL, respectively. The reactions were followed in chiral HPLC and the enantiomeric excess of the unreacted 4-methoxymandelonitrile benzoate was calculated. Conversion was determined based on the concentration of formed benzoic acid and unreacted 4-methoxymandelonitrile. Figure 30 summarizes the results of the hydrolases which exhibited activity.

Table 6: Assigned number and specifications of the hydrolases screened in the hydrolysis of (±)-4-methoxymandelonitrile benzoate in a 1:1 mixture of *i*Pr_2O and phosphate buffer pH 7 (100 mM).

Exp. n°	Name	Provider	Enzyme type	Origin
1	SPRIN imibond THERMOLYSIN	Sprin Technologies	protease	*Geobacillus* sp.
2	SPRIN epobond THERMOLYSIN	Sprin Technologies	protease	*Geobacillus* sp.
3	Protease from Bacillus Licheniformis	Sigma Aldrich	protease	*Bacillus licheniformis*
4	CALA L	Novozymes	lipase	*Candida antarctica*
5	Porcine PEM	Novozymes	protease mixture	*Sus domesticus*
6	Novozym 388	Novozymes	lipase	*Rhizomucor miehei*
7	Lipex 100L	Novozymes	lipase	*Aspergillus oryzae*
8	Acylase "Amano"	Amano Enzyme Inc.	acylase	*Aspergillus melleus*
9	Esperase 8.0 L	Novozymes	protease	*Bacillus lentus*
10	Lipase AK "Amano" 20	Amano Enzyme Inc.	lipase	*Pseudomonas fluorescens*
11	Protease N "Amano"	Amano Enzyme Inc.	protease	*Bacillus subtilis*
12	Lipase AYS "Amano"	Amano Enzyme Inc.	lipase	*Candida rugosa*
13	Protease S "Amano"	Amano Enzyme Inc.	protease	*Bacillus* sp.
14	Lipase AS "Amano"	Amano Enzyme Inc.	lipase	*Aspergillus niger*
15	Lipase PS "Amano" SD	Amano Enzyme Inc.	lipase	*Bulkholderia cepacia*
16	Neutrase 0.8 L	Novozymes	metalloprotease	*Bacillus amyloliquefaciens*
17	Savinase 16L, Type EX	Novozymes	protease	*Bacillus lentus*
18	Lipase from porcine pancreas, Type II	Sigma Aldrich	lipase	*Sus domesticus*

Exp. n°	Name	Provider	Enzyme type	Origin
19	ASSEMBLASE liquid	DSM Anti-Infectives	amidase	*Escherichia coli*
20	BIOCATALYST CALB 10L	Fermenta Biotech Ltd	lipase	*Candida antarctica*
21	Lipase R "Amano"	Amano Enzyme Inc.	lipase	*Penicillium roqueforti*
22	Lipase AY "Amano" 30SD-K	Amano Enzyme Inc.	lipase	*Candida rugosa*
23	Lipase MH "Amano" 10SD	Amano Enzyme Inc.	lipase	*Mucor javanicus*
24	Lipase A "Amano" 12-K	Amano Enzyme Inc.	lipase	*Aspergillus niger*
25	Lipase DF "Amano" 15-K	Amano Enzyme Inc.	lipase	*Rhizopus oryzae*
26	Lipase R "Amano"-K	Amano Enzyme Inc.	lipase	*Penicillium roqueforti*
27	Papain from papaya latex, P3375-25G	Sigma Aldrich	protease	*Carica papaya*
28	Alcalase	Clea Technologies	protease	*Bacillus licheniformis*
29	ECS-PLE06	Enzymicals	esterase	*Sus domesticus*
30	Trypsin from bovine pancreas cat: 93610	Fluka, Bio Chemika	protease	*Bos taurus*
31	Esterase, from porcine liver, crude.	Sigma Aldrich	esterase	*Sus domesticus*
32	CES P-1	Amano Enzyme Inc.	protease	ND [1]
33	CES P-2	Amano Enzyme Inc.	protease	ND [1]
34	CES P-3	Amano Enzyme Inc.	protease	ND [1]
35	CES L-1	Amano Enzyme Inc.	lipase	ND [1]
36	CES L-2	Amano Enzyme Inc.	lipase	ND [1]
37	CES L-3	Amano Enzyme Inc.	lipase	ND [1]
38	CES L-4	Amano Enzyme Inc.	lipase	ND [1]
39	CES L-5	Amano Enzyme Inc.	esterase	ND [1]
40	CES E-1	Amano Enzyme Inc.	esterase	ND [1]
41	CES E-2	Amano Enzyme Inc.	esterase	ND [1]

[1] ND: Not disclosed

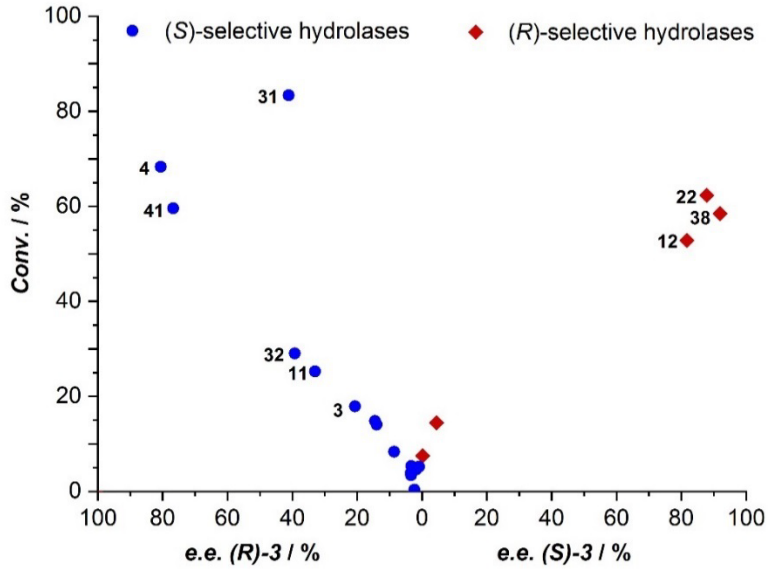

Figure 30. Conversion and enantiomeric excess (e.e.) of the remaining 4-methoxymandelonitrile benzoate after 18 hours of hydrolysis reaction catalyzed by the hydrolases in a 1:1 mixture of *i*Pr_2O and phosphate buffer pH 7 (100 mM).. The number next to each data point indicates the hydrolase to which it corresponds (see Table 6). Hydrolases 5, 7, 8, 9, 14, 17, 18, 24, 28, 29 and 33 showed low activity and/or selectivity and their numbers are therefore not specified on the graph. Hydrolases with no activity are not shown.

As expected, most of the screened hydrolases show a preference for (*S*)-4-methoxymandelonitrile benzoate. It must be noted here that, since the nitrile group has a higher priority than the *p*-methoxyphenyl group according to Cahn–Ingold–Prelog rules [234], most lipases will catalyze the acylation of the (*S*) enantiomer preferentially, following Kazlauskas' rule for secondary alcohols [144]. Based on the hydrolysis screening and on the availability of immobilized hydrolases, several enzymes with high activity and affinity for (*S*)- or (*R*)-4-methoxymandelonitrile benzoate were selected for their evaluation in the transesterification reaction using racemic 4-methoxymandelonitrile as substrate. Lipase AY (*Candida rugosa* lipase, CRL) from Amano was selected for its enantiopreference for (*R*)-4-methoxymandelonitrile benzoate. Although Alcalase had shown low activity in the hydrolysis screening and slight enantiopreference for the (*S*)-enantiomer, it is known that this enzyme presents opposite enantiopreference to lipases in organic solvents and that this selectivity may change in aqueous medium [145]. Therefore, it was also included in the transesterification screening. *Candida antarctica* lipase A (CALA) and pig liver esterase (PLE) were selected for their enantiopreference for (*S*)-4-methoxymandelonitrile benzoate. Furthermore, *Candida antarctica* lipase B (CALB) was also tested. The enzymes were evaluated in a dynamic kinetic resolution (DKR) in which 3 Å molecular sieves served both as drying agent to avoid hydrolysis and as non-selective catalyst for the hydrocyanation of 4-anisaldehyde. For the hydrolase-catalyzed transesterification reaction, vinyl benzoate was selected as acyl donor. As can be seen in Table 7, both Lipase AY and Alcalase

showed enantiopreference for the (*S*)-enantiomer, with low selectivity in both cases. In the case of Alcalase, the result is consistent with our observation during the hydrolysis test. Regarding the change in enantiopreference exhibited by Lipase AY, Jin *et al.* reported on the effect of the reaction medium on the enantioselectivity of CRL, which could be reversed due to variations of the racemic temperature caused by different solvents [235]. CALB and PLE showed no activity under the transesterifications conditions, whereas CALA showed low activity but with a fair enantiopreference for the (*S*)-enantiomer, in accordance with the hydrolysis test.

Table 7: Results of the hydrolase screening for the benzoylation of 4-methoxymandelonitrile in a DKR using 3 Å molecular sieves as hydrocyanation catalyst in *i*Pr_2O. The hydrolase and vinyl benzoate were added after 20 h of hydrocyanation reaction to allow for sufficient formation of the cyanohydrin.

Enzyme	Immobilization method and support	Conversion (%)[1]	Enantiopreference (*S*)-3 or (*R*)-3	e.e. 3 (%) [2]
Lipase AY from Amano	Adsorbed on macroporous methyl methacrylate/styrene copolymer beads	13	(*S*)-3	11
Alcalase	Covalently immobilized on macroporous polymethylmethacrylate beads functionalized with amine groups	2	(*S*)-3	67
CALA	Covalently immobilized on macroporous polymethylmethacrylate beads functionalized with oxirane groups	3	(*S*)-3	73
CALB [3]	Adsorbed on an acrylic resin	0	-	-
PLE	Covalently immobilized on macroporous polymethylmethacrylate beads functionalized with oxirane groups	0	-	-

[1] Total conversion from 4-anisaldehyde to 4-methoxymandelonitrile benzoate 4 hours after the addition of the hydrolase and vinyl benzoate. [2] E.e. of the major enantiomer of 4-methoxymandelonitrile benzoate formed. [3] Commercial Novozym 435 was used. All other enzymes were immobilized at Viaym B.V., Delft, The Netherlands.

Due to the lack of a hydrolase with enantiopreference for the (*R*)-cyanohydrin, it was decided to focus solely on the concurrent bi-enzymatic synthesis of (*S*)-4-methoxymandelonitrile benzoate, for which CALA was selected for its combination with *Me*HNL based on the DKR test. CALA is a robust industrial enzyme [154,236], and was shown to exhibit acyltransferase activity even in aqueous media [156,157], which was deemed an attractive feature in our envisioned cascade. To ensure its optimal combination with the HNL-catalyzed hydrocyanation in a concurrent fashion, it was decided to immobilize CALA by adsorbing it on Relizyme EXE309. This is a macroporous bead based on a methyl methacrylate/styrene copolymer that was recommended by the manufacturer for effective lipase adsorption.

3.1.5. Selection of benzoyl donor

A crucial step in the development of the intended cascade was the identification of a suitable benzoyl donor that would facilitate the CALA-catalyzed transesterification. For this reaction to take place, an activated benzoyl donor was required [149]. Enol esters are highly activated acyl donors and have been extensively used in lipase-catalyzed transesterifications [129,149]. As an alternative to enol esters, several studies have proposed oxime esters, which are generally considered quasi-irreversible acyl donors [149,237–240]. Another activated ester, reported by Sakulsombat *et al*. on the successful acetylation of cyanohydrins catalyzed by *Burkholderia cepacia* lipase, is phenyl acetate [241]. Based on this information, vinyl benzoate, acetoxime benzoate and phenyl benzoate were studied in the transesterification reaction of 4-methoxymandelonitrile (see Figure 31).

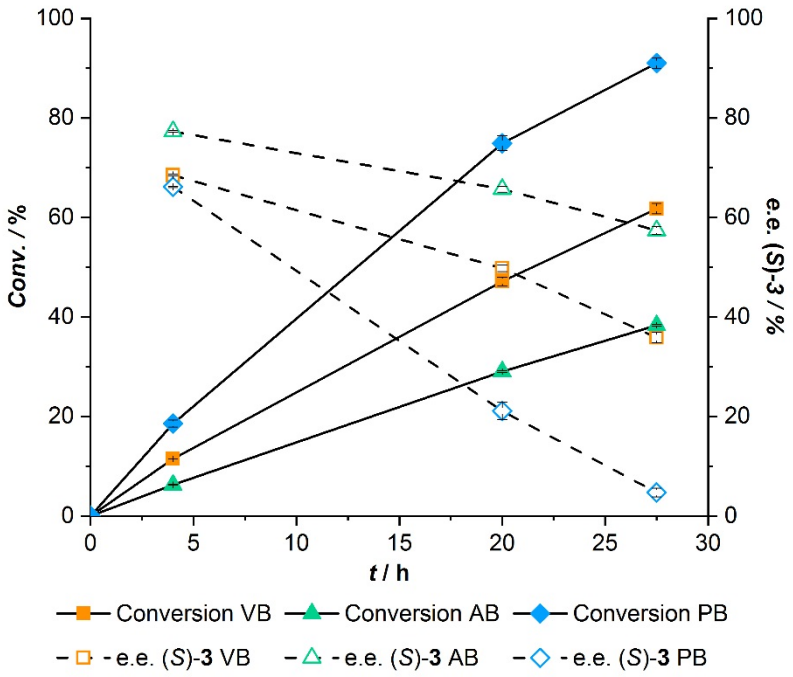

Figure 31. Conversion and enantiomeric excess (e.e.) values obtained for the immobilized CALA-catalyzed benzoylation of 67 mM (±)-4-methoxymandelonitrile using 200 mM vinyl benzoate (VB), acetoxime benzoate (AB) or phenyl benzoate (PB) in diisopropyl ether.

As shown in Figure 31, all three activated benzoyl donors are accepted by CALA in the benzoylation of 4-methoxymandelonitrile. Phenyl benzoate afforded the highest reaction rate, followed by vinyl benzoate and, finally, acetoxime benzoate. The enantioselectivity of the reaction was not significantly affected by the donors, resulting in an enantiomeric ratio (E value) [242] of 8 when vinyl benzoate was used and 6 when acetoxime benzoate or phenyl benzoate were used.

Among the three tested donors, vinyl benzoate is the only one that can yield an irreversible benzoylation of 4-methoxymandelonitrile, due to the tautomerization of the byproduct to acetaldehyde. This constitutes an advantage for the transesterification reaction, but acetaldehyde might compete with 4-anisaldehyde as a substrate for *Me*HNL. After confirming that *Me*HNL could catalyze the hydrocyanation of acetaldehyde to yield lactonitrile, vinyl benzoate was ruled out as suitable benzoyl donor for the cascade approach.

Phenyl benzoate and acetoxime benzoate are both activated donors due to the poor nucleophilicity of the byproducts (phenol and acetone oxime), although they do not yield irreversible transesterifications. Given that phenyl benzoate afforded considerably higher transesterification rates than acetoxime benzoate, and after confirming that phenyl benzoate as well as the byproduct phenol did not exert a negative effect on the hydrocyanation reaction (see section 3.1.11., Figure 41), it was selected for the cascade synthesis of (*S*)-4-methoxymandelonitrile benzoate.

3.1.6. Influence of reaction temperature

In general, temperature affects enzymatic stability and has an important effect on the reaction rate of enzyme-catalyzed reactions and their enantioselectivity. Depending on whether the reaction takes place below or above the racemic temperature, a decrease in temperature will increase or decrease the enantioselectivity, respectively.

According to literature, *Me*HNL shows optimal hydrocyanation activity at ~40 °C [71]. A reduction in the reaction temperature below 40 °C would decrease the enzymatic activity, but is expected to slightly increase its enantioselectivity, since *Me*HNL displays an elevated racemic temperature of 580 °C in the hydrocyanation of phenylpropionaldehyde in dibutylether [14]. Furthermore, in several cases, decreasing the reaction temperature has been shown to reduce the rate of the nonenzymatic hydrocyanation of 4-anisaldehyde to a higher extent than the enzymatic reaction, which would also contribute to increase the enantiomeric excess (e.e.) of the cyanohydrin [243–245]. Finally, the reaction must be performed at a rather low temperature, since the boiling point of HCN is 25.6 °C [246]. Based on this information, hydrocyanation reactions were performed at 5, 10, and 20 °C.

Within the studied temperature range, the hydrocyanation rate increased moderately with the reaction temperature (see Figure 32). On the other hand, the enantioselectivity of the enzymatic reaction slightly increased at lower temperatures, as expected. These results suggest that the optimal reaction temperature, which would afford excellent enantioselectivity with a satisfactory reaction rate, would be 10 °C.

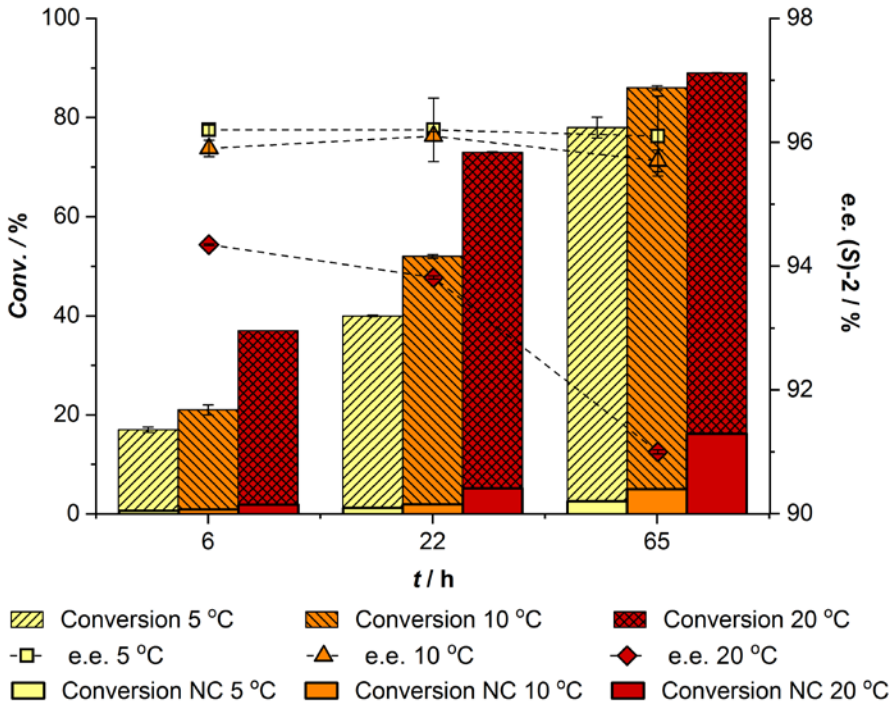

Figure 32. Effect of reaction temperature on the non-immobilized *Me*HNL-catalyzed hydrocyanation of 100 mM 4-anisaldehyde in a biphasic system using 6.5 equivalents of HCN in a 1:8 mixture of 500 mM citrate buffer at pH 5 and *i*Pr_2O. Negative control (NC) shows the rate of the unselective background reaction.

In the case of CALA, based on the data from kinetic resolution studies, the lipase was expected to show increased enantioselectivity with lower temperatures [247,248]. However, immobilized CALA has been reported to display a temperature optimum of 90 °C [249], thus the reaction will be limited by low rates at low temperatures.

The effect of reaction temperature on the CALA-catalyzed benzoylation of racemic 4-methoxymandelonitrile was studied in diisopropyl ether without added water in the range of 5 to 25 °C. The results showed that, when reducing the temperature, the enantioselectivity of CALA was slightly enhanced (E value of 7 at 5 and 10 °C and 6 at 25 °C), although this was at the expense of a pronounced reduction of reaction rate, as shown in Figure 33. Within the studied temperature range, the CALA-catalyzed benzoylation of 4-methoxymandelonitrile can be achieved in relatively high yields with optimal performance at 25 °C. Although CALA shows preference for conversion of the (*S*)-enantiomer, it is not selective enough to afford an enantiopure product. However, when preceded by an enantioselective hydrocyanation, the transesterification reaction can enhance the enantiopurity of the final product. Therefore, the observed minor effect of reaction temperature on the enantiomeric ratio can be neglected.

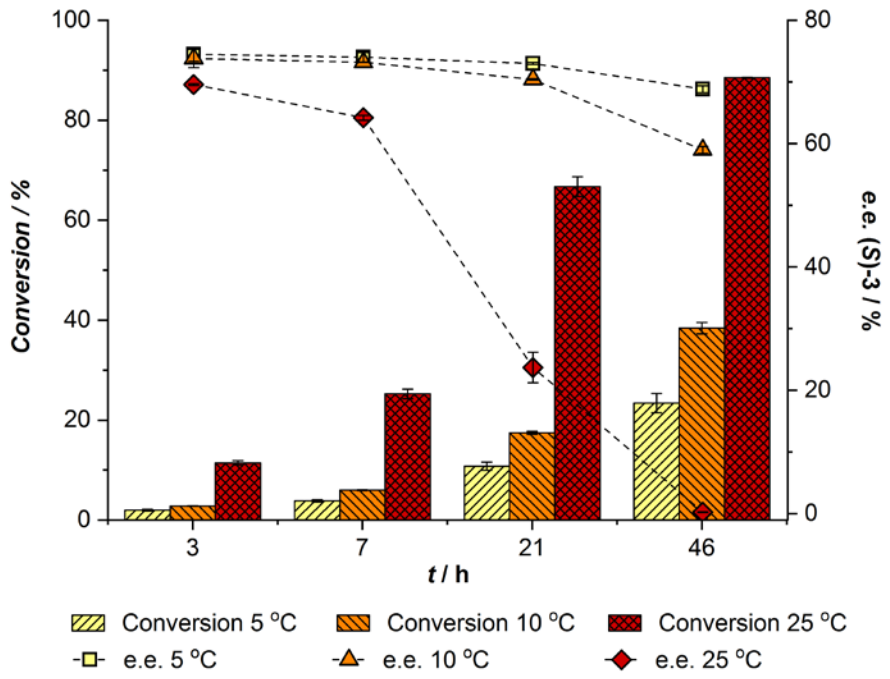

Figure 33. Effect of reaction temperature on immobilized CALA-catalyzed benzoylation of 65 mM (±)-4-methoxymandelonitrile using 200 mM phenyl benzoate in diisopropyl ether.

3.1.7. Evaluation of CALA-D122L mutant

Although CALA has been shown to present acyltransferase activity even in water-rich media [156,157], it is not fully selective towards transesterification and also catalyzes hydrolysis reactions, thereby releasing free acids. This not only decreases the reaction efficiency, but may eventually lead to inhibition of the lipase or the HNL in our envisioned cascade. Aiming at increasing the reaction selectivity of CALA towards transesterification, Müller *et al.* created several CALA mutants *via* rational design [250]. Introducing the single mutation Asp122Leu afforded a variant with enhanced acyltransferase selectivity, producing a significantly lower amount of free acids in transesterification reactions, while retaining all other characteristics of the WT.

CALA-D122L was evaluated as an alternative to CALA in order to suppress the hydrolysis reaction and, thus, minimize inhibition of the enzymes (see section 3.1.11.). The variant was immobilized on Relizyme EXE309, following the same procedure as for the wild-type lipase and the different benzoyl donors were also tested to ensure that the optimal conditions were found (see Figure 34). This variant showed a marked preference for phenyl benzoate over vinyl benzoate and acetoxime benzoate. Surprisingly, in this case the vinyl ester did not afford higher reaction rate than the acetoxime ester. Furthermore, a temperature screening was performed for the benzoylation of (±)-4-methoxymandelonitrile catalyzed by CALA-D122L. As shown in Figure 35, a

pronounced decrease in enzymatic activity was observed when reducing the reaction temperature from 25 to 10 °C.

The chemoselectivity of both CALA and CALA-D122L was then evaluated at the optimal temperature value within the studied range, using phenyl benzoate as donor in the benzoylation of (±)-4-methoxymandelonitrile. After immobilization, both enzymes were dried under high vacuum overnight to ensure that differences in the level of dryness of the immobilisates did not affect the results. Figure 36 shows that, unexpectedly, under the used conditions the mutant exhibits a higher hydrolase activity than the wild-type. Based on these results and given the higher accessibility of commercial WT CALA, the enzymatic cascade synthesis of (*S*)-4-methoxymandelonitrile benzoate was further optimized using wild-type CALA.

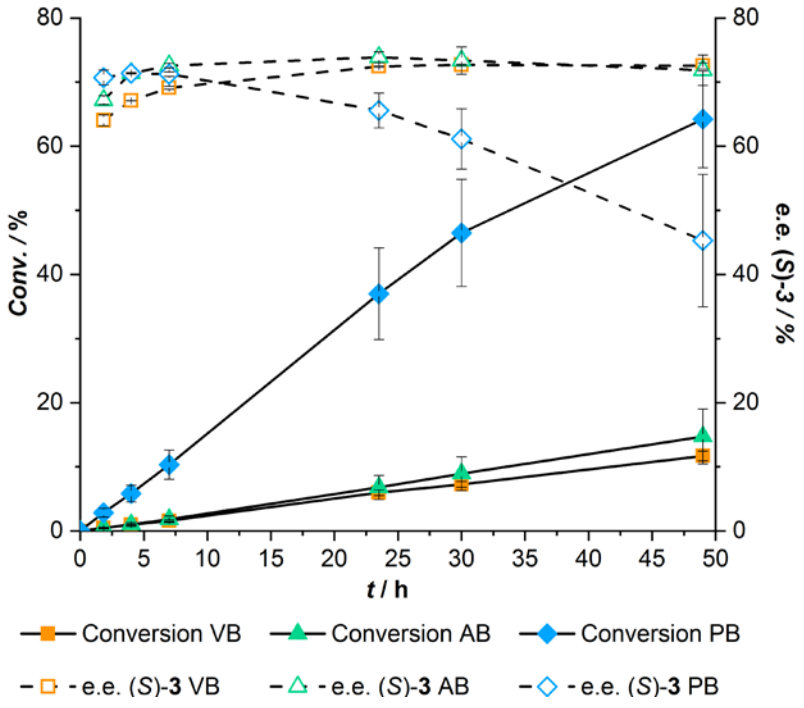

Figure 34. Conversion and enantiomeric excess (e.e.) values obtained for the CALA-D122L-catalyzed benzoylation of 67 mM (±)-4-methoxymandelonitrile using 200 mM vinyl benzoate (VB), acetoxime benzoate (AB) or phenyl benzoate (PB) in diisopropyl ether.

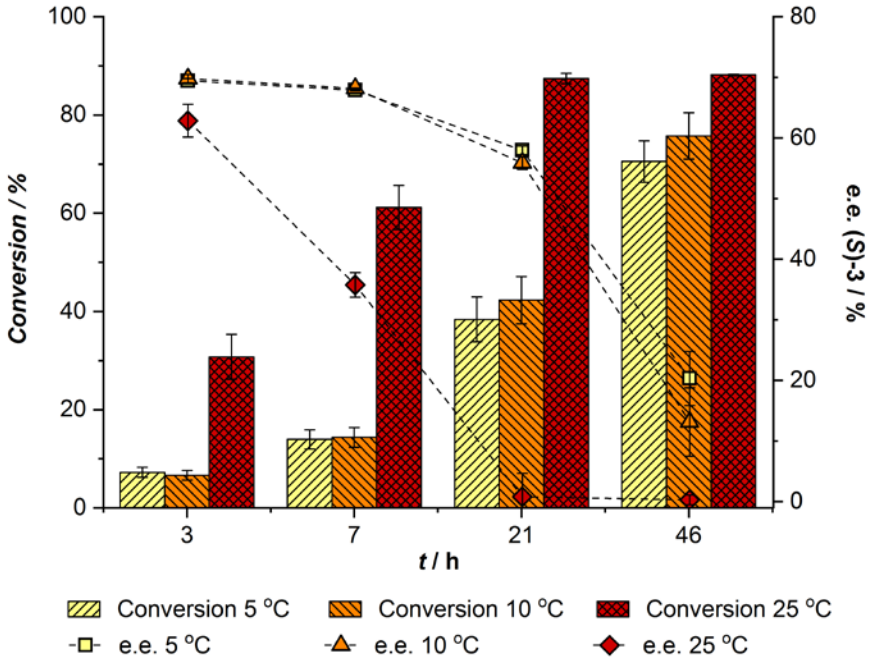

Figure 35. Effect of reaction temperature on the benzoylation of 65 mM (±)-4-methoxymandelonitrile using 200 mM phenyl benzoate in diisopropyl ether, catalyzed by the CALA-D122L variant.

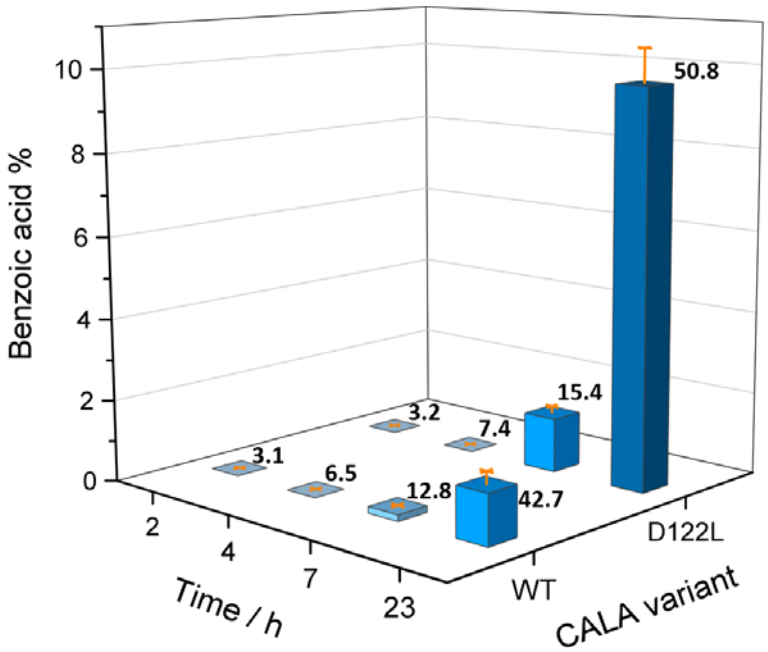

Figure 36. Chemoselectivity of CALA and CALA-D122L on the benzoylation of 65 mM (±)-4-methoxymandelonitrile using 200 mM phenyl benzoate at 25 °C in diisopropyl ether. Transesterification leads to 4-methoxymandelonitrile benzoate (E), whereas hydrolysis leads to benzoic acid (BA). The numbers next to the bars correspond to the sum [BA]+[E], in mM. The vertical axis in the graph represents the proportion of benzoic acid that is formed per total of phenyl benzoate converted, using the formula: BA% = 100 × [BA] / ([BA]+[E]).

3.1.8. Selection of a suitable carrier for the immobilization of MeHNL

A screening of different carriers for the immobilization of *Me*HNL *via* adsorption was performed. Crystalline cellulose and Celite have been widely used for HNL immobilization, affording high activities and selectivities in organic solvents [25,85,158,159,251,252]. Furthermore, Celite has been used to control water activity in organic media [253]. In a recent study of various supports for the immobilization of *Me*HNL, silica gel exhibited very high activity recovery [254]. Based on this information, microcrystalline cellulose (MCC), Celite R-633 (which has been previously used for immobilization of *At*HNL and *Hb*HNL) [25,159] and several silica supports were used as carriers for *Me*HNL. The resulting immobilisates were tested in the hydrocyanation of 4-anisaldehyde in a controlled low-water medium (see Table 8).

Under the tested conditions, most *Me*HNL formulations performed poorly, compared with the excellent yield and selectivity values obtained for the hydrocyanation of 4-anisaldehyde in a biphasic medium using free *Me*HNL (see Figure 32). This observation could be partially attributed to the reported lower activity and selectivity of *Me*HNL when working at reduced water content [85,158]. Furthermore, it was observed that Celite R-633 and the silica carriers catalyzed the unselective hydrocyanation, thus contributing to forming of the unwanted enantiomer. Nevertheless, the screening clearly identified Celite R-633 as the best carrier for *Me*HNL, with the highest activity and selectivity of the resulting biocatalyst (enzyme loading = 0.41 U/mg), which afforded a conversion of 82% and an e.e. value of 93% after 2 h under the studied conditions. However, the hydrocyanation reaction reached plateau shortly after 2 hours and, as the reaction continued, the e.e. dropped to 69%, with 86% conversion after 25 hours. This decrease in e.e. after long reaction times is due to the mentioned chemical background reaction catalyzed by the carrier. In order to minimize the catalytic effect of Celite R-633, the cell-free extract containing *Me*HNL was concentrated as much as possible and adsorbed on the minimum amount of carrier (enzyme loading is 0.79 U/ mg carrier). The enzymatic activity of the immobilisate was determined as 0.03 U/mg according to the procedure described in section 2.2.2.4.

Table 8: Results of hydrocyanation of 100 mM 4-anisaldehyde with 6.5 equivalents of HCN catalyzed by immobilized *Me*HNL in diisopropyl ether in a controlled water medium.

Support	Enzyme loading (U enz. / mg carrier)	mg immobilisate / mL of reaction	Reaction time (h)	Conversion (%)	e.e. (S)-2 (%)	Conversion NC (%) [1]
MCC [2]	0.36	14	23	18	48	ND [3]
Celite R-633	0.22	23	23	63	60	ND
Celite R-633	0.41	30	2	82	93	-
			25	86	69	27
SP53D-11785	0.41	30	2	12	76	-
			25	54	60	33
SP 540-10297	0.41	30	2	14	62	-
			25	70	35	51
SYLOID 244 FP	0.41	30	2	7	42	-
			25	48	26	23
SYLOID AL1-FP	0.41	30	2	10	47	-
			25	78	24	23
Perkasil SM 660	0.41	30	2	3	99	-
			25	22	48	16

[1] NC = negative control where the support is added instead of the immobilized enzyme. [2] Microcrystalline cellulose. [3] Not determined.

3.1.9. Influence of water activity

When working with enzymes in organic solvents, their activity is greatly affected by the water content in the reaction medium. This variable is best quantified in terms of thermodynamic water activity (a_w), which is equal in all phases in equilibrium [255]. Water is believed to act as a molecular lubricant, increasing the conformational flexibility of enzymes and, thus, their catalytic activity [256]. The water content also affects enzyme selectivity in a complex way, which involves interactions with the reaction medium and the substrates [158].

In the case of HNLs, it has been shown that when working at low water activities, the enzymes are insufficiently hydrated, resulting in activity and selectivity losses [73,85,158]. Lipases, on the other hand, can generally withstand lower water content [257], and some studies have shown that a_w does not significantly influence the enantioselectivity of lipases [158,257–259]. Furthermore, water competes with the substrate alcohol (in this case, cyanohydrin) for the nucleophilic attack of the acyl-enzyme intermediate, leading to ester hydrolysis [260].

A prerequisite for the combination of both enzymes in a concurrent mode is to find a suitable a_w range that allows for sufficient *Me*HNL activity and high selectivity, while minimizing ester hydrolysis catalyzed by CALA. In order to evaluate the a_w effect on both enzymatic reactions, a salt hydrate system that could cover a wide range of a_w values was selected: $Na_2HPO_4/Na_2HPO_4{\cdot}2H_2O/Na_2HPO_4{\cdot}7H_2O/Na_2HPO_4{\cdot}12H_2O$. These salt pairs afford water activity values of 0.15, 0.57 and 0.74, respectively, at 20 °C [222]. The hydrocyanation and benzoylation reactions were studied independently using immobilized *Me*HNL and CALA and the three salt pairs.

Before evaluating the influence of a_w on *Me*HNL, the effect of the phosphate salt hydrate pairs on the background hydrocyanation reaction was studied. The chemical hydrocyanation of 100 mM 4-anisaldehyde in diisopropyl ether was performed using 6.5 equivalents of HCN and 0.5 mmol salt pair per mL of reaction. As can be seen in Figure 37, this experiment revealed that the $Na_2HPO_4/Na_2HPO_4{\cdot}2H_2O$ pair could convert 32% of the aldehyde in 24 h, whereas the other two salt pairs afforded a much lower chemical background reaction rate with only 4% conversion after 24 hours. The negative control, where no salt was added, showed 1% conversion.

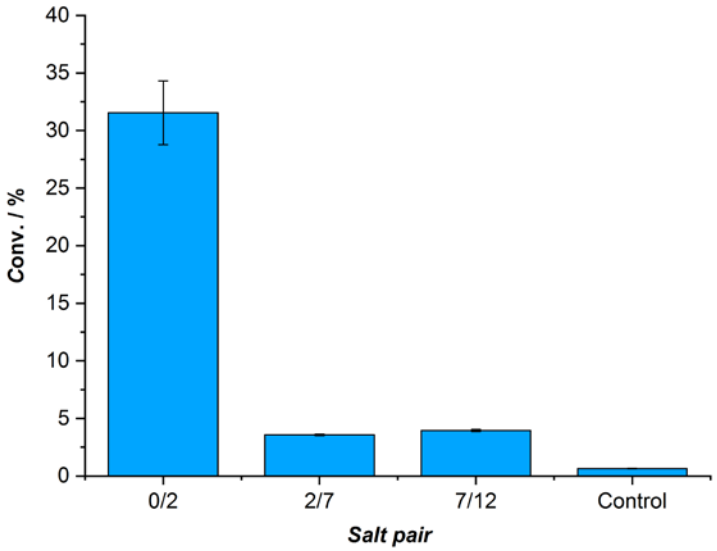

Figure 37. Effect of phosphate salt hydrate pairs (0.5 mmol / mL) on the non-enzymatic hydrocyanation of 100 mM 4-anisaldehyde using 6.5 equivalents of HCN in iPr_2O. The salt pairs used are $Na_2HPO_4/Na_2HPO_4{\cdot}2H_2O$ (0/2), $Na_2HPO_4{\cdot}2H_2O/Na_2HPO_4{\cdot}7H_2O$ (2/7), $Na_2HPO_4{\cdot}7H_2O/Na_2HPO_4{\cdot}12H_2O$ (7/12). No salt pair was added in the control reaction. Conversion and e.e. values taken after 24 hours of reaction.

The effect of the three water activity values provided by the phosphate salts on the *Me*HNL-catalyzed hydrocyanation of 4-anisaldehyde was then evaluated (see Figure 38). Results at a_w = 0.15 are difficult to interpret due to the above-mentioned catalytic effect of the salt. It seems,

however, that the enzyme is hardly active at this low water activity. Comparison of the results at the two highest water activity values, where the background reaction is similarly low, shows that the activity and selectivity of *Me*HNL increased with increasing a_w. Hence, to ensure a high e.e. of the resulting cyanohydrin, it is necessary to work at a high a_w for the combination of *Me*HNL and CALA.

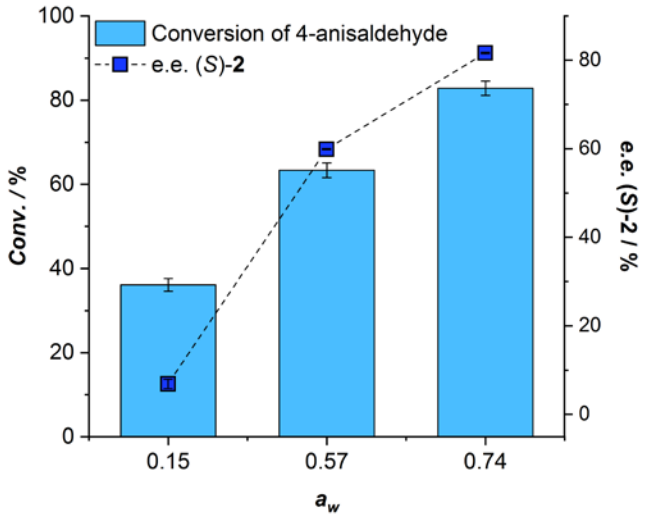

Figure 38. Effect of water activity on the *Me*HNL-catalyzed hydrocyanation of 90 mM 4-anisaldehyde using 6.5 equivalents of HCN in diisopropyl ether. Conversion and e.e. values taken after 23 hours of reaction.

In the case of CALA, at a_w = 0.57 and below, no significant difference in the enantioselectivity of the enzyme (E = 5) or in the selectivity for transesterification over hydrolysis was observed (see Figure 39). When working at a_w = 0.74, however, the hydrolysis rate increased significantly at the expense of the transesterification reaction. Although the enantioselectivity also increased under these conditions (E = 9), it is not a sufficient improvement to compensate for the increased hydrolysis rate. Considering the observed effects of water activity on *Me*HNL and CALA, it was concluded that it should be possible to combine both enzymatic reactions at a_w = 0.57.

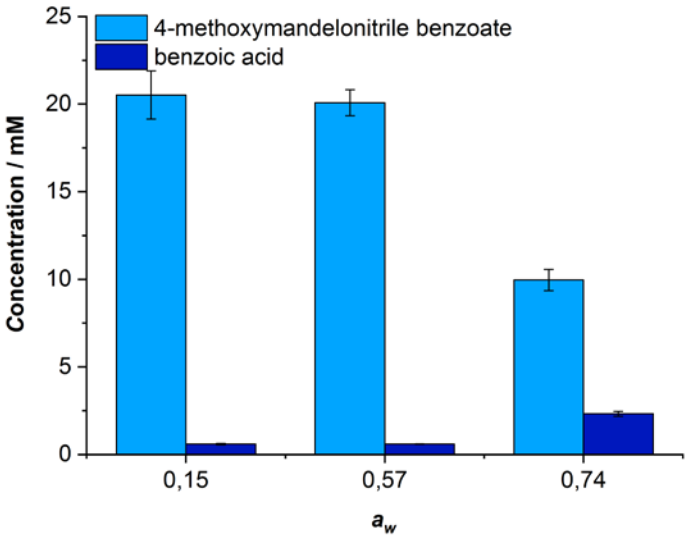

Figure 39. Effect of the different phosphate hydrate pairs on the CALA-catalyzed benzoylation of 66 mM (±)-4-methoxymandelonitrile using 200 mM vinyl benzoate in diisopropyl ether after 22 hours of reaction.

3.1.10. Alternative solvents and cyanide sources for the MeHNL-catalyzed hydrocyanation

Solvents with higher hydrophobicity than the widely used *t*BME and *i*Pr_2O, such as n-hexane (log *P* = 3.90) and n-octanol (log *P* = 5.18), have been reported to enhance the enzymatic activity of several hydroxynitrile lyases [73,85]. Additionally, due to the lower solubility of the benzoylated product **3** in less polar solvents, using them could further enhance the yield of our cascade by *in situ* product removal through product precipitation. Therefore, cyclohexane (log*P* = 3.44) and n-heptane (log*P* = 4.66) were selected for their evaluation in the *Me*HNL-catalyzed hydrocyanation of 4-anisaldehyde. Toluene (log*P* = 2.73) was not tested, since a slight decrease in the *Me*HNL-catalyzed hydrocyanation activity with respect to *t*BME as solvent was reported [73] and CALA also performed poorly in this solvent (data not shown).

The low solubility of HCN in cyclohexane and n-heptane – the maximum HCN concentration achieved following the procedure described in section 2.1.1.1. was 5 mM – prompted us to use acetone cyanohydrin as cyanide source. The *Me*HNL-catalyzed *in situ* cleavage of acetone cyanohydrin, which yields acetone and HCN, is a safer alternative to free HCN and, furthermore, it affords a better solubility of the cyanide source in apolar solvents than when using free HCN. Thus, an experiment was performed to evaluate both the alternative, safer cyanide source and to select the best solvent. The hydrocyanation of 4-anisaldehyde catalyzed by immobilized *Me*HNL using 6.5 equivalents of acetone cyanohydrin was performed in *i*Pr_2O, *t*BME, heptane and cyclohexane at 10 °C. To evaluate the solvents under the same water activity conditions, $Na_2HPO_4 \cdot 2H_2O$ was added to the reaction mixture, setting the a_w value at 0.57. Using acetone cyanohydrin as cyanide donor, however, afforded less than 1% conversion after 18 hours of

reaction in all cases. In parallel, an experiment was performed under the same conditions using a solution of HCN (6.5 equivalents) instead of acetone cyanohydrin in *i*Pr_2O and *t*BME. As already demonstrated with the free *Me*HNL-catalyzed hydrocyanation reaction in a biphasic system (see Figure 26), the reaction performed in *i*Pr_2O with immobilized MeHNL was more than 2-fold faster than when performed in *t*BME, albeit with no significant effect on the product e.e. Based on these results, it was decided to continue using free HCN in *i*Pr_2O.

3.1.11. Cross interactions

When performing several reactions in one-pot, the reagents, products, or byproducts of one reaction may affect the other reactions. This was already illustrated in section 3.1.5. by the example of the benzoyl donor vinyl benzoate, which upon transesterification afforded the byproduct acetaldehyde that competed with 4-anisaldehyde for the *Me*HNL-catalyzed hydrocyanation reaction. Thus, for an optimized cascade, the effect of hydrocyanation reagents on the CALA-catalyzed transesterification reaction as well as the influence of the benzoyl donor and the transesterification byproduct on the *Me*HNL-catalyzed hydrocyanation reaction was evaluated. Further, the influence of the side product benzoic acid on both transesterification and hydrocyanation reactions was studied.

The influence of 4-anisaldehyde and HCN on the reaction rate and selectivity of the CALA-catalyzed benzoylation of 4-methoxymandelonitrile was evaluated. As shown in Figure 40A, both 4-anisaldehyde and HCN exert a moderate negative effect on the benzoylation rate. Moreover, both compounds reduce the selectivity of CALA towards transesterification (see Figure 40B). Regarding the enantioselectivity of the benzoylation reaction, it was not significantly affected by the presence of either of the hydrocyanation substrates, with the E values varying between 5 and 6. Similarly, the effect of benzoic acid on CALA was studied in a benzoylation reaction of 70 mM (±)-4-methoxymandelonitirile containing one equivalent of benzoic acid. As a result, the reaction rate was 20% lower than that of the control.

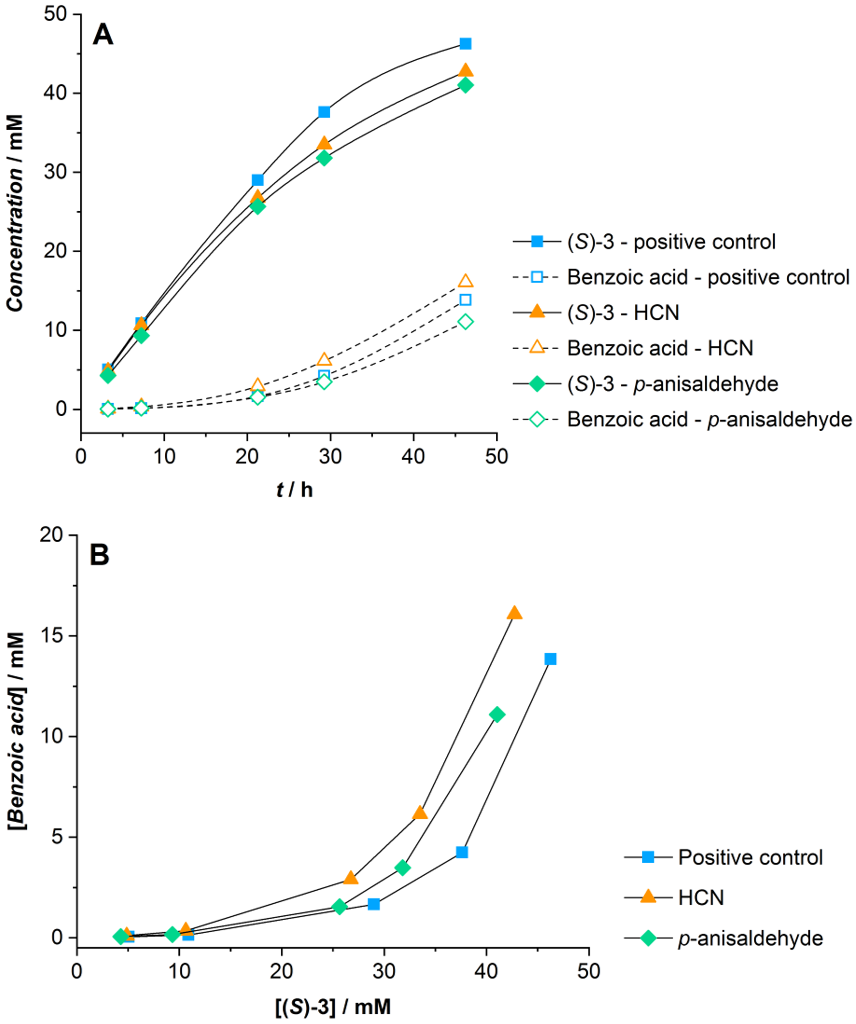

Figure 40. Effect of 60 mM 4-anisaldehyde and 209 mM HCN on the transesterification and hydrolysis rate of CALA (**A**) as well as its selectivity towards transesterification over hydrolysis (**B**) using 65 mM (±)-4-methoxymandelonitrile and 200 mM phenyl benzoate.

The influence of phenyl benzoate and its leaving group, phenol, on the *Me*HNL-catalyzed hydrocyanation of 4-methoxymandelonitrile was studied. Addition of either three equivalents of phenyl benzoate or phenol to the hydrocyanation reaction afforded (*S*)-4-methoxymandelonitrile with the same yield and enantiopurity as the control reaction (see Figure 41).

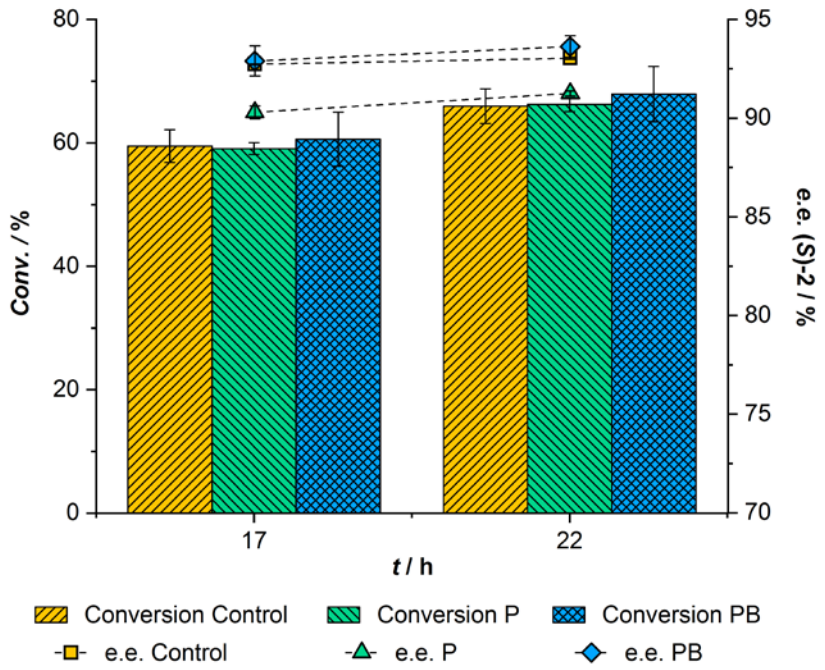

Figure 41. Effect of 300 mM phenol (P) or 300 mM phenyl benzoate (PB) on *Me*HNL-catalyzed hydrocyanation of 100 mM 4-anisaldehyde using 6 equivalents of HCN in *i*Pr_2O.

To evaluate the effect of the side product benzoic acid on the hydrocyanation reaction, an experiment was performed with addition of different amounts of acid to the reaction mixture. As shown in Figure 42, benzoic acid exerts a strong negative effect on the hydrocyanation rate of *Me*HNL. Thus, in order to achieve a cascade synthesis of (*S*)-**3** with high yield and selectivity, the CALA-catalyzed hydrolysis of phenyl benzoate and **3** should be minimized as much as possible. This observation is not surprising, since benzoic acid has previously been reported as a competitive inhibitor for other hydroxynitrile lyases [98,261,262]. Based on these results, the observed negative effect of benzoic acid on CALA is minor when compared to its effect on *Me*HNL.

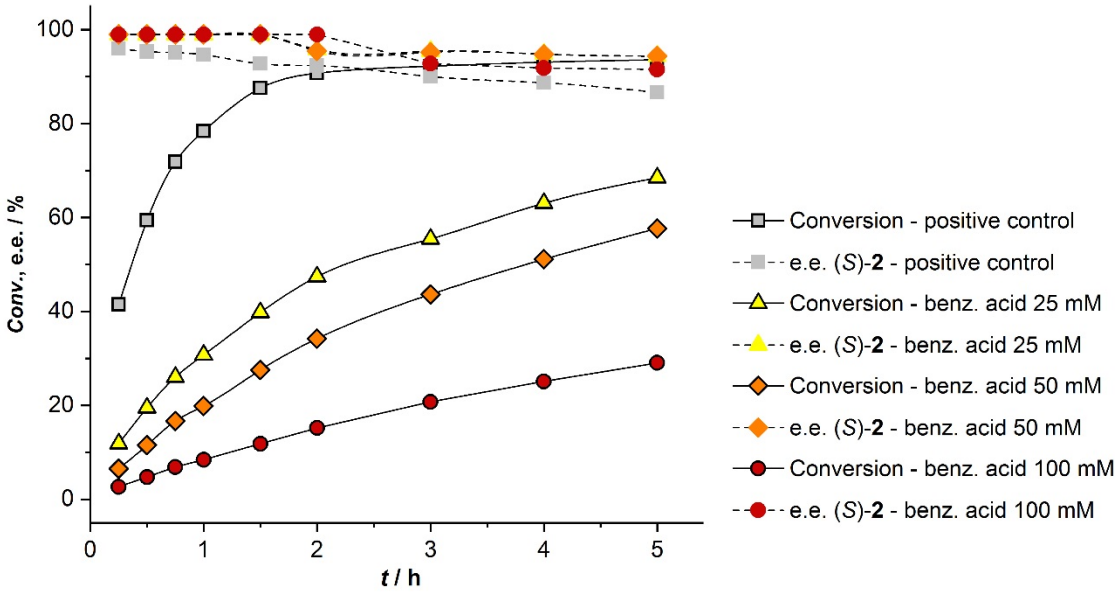

Figure 42. Effect of 25, 50, or 100 mM benzoic acid on the *Me*HNL-catalyzed hydrocyanation of 100 mM 4-anisaldehyde using 6.5 equivalents of HCN in *i*Pr$_2$O. With exception of the positive control, the enantiomeric excess values overlap at short reaction times.

3.1.12. Cascade synthesis of (S)-4-methoxymandelonitrile benzoate

For the first cascade synthesis test (see Table 9, entry 1), the used reaction conditions in terms of enzyme amount, temperature, water buffering salts and the time point of CALA addition were selected based on the results obtained before. The reaction temperature was set at 10 °C, $Na_2HPO_4{\cdot}2H_2O/Na_2HPO_4{\cdot}7H_2O$ was added to set the water activity to $a_w = 0.57$, and the lipase was added after 16 h of hydrocyanation reaction with the idea to minimize the exposure of *Me*HNL to benzoic acid. In this first reaction, a low reaction rate of the overall process was observed, resulting in only 10.5% conversion to the corresponding ester with a fair e.e. of 89% after 47 h reaction time. The results, however, showed that both enzymes were simultaneously active after adding the lipase to the reaction mixture, since the 4-anisaldehyde was further converted and (*S*)-4-methoxymandelonitrile benzoate was also formed. The same process was repeated at 25 °C (Table 9, entry 2) resulting in a significantly improved reaction rate, while maintaining the enantiomeric excess of the ester. Based on these observations, all further reactions were performed at room temperature (20 °C).

For comparison, in experiment 3 (Table 9, entry 3) a concurrent approach, where both enzymes were added from the beginning, was tested. Due to the inhibitory effect of 4-anisaldehyde and HCN on the acyltransferase activity of CALA, a higher amount of lipase was added. This approach significantly improved the enantiopurity of the final ester (97% e.e.), while maintaining a good reaction rate. After 30.5 hours of reaction, 10 mM cyanohydrin was still

present in the reaction mixture. This suggested that the transesterification rate was not too high in comparison to the *Me*HNL-catalyzed hydrocyanation. Therefore, it was decided to maintain the CALA/*Me*HNL ratio for further reactions. Strikingly, the results could be further improved by omitting the water buffering salts from the system (Table 9, entry 4). Elimination of these salts provided overall higher yield and selectivity, which may be explained by the previously identified negative effect of low water activity on the enzymatic hydrocyanation reaction. Moreover, comparison of the benzoic acid concentration in experiments 3 and 4 indicated that in the former cascade (including the salts) the hydrolysis reaction was not suppressed to a higher extent than in the latter (without salts). Thus, the use of the salt hydrate pair did not further reduce the hydrolysis reaction in the studied system.

Salt-free experiments with varying initial amounts of benzoyl donor (Table 9, entries 4–6) showed a detrimental effect of higher donor concentrations on the hydrocyanation reaction, while the amount of hydrolysis side product, benzoic acid, increased substantially. In all cases, however, excellent enantiopurity of (*S*)-4-methoxymandelonitrile benzoate (99% e.e.) was maintained throughout the process. These results prompted us to test gradual addition of phenyl benzoate to the process, which was found to minimize the hydrolytic side reaction at the expense of some loss in the benzoylation reaction rate (see Table 9, entry 7), leading to 64% yield of ester **3** (98% e.e.) in 49 h, with 50% less benzoic acid produced compared to Table 9, entry 5.

Furthermore, the possibility of decreasing the amount of HCN used in the cascade was also tested. However, when performing the cascade using 5 instead of 6.5 equivalents of HCN (using the same conditions detailed in Table 9, entry 7), after 122 hours only 60 mM (*S*)-**3** was produced with a poor enantiomeric excess of 87%. Similarly, a decrease in yield and enantioselectivity of (*S*)-**2** was observed in the immobilized *Me*HNL-catalyzed hydrocyanation of 4-anisaldehyde when decreasing the HCN concentration (see Figure 43).

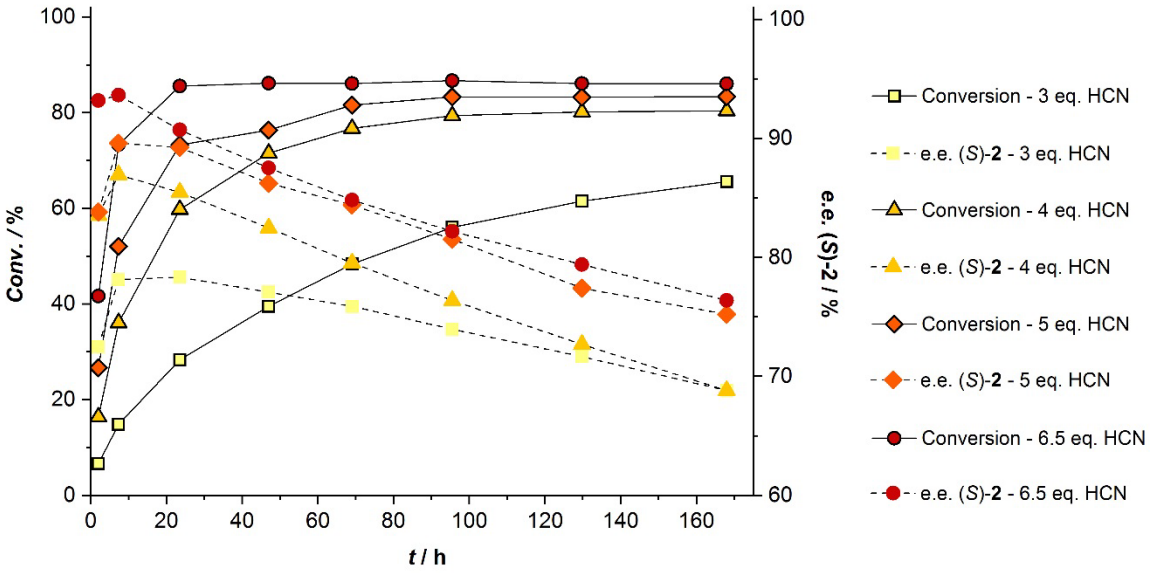

Figure 43. Hydrocyanation of 100 mM 4-anisaldehyde catalyzed by immobilized *Me*HNL using 3-6.5 equivalents of HCN in iPr$_2$O at 20 °C.

Finally, it was hypothesized that a reduction of the lipase units could further decrease the amount of formed benzoic acid. Using 0.5 U/ml CALA afforded ester **3** (98% e.e.) with 81% yield in 122 h, with a total conversion of 4-anisaldehyde of 95% (see Table 9, entry 8). The reaction time required for high conversion values could be reduced by approximately one day when the reaction temperature was increased from 20 to 25 °C (see Table 9, entry 10). For comparison, a *Me*HNL-catalyzed hydrocyanation reaction was performed in parallel to the concurrent cascade reaction from Table 9, entry 8, under the same conditions. After 24 hours the hydrocyanation had reached plateau with a conversion of 85% and an e.e. of just 91%, whereas the bi-enzymatic approach reached also 85% yield of (*S*)-**3** if allowed to react for 164 hours, with an improved e.e. of 96%, as shown in entry 8 of Table 9.

After careful optimization of the variables influencing both enzymatic reactions, the successful concurrent cascade synthesis of (*S*)-4-methoxymandelonitrile benzoate starting from 4-anisaldehyde and catalyzed by *Me*HNL and CALA was accomplished. Systematically studying each enzymatic reaction first was key for their effective combination. When developing the one-pot cascade, however, further fine-tuning of reaction conditions was required to achieve optimal performance. This way, 95% conversion of **1** with 81% yield of the final ester (*S*)-**3** and excellent enantiopurity of 98% e.e. was achieved.

Table 9: Cascade synthesis of (S)-4-methoxymandelonitrile benzoate catalyzed by immobilized *Me*HNL and CALA starting from 100 mM 4-anisaldehyde and 650 mM HCN using 200–400 mM phenyl benzoate in *i*Pr_2O. Reactions were performed in duplicate and relative standard deviations were generally below 2%.

Exp	T (°C)	Equiv. Phenyl benzoate	*Me*HNL (U/mL) [1]	CALA (U/mL) [2]	Time (h)	[1] (mM)	[2] (mM)	e.e. (*S*)-2 (%)	[3] (mM)	e.e. (*S*)-3 (%)	[benzoic acid] (mM)
1[3]	10	3	0.21	0.50 [4]	16	90	10	58	-	-	-
					47	82	7	12	11	89	ND
2[3]	25	3	0.21	0.50 [5]	15	75	25	63	-	-	-
					24	59	11	15	30	90	ND
3[3]	20	2	0.26	2.20	31	47	10	70	43	97	64
4	20	2	0.26	2.20	31	23	21	92	56	99	57
					73	15	23	86	62	98	111
5	20	3	0.26	2.20	31	33	8	76	59	99	109
6	20	4	0.26	2.20	31	45	4	68	51	99	140
7	20	3 [6]	0.26	2.20	49	18	19	74	64	98	56
					122	15	13	79	72	93	210
8	20	3 [6]	0.26	0.50	122	5	14	60	81	98	50
					164	4	11	61	85	96	94
9	20	0	0.26	0	24	15	85	91	-	-	-
10	25	3 [6]	0.26	0.50	94	7	13	46	80	97	39

[1] Activity of immobilized *Me*HNL: 0.03 U/mg. [2]Activity of immobilized CALA: 0.11 U/mg. [3] $Na_2HPO_4{\cdot}2H_2O/Na_2HPO_4{\cdot}7H_2O$ was added (0.34 mmol per mL of reaction). [4] CALA was added after 16 h. [5] CALA was added after 15 h. [6] Gradual addition: Each 1 equivalent of phenyl benzoate was added at the beginning, after 24 h, and after 48 h.

3.2. Novel multi-catalytic route for the synthesis of an *N*-acyl-β-amino alcohol

3.2.1. Design of a 2-step catalytic synthetic route towards (S)-tembanide

As discussed in chapter 1.2, the synthesis of enantiopure β-amino alcohols and their derivatives has been traditionally achieved *via* derivatization of the limited chiral pool of amino acids. However, given the high versatility of these compounds and their multiple biomedical applications, researchers have focused on the development of new chiral routes that do not rely on the availability of a chiral precursor. In this context, the current trend towards more efficient chemical transformations promotes not only the use of catalysts, rather than using activated compounds, but also the reduction of work-up steps by combining two or more reactions into sequential or concurrent cascades [17–19,263–265]. Considering this trend, a cascade synthesis of (*S*)-tembamide (**4**) starting from 4-anisaldehyde (**1**) was envisioned (see Figure 44).

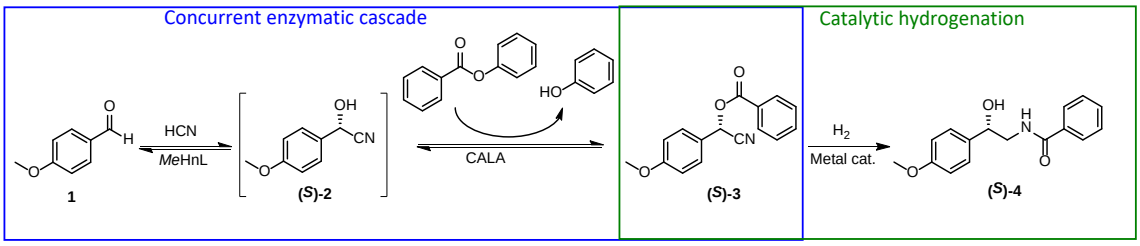

Figure 44. Catalytic asymmetric cascade route towards (*S*)-tembamide.

The first step consists in a concurrent bi-enzymatic synthesis of (*S*)-4-methoxymandelonitrile benzoate ((*S*)-**3**), using immobilized *Me*HNL and CALA as catalysts. In a second step, the nitrile group is catalytically reduced to give (*S*)-tembamide ((*S*)-**4**). The catalytic hydrogenation of acylated cyanohydrins is an approach reported by Veum *et al.* [174], which initially forms an amino-ester intermediate that spontaneously undergoes acyl transfer to yield the corresponding 1,2-hydroxyamide. Our designed pathway towards (*S*)-tembamide constitutes a fully catalytic route that reduces the number of work-up steps with respect to the reported routes [42,43,52–55,44–51] and avoids isolation of the unstable cyanohydrin (*S*)-**2**.

The combination of *Me*HNL and CALA to convert 4-anisaldehyde into (*S*)-4-methoxymandelonitrile benzoate ((*S*)-**3**) in organic solvent could be accomplished by carefully selecting the acylating agent and further optimizing the reaction conditions, as described in section 3.1. The present section focuses on the identification of a proper catalyst and reaction conditions to reduce the chiral acylated cyanohydrin (*S*)-**3** to form (*S*)-tembamide with the highest selectivity.

Besides the intrinsic catalytic nitrile hydrogenation side reactions leading to secondary and tertiary amines depicted in Figure 19, selectivity is very important, since the reactions at other functional groups in the molecule would result in other undesired side products. For example, the C–O bond of the benzyloxy group is especially susceptible to hydrogenolysis, due to the phenyl ring of the cyanohydrin fragment (see Figure 45) [174,266,267]. Furthermore, the hydrogenation conditions may affect the chiral center of the reactant resulting in racemization [189]. For example, even under optimized conditions, Veum *et al.* observed in their study on the catalytic hydrogenation of (*S*)-mandelonitrile acetate a decrease in enantiopurity of the resulting (*S*)-*N*-(2-hydroxy-2-phenylethyl)acetamide (*i.e.*, a decrease in e.e. from 95% to 75%) [174]. In contrast, Hertzberg *et al.* accomplished the hydrogenation of benzylic *O*-acyl cyanohydrins with little or no racemization using milder temperature [268,269].

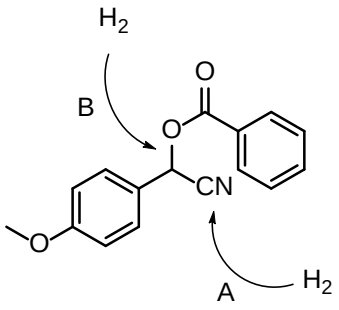

Figure 45. In addition to the desired hydrogenation of the nitrile group (A), 4-methoxymandelonitrile benzoate may undergo hydrogenolysis of the C–O bond in the benzyloxy group (B) under catalytic hydrogenation conditions.

3.2.2. Catalyst screening

Previous studies have shown that the combination of amorphous Ni catalysts with $NaBH_4$ or KBH_4 in alcohol solvents can selectively reduce nitriles – which are generally not reduced when using the borohydride alone [182] – under conditions that were compatible with ester groups [181,182]. Based on this information, we presumed that a Raney Ni-$NaBH_4$ transfer hydrogenation of compound **3** should provide higher selectivity towards primary amines (vs catalytic hydrogenation) as well as suitable functional group tolerance, at the expense of increased metal waste. Therefore, we initially investigated the reduction of (±)-**3** using 4 mol equivalents of $NaBH_4$ and 0.25 g of Raney Ni per gram of substrate in ethanol or *tert*-butanol at room temperature. ^{1}H NMR analysis showed that compound **3** was fully converted in both cases after 2 hours, but no tembamide was formed. This was thought to be due to poor chemoselectivity, leading to the reduction of the benzyloxy C-O bond. Since the advantage of this approach should be higher selectivity, no additional efforts were directed to further investigate and optimize this concept.

As discussed in section 1.5, the chemoselectivity of the catalytic hydrogenation of nitriles greatly depends on the catalyst's nature, although other factors such as the substrate structure, the loading of catalyst, reaction temperature and hydrogen pressure also have an impact on the reaction outcome. In order to hydrogenate the nitrile in compound (*S*)-**3** with the highest yield towards (*S*)-tembamide, minimizing the hydrogenolysis of the C−O bond from the benzyloxy group and the formation of secondary and tertiary amines, a transition metal catalyst screening was performed. With the idea of achieving the total synthesis of tembamide in a one-pot-two-step fashion, the initial screening was performed under mild conditions that could facilitate the overall process, including potential recycling of the enzymes. Additionally, by working under milder conditions we hoped to improve the enantioretention of the chiral center with respect to the loss in chirality observed by Veum *et al.* [174]. The hydrogenation reactions were carried out at room temperature under 1 bar of H_2 in dioxane, this being the solvent of choice in the optimized catalytic nitrile hydrogenation reactions previously reported [174,268,269].

Table 10 shows the results of the metal-catalyzed conversion of (±)-**3** under the aforementioned conditions. Although conversion of the substrate was observed in all cases, not all the catalysts afforded tembamide as a product, and only low chemoselectivity towards the desired product was observed in the cases where tembamide was formed.

While Pd on carbon (Pd (C)) afforded full conversion of (±)-**3**, tembamide was not formed. ^{1}H NMR spectroscopy identified benzoic acid as one of the reaction products and a control reaction under N_2 atmosphere afforded no conversion of the acyl cyanohydrin, indicating that benzoic acid was formed *via* hydrogenolysis (see Table 10, entry 1).

Raney Co and Ni on Al_2O_3/SiO_2 (Ni@Al_2O_3/SiO_2 65%) catalyzed the hydrogenation of (±)-**3** with low conversion (see Table 10, entries 2 and 3). Raney Co is frequently used at high dihydrogen pressure and elevated temperature [270], which might explain its poor performance under the initial screening conditions. It is, nevertheless, an attractive catalyst because of its typically high chemoselectivity, especially when seeking to reduce nitrile groups in the presence of other potentially reactive moieties [270]. Regarding Ni@Al_2O_3/SiO_2 65%, it has been shown that the catalytic activity of Ni on alumina can be enhanced after a pre-activation treatment under high H_2 pressure and high temperature [174]. This might also be the case for Rh on Al_2O_3 (Table 10, entry 7), which afforded tembamide in negligible yields.

Raney Ni, Rh on silica (Rh@SiO_2 1%) and Rh on carbon exhibited high conversion of the ester (> 90%) along with similar chemoselectivity towards tembamide, with yields ranging between 4% and 5% (see Table 10, entries 4, 5 and 6). $RhCl_3 \cdot 3H_2O$ and $RuO_2 \cdot H_2O$, which catalyzed the hydrogenation of (±)-**3** with lower conversion, but without tembamide formation, were not

further considered (see Table 10, entries 8 and 9). The hydrogenation using Rh@SiO_2 1% was also performed in diisopropyl ether (*i*Pr_2O), resulting in higher selectivity compared to the reaction in dioxane (Table 10, entry 10). Since the first two enzymatic reactions of the final cascade are performed in diisopropyl ether, this solvent was chosen for further optimization.

Table 10: Catalyst screening for the catalytic hydrogenation of 19 mM (±)-**3** at room temperature (25 °C) under 1 bar of H_2.

Entry	Catalyst	Catalyst loading (g/g) [1]	Solvent	Conversion (%)	Tembamide yield (%) [2]	Selectivity (%) [3]
1	Pd (C) [4]	0.25	dioxane	100	0	0
2	Raney Co 86% slurry	2.2	dioxane	23	0.1	0.2
3	Ni@Al_2O_3/SiO_2 65%	1	dioxane	19	0	0
4	Raney Ni 50% slurry	2	dioxane	92	4.4	4.9
5	Rh (C) 5%	1	dioxane	100	4.5	4.5
6	Rh@SiO_2 1%	3	dioxane	38	1.1	2.9
7	Rh@Al_2O_3 5%	1	dioxane	53	0.3	0.6
8	$RhCl_3 \cdot 3H_2O$	1	dioxane	47	0	0
9	$RuO_2 \cdot H_2O$	1	dioxane	37	0	0
10	Rh@SiO_2 1%	3	*i*Pr_2O	45	4	8.9

[1] g of catalyst / g of starting material. [2] Yield determined by HPLC analysis. [3] Selectivity calculated as (tembamide yield)/(conversion)×100. [4] A negative control using Pd (C) under N_2 atmosphere was performed.

In contrast to the results obtained by Veum *et al.* using 120 °C and 20 bar of H_2 as optimized conditions [174], our initial catalyst screening results performed at room temperature and 1 bar of H_2 afforded only very low yields of tembamide. Hence, we speculated that the catalysts' chemoselectivity to hydrogenate the nitrile moiety instead of the C−O bond could be enhanced by increasing the temperature and/or H_2 pressure. Additionally, the intramolecular acyl migration might be facilitated by increased temperatures. Therefore, a second catalyst screening was performed at 100 °C under 5 bar of H_2 (see Table 11). For this purpose, the catalysts that had afforded tembamide under the initial conditions, as well as Ni@Al_2O_3/SiO_2 65% (which was expected to perform better after pre-activation under high temperature and H_2 pressure) were selected.

Table 11: Catalyst screening for the catalytic hydrogenation of (±)-**3** 19 mM under 100 °C and 5 bar of H_2 in diisopropyl ether. Reactions stopped after 2.5 hours of reaction.

Entry	Catalyst	Catalyst loading (g/g) [1]	Conversion (%)	Tembamide yield (%) [2]	Selectivity (%) [3]
1	Ni@Al_2O_3/SiO_2 65% [4]	1	94	12	12
2	Raney Ni 50% slurry	3.5	100	25	25
3	Raney Co 86% slurry	3.5	69	13	19
4	Rh (C) 5%	1	100	0	0
5	Rh@SiO_2 1%	2.5	100	0	0
6	Rh@Al_2O_3 5% [4]	1	100	0	0

[1] g of catalyst / g of starting material. [2] Yield determined by HPLC analysis. [3] Selectivity calculated as (tembamide yield)/(conversion)×100. [4] Catalyst was preactivated at 120 °C under 10 bar of H_2 in *i*Pr_2O.

As expected, the pre-activation of Ni@Al_2O_3/SiO_2 65% as well as the higher temperature and hydrogen pressure allowed for the formation of tembamide (see Table 11, entry 1). In the case of the Raney catalysts, the selectivity towards tembamide was greatly increased with respect to the initial screening (Table 11, entries 2 and 3). Surprisingly, none of the rhodium catalysts afforded the desired product under the new reaction conditions, although full conversion was reached in these cases (see Table 11, entries 4, 5 and 6). Although the catalytic hydrogenation of nitriles has been widely studied, there is no general method that affords the desired products with highest selectivity and yields, and therefore, optimization of the reaction parameters is always required for optimal results. In this context, there appears to be no clear trend in the reported effect of temperature and H_2 pressure on the reaction selectivity [177,184,190,271]. The effect of H_2 pressure has been reported to directly influence the relative hydrogenation/condensation rates involved in the synthesis of primary, secondary and tertiary amines [177]. The higher yields observed when increasing the temperature in the case of Ni and Co catalysts may be attributed to a positive change in the relative ratios of the hydrogenation/hydrogenolysis and the hydrogenation/condensation rates. In addition, the higher temperature may also favor the acyl migration necessary for the formation of tembamide.

In order to better understand the reaction and the process leading to the formation of undesired products, the stability of (±)-tembamide was evaluated in parallel under hydrogenating conditions in the presence of Ni@Al_2O_3/SiO_2 65%. After 2 hours of reaction, 30% of tembamide had been depleted and several degradation products were observed in HPLC. A control in the absence of catalyst showed no reaction, indicating that the degradation of tembamide was due to a hydrogenation process.

3.2.3. Selection of catalyst and optimization of reaction temperature

Given the superiority of the Raney catalysts in terms of selectivity towards tembamide, a reaction temperature optimization was performed under 5 bar of H_2 in order to select the best catalyst (see Figure 46).

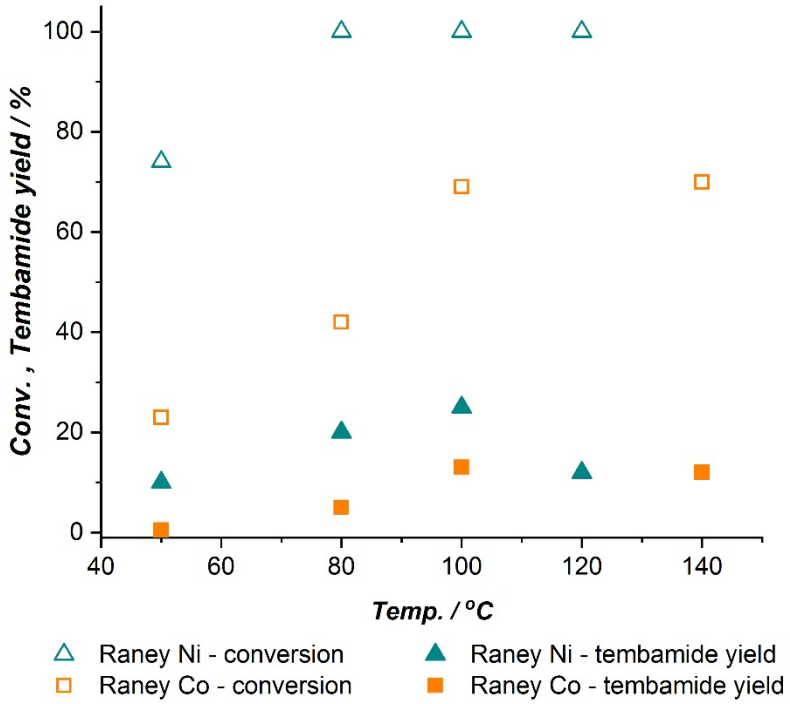

Figure 46. Effect of reaction temperature on the hydrogenation of 19 mM (±)-**3** catalyzed by Raney Ni and Raney Co under 5 bar of H2 in *i*Pr_2O, using 3.5 grams of catalyst per gram of substrate. Reactions performed at 80 °C and below were run for 5 hours, whereas reactions run at 100 °C and above where stopped after 2.5 hours.

Raney Ni showed a temperature optimum around 100 °C, while lower yields of tembamide were obtained at higher and lower temperatures. Raney Co performed best also at 100 °C, since increasing the temperature up to 140 °C did not afford higher conversion or yield towards tembamide. Both catalysts were then tested at 100 °C and 10 bar of H_2. In the case of Raney Ni, lower selectivity towards tembamide was observed (21% tembamide yield, 100% conversion), whereas Raney Co afforded slightly higher conversion (76%) and tembamide yield (17%) than at lower pressure. The results indicate that Raney Co generally requires higher temperature and H_2 pressure to afford tembamide with similar selectivity as Raney Ni, albeit with lower reaction rate. Since variations in the H_2 pressure did not have a strong effect on the reaction performance, this parameter was set at 5 bar and Raney Ni was selected for further optimization of the reaction conditions.

Having selected the catalyst, a test was performed to evaluate the enantioretention of the chiral center during the hydrogenation reaction. The hydrogenation of 19 mM (*R*)-4-methoxymandelonitrile benzoate (99% e.e.) catalyzed by Raney Ni at 100 °C under 5 bar of H_2, afforded 25% (*R*)-tembamide with 98% e.e..

3.2.4. Identification of side products and further optimization of reaction parameters

Using high resolution GC−MS analysis of a crude reaction mixture obtained after hydrogenation, three major side products were identified (Figure 47, compounds **5** - **7**). Formation of benzoic acid (**5**) and 4-methoxy benzyl cyanide (**7**) can be explained by hydrogenation of the benzylic C−O bond of compound **3**. The presence of the secondary amine **6** is supported by the mechanism proposed in Figure 19, involving reduction products of compound **7** and possibly other reaction intermediates. We infer that hydrogenolysis of the benzylic C−O bond is one of the major side reactions, which leads to products such as **6** and **7** that can trigger the formation of other side products such as secondary and tertiary amines, further depleting the tembamide yield. Previous reports have indicated that the addition of NH_3 minimizes the formation of secondary and tertiary amines [185,186]. However, this additive can also result in the formation of other undesired products, as observed by Veum *et al.* for the catalytic hydrogenation of acylated cyanohydrins [174]. Furthermore, we surmised that if the nitrile hydrogenation takes place selectively, the β-amino ester quickly undergoes transacylation to tembamide and, thus, will not participate in secondary amine formation pathways. Based on these considerations, no efforts were made towards the addition of additives such as NH_3 to avoid secondary and tertiary amine formation.

Additionally, NMR analysis of a column chromatography fraction established the presence of the side product **8** (Figure 47). The amine formed *via* hydrogenation of compound **7** may react in a nucleophilic acyl substitution with another species bearing a benzoyl group to yield compound **8**. Alternatively, this side product may result from the hydrogenolysis of the C−OH bond after tembamide formation, considering that tembamide was shown to react under hydrogenating conditions. Therefore, the identification of an optimal reaction time to avoid tembamide degradation appears to be crucial.

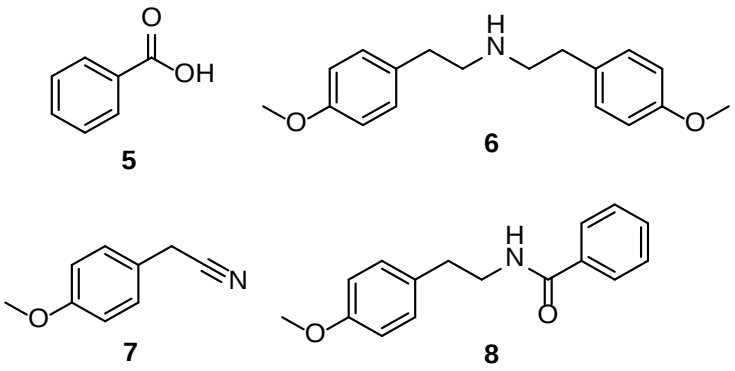

Figure 47. Identified major side products of the hydrogenation of 4-methoxymandelonitrile benzoate.

The presence of water in the reaction medium also influences the catalytic hydrogenation of nitriles, but, so far, the studies on the specific effect of water on the product distribution and reaction rate are inconclusive. Volf *et al.* reported increased reaction rate and selectivity towards primary amines upon addition of water when using unsupported Ni and Co catalysts, while the contrary effect is observed when using supported catalysts [272]. In the case of Pt(C)-catalyzed hydrogenation of benzonitrile, increased selectivity towards primary amines was reported when small quantities of water were added [273]. However, it has also been claimed that water increases the reaction rate, while having only a negligible effect on the chemoselectivity when supported Pt and Ru catalysts are used [274]. Veum *et al.* observed a slightly positive effect on the reaction yield when adding water in the hydrogenation of aliphatic acylated cyanohydrins, but reported no effect on benzylic acylated cyanohydrins [174]. Additionally, studies on acyl migration of monoacylglycerols have shown that water addition influences the migration rate, which could also affect the yield of tembamide in our reaction [275]. Furthermore, the addition of water could increase the risk of hydrolysis of benzoylated species. To evaluate the effect of water on the hydrogenation of (±)-**3**, two experiments were carried out (Table 12, entries 1 & 2) where water was either removed or added to the system. The addition of 4 Å molecular sieves to remove water had a slightly negative effect on the yield towards tembamide compared to reactions without molecular sieves (Table 12, entry 2). This might imply that small quantities of water have, actually, a beneficial effect on the catalyst performance, whereas a complete removal would be counterproductive. The addition of 2.5% v/v water, however, resulted in a dramatically lower yield of tembamide and a higher concentration of benzoic acid (5.7 mM when using molecular sieves vs 8 mM with water addition). Unfortunately, we cannot differentiate to what extent this is caused by increased hydrogenolysis, hydrolysis or other processes. Therefore, no further experiments were directed towards optimizing the amount of water in the reaction medium and it was decided to proceed without further removal or addition of water.

Table 12: Optimization of parameters influencing the yield towards tembamide in the hydrogenation of (±)-**3** catalyzed by Raney Ni at 100 °C under 5 bar of H_2 in diisopropyl ether.

Entry	Catalyst loading (g/g) [1]	(±)-3 (mM)	Additive	Reaction time (h)	Conversion (%)	Tembamide yield (%) [2]	Selectivity (%) [3]
1	3.5	19	4 Å molecular sieves[4]	2.5	100	21	21
2	3.5	19	2.5% Milli-Q water	2.5	100	6	6
3	3.5	19	-	2	100	24	24
4	0.5	19	-	1	100	27	27
5	0.25	19	-	1	96	20	21
6	0.5	112	-	2	98	16	16
7	0.5	84	-	2	95	17	18

[1] g of catalyst / g of starting material. [2] Yield determined by HPLC analysis. [3] Selectivity calculated as (tembamide yield)/(conversion)×100. [4] A small spatula point of molecular sieves, previously crushed and pre-activated in vacuum oven, was added.

The catalyst loading and substrate concentration were also expected to impact the reaction performance. First, the catalyst loading was adjusted (see Table 12, entries 3-5). A reduction of the catalyst/substrate ratio was desirable in terms of atom economy and could potentially alter the selectivity of the reaction. An experiment was performed decreasing the Raney Ni loading to 0.5 $g/g_{substrate}$, whereupon a slight increase in selectivity was observed. Further decreasing the catalyst loading to 0.25 $g/g_{substrate}$ resulted in a lower tembamide yield. Thus, for future experiments the catalyst loading was set to 0.5 $g/g_{substrate}$.

In order to evaluate the effect exerted by the substrate concentration, a hydrogenation experiment was performed starting from a saturated solution of (±)-**3** (Table 12, entry 6). Also, based on the concentration of the ester obtained *via* the biocatalytic cascade, a hydrogenation reaction using 84 mM (±)-**3** was performed (Table 12, entry 7). Increasing the concentration of 4-methoxymandelonitrile benzoate had a negative influence on the selectivity of the hydrogenation reaction, leading to a decreased tembamide yield. We hypothesize that this detrimental effect associated with an increased substrate concentration results from a competition between the *O*-benzoyl cyanohydrin and the partially reduced imino intermediate (see Figure 19, compound II) on the catalyst surface, where compound **3** outcompetes the imino intermediate at higher concentrations. This situation, combined with the higher concentration of free amines – resulting from a higher substrate concentration – would increase the rate of the condensation reaction between the imino intermediate and the amines, and therefore limit the hydrogenation of intermediate II that should eventually lead to tembamide.

The optimization of the hydrogenation conditions was performed intermittently in a time span of three years. Raney Ni was purchased fresh at the beginning of this project and when the Raney Ni-catalyzed hydrogenation of **3** was performed under the optimized conditions (100 °C, 5 bar of H_2, using 0.5 g catalyst per gram of substrate, with a substrate concentration of 19 mM in *i*Pr_2O) after 3 years, it was found that the catalyst had lost activity (see Table 13, entry 1). Raney Ni generally underwent several washing cycles before adding it to the reaction solution, in order to avoid hydrolysis. After two initial washes with demineralized water to remove aluminum salts and ensure neutral pH, it was rinsed two times with ethanol and finally two times with diisopropyl ether to remove the water. However, the observed loss of catalytic activity over time prompted us to evaluate the effect of washing the catalyst. Two hydrogenation experiments were performed using the aged Raney Ni, which was either washed following the mentioned procedure (Table 13, entry 1) or simply centrifuged to remove the supernatant (Table 13, entry 2).

Table 13: Effect of catalyst washing in the Raney Ni-catayzed hydrogenation of (±)-**3** at 100 °C under 5 bar of H_2 in diisopropyl ether. For this experiment, 0.5 g of aged Raney Ni (3 years old) was used per gram of substrate.

Entry	(±)-3 (mM)	Pre-treatment	Conversion (%)	Tembamide yield (%) [1]	Selectivity (%) [2]
1	19	Washed & centrifuged	23	2	9
2	19	Centrifuged	73	15	20

[1] Yield determined by HPLC analysis. [2] Selectivity calculated as (tembamide yield)/(conversion)×100. Reactions stopped after 2 hours.

As shown in Table 13, surprisingly, washing the catalyst actually reduced the hydrogenation rate by 70% and also significantly decreased the selectivity towards tembamide. The washing procedure, thus, did not have the expected positive effect, but rather lowered the reaction performance. A possible explanation for the change in selectivity could be that alkaline salts contained in the slurry (pH = 10.3) might actually favor the formation of primary amines over secondary and tertiary amines [188]. However, the results obtained here are not in agreement with previous experiments on the effect of washing Raney Ni, where no effect was observed on the catalyst's activity after washing several times with water [276].

3.2.5. Preparative synthesis of (S)-tembamide

As a proof of concept, once all hydrogenation conditions had been optimized, we aimed for a preparative one-pot, two-step chemo-enzymatic synthesis of (*S*)-tembamide. Based on our previous studies [277], the enzymatic cascade leading to (*S*)-**3** afforded a crude solution containing approximately 80-85 mM (*S*)-**3**, 10-15 mM **2**, 5-10 mM **1**, 180 mM phenyl benzoate, 40

mM benzoic acid and a maximum of 550 mM HCN. Given the high concentration of HCN and its susceptibility to hydrogenation [278,279], its effect on the hydrogenation of **3** was evaluated. For optimal selectivity, a concentration of **3** in the range of 20 mM was selected, for which the biocatalytic crude reaction mixture would undergo a 4-fold dilution prior to the reduction step. Therefore, the final HCN concentration in the autoclave was estimated to be around 120 mM. Thus, a hydrogenation reaction of 19 mM (±)-**3** with addition of 120 mM HCN and a control reaction without HCN were performed, using unwashed Raney Ni under 5 bar of H_2. For safety reasons, a setup was used that limited the reaction temperature to 70 °C. After 1 hour, the control reaction had afforded 60% conversion of (±)-**3**, whereas the reactor containing HCN showed no conversion of the benzoylated cyanohydrin. These results established the need to evaporate the crude reaction mixture from the enzymatic cascade in order to eliminate the HCN, followed by subsequent re-dissolution in *i*Pr_2O prior to the hydrogenation step.

The required evaporation of the biocatalytic reaction crude mixture opened up the possibility to use a different solvent for the hydrogenation step. A qualitative evaluation of solvents performed at 100 °C under 5 bar of H_2, showed that the selectivity towards tembamide decreased in the following order: *i*Pr_2O > 1,4-dioxane ≈ *t*BME > methyl benzoate > isopropanol > toluene. Therefore, 1,4-dioxane was tested once more under optimized conditions, being this the preferred solvent for catalytic hydrogenations of acyl cyanohydrins in the literature [174,268,269]. However, after 40 minutes of hydrogenation catalyzed by unwashed Raney Ni in 1,4-dioxane, almost full conversion was reached (98%) but only 14% tembamide was formed. In light of this result, diisopropyl ether was maintained as solvent for the preparative chemo-enzymatic synthesis of (*S*)-tembamide.

In the first attempt to synthesize (*S*)-tembamide from the re-dissolved biocatalytic reaction crude containing 19 mM (*S*)-**3** (97% e.e.) using unwashed Raney Ni under the optimized conditions, the hydrogenation reaction was stopped after 40 minutes. With such short reaction time, a conversion close to 100% and a maximum yield of tembamide was aimed for by avoiding excessive product degradation due to a long reaction time. However, the reaction proved to be much slower than when starting from pure **3**, resulting in a conversion of 45% and affording tembamide with 9% yield (95% e.e.). The decrease in reaction rate was attributed to the presence of other species that can also undergo hydrogenation, especially phenyl benzoate, which is present in much higher concentration than (*S*)-**3**. Therefore, a longer reaction time was required to achieve full conversion. Regarding the enantioretention, the enantiomeric excess of tembamide experienced only a minor loss, as had been confirmed previously during the hydrogenation of (*R*)-**3** (see section 3.2.3.).

Once all hydrogenation reaction parameters were defined, the synthesis of (*S*)-tembamide starting from 300 mg 4-anisaldeyde was performed. The scaled-up biocatalytic cascade (22 mL) afforded (*S*)-**3** with 80% yield and 99% e.e. After separation of the immobilized enzymes and evaporation of the volatiles, the crude was re-dissolved in diisopropyl ether to a concentration of 21 mM (95 mL) and the hydrogenation reaction was performed under the optimal conditions for 90 minutes. Chiral HPLC analysis showed that (*S*)-tembamide had been successfully synthetized with 32% yield and 98% e.e.. Column chromatography purification followed by recrystallization of the enriched fractions afforded colorless crystals of pure (*S*)-tembamide with excellent enantiopurity (98% e.e.), albeit with a total isolated yield of 15% (91 mg).

While intermediate (*S*)-**3** was obtained with a fair yield, the low selectivity of the nitrile hydrogenation resulted in total HPLC yield of the 2-step cascade of only 26%, although (*S*)-tembamide was obtained with an excellent enantiomeric excess of 98%. Nevertheless, the 32% yield of the hydrogenation step obtained in this experiment is higher than the maximum yield obtained during the optimization of the hydrogenation of pure (±)-**3** (27%, as reported in Table 7, entry 4). It is hard to determine to what extent the factors that differentiate the preparative scale experiment from the optimized hydrogenation of pure **3** – such as the presence of other species, combined with the longer reaction time or the larger reaction volume – may have influenced the reaction chemoselectivity in order to afford a higher yield. Most likely, the fact of not washing the catalyst contributed to this improvement, as suggested by the results from Table 13.

3.3. HheG engineering for enhanced cyanolytic activity

3.3.1. Expression test of HheG in 96-deep-well plates

Prior to developing a method for the evaluation of the cyanolytic activity of HheG mutant libraries, it was necessary to identify optimal conditions for HheG over-expression in 96-deep-well plates. The selected host organism for the production of recombinant HheG is *Escherichia coli* (*E. coli*) BL21 (DE3) Gold, which provides a well-established platform for protein expression, given its fast growth kinetics, capacity to easily reach high density cultures, inexpensive media required and fast and easy transformation with exogenous DNA [280]. *E. coli* BL21 (DE3) Gold carrying the pET-28a(+)-hheG vector was used for this purpose [122], which provides His-tagged HheG, facilitating its purification when necessary. In a previous expression test performed by Julia Koopmeiners, 22 °C had been identified as the optimal expression temperature affording the highest amount of soluble protein [123]. Therefore, our aim was to determine the best expression time for the production of HheG in 96-deep-well plates. Expression was carried out using TB

medium, this being richer than LB and lacking NaCl, which might lead to interfering halogenation reactions later on. An overnight pre-culture was diluted 9× with medium and expression was induced by adding 0.2 mM IPTG. The cultures were incubated for a total of 48 h at 22 °C, OD_{600} of each well was measured after 3.5, 7, 24 and 48 h and the cell pellets of duplicate samples corresponding to an OD_{600} = 1 for the first time point and OD_{600} = 2 for all other time points were stored at -20 °C. Additionally, the content of each one well was withdrawn after 24 h (A6) and 48 h (A8) of incubation and the cell pellets were stored at -20 °C for future evaluation of the biocatalytic activity. As can be seen in Figure 48, SDS-PAGE of the soluble (S) and pellet (P) fractions of the samples taken at each time point showed a higher concentration of insoluble protein than of soluble protein in the range of 30 kDa. This corresponds to HheG, which, together with the His-tag, has a predicted molecular weight of 29.9 kDa [112].

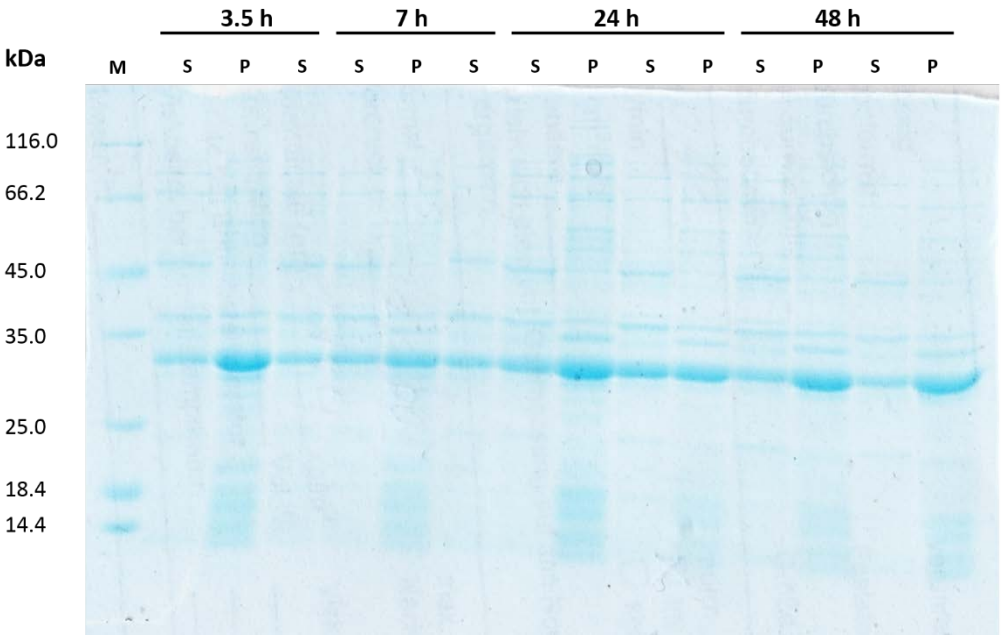

Figure 48. Progression of protein expression over time (3.5 h, 7 h, 24 h and 48 h after induction) in the expression test of HheG in deep-well plate format using pET-28a(+)-hheG vector in *E. coli* BL21 (DE3) Gold as expression host. The soluble protein fractions (S) were obtained after incubation of the cell pellets with the cell lysis reagent B-PER (40 µL) and subsequent centrifugation to remove cell debris. The insoluble pellet fraction (P) after centrifugation was resuspended in 40 µL B-PER. For samples collected after 3.5 h, 20 µL B-PER was used both for cell lysis and resuspension of the insoluble fraction. Both S and P samples were 4× diluted with Milli-Q® water and incubated with 33% (v/v) loading dye before loading 7 µL in each lane. Samples were taken in duplicate for all time points. All samples were loaded on the gel except for the insoluble pellets of each one duplicate after 3.5 h and 7 h of incubation.

The higher concentration of HheG in the insoluble pellet could be due to an incomplete lysis caused by insufficient incubation time with the cell lysis reagent B-PER or due to a significant production of the protein in inclusion bodies. However, the amount of soluble protein might be enough for the catalytic evaluation of HheG variants. What must be noted is that expression of

HheG was practically constant over time, when normalized with respect to the OD_{600} value, since the intensity and size of the HheG band does not change significantly between samples of different time points.

To evaluate the suitability of the expression procedure for activity screening of HheG mutant libraries, cyanolysis reactions using the cell content of wells A6 (24 h, OD_{600} = 6) and A8 (48 h, OD_{600} = 7) were performed. The cyanolysis of 10 mM cyclohexene oxide using 20 mM CN^- in 50 mM phosphate buffer at pH 8.0 was performed by adding the reagent solutions directly to the thawed cell pellets with subsequent incubation at 25 °C and 800 rpm. For reaction analysis, an achiral GC method was developed for the separation of substrate and product, and a suitable internal standard was selected. After 4 h of reaction, the products of both reactions were extracted with *t*BME and the conversion was determined using the newly developed GC method. The GC chromatograms in Figure 49 show that both A6 and A8 exhibited similar conversion values (10% and 11.5%, respectively), indicating that an expression time of 24 h is sufficient for the evaluation of mutant libraries in 96-deep-well plates.

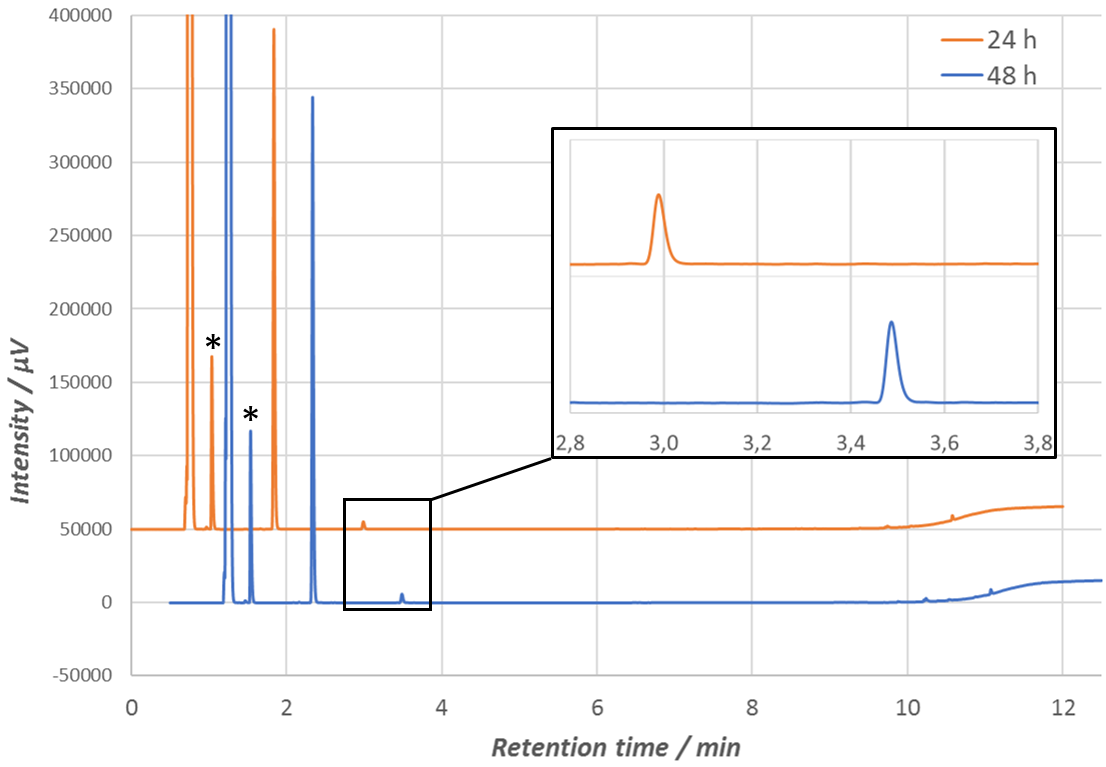

Figure 49. GC chromatograms of the cyanolysis reaction of cyclohexene oxide catalysed by the cell pellets of *E. coli* BL21 (DE3) Gold pET-28a(+)-hheG from the expression test 24 h (orange) and 48 h (blue) after induction. Reactions were performed at room temperature for 4 hours. Cyclohexene oxide peaks are identified with an asterisk (*) and the peaks of the product 2-cyanocyclohexanol are amplified and highlighted with a black box.

3.3.2. Site-saturation mutagenesis of HheG at position T154

As mentioned in section 1.6.1., the direct transfer of the cyanolysis-enhancing mutation T134A of HheC to HheG (*i.e.* T154A) performed by Julia Koopmeiners did not lead to a mutant with improved cyanolytic activity. However, due to the location of Thr154 near the catalytic triad, it was deemed an important residue and, given the relevance of HheG for its ability to convert cyclic epoxides as well as a range of acyclic di-substituted epoxides [115], further efforts were directed towards generating putative variants with higher cyanolytic activity. To this end, position 154 of HheG was randomized using site-saturation mutagenesis (SSM) with primers carrying an NNS codon. For this, vector pET-28a(+)-hheG was amplified using QuikChange® PCR with the degenerated forward (fwd) and reverse (rev) primers [281,282]. Two pairs of NNS-T154 forward and reverse primers with different lengths were used in separate PCR reactions in order to maximize the chances of success, ensuring that enough PCR product was available for transformation. After the PCR reaction, the parental DNA was digested using DpnI and the product was analyzed on an agarose gel. As shown in Figure 50, although PCR product was obtained in both reactions, the longer primers NNS-T154-2-fwd and -rev afforded a higher concentration of PCR product. The absence of other bands indicated that the PCR proceeded without errors.

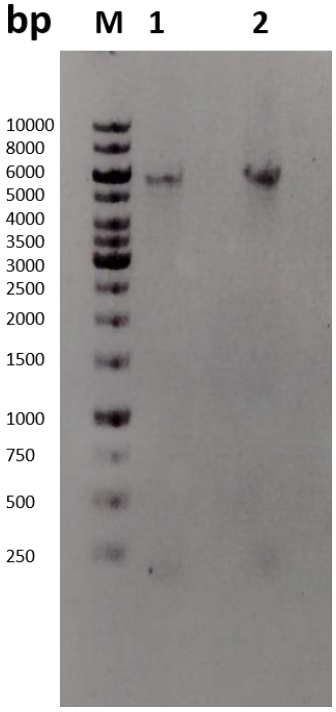

Figure 50. QuikChange® PCR products using degenerate primers NNS-T154-1-fwd and -rev (1) as well as NNS-T154-2-fwd and -rev (2). The first lane corresponds to Thermo Scientific GeneRuler 1kb DNA Ladder.

Chemically competent *E. coli* DH5α cells were transformed with the respective PCR products [pET-28a(+)-hheG(NNS-T154-1) and pET-28a(+)-hheG(NNS-T154-2] and transferred to LB Agar plates containing kanamycin. Around 70 and 160 colonies were obtained for the libraries generated with primer pairs NNS-T154-1 and NNS-T154-2, respectively, which is in accordance with the difference in the band intensity on the agarose gel. The number of colonies covers the expected library size in order to achieve 95% coverage of all possible substitutions (*oversampling factor* × (*number of possible bases* ^ *number of positions at codon* = $3\times(4^2\times2^1)$ = 96) [209]. From each agar plate, two colonies were picked for sequencing, showing that the wild-type codon ACC (threonine) had been substituted by CCC (proline), CAG (glutamine), CAC (histidine) and GGC (glycine) (see Figure 51). This result suggested a high quality of the SSM library, indicating that probably all 20 amino acids were present in the library. The colonies of both plates were combined and plasmid DNA was isolated. Successful mutagenesis was confirmed after sequencing of the isolated vector library (see Figure 51).

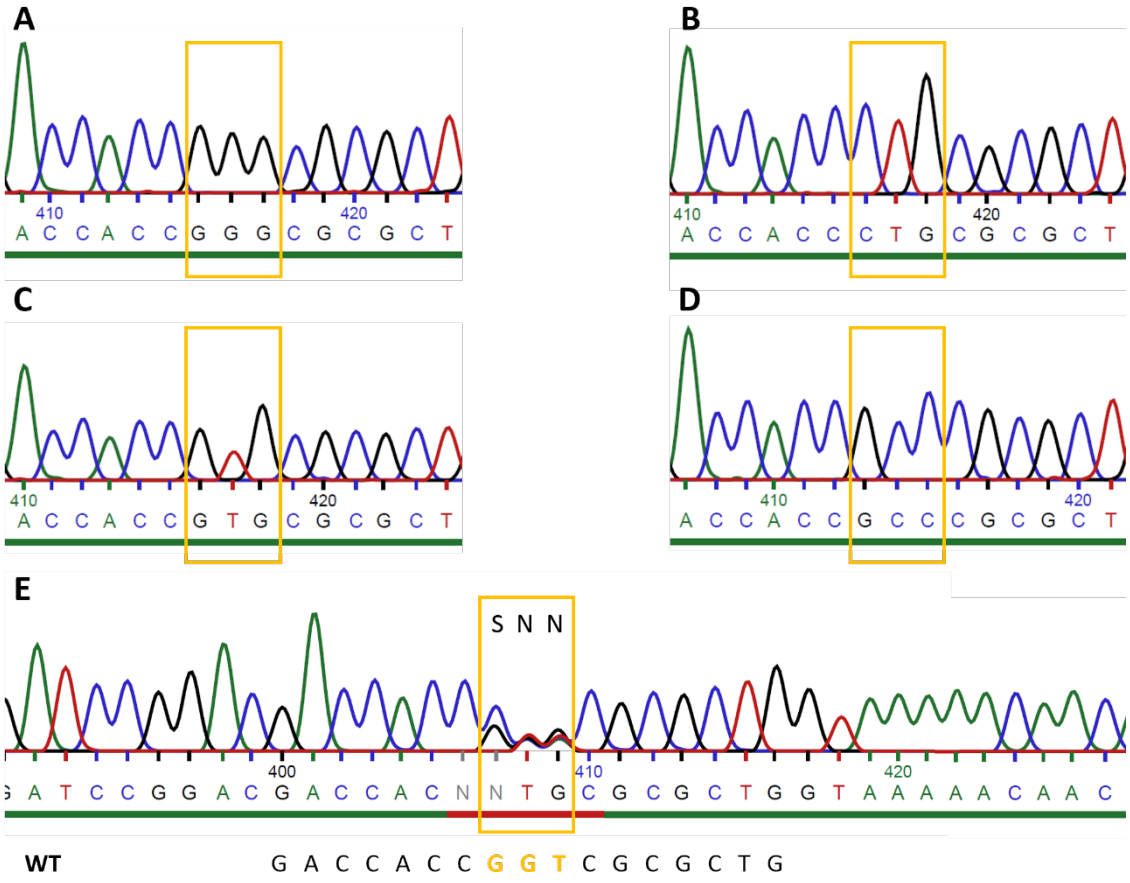

Figure 51. Sequencing result of single colonies (A-D) as well as the combined plasmid library (E) from the site-saturation mutagenesis of HheG at position 154. The reverse complement sequence is shown with position 154 highlighted with a yellow box. For comparison, the reverse complement sequence of wild-type HheG is shown underneath the combined plasmid library sequence.

The library DNA was transformed into chemically competent *E. coli* BL21 (DE3) Gold cells and 92 of the resulting colonies were transferred into a 96-well microtiter plate for cultivation and protein expression. The mutant library was subsequently screened for cyanolytic activity using cyclohexene oxide as substrate, as described in Section 2.2.2.3. (see Figure 52). As shown in Table 14, none of the library colonies exhibited higher activity than the WT control.

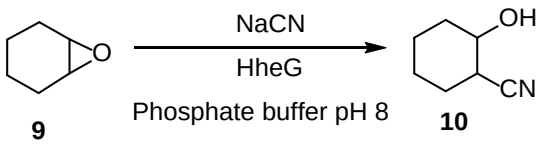

Figure 52. Cyanide-mediated epoxide ring-opening of cyclohexene oxide was used as screening assay for cyanolytic activity of HheG variants.

Table 14: Results of the cyanolysis of cyclohexene oxide catalysed by HheG SSM mutants at position T154. The values show the conversion (%) of cyclohexene oxide to 2-cyanocyclohexanol after 5 h 45 min. Reactions were performed using whole cells expressed in 96-deep-well plates, 10 mM cyclohexene oxide and 20 mM NaCN. Grey indicates empty vector (negative) controls and green shows HheG wild-type controls. Blue marks variants with at least 60% relative activity with respect to the wild-type controls.

	1	**2**	**3**	**4**	**5**	**6**	**7**	**8**	**9**	**10**	**11**	**12**
A	26.7	5.5	17.6	9.0	6.3	0	0	0	0	0	5.2	8.7
B	0	0	0	4.1	24.7	0	0	4.4	9.8	0	19.4	0
C	0	0	0	7.2	0	4.1	0	0	0	0	0	7.8
D	4.1	0	5.5	0	10.4	0	26.8	10.7	3.7	7.0	7.6	12.4
E	13.7	4.5	8.9	4.7	0	0	4,0	0	0	15.1	11.5	0
F	8.1	0	0	0	0	0	0	10.8	14.6	10.8	7.7	0
G	10.3	10.2	4.3	5.6	18.9	0	0	0	0	0	14.0	0
H	0	6.0	0	5.2	11.1	4.2	10.2	0	9.2	3.9	5.2	0

Low conversion values may be attributed to a lower enzymatic activity but could also be due to a lower expression efficiency. Therefore, the colonies that exhibited the highest conversion values, with a relative conversion of 65% or higher with respect to the WT controls were sequenced. Variants B5, B11 and A3 were all found to be WT (all presenting the ACG codon from the wild-type gene), whereas G5 carried a leucine in position 154. Since HheG WT afforded a conversion that was 40% higher than HheG T154L and given that all other colonies with acceptable activity contained also WT HheG, no further efforts were directed towards improving the cyanolytic activity of HheG by mutagenesis of position 154. These results indicate that, probably due to the structural differences between HheG and HheC in the surroundings of the

active site, residues of HheC that are likely to yield variants with improved properties upon mutagenesis are not necessarily transferrable to HheG.

3.3.3. Evaluation of SSM library of HheG at position T195

To verify the results obtained by Janine Mayer for the library at position T195 (see section 1.6.1), a screening was performed according to the procedure described in section 2.2.2.3. When performing the screening *via* a cyanolysis of cyclohexene oxide starting from 2-chlorocyclohexanol (see Figure 22 B), putative mutants with higher cyanolytic activity might be overlooked if they present a decreased activity in the dehalogenation of 2-chlorocyclohexanol. Therefore, the direct cyanide-mediated epoxide ring-opening constitutes a more reliable screening method. As can be seen in Table 15, cyanolysis of 10 mM cyclohexene oxide using 2 equivalents of cyanide afforded 2-cyanocyclohexanol in the range of 5-9 % conversion for the HheG wild-type controls, whereas no conversion was detected for the negative controls after 5 hours and 30 minutes. In contrast to the procedure followed by Janine Mayer for the direct cyanolysis of cyclohexene oxide in the screening of the HheG N196-NNS library, where the empty vector controls afforded on average 78% relative activity with respect to wild-type HheG [212], the cyanolysis screening test under the conditions reported here allows for a wider dynamic range, facilitating the identification of putatively more active mutants.

Table 15: Results of the cyanolysis screening of library HheG T195-NNS using cyclohexene oxide as substrate. The values show the conversion (%) of cyclohexene oxide to 2-cyanocyclohexanol after 5 h 30 min. Reactions were performed using whole cells expressed in 96-deep-well plates, 10 mM cyclohexene oxide and 20 mM NaCN. Grey indicates empty vector (negative) controls and green shows HheG wild-type controls. Yellow marks a conversion up to 2-fold higher than the mean conversion of HheG wild-type controls, and orange marks a conversion between 2-fold and 3-fold higher.

	1	**2**	**3**	**4**	**5**	**6**	**7**	**8**	**9**	**10**	**11**	**12**
A	0	8.0	0	0	0	0	23.8	0	0	6.4	5.1	0
B	13.6	0	20.9	0	0	0	0	12.1	0	0	0	0
C	0	0	0	0	0	0	0	12.5	0	0	23.8	0
D	0	11.6	13.7	0	0	0	8.2	0	0	0	0	0
E	0	0	12.4	21.8	0	0	0	0	0	0	0	0
F	0	0	0	14.1	0	0	0	0	21.4	0	14.9	0
G	0	0	0	0	0	0	0	0	0	0	0	0
H	0	6.9	0	0	0	18.6	0	0	20.4	0	8.8	0

From the screened variants, 15 afforded a conversion at least 50% higher than the wild-type control, of which seven variants showed a 2-fold conversion increase or higher. With this, the

results follow the same trend observed by Janine Mayer in the cascade screening starting from 2-chlorocyclohexanol (see Table 16) [212].

Table 16: Results of the activity screening of library HheG T195-NNS in the cascade synthesis of 2-cyanocyclohexanol starting from 2-chlorocyclohexanol performed by Janine Mayer. The values show the conversion (%) of 2-chlorocyclohexanol to 2-cyanocyclohexanol after 42 h. Reactions were performed using whole cells expressed in 96-deep-well plates, 20 mM cyclohexene oxide and 40 mM NaCN. Grey indicates empty vector (negative) controls and green shows HheG wild-type controls. Yellow marks a conversion up to 3-fold higher than the mean conversion of HheG wild-type controls, and orange marks a conversion at least 3-fold higher. Modified from [212].

	1	2	3	4	5	6	7	8	9	10	11	12
A	0.9	20.0	1.6	2.1	1.2	1.0	73.0	4.0	2.9	11.7	15.8	0.9
B	57.8	3.2	75.9	1.3	2.2	2.1	1.5	41.6	0.9	0.2	1.4	0.4
C	1.0	1.4	1.1	2.1	1.8	1.7	1.1	33.1	3.5	3.2	55.7	1.3
D	1.8	52.0	49.9	1.0	1.5	0.8	15.4	1.1	1.1	1.0	0.4	1.7
E	4.8	1.3	42.8	71.4	1.6	0.9	1.1	1.2	0.9	3.4	1.4	1.1
F	2.2	2.1	1.2	46.3	4.2	3.9	0.9	0.9	65.2	0.7	41.2	1.6
G	1.5	0.9	1.1	1.1	1.4	1.0	3.2	1.4	1.1	0.8	0.7	0.9
H	0.7	16.8	2.8	3.6	1.0	66.6	1.7	1.0	62.7	0.8	15.1	0.6

The six variants presenting the highest activity (A7, B3, C11, E4, F9, H9) in the cyanolysis assay starting from cyclohexene oxide were sequenced. Although they afforded a conversion at least 2-fold higher than the HheG WT control, all of them carried a threonine in position 195, all presenting the ACC codon from the wild-type gene, except for E4 (ACG). The fact that 5 out of 86 variants composing the SSM library carried the wild-type HheG gene sequence, suggests that the quality of the library is not optimal, and it is possible that not all 20 possible amino acids at position 195 are covered by the mutants on the plate. However, *via* mutagenesis at other sites, Janine Mayer identified other promising variants with higher cyanolytic activity, namely mutant N196M and mutant I104M + N196M. Therefore, no further efforts were directed towards improving the activity of HheG in the cyanide-mediated epoxide ring-opening reaction by mutagenesis of position T195. Engineering of HheG based on the *in silico* design performed by Elia Calderini afforded several mutants with increased activity in the azidolysis of cyclohexene oxide, as well as variants with increased or inversed selectivity, showing the usefulness of this approach [211,212]. However, in the case of the cyanide-mediated epoxide ring-opening reaction, only one mutant afforded higher conversion than wild-type HheG. This suggests that the success in the improvement of HheG's activity *via* site directed mutagenesis not only depends on the selection of the right residues, but also seems to depend on the nucleophile that will be used for the epoxide ring-opening reaction.

4. Discussion

In this thesis, a novel chemo-enzymatic cascade for the synthesis of the β-amino alcohol derivative (*S*)-tembamide was designed and optimized. The developed route starts with a concurrent bi-enzymatic synthesis of intermediate (*S*)-4-methoxymandelonitrile benzoate starting from 4-anisaldehyde and catalyzed by immobilized *Me*HNL and CALA. The second and final step consists in the Raney Ni-catalyzed hydrogenation of the nitrile moiety and spontaneous acyl migration to yield (*S*)-tembamide with high enantiopurity. In order to achieve the first step, both enzymatic hydrocyanation and benzoylation reactions were initially studied separately and their combination was optimized to ensure the maximum chemo- and enantioselectivity of the cascade. In parallel, the catalytic reduction of the nitrile was investigated, selecting a suitable catalyst and the optimal conditions to reach the highest selectivity and enantioretention. Finally, as a proof of concept, the preparative synthesis of (*S*)-tembamide starting from 4-anisaldehyde was achieved in a 2-pot 2-step fashion using the developed cascade.

In addition, engineering of HheG was explored using site-saturation mutagenesis in order to improve its cyanolytic activity for the conversion of cyclic epoxides into chiral β-hydroxynitriles.

4.1. Concurrent bi-enzymatic cascade synthesis of (*S*)-4-methoxymandelonitrile benzoate

4.1.1. Lipase screening

Initially, the aim of this project was to synthesize both (*S*)- and (*R*)-4-methoxymandelonitrile benzoate using two pairs of HNL and hydrolase with matching enantioselectivity. In the initial hydrolase screening based on the hydrolysis of racemic 4-methoxymandelonitirile benzoate, most of the enzymes showed preference for the (*S*)-enantiomer. As already pointed out in section 3.1.4., since the nitrile group has a higher priority than the 4-methoxyphenyl group according to Cahn–Ingold–Prelog rules [234], most lipases will catalyze the acylation of the (*S*)-enantiomer preferentially, following Kazlauskas' rule for secondary alcohols [144]. Lipase AY (*Candida rugosa* lipase, CRL) from Amano (Amano Enzyme Inc., Nagoya, Japan) was one of the few that preferentially hydrolyzed (*R*)-4-methoxymandelonitrile benzoate. It has been previously reported that the stereoselectivity of CRL strongly depends on the structure of the alcohol, showing reverse enantioselectivity with cyanohydrin substrates [127,283]. However, to our surprise, none of the immobilized hydrolases tested in the benzoylation reaction could afford the conversion of (*R*)-4-methoxymandelonitrile preferentially over (*S*)-4-methoxymandelonitrile. Here, two enzymes

with unexpected behavior can be pointed out. CRL, on one side, showed enantiopreference for (*R*)-**3** during the hydrolysis test, whereas it preferentially benzoylated (*S*)-**2**. While the hydrolysis test was performed in a biphasic medium (phosphate buffer/*i*Pr_2O), pure *i*Pr_2O was used for the benzoylation reaction. Differences in the reaction medium have been shown to significantly influence the racemic temperature of CRL in the hydrolysis of ketoprofen vinyl ester [235]. Jin *et al*. observed that variation of the reaction solvents and water-solvent mixtures led to a change in the enantioselectivity, which, they surmised, could be due to changes in the conformational flexibility and solvation of the substrate. Alcalase (subtilisin), however, preferentially converted the (*S*)-enantiomer in both tests. This was an unforeseen result, since it is known for presenting opposite enantiopreference to lipases in organic solvents. Nevertheless, Savile and Kazlauskas' studies on the enantioselectivity of subtilisins toward secondary alcohols showed that this not only depends on the substituents' size but also on their hydrophobicity and the reaction solvent (see Figure 53) [145]. Since these enzymes bind substrates in an extended conformation, only one pocket (S_1') is available for the binding of one substituent, while the other substituent is solvated by the solvent. The size of S_1' is large enough to accommodate aryl groups with small substituents in *para* position. When the two substituents present similar hydrophobicity or when the reaction takes place in non-polar organic solvents, the traditional rule based on substituent size applies (Figure 53 A). However, when the reaction takes place in water or in polar solvents, the less hydrophobic substituent will be better solvated by the solvent and this will determine the enzyme's enantioselectivity (Figure 53 B, C, D). In the case of 4-methoxymandelonitrile, the hydrophobicity of the 4-methoxyphenyl group is similar to that of a phenyl ring [284], which would explain the preferred hydrolysis of (*S*)-**3** in water, since the nitrile would be solvated while the 4-methoxyphenyl group is accommodated in the enzyme's pocket, as shown in Figure 53 C. However, diisopropyl ether is a relatively non-polar solvent and, thus, the enantioselectivity of subtilisin should be explained with the simplified rule depicted in Figure 53 A, leading to the benzoylation of (*R*)-**2** preferentially. Therefore, the unexpected enantioselectivity of Alcalase in the benzoylation of (±)-**2** cannot be rationalized. It might be possible to further decrease the enzyme's already poor enantioselectivity by changing to an apolar solvent such as heptane. This might afford the combination of Alcalase with *Pa*HNL for the synthesis of (*R*)-4-methoxymandelonitrile benzoate, with the enantioselectivity of the benzoylation reaction being almost negligible.

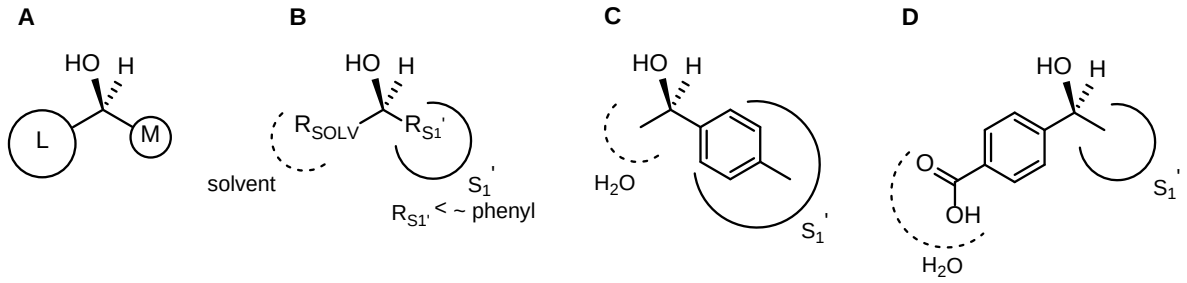

Figure 53. Models (A & B) predicting the enantioselectivity of subtilisins based on the size and hydrophobicity of the substituents in secondary alcohols. The rules predict that A) the faster reacting secondary alcohol enantiomer in a subtilisin-catalyzed reaction is the (*S*)-enantiomer, provided that the larger substituent (L) has higher priority than the smaller one (M) according to Cahn-Ingold-Prelog rules; B) Substituent R_{SOLV} remains in the solvent, while $R_{S1'}$ is accommodated in the S_1' pocket. For example, in C the less hydrophobic methyl group is better solvated than the 4-toluyl group, which leads to *R*-selectivity. However, in example D, the carboxylic acid moiety in *para*-position of the phenyl ring facilitates its solvation in water and, thus, the (*S*)-enantiomer is converted preferentially. Modified from [145].

Ideally, in order to select the most suitable enzyme for a specific reaction, the screening must be performed using the same reaction and under the same conditions that will be eventually used in the final process. Or, in Frances Arnold's words "You get what you screen for" [285]. However, a high throughput screening is not always available for the reaction of interest and, in this case, the immobilization of all 41 hydrolases in order to ensure that their activities would be retained in a benzoylation reaction performed in organic solvent was deemed too time-consuming. Nevertheless, rescreening all hydrolases for the benzoylation of (±)-**2** in organic solvent might have pointed at other lipases with enhanced selectivity towards the (*R*)-enantiomer. Furthermore, some of the enzymes exhibiting (*R*)-enantiopreference in the hydrolysis test were not available in immobilized form and their evaluation in the benzoylation reaction was not considered. The selection of an appropriate hydrolase for the preparation of (*R*)-**3** was set aside as a future goal and all further efforts were directed towards optimizing the cascade synthesis of (*S*)-**3**.

4.1.2. Optimization of the cascade synthesis of (S)-3 catalyzed by MeHNL and CALA

4.1.2.1. Alternative benzoyl donors

When performing the concurrent bi-enzymatic cascade synthesis of (*S*)-4-methoxymandelonitrile benzoate under the optimized conditions (see Table 9, entry 8), it was observed that after about 150 hours of reaction the concentration of cyanohydrin **2** remained constant at 11 mM. It could not be further converted to **3** by CALA, which continued catalyzing the hydrolysis of phenyl benzoate, as shown in Figure 54. This seems to indicate a rather low affinity of the lipase for 4-methoxymandelonitrile, which, at low concentrations, cannot compete

with the water present in the reaction medium for the acyl-enzyme complex. Hence, hydrolysis is the main reaction taking place in the end. However, since the benzoylation of cyanohydrin **2** using phenyl benzoate as donor is not irreversible – the byproduct phenol is not a good nucleophile but the reaction is reversible – this may also partially account for the reaction not being quantitative. Furthermore, the formation of phenol as byproduct not only reduces the cascade's atom economy, but may also lead to dead-end inhibition of the lipase [286].

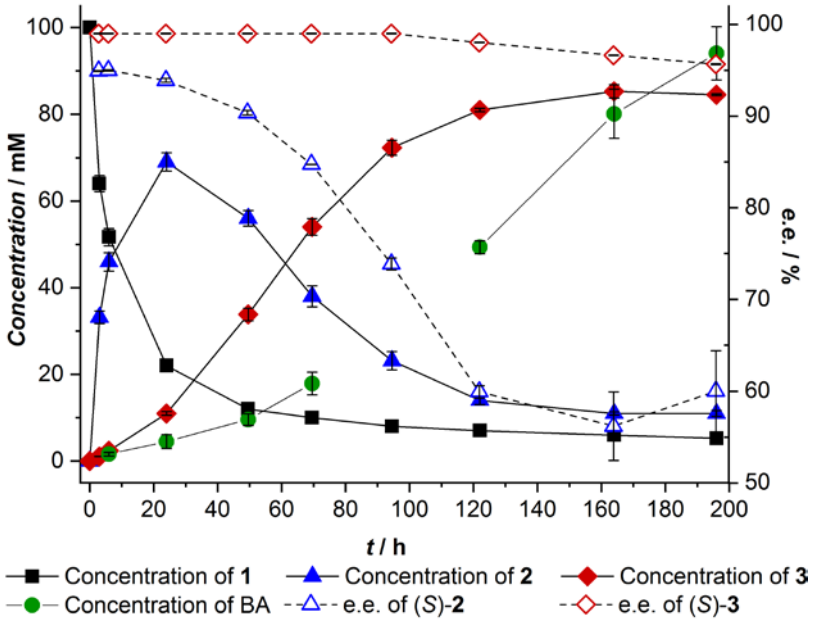

Figure 54. Optimized concurrent bi-enzymatic cascade synthesis of (*S*)-4-methoxymandelonitrile benzoate catalyzed by immobilized *Me*HNL and immobilized CALA starting from 100 mM **1** using 6.5 equivalents of HCN (Table 9, entry 8). The concentration of benzoic acid (BA) at time point = 95 h could not be determined.

The use of an alternative irreversible benzoyl donor in this concurrent cascade might not only increase the atom economy but, if selected wisely and provided that no relevant undesired cross interactions take place, could help drive the equilibrium to completion. For example, isopropenyl benzoate would afford an irreversible benzoylation reaction, since the byproduct immediately tautomerizes to acetone. Acetone is not as reactive as acetaldehyde towards hydrocyanation and, thus, might not significantly affect the hydrocyanation rate of 4-anisaldehyde, as it occurred when using vinyl benzoate as donor. However, isopropenyl benzoate is not commercially available and therefore, was not evaluated in this thesis.

As mentioned in section 1.4.2., Purkarthofer *et al.* reported an interesting concurrent approach for the synthesis of ethoxycarbonylated (*R*)-mandelonitrile catalyzed by *Pa*HNL adsorbed on Celite [165]. They used ethyl cyanoformate as both cyanide source and acylating agent and, while the HNL catalyzed the hydrocyanation, the Celite catalyzed the acylation of the

cyanohydrin (see Figure 18, scheme I). Based on this approach, one could imagine that a similar approach could be used in the present cascade, as shown in Figure 55. Although this would lack the additional selectivity achieved when using CALA as catalyst, the process might benefit from a higher atom economy and suppression of hydrolysis, which would, in turn, benefit the *Me*HNL-catalyzed hydrocyanation. However, some tests performed during the optimization of the bi-enzymatic cascade suggest that this approach would probably not work. As control reactions, the synthesis of **3** starting from aldehyde **1** was also attempted using Celite R-633 and CALA (negative control for the immobilized *Me*HNL), *Me*HNL and EXE309 (negative control for the immobilized CALA) or Celite R-633 and EXE309 (negative control for both immobilized enzymes). In the first case, formation of (*S*)-**3** was observed, albeit with lower enantiopurity than in the bi-enzymatic cascade. In contrast, the other negative controls only afforded cyanohydrin **2** – enantiopure in the first case, racemic in the double negative control – indicating that Celite R-633 only catalyzes the hydrocyanation reaction, but not the transesterification.

Figure 55. Proposed alternative concurrent chemo-enzymatic synthesis of (*S*)-4-methoxymandelonitrile benzoate catalyzed by *Me*HNL and Celite R-633.

4.1.2.2. Effect of HCN excess on hydrocyanation rate and product enantiopurity

A logical assumption when planning a concurrent cascade involving a hydrocyanation and subsequent benzoylation would be that, upon successful combination, a lower excess of HCN would be required. Once the suitable conditions for the concurrent *Me*HNL- and CALA-catalyzed cascade were determined, it was attempted to decrease the equivalents of HCN from 6.5 to 5. This resulted in lower reaction rates together with a decrease in the product enantiomeric excess (see section 3.1.12.). To understand this result, the effect of varying the equivalents of cyanide on the enzymatic hydrocyanation rate and product enantiopurity was evaluated. Immobilized *Me*HNL-catalyzed hydrocyanation of 100 mM 4-anisaldehyde using 3, 4, 5 or 6.5 equivalents in diisopropyl ether (without addition of phosphate salt hydrates) established a strong negative effect of decreasing the HCN excess not only on the reaction rate but, strikingly, on the enantiopurity of cyanohydrin **2** (see Figure 43). This result is in accordance with the observed lower product e.e. when decreasing the HCN excess in the cascade synthesis. However, when the hydrocyanation reaction was performed using non-immobilized *Me*HNL in a biphasic system, a different trend was observed. As shown in Figure 56, decreasing the HCN excess from 5 to 3

equivalents had a negative effect on the hydrocyanation rate at a late stage and, as expected, the maximum conversion decreased when using less HCN. However, although a slightly lower enantiopurity of (*S*)-**2** was observed when decreasing the HCN equivalents (variations of e.e. between 91% and 92% at plateau), this effect was almost negligible when compared to the observations using immobilized *Me*HNL in diisopropyl ether (variations between 69% and 75% at plateau when using 3–5 equivalents of HCN).

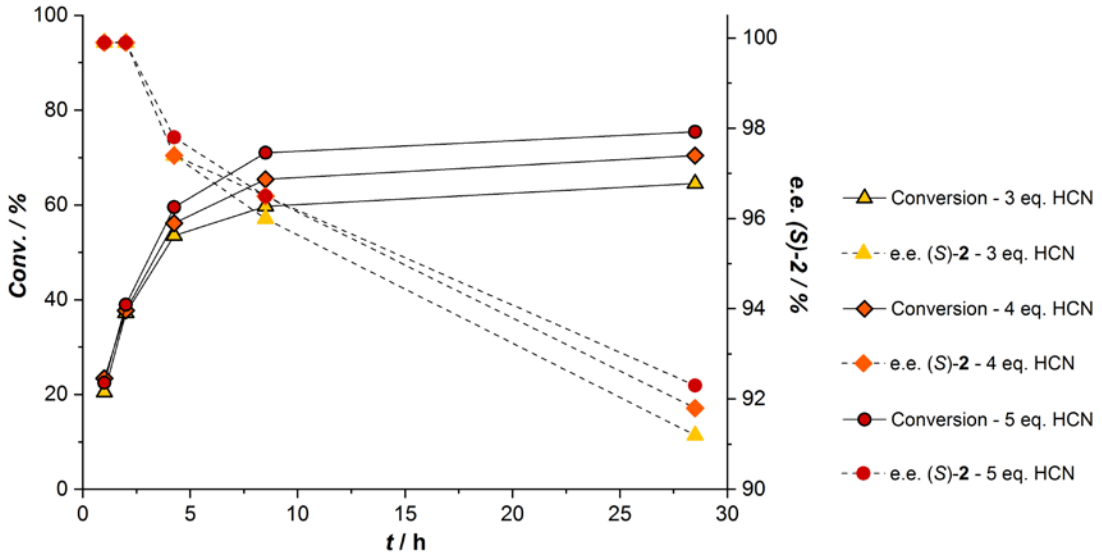

Figure 56. Hydrocyanation of 100 mM 4-anisaldehyde catalyzed by non-immobilized *Me*HNL using 3-5 equivalents of HCN in a 1:8 mixture of 500 mM citrate buffer pH 5 and diisopropyl ether at 20 °C.

Increasing the available concentration of cyanide in hydrocyanation reactions should reduce the degree to which back conversion (cyanogenesis) takes place [287]. This should, thus, decrease the racemization rate and can explain the general trend observed for the variations of product enantiopurity with HCN concentration. However, this on its own does not explain the differences observed between the immobilized and non-immobilized *Me*HNL systems. The main difference between these two systems, besides the reaction solvent mixture, is the presence or absence of the enzyme support, Celite R-633. As described in section 3.1.8., this support also catalyzes the non-selective hydrocyanation of 4-anisaldehyde. Therefore, we infer that the Celite-catalyzed racemization *via* cyanogenesis and hydrocyanation accounts for the more pronounced effect of decreasing HCN excess on the product enantiopurity in the system using immobilized *Me*HNL. This demonstrates the importance of choosing a suitable immobilization support and suggests that decreasing the HCN excess might be possible without compromising the enantiopurity of the product in the developed concurrent bi-enzymatic cascade. This might be achieved if, by further studying the alternatives for *Me*HNL immobilization, a support could be found that does not

catalyze the non-selective hydrocyanation reaction and maintains the enzyme's activity under the optimized conditions.

4.1.2.3. Control of water activity to suppress hydrolysis

Already at the beginning of this project, the water content in the reaction medium was considered a crucial factor that had to be optimized for the successful combination of an HNL and a hydrolase. It was decided to use disodium phosphate salts with different levels of hydration to establish and control a low water activity. This was expected to overall favor the bi-enzymatic cascade by suppressing hydrolysis – thus limiting the concentration of benzoic acid –, in spite of the proven negative effect that the selected salt pair exerted on the activity of *Me*HNL and the decrease of product e.e. due to its catalytic activity on the non-selective hydrocyanation (see section 3.1.9. Figures 37 and 38). However, during the optimization of the concurrent cascade, it was observed that the salt hydrates did not hamper the formation of benzoic acid (see section 3.1.12. Table 9, entries 3 and 4). This contradicts the results obtained during the evaluation of the effect of the salt pairs on the chemoselectivity of CALA. When performing the CALA-catalyzed benzoylation of **2** (containing a small amount of **1** as impurity) in *i*Pr_2O as an isolated step using the pair $Na_2HPO_4{\cdot}2H_2O/Na_2HPO_4{\cdot}7H_2O$, the hydrolytic reaction constituted only 3% of the enzyme's activity after 24 hours at 20 °C (see section 3.1.9. Figure 39). However, in the concurrent bi-enzymatic cascade, of the total amount of phenyl benzoate reacted after 31 hours at 20 °C, 40% was converted to benzoic acid when using the same salt pair (Table 4, entry 3). This suggests that the conditions of the water activity test and the final reaction conditions cannot be directly compared. Performing the transesterification as part of the cascade in a concurrent fashion supposes the addition of several components that were not present in the water activity evaluation experiments from section 3.1.9.. Two of these components are known to have an impact on the water activity. On one hand, Celite R-633 has been shown to control the water activity when used as an additive or as an enzyme support, by adsorbing the water present in the reaction medium [130,288]. Although the immobilized *Me*HNL was treated under high vacuum, it could have absorbed water from the environment when stored in the refrigerator and might have released part of this water, which could form the salt pair with higher hydration level ($Na_2HPO_4{\cdot}7H_2O/Na_2HPO_4{\cdot}12H_2O$). Nevertheless, when performing the CALA-catalyzed benzoylation of **2** using the reaction mixture crude proceeding from a non-immobilized *Me*HNL-catalyzed hydrocyanation of **1**, again high amounts of benzoic acid were formed (see Figure 58B). This suggests that Celite R-633 is probably not significantly increasing the water activity. On the other hand, it has been reported that when gaseous HCN is present in the reaction medium, the equilibration of a_w is not possible [73,158]. Although the authors did not provide experimental or

theoretical support for this statement, it cannot be ruled out as a possible explanation for the observations here reported.

4.1.3. Evaluation of the concurrent bi-enzymatic cascade synthesis of (S)-3

The results of chapter 3.1 demonstrate that the concurrent combination of a *Me*HNL-catalyzed hydrocyanation with a CALA-catalyzed transesterification is possible after careful investigation of the individual reactions in search for compatible conditions. However, further optimization is required to improve the cascade, since 5% residual 4-anisaldehyde could not be converted by *Me*HNL (see Table 9, entry 8 and Figure 54). Presumably, this is due to an observed increase of benzoic acid concentration as the cascade proceeds, as also shown in Figure 54. Furthermore, as already discussed in section 4.1.2.1, CALA does not catalyze the benzoylation of **2** to completion, but maintains its hydrolytic activity, further increasing the amount of benzoic acid. In section 3.1.7. the use of an engineered lipase, CALA-D122L, for which reduced hydrolytic activity had been reported, was evaluated. However, this mutant exhibited less selectivity towards the transesterification reaction versus hydrolysis, when compared to the wild-type (see Figure 36). For this assay, both lipases were immobilized following the same procedure, so the amount of water retained in the immobilisates was expected to be very similar. Nevertheless, a more reliable experiment should have included the sodium phosphate hydrate pair initially selected for the cascade. This, in principle, would have ensured that both reactions were performed under equal water activity and might have rendered other results.

By comparison of the sequence and 3D models of CALA with lipases with enhanced acyltransferase activity (CduLAc from *Candida dubliniensis* and CpLIP2 from *Candida parapsilosis*) Jan *et al.* identified residue Glu370 in CALA as a key residue for the acyltransferase activity [289]. Mutant CALA E370A, obtained by rational design, exhibited a drastic increase in acyltransferase activity, which might afford higher yields and selectivity in the herein reported cascade synthesis of (*S*)-4-methoxymandelonitrile benzoate.

When comparing the optimized concurrent cascade (Table 4, entry 8 and Figure 54) with the enzymatic hydrocyanation performed under the same conditions (see Table 9, entry 9 and Figure 57), it can be concluded that the CALA-catalyzed benzoylation of (*S*)-**2** coupled to the *Me*HNL-catalyzed hydrocyanation of **1** can shift the equilibrium of the latter by removal of the unstable intermediate. Whereas the isolated hydrocyanation reaction reaches a maximum yield of (*S*)-**2** of 85%, with an e.e. of 91%, the bi-enzymatic reaction affords a total conversion of 4-anisaldehyde of 95%, with 81% yield of (*S*)-**3** and an e.e. of 98% for the benzoylated cyanohydrin. If the reaction

is allowed to proceed, although the hydrocyanation reaction is negligible at this point, (*S*)-**3** can be reached in 85% yield with a fair e.e. of 96%.

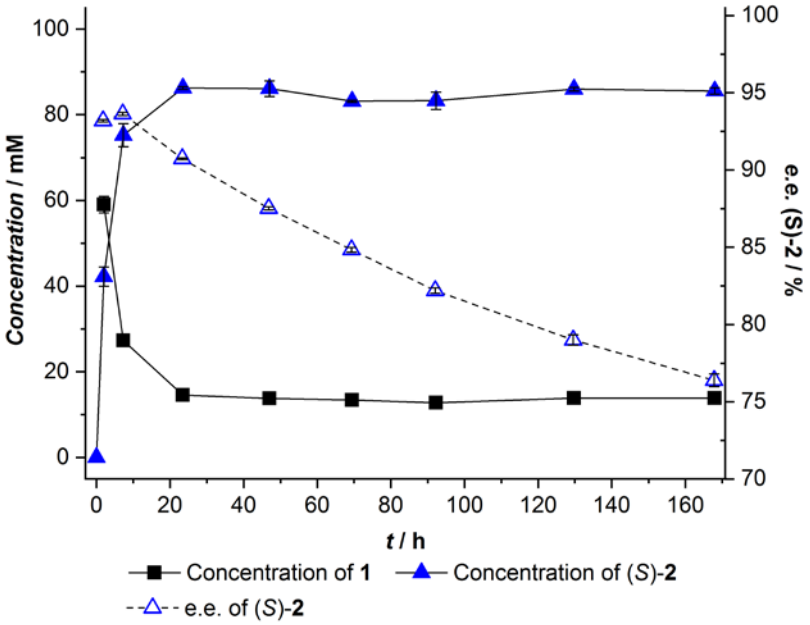

Figure 57. Hydrocyanation of 100 mM 4-anisaldehyde using 6.5 equivalents of HCN, catalyzed by immobilized *Me*HNL under the conditions used for the optimized concurrent bi-enzymatic synthesis of (*S*)-**3**. This reaction corresponds to entry 9 from Table 9.

Moreover, it is interesting to compare the optimized concurrent process with a sequential cascade. A sequential approach benefits from the fact that each enzyme can work under optimal conditions. Thus, the hydrocyanation of 4-anisaldehyde can be performed using free *Me*HNL in a biphasic system under the optimal temperature. After reaching plateau, the reaction mixture may be dried after removal of the aqueous phase and the benzoylation reaction may start upon addition of the lipase and benzoyl donor under optimal temperature. For comparison, the sequential bi-enzymatic synthesis of (*S*)-**3** was performed under the optimal conditions found for each reaction within the studied range. Cell-free extract containing *Me*HNL was used for the hydrocyanation of 4-anisaldehyde using 6.5 equivalents of HCN in a biphasic system at 10 °C (see Figure 58A). After 46 hours, the reaction had reached plateau, affording (*S*)-**2** with 89% yield and 96% e.e. After completion, the aqueous phase was pipetted out and the reaction crude mixture was dried over anhydrous magnesium sulphate, which was then filtered off prior to addition of immobilized CALA and 3 equivalents of phenyl benzoate. The benzoylation reaction was performed at 25 °C. A higher activity is expected when raising the temperature further [249], but this would accelerate the cyanogenesis reaction. Due to the increase in temperature, a slight increase in the concentration of **1** was observed (from 11 mM to 12 mM). After 45 hours the

benzoylation had reached plateau, yielding 81% (*S*)-**3** with 98% e.e (see Figure 58B). This demonstrates that the equilibrium shift of the hydrocyanation reaction, enabled by its combination with the lipase-catalyzed benzoylation reaction in a concurrent fashion, actually compensates for the lower activity and selectivity that both enzymes exhibit due to not working under optimal conditions. Indeed, while allowing for each enzyme to work under optimal conditions, the reaction performed in a sequential mode does not offer higher conversion or enantiopurity values than the concurrent approach.

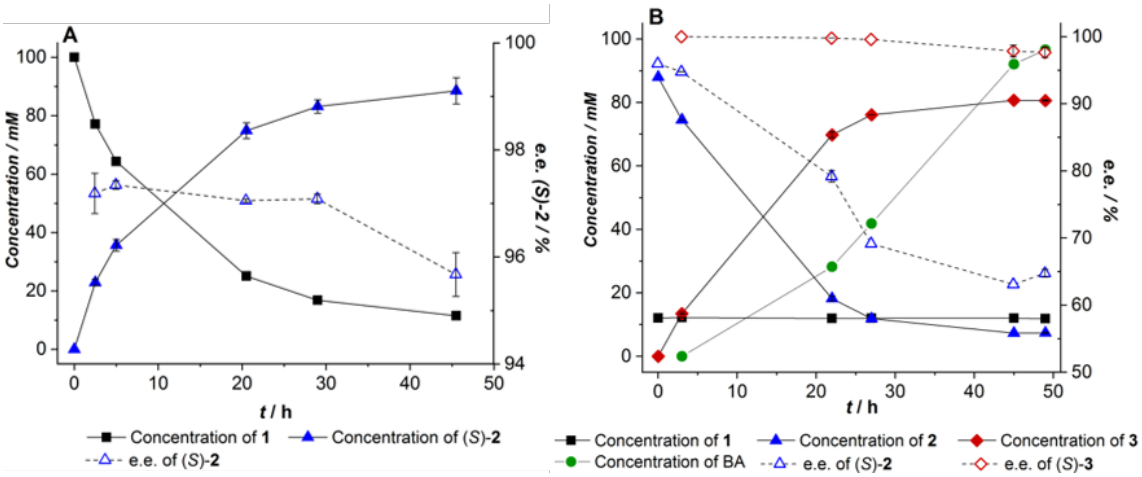

Figure 58. A) Hydrocyanation of 100 mM 4-anisaldehyde using 6.5 equivalents of HCN, catalyzed by non-immobilized *Me*HNL in a 1:10 mixture of 500 mM citrate buffer at pH 5 and *i*Pr$_2$O at 10 °C. B) Benzoylation of dried reaction mixture proceeding from the hydrocyanation reaction, catalyzed by immobilized CALA using 3 equivalents of phenyl benzoate at 25 °C. BA corresponds to benzoic acid. The amounts of *Me*HNL and CALA used for this experiment are adjusted according to the amount used in Table 9, entry 8.

Performing enzymatic or chemo-enzymatic cascades in a concurrent fashion does not always offer better results than the equivalent sequential cascades. Even though performing the reactions simultaneously may offer advantages such as shifting equilibria and co-factor and co-substrate recycling, often, incompatibilities between the different catalysts' requirements and cross interactions can actually lead to lower yields. An example of a bi-enzymatic cascade in which the sequential approach offers better results than the concurrent cascade was reported by Sehl *et al.* [290]. They envisioned a cascade for the synthesis of (1*R*,2*S*)-norephedrine and (1*R*,2*R*)-norseudoephedrine from benzaldehyde and pyruvate, catalyzed by thiamine diphosphate (ThDP)-dependent acetohydroxyacid synthase I (AHAS-I) from *E. coli* and *S*- or *R*-selective ω-transaminases, respectively (see Figure 59). The advantage of a concurrent approach was the possibility to continuously remove the byproduct from the transaminase-catalyzed reductive amination of intermediate phenylacetylcarbinol (PAC), pyruvate, by recycling it in the AHAS-I-catalyzed decarboxylation reaction and subsequent carboligation with benzaldehyde. This would

afford a significant increase in the reductive amination reaction yield and would additionally improve the atom efficiency by reducing waste production. However, they encountered a major problem in the concurrent synthesis of norephedrine, catalyzed by AHAS-I and *Cv*-(*S*)TA from *Chromobacterium violaceum*, as a result of cross-reactivity. Due to the higher reactivity of aldehydes over ketones and steric constraints in the active site of the transaminase, *Cv*-(*S*)TA offered a 17-fold higher initial rate in the transamination of benzaldehyde than with PAC. As a consequence, when the reaction was performed in a concurrent fashion, 98% of the benzaldehyde was converted to undesired benzylamine. In this case, the best results were obtained in a sequential approach were the transaminase was added after benzaldehyde had been fully converted, followed by a second carboligation step after addition of fresh AHAS-I and benzaldehyde. Furthermore, they observed inactivation of *Cv*-(*S*)TA, which had to be added again freshly after the second carboligation step. This way, a norephedrine yield of 65% (relative to the total benzaldehyde reacted) could be achieved when performing the reaction as a sequential recycling cascade. This is an example of how cross-interactions and enzyme inactivation due to reaction components can hamper the successful combination of multiple enzymes in concurrent cascades.

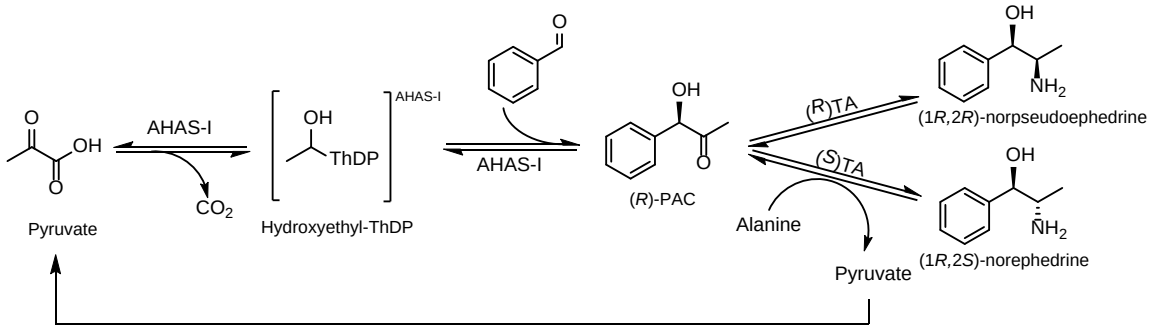

Figure 59. Bi-enzymatic recycling cascade synthesis of nor(pseudo)ephedrine catalyzed by AHAS-I and *S*- or *R*-selective ω-transaminases, developed by Sehl *et al.* [290].

The herein reported bi-enzymatic synthesis of (*S*)-4-methoxymandelonitrile benzoate is the first example of a successful concurrent cascade involving an HNL and a lipase in which both enzymes maintain enough activity and selectivity to yield an enantiopure acylated cyanohydrin with good yield. In principle, this approach can be transferred to the synthesis of other acylated cyanohydrins. In any case, a key requirement for success will be the application of a lipase with high selectivity for transesterification over hydrolysis in microaqueous media. Recently, Subileau *et al.* carried out an extensive kinetic characterization of 13 lipases to evaluate their acyl transferase activity and proposed a methodology for the classification of lipases according to their acyltransferase character [291]. These lipases were divided into three categories depending on

the ratio of their apparent transfer/hydrolysis rates constant [$(K_t/K_h)_{app}$]. Those with the highest acyltransferase character were CalLAc5 from *Candida albicans* and CduLAc from *Candida dubliniensis*, which afforded $(K_t/K_h)_{app}$ values of 1660 and 1357 respectively (as comparison, the calculated $(K_t/K_h)_{app}$ ratio of CALA was 27).

A few years ago, Brahma *et al.* developed a multistep continuous approach for the synthesis of chiral *O*-acetylcyanohydrins with safe generation of HCN [292]. In a first packed bed reactor (PBR), CALB catalyzed the hydrolysis of ethyl cyanoformate, generating HCN which was used in a second PBR for the *At*HNL-catalyzed hydrocyanation of a range of aromatic aldehydes. Finally, in-line chemical acetylation allowed for the isolation of the more stable acetylated cyanohydrins. Inspired by the flow process reported by Brahma, the possibility of adapting the biocatalytic generation of cyanide to the herein developed bi-enzymatic cascade for the synthesis of 4-methoxymandelonitrile benzoate was considered as a measure to improve the safety of the process. A preliminary experiment where either CALA or CALB were introduced in a reaction mixture containing immobilized *Me*HNL, ethyl cyanoformate and 4-anisaldehyde showed that, indeed, the reaction containing CALB led to the formation of 4-methoxymandelonitrile, but no product was formed in the reaction containing CALA. This opens up the possibility of developing a 2-step flow cascade where HCN would be safely generated by CALB-catalyzed hydrolysis of ethyl cyanoformate in a first PBR and, after adjusting the water activity of the outflow, this could be transferred to a second reactor where the formation and benzoylation of 4-methoxymandelonitrile would take place. Furthermore, implementing the reaction in flow mode might help reduce the accumulation of benzoic acid over time, which should improve the performance of the cascade.

4.2. Novel multi-catalytic route for the synthesis of (*S*)-tembamide

4.2.1. Catalyst screening and optimization of nitrile hydrogenation

4.2.1.1. Selectivity of the catalytic hydrogenation of 3

As indicated by the identification of the major side products from the hydrogenation of **3** (see Figure 47), one of the main side reactions significantly lowering the yield of tembamide is the hydrogenolysis of the C−O bond of the benzyloxy group as depicted in Figure 45. The susceptibility of benzyl groups attached to oxygen atoms to undergo hydrogenolysis has been known for long. Benzyl alcohol is reduced rapidly and quantitatively to yield toluene [293]. Similarly, nuclear substituted benzyl alcohols, such as 4-methoxybenzyl alcohol, also undergo hydrogenolysis to yield the corresponding toluene derivative (see Figure 60) [294]. This, together

with the identification of compound **8** (Figure 47), suggests that the hydrogenolysis of the C-OH bond in tembamide is likely one of the major reactions taking place when tembamide is subjected to hydrogenation conditions (see section 3.2.2.). Furthermore, esters from benzyl alcohols are also especially reactive towards hydrogenolysis, yielding toluene and the corresponding acid [293]. This reaction is typically – but not exclusively – catalyzed by Pd (C), which explains the results obtained when using this catalyst (see section 3.2.2., Table 10, entry 1).

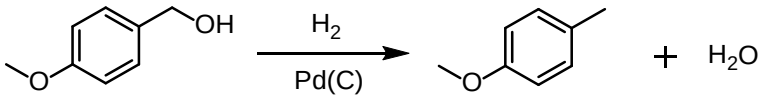

Figure 60. Examples of nuclear substituted benzyl alcohols that smoothly undergo hydrogenolysis [294].

The selectivity towards primary amines in the catalytic hydrogenation of nitriles may be enhanced by addition of ammonia or an appropriate base [186]. As already explained in section 3.2.4., the addition of ammonia was not considered, since it had been shown to lead to other side products in the hydrogenation of *O*-acyl cyanohydrins [174]. The addition of other bases, such as NaOH, LiOH or Na_2CO_3, has been shown to increase the ratio of primary to secondary amine [188,295], which is suggested to act, partly, by decreasing the concentration of Lewis acid sites on the catalyst surface [295], which are known to catalyze condensation reactions [296]. Therefore, it would be interesting to evaluate the addition of bases in future experiments for further optimization of the process.

In section 3.2.4. the effect of substrate concentration was evaluated, showing that higher concentrations led to lower selectivity towards tembamide. It was hypothesized that this was due to competition of the substrate **3** and the imino intermediate (Figure 19, compound II) on the catalyst surface, as well as a higher concentration of free amine, both situations leading to an increase in the condensation rate. Although some authors have claimed that the condensation reaction between imino intermediates and amines takes place on the catalyst surface [274,295], it is clear that a higher concentration of free amine resulting from a higher substrate concentration will increase the condensation rate. In this context, researchers have managed to improve the selectivity towards primary amines by decreasing the concentration of free amines, either by forming salts with acids or *via* acylation of the amine with acetic anhydride, for example [186]. In the present case, the intramolecular acyl migration leading to tembamide would decrease the amount of free amine, theoretically increasing the selectivity towards primary amines. Since the acyl shift is expected to be a fast reaction, we surmised that the addition of acids to decrease the concentration of primary amine would not significantly improve the yield of tembamide. On the one hand, the formation of amine salts proceeding from the reduction of

compound **7** should, indeed, decrease the amount of free amines that can react with the imino intermediates resulting from the hydrogenation of **3**, thereby decreasing the rate of undesired condensation reactions. On the other hand, however, the formation of amine salts of the β-amino ester intermediate resulting from hydrogenation of **3** would decrease the efficiency of the intramolecular acyl migration.

As commented in section 1.5., regarding the nature of the catalyst, there is a general selectivity trend whereby Ni and Co catalysts often offer high activity and selectivity towards primary amines, whereas Pd and Pt usually yield secondary or tertiary amines [184]. A mechanistic proposal reported by Krupka explains this behaviour based on the preferences of the catalysts for binding reaction intermediates (see Figure 61) [184].

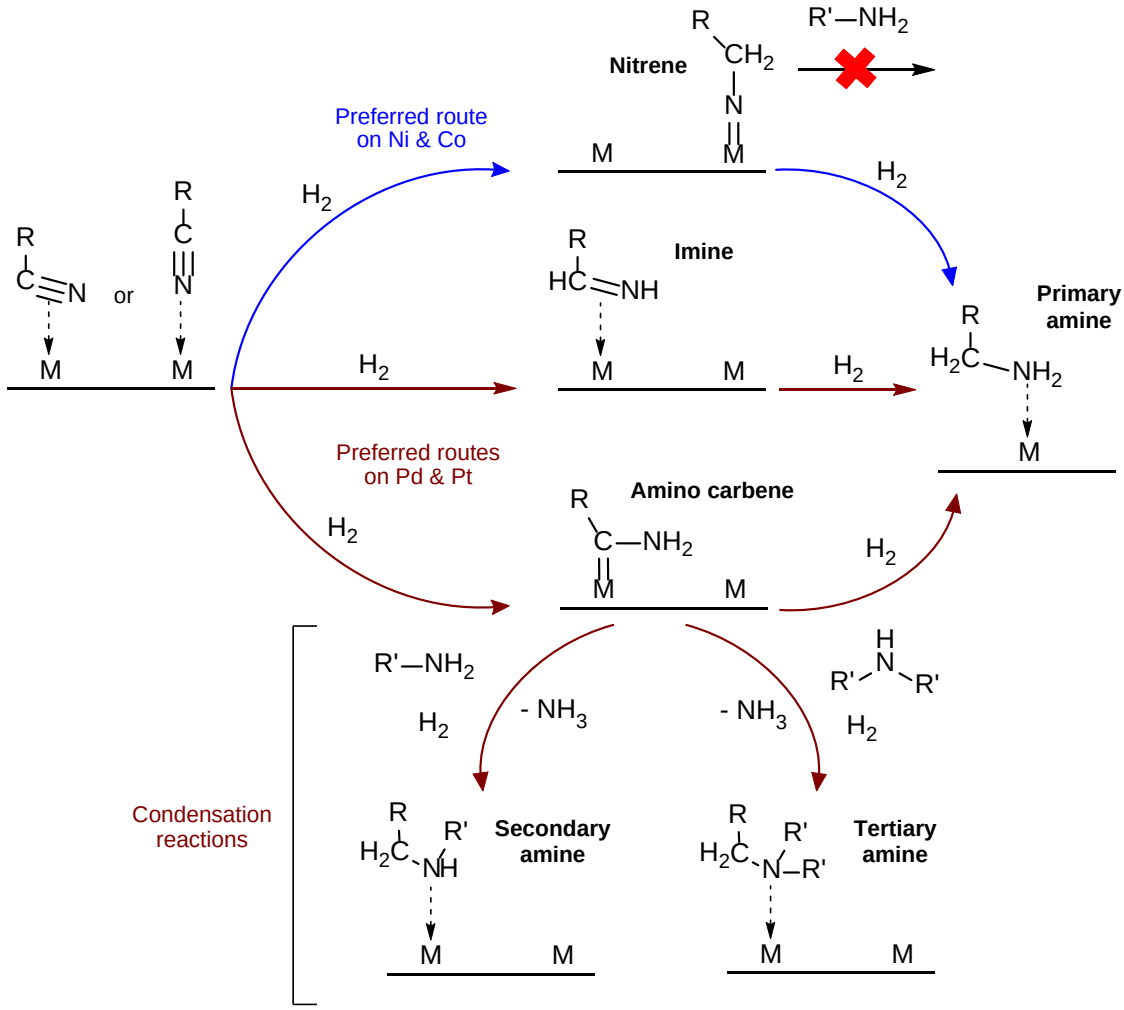

Figure 61. Mechanistic model of surface reactions suggested by Krupka *et al.* for the nitrile hydrogenation catalyzed by heterogeneous metal catalysts. For clarity, the condensation reactions of the surface imine species are not included in the scheme. M represents the active site corresponding to one or more surface atoms of the metal. Modified from [184].

As illustrated in Figure 61, under normal hydrogenation conditions (*i.e.* under high H_2 pressure and below 150 °C), Ni and Co prefer to bind reaction intermediates *via* the free electron pair of the nitrogen, whereas Pd and Pt preferentially form intermediates bound onto the metal surface *via* the α carbon or the π-system of an N=C double bond. Regarding the catalysts screened in this project, the results in terms of yield of tembamide are in agreement with the aforementioned trend. This could indicate that the selectivity in this case does not only depend on the hydrogenation/hydrogenolysis ratio but, in fact, successfully preventing condensation reactions might increase the yield of tembamide.

4.2.1.2. Catalytic activity and selectivity of Raney Ni

Regarding the selected catalyst, Raney Ni, for the reduction of 4-methoxymandelonitrile benzoate several aspects can affect its activity and selectivity. It has been reported that the activity of this catalyst may vary with small changes in the purity of the substrate [297], which might partly explain the difference in reaction rate observed when changing from pure 4-methoxymandelonitrile benzoate to the crude reaction mixture proceeding from the bi-enzymatic synthesis of this substrate. Additionally, the use of certain metallic promoters, such as molybdenum or chromium, can significantly improve the activity of Raney Ni on the hydrogenation of different functional groups [298]. This strategy was not considered within this project, but may be worth investigating, as it might also affect the catalyst's selectivity. For example, the addition of chromium chloride was found to inhibit the hydrogenolysis of benzyl alcohols [299], which could improve the selectivity in the herein reported synthesis of tembamide. Other non-metal additives such as formaldehyde or carbon monoxide have also been shown to improve selectivity towards primary amines in Raney Ni-catalyzed nitrile hydrogenations [300].

Raney Ni is prepared by reacting a nickel-aluminum alloy powder with sodium hydroxide, creating a sponge-like catalyst with high surface area, which contains a large amount of adsorbed hydrogen. Storage of this catalyst in water promotes surface oxidation, which can be delayed if stored under hydrogen atmosphere [298]. When attempting to perform the preparative cascade synthesis of (*S*)-tembamide, it was observed that the Raney Ni slurry had partially lost its activity after being stored for over 3 years. Although at this point it was decided to purchase a new Raney Ni catalyst, it is important to ensure maximum activity for the correct comparison of the different reactions performed during the optimization. It has been reported that ultrasound treatment of aged Raney Ni can restore its initial activity by removing passivating surface impurities [301]. Therefore, for optimal comparison of reactions performed within a time span of several years, this procedure should have been adopted prior to the hydrogenation reactions.

4.2.2. Preparative synthesis of (S)-tembamide

The initial idea for the envisioned catalytic synthesis of tembamide involved a 1-pot 2-step approach, which would minimize intermediate downstream and purification steps, reducing solvent waste and decreasing unit operations if successfully applied in an industrial scale. In this approach, the hydrogenation of the nitrile group would take place after the biocatalytic step, ideally without an intermediate work-up procedure. However, after observing that the presence of HCN in high concentration inhibited the hydrogenation of **3**, it became clear that evaporation of this compound was required prior to the hydrogenation step. There are few examples of concurrent chemo-enzymatic tandem reactions in literature [45,263,302], due to the often different requirements of the chemical catalysts and enzymes and the frequent cross-reactivity issues. Usually, an intermediate work-up step is required in order to adjust the reaction conditions (e.g. dilution, removal of inhibiting components, etc.). Furthermore, concurrent approaches are not necessarily preferred over step-wise cascades, for they both share the major advantage of avoiding the isolation of intermediates and minimizing downstream-processing steps. Supposing a large-scale production of (*S*)-tembamide, the reaction crude mixture after the biocatalytic step could be filtered to separate the enzyme immobilisates, provided that the enzymes can be recycled several times, and transferred into a second reactor where – after evaporation of the volatiles and re-dissolution of the reaction mixture – the catalytic hydrogenation would take place. However, if the recycling of the enzymes were not feasible or advantageous, the facility footprint could be reduced by using a single reactor where both the biocatalytic step and the subsequent catalytic hydrogenation – after evaporation of the volatiles and re-dissolution – would take place.

After optimization of all reactions, the combination of the bi-enzymatic concurrent cascade synthesis of (*S*)-**3** with the subsequent Raney Ni-catalyzed hydrogenation reaction allowed for a fully catalytic 2-step synthesis of (*S*)-tembamide in preparative scale. While intermediate (*S*)-**3** was obtained with a fair overall yield of 80% (99% e.e.), the low selectivity of the nitrile hydrogenation resulted in a poor yield of 32% for the last step. Therefore, the total HPLC yield of the 2-step cascade is 26%, although the total isolated yield of (*S*)-tembamide was 15%. However, the enantiopurity of the synthesized (*S*)-tembamide was outstanding, with a minor loss of 1% during the hydrogenation step in contrast to the low enantioretention observed under the harsher conditions employed by Veum *et al.* on the hydrogenation of benzylic acyl cyanohydrins [174].

The herein developed cascade constitutes the first totally catalytic route for the synthesis of (*S*)-tembamide. Furthermore, it affords the desired product in just 2 steps, requiring no isolation

of reaction intermediates, thus theoretically reducing waste generation when compared to a traditional 3-step approach with work-up of intermediates. However, although the product is obtained with excellent enantiopurity (98%), the low overall isolated yield renders the application of this cascade in a productive scale highly unprofitable. In order to afford a competitive production of (*S*)-tembamide following the reported procedure, optimization of the hydrogenation step reaction is key. Additionally, if performed in an industrial scale, the purification of tembamide would presumably be achieved solely by crystallization, most likely affording higher isolated yields.

Only four of the previously developed chiral routes for the synthesis of tembamide employ enzymes (see Figure 4) [42–45], whereas most of the alternative approaches introduce the chiral center using expensive metal complexes or chiral catalysts that must be synthesized previously [46–55]. Among the enzymatic processes, an interesting approach is that developed by Schrittwieser *et al.* for the synthesis of (*S*)-tembamide with 73% isolated yield and 99% e.e. (see Figure 4, first reaction scheme) [42]. This cascade is performed in a 1-pot 4-step fashion, thus also avoiding isolation of intermediates and greatly reducing waste generation. As comparison, the route proposed by Yadav *et al.* may be considered (see Figure 4, second reaction scheme) [43], since both approaches involve the same chemical transformations, albeit with complementary enantioselectivity of the chiral step (it is worth mentioning that the azido ketone used as starting compound by Yadav is not commercial and must be previously synthesized). In many cases, purification is achieved *via* column chromatography and, thus, the silica gel and solvents employed greatly contribute to increasing the environmental factor (E factor = kg waste/kg product) [303]. While Yadav's chemo-enzymatic approach afforded (*R*)-tembamide in 85% yield, the purification of the azido alcohol intermediate using column chromatography increased the E factor of the downstream processes (isolation and purification) by a factor 3, as calculated by Schrittwieser [42]. In the case of Yadav, carrot root was used as enzyme source, considerably reducing the catalyst price when compared to Schrittwieser's approach, which uses proprietary enzymes from Codexis (Redwood City, CA, USA). However, the fact of not using purified enzyme results in a significant increase of the E factor for the reaction, almost 25-fold higher than in Schrittwieser's cascade, as calculated by Schrittwieser in the *Supplementary information 2* [42], since the mass of carrot root needed to convert one Kg of substrate B is much higher than the mass of pure KRED-NADH-110 needed to convert the same amount of B (see Figure 4 for reaction schemes). The calculation of the E factor of Schrittwieser's approach excludes the waste generated during enzyme production and purification, since it is included in the equation as purified catalyst, whereas the carrot root that dramatically increases the E factor in the case of Yadav is neither expensive nor a toxic waste. This illustrates how, although the E factor is a

concept than can help assess the efficiency and the greenness of a process, it is crucial to evaluate not only the numbers but to focus also on what are the components of the generated waste. A simple calculation of the E factor for the herein reported cascade is shown in Table 17.

Table 17: Calculation of the E factor and the solvent/product ratio for the developed catalytic cascade for the synthesis of (*S*)-tembamide. The solvents are not included in the calculation of the E factor, but their use is evaluated separately as (mL of solvent) / (g of isolated product). A distinction is made between the reagents and solvents used for the reactions and those used for the purification of tembamide, and the total values are displayed in the last row.

Material	Mass (g) [1]	E factor [2]	Solvent (mL)	Solvent (mL/g)
		Reaction		
1	0.300	0.16		
HCN	0.386	3.72		
Phenyl benzoate	1.320	10.64		
*Me*HNL	0.190	2.09		
CALA	0.137	1.50		
H_2 [3]	0.022	0.21		
Raney Ni	0.224	2.46		
2	-	0.59		
Phenol	-	1.82		
Other side products [4]		3.51		
iPr_2O			115	1264
Total reaction		***26.7***		***1264***
		Purification		
Silica gel	60	659.34		
Heptane			1000	10989
AcOEt			600	6593
Total purification		***659.3***		***17582***
TOTAL PROCESS		***686.0***		***18846***

[1] Mass of reagents, reactants or catalysts. [2] Calculated as (mass of material after reaction) / (mass of isolated tembamide). [3] For comparison with Schrittwieser's calculations, 5 equivalents of H_2 are considered. [4] Considering the HPLC yield of tembamide (32%) and full conversion of **3**, for simplicity, benzoic acid, as well as other side products were calculated as (mass of **3** formed in the bi-enzymatic cascade) × 0.68. Furthermore, hydrolysis and hydrogenation of phenyl benzoate was not taken into account. These assumptions do not affect the total E factor of the reaction.

Table 17 shows that the reaction has yet to be improved in order to be comparable to other routes such as those developed by Schrittwieser [42], Lee [50], Baeza [54] and Brown [53] (see Table 18). The reaction E factor is comparable to the chemo-enzymatic route developed by Kamal [44], and 3-fold lower than Yadav's approach [43] (see Table 18). However, if the downstream processes are considered, this process shows an E factor which is much higher than any of the calculated E factors for the other routes in Table 18. The relatively high E factor for the reaction is partly due to the excess of HCN required and, especially, the excess of phenyl benzoate used since it carries a phenyl group that only contributes to decreasing the atom economy. Furthermore, the fact that the enzymes are immobilized and the low yield of the hydrogenation reaction also contribute to increasing the E factor of the reaction. In contrast, the procedures

developed by Schrittwieser, Lee, Baeza and Brown use benzoyl chloride for the acylation step in equimolar amount or with a low excess, they reach relatively high yields (always above 75%) for all their reaction steps and use generally low catalyst loading and low excess of reagents, which accounts for the lower E factors achieved. Further optimization of the herein developed reaction might decrease the required excess of phenyl benzoate or substitute this by a smaller benzoyl donor. Regarding the enzymes, if these can be recycled, they must be excluded from the E factor equation. The extremely high E factor corresponding to the purification step is due to the cumbersome column chromatography purification, which requires a high amount of silica. Further optimization of the purification step might significantly decrease these values.

Table 18: E factor and solvent/product ratio of different chiral routes for the synthesis of tembamide. Excluding the values of this thesis, all calculations were performed by Schrittwieser *et al.* (article and Supplementary information 2) [42].

Article	Steps [1]	Yield (%) [2]	E factor reaction [3]	Total E factor [4]	Solvent (mL/g)
This thesis	4 (1)	15	26.7	686.0	18846
Schrittwieser *et al.* 2013	4 (1)	73	3.2	11.1	309
Lee *et al.* 2007	5 (5)	62	4.4	57.8	1600
Baeza *et al.* 2005	3 (2)	65	5.8	23.3	1031
Kamal *et al.* 2004	5 (4)	42	19.7	114.9	1801
Yadav *et al.* 2001	3 (2)	85	77.8	97.5	826
Brown *et al.* 1993	3 (3)	72	5.2	14.6	483

[1] Number of chemical transformations (number of individual steps with product isolation). [2] Total isolated yield. [3] E factor for the reactions, excluding downstream processes and solvents. [4] Total E factor, excluding solvents.

The process recently developed by Liardo *et al.* is another interesting example of a successful sequential chemo-enzymatic cascade for the synthesis of several β-hydroxy amides that can be further converted to yield (*S*)- or (*R*)-tembamide [45]. Although the process involves five chemical transformations, (*S*)- tembamide was obtained in a fair 77% yield, with 99% e.e. The calculation of the E factor for this approach is, however, not possible, since they do not provide all the required information regarding reagent equivalents, amount of solvent and isolation or purification steps.

It can be concluded, based on the calculations of the E factor and the isolated yields of tembamide, that the herein developed chemo-enzymatic cascade cannot compete with many other preexisting routes for the synthesis of (*S*)-tembamide in terms of efficiency and waste production. The low chemoselectivity of the nitrile hydrogenation step results in an extremely low overall yield, which makes this a much less efficient route. The identification of the major side products from this last step, together with the limited improvements on the yield of tembamide achieved during the reaction optimization, demonstrated the difficulty of controlling the reaction

chemoselectivity. Nevertheless, the yield might be further enhanced when working with a fed batch system, thereby lowering the observed detrimental effect of high substrate concentrations. Furthermore, on-line reaction monitoring would allow studying the effect of the reaction parameters on the rate of side product formation, which might further contribute to optimizing the overall reaction.

The herein developed approach is potentially transferrable to the synthesis of other *N*-acyl-β-amino alcohols, for which higher selectivity is expected when using aliphatic aldehydes as starting material, since the C–O bond would be less susceptible to hydrogenolysis (see Figure 45). However, based on the experience gained in this project and other literature examples, it seems likely that an optimization of the hydrogenation reaction parameters would be required in each case in order to maximize the yield, since there is still no general robust method for the selective hydrogenation of nitriles in compounds bearing other reactive groups [174,268,269].

4.3. Engineering of HheG *via* site-saturation mutagenesis

The purpose of this part of the project was to improve the catalytic activity of HheG in the cyanolysis of epoxides using site-saturation mutagenesis. HheG is an HHDH of special interest for it is capable of converting cyclic epoxides, as well as a range of acyclic vicinally di-substituted epoxides [115]. However, its cyanolytic activity is rather poor, limiting the synthesis of cyclic or vicinally di-substituted β-cyanohydrins on preparative scale. HheC – the only HHDH used in an industrial process [201] – presents generally higher activity and enantioselectivity than other HHDHs and has been widely studied. Previous studies aiming at improving the cyanolytic activity of HheG were based or aided by structural alignments between this enzyme and HheC. This was done either by selecting structurally homologous residues that had led to significantly higher cyanolytic activity of HheC upon mutation [117], or by aligning the crystal structure of HheG with the structure of HheC bound to (*R*)-4-cyano-3-hydroxybutyrate or styrene oxide in order to select promising amino acid exchanges that might improve the interaction with the docked ligands [211]. In this thesis, the former approach was used, and a site-saturation mutagenesis library was generated for position Thr154, since mutagenesis of the homologous residue in HheC (Thr134) improved the enzyme's cyanolytic activity [117,118].

Contrary to expectations, the screening of the constructed SSM library at position T154 did not afford any variants with improved cyanolytic activity. Sequencing of the four variants with highest activity (maximum activity decrease of 35% with respect to the conversion reached using the wild-type controls) showed that they were all WT except for one, carrying leucine at position

154 (see section 3.3.2.). The number of screened variants (92) is close to the theoretical number to cover the expected library size in order to achieve 95% coverage of all possible substitutions (96). Also, sequencing of the combined vectors of all generated colonies and of four single colonies picked randomly suggested a good quality of the mutant library (see Figure 51). Furthermore, variants B5, B11 and A3 are probably the only ones carrying a threonine at position 154, also suggesting a high probability that the majority of all 20 amino acids is represented in the generated library. Therefore, it does not seem likely that the lack of variants with enhanced cyanolytic activity is due to a poor library quality. As reported by Koopmeiners, HheG and HheC do not only share low sequence identity (26%), but the structure of their active sites is very different (see section 1.3.2., Figure 14) [112,117]. Therefore, it may not be surprising that residue T154 of HheG does not have the same impact on cyanolytic activity as the structurally homologous residue T134 in HheC. In the case of HheC, fluorescence experiments indicated that mutation T134A had only a minor effect on the binding of cyanide and bromide, suggesting that the increase of cyanolytic activity was caused by reactivity differences and not an increased binding affinity [118]. Structural analysis demonstrated that the anion binding site, as well as the site binding the R group connected to the secondary carbon of the epoxide remained unchanged. Furthermore, there were no detectable changes in the position and orientation of the catalytic triad (Ser132, Tyr145 and Arg149). However, residue T134 in HheC forms a hydrogen bond with Ser132, which donates a hydrogen bond to the oxygen atom of the substrate epoxide or alcohol. Therefore, the loss of this H bond upon replacing Thr by Ala in position 134 led to an enhancement of the cyanolytic activity of HheC. In the case of HheG, it seems that threonine at position 154 is required to maintain the enzyme's cyanolytic activity and, probably, structural differences in the immediate proximity of the active site between HheG and HheC account for these results.

Regarding the differences in activity observed between the wild-type controls and clones identified as wild-type HheG in the SSM library at position T154 (*i.e.* B5, B11 and A3, with a maximum activity decrease of 35% with respect to the WT control, see Table 14), these can be explained by a difference in the amount of recombinantly expressed HheG in the different wells. Variations in temperature and aeration could account for differences in the levels of expression from one well to another. Furthermore, although the size of the cell pellets was estimated to be constant along the plate, differences in the cell density due to temperature and aeration variations would also have an impact on the amount of protein expressed in each well. Furthermore, it is possible that other unidentified factors could have contributed to this difference in conversion between the WT controls and the WT clones from this library. A screening experiment performed using a 96-deep-well plate containing only WT controls for the cyanide-mediated epoxide ring-opening of cyclohexene oxide showed a standard deviation of

16% (data not shown), which corresponds to, approximately, 50% of the difference observed between the WT controls and the mutants carrying Thr in position 154 in the generated library. The differences in conversion observed between the WT controls and the clones identified as WT in the screening of SSM library at position T195, however, are much more significant. Certain clones bearing threonine at position 195 afforded more than 3-fold higher conversion of cyclohexene oxide than the WT controls. This difference cannot be simply explained by variations in expression level due to the different locations on the plate. Most likely, this is due to the fact that the WT controls were picked from a several years-old glycerol stock of *E. coli* BL21 (DE3) Gold carrying the pET-28a(+)-hheG vector. Long term storage of expression strains is usually not recommended, since they tend to lose their plasmids due to endonuclease or recombinase activity (*E. coli* DH5α cells are *endA and recA* negative, while *E. coli* BL21 (DE3) Gold cells are not) [304] or by mutations causing spontaneous antibiotic resistance, therefore eliminating the selectivity effect of the medium. This, together with the possible accumulation of other mutations over time that might decrease the expression rate of HheG, could explain the extremely low conversion values observed for the WT controls. For the construction of SSM library at position T154, the WT controls were inoculated from a fresh glycerol stock and, thus, these exhibited much higher activity (average of 27% conversion afforded by the WT controls of the SSM library at position 154 after a reaction time of 5 h 45 min *versus* an average of 7% conversion afforded by the WT controls of the SSM library at position 195 after a reaction time of 5 h 30 min).

The results of this side project may be used as a small example to illustrate the complexity of the relationship between enzymes' sequence, structure and function. As exemplified by Schallmey's success in improving the cyanolytic activity of HheC *via* single point mutation at position T134 – identified after comparison of the sequences of HheC, $HheB_{Myc}$ from *Mycobacterium sp*. strain GP1 and $HheB_{Cor}$ from *Corynebacterium* [118] – amino acid exchanges that allow for the improvement of certain characteristics in some enzymes may in some cases be successfully transferred to other enzymes from the same family. However, as shown in this thesis and previously reported by Julia Koopmeiners [117], this transfer of beneficial mutations to other enzymes does not always work out as expected.

5. References

1. Turner, N.J.; Humphreys, L. *Biocatalysis in Organic Synthesis*; The Royal Society of Chemistry, 2018.
2. Schrewe, M.; Julsing, M.K.; Bühler, B.; Schmid, A. Whole-cell biocatalysis for selective and productive C–O functional group introduction and modification. *Chem. Soc. Rev.* **2013**, *42*, 6346–6377.
3. Lin, B.; Tao, Y. Whole-cell biocatalysts by design. *Microb. Cell Fact.* **2017**, *16*, 1–12.
4. Reetz, M.T. Biocatalysis in organic chemistry and biotechnology: past , present , and future. *J. Am. Chem. Soc.* **2013**, *135*, 12480–12496.
5. Pasteur, M., L. Mémoire sur la fermentation de l'acide tantrique. *C. R. Hebd. Seances Acad. Sci.* **1858**, *46*, 615–618.
6. Fischer, E. Influence of configuration on the action of enzymes. *Ber. Dtsch. Chem. Ges.* **1894**, *27*, 2985–2993.
7. Zaks, A; Klibanov, A. M. Enzymatic catalysis in organic media at 100 degrees C. *Science* **1984**, *224*, 1249–1251.
8. Zaks, A.; Klibanov, A.M. Enzyme-catalyzed processes in organic solvents. *Proc. Natl. Acad. Sci.* **1985**, *82*, 3192–3196.
9. Buchholz, K.; Kasche, V. *Biocatalysts and enzyme technology*; Wiley-Blackwell , Hoboken, USA, 2006; Vol. 2.
10. Sheldon, R.A.; Arends, I.; Hanefeld, U. Introduction: Green Chemistry and Catalysis. In *Green Chemistry and Catalysis*; Wiley-VCH Verlag GmbH & Co. KGaA, Weinheim, Germany, 2007; pp. 1–47.
11. Choi, J.M.; Han, S.S.; Kim, H.S. Industrial applications of enzyme biocatalysis: Current status and future aspects. *Biotechnol. Adv.* **2015**, *33*, 1443–1454.
12. Gröger, H.; Asano, Y. *Enzyme Catalysis in Organic Synthesis*; Wiley-VCH Verlag GmbH & Co. KGaA, Weinheim, Germany, 2012; pp. 1–42.
13. Constable, D.J.C.; Dunn, P.J.; Hayler, J.D.; Humphrey, G.R.; Leazer, J.L.; Linderman, R.J.; Lorenz, K.; Manley, J.; Pearlman, B.A.; Wells, A.; et al. Key green chemistry research areas - A perspective from pharmaceutical manufacturers. *Green Chem.* **2007**, *9*, 411–420.
14. Reetz, M.T. What are the limitations of enzymes in synthetic organic chemistry? *Chem. Rec.* **2016**, *16*, 2449–2459.
15. Sperl, J.M.; Sieber, V. Multienzyme cascade reactions—status and recent advances. *ACS Catal.* **2018**, 2385–2396.
16. France, S.P.; Hepworth, L.J.; Turner, N.J.; Flitsch, S.L. Constructing biocatalytic cascades: In vitro and in vivo approaches to de novo multi-enzyme pathways. *ACS Catal.* **2017**, *7*, 710–724.
17. Gröger, H.; Hummel, W. Combining the "two worlds" of chemocatalysis and biocatalysis towards multi-step one-pot processes in aqueous media. *Curr. Opin. Chem. Biol.* **2014**, *19*, 171–179.
18. Gröger, H.; Hummel, W. Chemoenzymatic multistep one-pot processes. In *Cascade Biocatalysis: Integrating Stereoselective and Environmentally Friendly Reactions;* Wiley-VCH Verlag GmbH & Co. KGaA, Weinheim, Germany, 2014, pp. 427–456.
19. Schrittwieser, J.H.; Velikogne, S.; Hall, M.; Kroutil, W. Artificial biocatalytic linear cascades for preparation of organic molecules. *Chem. Rev.* **2018**, *118*, 270–348.
20. Ricca, E.; Brucher, B.; Schrittwieser, J.H. Multi-enzymatic cascade reactions: Overview and perspectives. *Adv. Synth. Catal.* **2011**, *353*, 2239–2262.
21. Makkee, M.; Kieboom, A.P.G.; Van Bekkum, H.; Roels, J.A. Combined action of enzyme and metal catalyst, applied to the preparation of D-mannitol. *J. Chem. Soc. Chem. Commun.* **1980**, 930–931.
22. Sheldon, R.A.; Arends, I.W.C.E.; Hanefeld, U. Process Integration and Cascade Catalysis. In

Green Chemistry and Catalysis; Wiley-VCH Verlag GmbH & Co. KGaA, Weinheim, Germany, 2007; pp. 389–408.

23. Abu, R.; Woodley, J.M. Application of enzyme coupling reactions to shift thermodynamically limited biocatalytic reactions. *ChemCatChem* **2015**, *7*, 3094–3105.
24. Muschiol, J.; Peters, C.; Oberleitner, N.; Mihovilovic, M.D.; Bornscheuer, U.T.; Rudroff, F. Cascade catalysis-strategies and challenges en route to preparative synthetic biology. *Chem. Commun.* **2015**, *51*, 5798–5811.
25. Hanefeld, U.; Straathof, A.J.J.; Heijnen, J.J. Enzymatic formation and esterification of (*S*) - mandelonitrile. *J. Mol. Catal. B Enzym.* **2001**, *11*, 213–218.
26. Reetz, M.T. New approaches to the use of amino acids as chiral building blocks in organic synthesis. *Angew. Chemie (International Ed. English)* **1991**, *30*, 1531–1546.
27. Bergmeier, S.C. The Synthesis of vicinal amino alcohols. *Tetrahedron* **2000**, *56*, 2561–2576.
28. Klingler, F.D. Asymmetric hydrogenation of prochiral amino ketones to amino alcohols for pharmaceutical use. *Acc. Chem. Res.* **2007**, *40*, 1367–1376.
29. Métro, T.-X.; Duthion, B.; Gomez Pardo, D.; Cossy, J. Rearrangement of β-amino alcohols via aziridiniums: a review. *Chem. Soc. Rev.* **2010**, *39*, 89–102.
30. Weng, C.; Zhang, H.; Xiong, X.; Lu, X.; Zhou, Y. Evolution of epoxides to synthesize β-amino alcohols. *Asian J. Chem.* **2014**, *26*, 3761–3768.
31. Li, G.; Chang, H.T.; Barry Sharpless, K. Catalytic asymmetric aminohydroxylation (AA) of olefins. *Angew. Chemie (International Ed. English)* **1996**, *35*, 451–454.
32. Donohoe, T.J.; Callens, C.K.A.; Flores, A.; Lacy, A.R.; Rathi, A.H. Recent developments in methodology for the direct oxyamination of olefins. *Chem. - A Eur. J.* **2011**, *17*, 58–76.
33. Burchak, O.N.; Py, S. Reductive cross-coupling reactions (RCCR) between C=N and C=O for β-amino alcohol synthesis. *Tetrahedron* **2009**, *65*, 7333–7356.
34. Ye, C.X.; Melcamu, Y.Y.; Li, H.H.; Cheng, J.T.; Zhang, T.T.; Ruan, Y.P.; Zheng, X.; Lu, X.; Huang, P.Q. Dual catalysis for enantioselective convergent synthesis of enantiopure vicinal amino alcohols. *Nat. Commun.* **2018**, *9*, 1–9.
35. Torssell, S. *Stereoselective Synthesis of Amino Alcohols : Applications to Natural Product Synthesis*; 2007; Doctoral thesis
36. Cheng, M.-J.; Tsai, I.-L.; Chen, I.-S. Chemical constituents from the root bark of formosan *Zanthoxylum ailanthoides*. *J. Chinese Chem. Soc.* **2003**, *50*, 1241–1246.
37. Johns, S.R.; Lamberton, J.A.; Tweeddale, H.J.; Willing, R.I. Alkaloids of *Zanthoxylum conspersipunctatum* (*Rutaceae*): The structure of a new alkaloid isomeric with protopine. *Aust. J. Chem.* **1969**, *22*, 2233–2236.
38. Shoeb, A.; Kapil, R.S.; Popli, S.P. Coumarins and alkaloids of *Aegle marmelos*. *Phytochemistry* **1973**, *12*, 2071–2072.
39. Somanathan, R.; Aguilar, H.R.; Ventura, G.R.; Smith, K.M. Syntheses of natural hydroxyamides using trimethylsilyl cyanide. *Synth. Commun.* **1983**, *13*, 273–280.
40. Cheng, M.J.; Lee, K.H.; Tsai, I.L.; Chen, I.S. Two new sesquiterpenoids and anti-HIV principles from the root bark of *Zanthoxylum ailanthoides*. *Bioorganic Med. Chem.* **2005**, *13*, 5915–5920.
41. Albonico, S.M.; Kuck, A.M.; Deulofeu, V. Tembamide from *Fagara hyemalis* (St. Hill.) Engler. *J. Chem. Soc.* **1967**, 1327–1328.
42. Schrittwieser, J.H.; Coccia, F.; Kara, S.; Grischek, B.; Kroutil, W.; D'Alessandro, N.; Hollmann, F. One-pot combination of enzyme and Pd nanoparticle catalysis for the synthesis of enantiomerically pure 1,2-amino alcohols. *Green Chem.* **2013**, *15*, 3318–3331.
43. Yadav, J.S.; Reddy, P.T.; Nanda, S.; Bhaskar Rao, A. Stereoselective synthesis of (*R*)-(-)-denopamine, (*R*)-(-)-tembamide and (*R*)-(-)-aegeline via asymmetric reduction of azidoketones by *Daucus carota* in aqueous medium. *Tetrahedron: Asymmetry* **2002**, *12*, 3381–3385.
44. Kamal, A.; Shaik, A.A.; Sandbhor, M.; Malik, M.S. Chemoenzymatic synthesis of (*R*)- and (*S*)-tembamide, aegeline and denopamine by a one-pot lipase resolution protocol.

Tetrahedron: Asymmetry **2004**, *15*, 3939–3944.

45. Liardo, E.; González-Fernández, R.; Ríos-Lombardía, N.; Morís, F.; García-Álvarez, J.; Cadierno, V.; Crochet, P.; Rebolledo, F.; González-Sabín, J. Strengthening the combination between enzymes and metals in aqueous medium: Concurrent ruthenium-catalyzed nitrile hydration - Asymmetric ketone bioreduction. *ChemCatChem* **2018**, *10*, 4676–4682.
46. Buchanan, D.J.; Dixon, D.J.; Scott, M.S.; Lainé, D.I. Short asymmetric syntheses of bioactive β-aryl ethanolamine derivatives via the highly diastereoselective delta lactol oxy-Michael addition. *Tetrahedron: Asymmetry* **2004**, *15*, 195–197.
47. Sadyandy, R. An asymmetric dihydroxylation route to (*R*)-(-)-octopamine, (*R*)-(-)-tembamide and (*R*)-(-)- aegeline. *Arkivoc* **2005**, *2005*, 36–43.
48. Cortez, N.A.; Aguirre, G.; Parra-Hake, M.; Somanathan, R. Synthesis of (*R*)-tembamide and (*R*)-aegeline via asymmetric transfer hydrogenation in water. *Tetrahedron: Asymmetry* **2013**, *24*, 1297–1302.
49. Tae Cho, B.; Kyu Kang, S.; Hye Shin, S. Application of optically active 1,2-diol monotosylates for synthesis of β-azido and β-amino alcohols with very high enantiomeric purity. Synthesis of enantiopure (*R*)-octopamine, (*R*)-tembamide and (*R*)-aegeline. *Tetrahedron: Asymmetry* **2002**, *13*, 1209–1217.
50. Lee, D.M.; Lee, J.C.; Jeong, N.; Lee, K.I. Asymmetric transfer hydrogenation of 2-tosyloxy-1-(4-hydroxyphenyl)ethanone derivatives: synthesis of (*R*)-tembamide, (*R*)-aegeline, (*R*)-octopamine, and (*R*)-denopamine. *Tetrahedron: Asymmetry* **2007**, *18*, 2662–2667.
51. Zhu, C.; Xia, Q.; Chen, X.; Liu, Y.; Du, X.; Cui, Y. Chiral metal–organic framework as a platform for cooperative catalysis in asymmetric cyanosilylation of aldehydes. *ACS Catal.* **2016**, *6*, 7590–7596.
52. Aguirre, G.; Salgado-rodríguez, A.; Flores-lópez, L.Z.; Parra-hake, M. Asymmetric synthesis of naturally occurring β -hydroxyamides (*R*)-tembamide and (*R*)-aegeline. *J. Mex. Chem. Soc.* **2001**, *45*, 21–24.
53. Brown, R.F.C.; Donohue, A.C.; Jackson, W.R.; McCarthy, T.D. Synthetic applications of optically active cyanohydrins. Enantioselective syntheses of the hydroxyamides tembamide and aegeline, the cardiac drug denopamine, and some analogues of the bronchodilator salbutamol. *Tetrahedron* **1994**, *50*, 13739–13752.
54. Baeza, A.; Nájera, C.; Sansano, J.M.; Saá, J.M. Binolam-AlCl: A two-centre catalyst for the synthesis of enantioenriched cyanohydrin *O*-phosphates. *Chem. - A Eur. J.* **2005**, *11*, 3849–3862.
55. Das, A.; Choudhary, M.K.; Kureshy, R.I.; Roy, T.; Khan, N.U.H.; Abdi, S.H.R.; Bajaj, H.C. Enantioselective Henry and aza-Henry reaction in the synthesis of (*R*)-tembamide using efficient, recyclable polymeric Cu(II) complexes as catalyst. *Chempluschem* **2014**, *79*, 1138–1146.
56. Bracco, P.; Busch, H.; von Langermann, J.; Hanefeld, U. Enantioselective synthesis of cyanohydrins catalysed by hydroxynitrile lyases – a review. *Org. Biomol. Chem.* **2016**, *14*, 6375–6389.
57. Holt, J.; Hanefeld, U. Enantioselective enzyme-catalysed synthesis of cyanohydrins. *Curr. Org. Synth.* **2009**, *6*, 15–37.
58. Gruber-Khadjawi, M.; Fechter, M.H.; Griengl, H. Cleavage and Formation of Cyanohydrins. In *Enzyme Catalysis in Organic Synthesis*; Drauz, K., Groger, H., May, O., Eds.; Wiley-VCH Verlag GmbH & Co, Weinheim, Germany, 2012; pp. 947–990.
59. Dehli, J.R.; Gotor, V. Enantio- and chemoselective bioreduction of β-keto nitriles by the fungus *Curvularia lunata*. *Tetrahedron: Asymmetry* **2000**, *11*, 3693–3700 .
60. Kataoka, M.; Shimizu, S.; Doi, Y.; Sakamoto, K.; Yamada, H. Microbial production of chiral pantothenonitrile through stereospecific reduction of 2'-ketopanthotenonitrile. *Biotechnol. Lett.* **1990**, *12*, 357–360.
61. DeSantis, G.; Zhu, Z.; Greenberg, W.A.; Wong, K.; Chaplin, J.; Hanson, S.R.; Farwell, B.; Nicholson, L.W.; Rand, C.L.; Weiner, D.P.; et al. An enzyme library approach to biocatalysis:

Development of nitrilases for enantioselective production of carboxylic acid derivatives. *J. Am. Chem. Soc.* **2002**, *124*, 9024–9025.

62. Itoh, T.; Mitsukura, K.; Kanphai, W.; Takagi, Y.; Kihara, H.; Tsukube, H. Thiacrown ether technology in lipase-catalyzed reaction: Scope and limitation for preparing optically active 3-hydroxyalkanenitriles and application to insect pheromone synthesis. *J. Org. Chem.* **1997**, *62*, 9165–9172.
63. Thomas, J.C.; Aggio, B.B.; Marques de Oliveira, A.R.; Piovan, L. High-throughput preparation of optically active cyanohydrins mediated by lipases. *European J. Org. Chem.* **2016**, *2016*, 5964–5970.
64. Jin, F.Z.; Zhao, C.C.; Ma, H.C.; Chen, G.J.; Dong, Y.B. Homochiral BINAPDA-Zr-MOF for heterogeneous asymmetric cyanosilylation of aldehydes. *Inorg. Chem.* **2019**, *58*, 9253–9259.
65. de Oliveira, A.; Alves, J.S.; de Lima, G.F.; De Abreu, H.A. Acidic and basic sites of M2DEBDC (M = Mg or Mn and E = O or S) acting as catalysts for cyanosilylation of aldehydes. *Polyhedron* **2018**, *154*, 98–107.
66. Ohkuma, T.; Kurono, N.; Sakaguchi, Y.; Yamauchi, K.; Yurino, T. Enantioselective cyanosilylation of alkynyl ketones catalyzed by combined systems consisting of chiral ruthenium(II) complex and lithium phenoxide. *Adv. Synth. Catal.* **2018**, *360*, 1517–1522.
67. Tsubogo, T.; Ishiwata, T.; Kobayashi, S. Asymmetric carbon-carbon bond formation under continuous-flow conditions with chiral heterogeneous catalysts. *Angew. Chemie - Int. Ed.* **2013**, *52*, 6590–6604.
68. Khan, N. ul H.; Kureshy, R.I.; Abdi, S.H.R.; Agrawal, S.; Jasra, R. V. Metal catalyzed asymmetric cyanation reactions. *Coord. Chem. Rev.* **2008**, *252*, 593–623.
69. Wühler, F.; Liebig, J. Notiz über die Bildung des Bittermandelöls. *Ann. der Pharm.* **1837**, *21*, 96–97.
70. Rosenthaler, L. Enzyme-effected asymmetric syntheses. *Biochem. Z.* **1908**, *14*, 238–253.
71. Dadashipour, M.; Asano, Y. Hydroxynitrile lyases: Insights into biochemistry, discovery, and engineering. *ACS Catal.* **2011**, *1*, 1121–1149.
72. Griengl, H.; Schwab, H.; Fechter, M. The synthesis of chiral cyanohydrins by oxynitrilases. *Trends Biotechnol.* **2000**, *18*, 252–256.
73. Paravidino, M.; Sorgedrager, M.J.; Orru, R.V.A.; Hanefeld, U. Activity and enantioselectivity of the hydroxynitrile lyase *Me*HNL in dry organic solvents. *Chem. - A Eur. J.* **2010**, *16*, 7596–7604.
74. Hanefeld, U. Immobilisation of hydroxynitrile lyases. *Chem. Soc. Rev.* **2013**, *42*, 6308–6321.
75. Lanfranchi, E.; Steiner, K.; Glieder, A.; Hajnal, I.; Sheldon, R.; Pelt, S.; Winkler, M. Mini-review: Recent developments in hydroxynitrile lyases for industrial biotechnology. *Recent Pat. Biotechnol.* **2013**, *7*, 197–206.
76. Henderson, R.K.; Jiménez-González, C.; Constable, D.J.C.; Woodley, J.M. EHS & LCA assessment for 7-ACA synthesis: A case study for comparing biocatalytic & chemical synthesis. **2008**, *4*, 180–192.
77. Hatti-Kaul, R.; Tornvall, U.; Gustafsson, L.; Borjesson, P. Industrial biotechnology for the production of bio-based chemicals –a cradle-to-grave perspective. *Trends Biotechnol.* **2007**, *25*, 119–124.
78. Pollard, D.J.; Woodley, J.M. Biocatalysis for pharmaceutical intermediates: the future is now. *Trends Biotechnol.* **2007**, *25*, 66–73.
79. Asano, Y.; Kawahara, N. A New S-Hydroxynitrile Lyase from *Baliospermum montanum* - Its structure, molecular dynamics simulation, and improvement by protein engineering. *Ind. Biotechnol.* **2016**, *12*, 91–97.
80. Wiedner, R.; Kothbauer, B.; Pavkov-Keller, T.; Gruber-Khadjawi, M.; Gruber, K.; Schwab, H.; Steiner, K. Improving the properties of bacterial *R*-selective hydroxynitrile lyases for industrial applications. *ChemCatChem* **2015**, *7*, 325–332.
81. Andexer, J.N.; Langermann, J. V.; Kragl, U.; Pohl, M. How to overcome limitations in

biotechnological processes - examples from hydroxynitrile lyase applications. *Trends Biotechnol.* **2009**, *27*, 599–607.

82. Liu, Z.; Pscheidt, B.; Avi, M.; Gaisberger, R.; Hartner, F.S.; Schuster, C.; Skranc, W.; Gruber, K.; Glieder, A. Laboratory evolved biocatalysts for stereoselective syntheses of substituted benzaldehyde cyanohydrins. *ChemBioChem* **2008**, *9*, 58–61.
83. Avi, M.; Griengl, H. Biocatalysis in Biphasic Systems: Oxynitrilases. In *Organic Synthesis with Enzymes in Non-Aqueous Media*; Carrea, G., Riva, S., Eds.; Wiley-VCH Verlag GmbH & Co, Weinheim, Germany, 2008; pp. 189–210.
84. Von Langermann, J.; Mell, A.; Paetzold, E.; Daußmann, T.; Kragl, U. Hydroxynitrile lyase in organic solvent-free systems to overcome thermodynamic limitations. *Adv. Synth. Catal.* **2007**, *349*, 1418–1424.
85. Costes, D.; Wehtje, E.; Adlercreutz, P. Hydroxynitrile lyase-catalyzed synthesis of cyanohydrins in organic solvents: Parameters influencing activity and enantiospecificity. *Enzyme Microb. Technol.* **1999**, *25*, 384–391.
86. Klibanov, A. Why are enzymes less active in organic solvents than in water? *Trends Biotechnol.* **1997**, *15*, 97–101.
87. Faber, K. *Biotransformations in Organic Chemistry*; 6th ed.; Springer-Verlag Berlin Heidelberg, Germany, 2011.
88. Sheldon, R.A.; van Pelt, S. Enzyme immobilisation in biocatalysis: Why, what and how. *Chem. Soc. Rev.* **2013**, *42*, 6223–6235.
89. Effenberger, F.; Foerster, S.; Kobler, C. State of the art and applications in stereoselective synthesis of chiral cyanohydrins. In *Biocatalysis in the Pharmaceutical and Biotechnology Industries*; Patel, R., Ed.; CRC Press, Taylor & Francis Group, Boca Raton, USA, 2007; pp. 677–698.
90. Dreveny, I.; Gruber, K.; Glieder, A.; Thompson, A.; Kratky, C. The hydroxynitrile lyase from almond: A lyase that looks like an oxidoreductase. *Structure* **2001**, *9*, 803–815.
91. Nanda, S.; Kato, Y.; Asano, Y. A new (*R*)-hydroxynitrile lyase from *Prunus mume*: Asymmetric synthesis of cyanohydrins. *Tetrahedron* **2005**, *61*, 10908–10916.
92. Mindrebo, J.T.; Nartey, C.M.; Seto, Y.; Burkart, M.D.; Noel, J.P. Unveiling the functional diversity of the alpha/beta hydrolase superfamily in the plant kingdom. *Curr. Opin. Struct. Biol.* **2016**, *41*, 233–246.
93. Hughes, J.; Carvalho, F.J.P.D.C.; Hughes, M.A. Purification, characterization, and cloning of α-hydroxynitrile lyase from cassava (*Manihot esculenta* Crantz). *Arch. Biochem. Biophys.* **1994**, *311*, 496–502.
94. Andexer, J.N.; Staunig, N.; Eggert, T.; Kratky, C.; Pohl, M.; Gruber, K. Hydroxynitrile lyases with α/β-hydrolase fold: Two enzymes with almost identical 3D structures but opposite enantioselectivities and different reaction mechanisms. *ChemBioChem* **2012**, *13*, 1932–1939.
95. Sulzbacher Caruso, C.; de Fátima Travensolo, R.; de Campus Bicudo, R.; de Macedo Lemos, E.G.; Ulian de Araújo, A.P.; Carrilho, E. α-Hydroxynitrile lyase protein from *Xylella fastidiosa*: Cloning, expression, and characterization. *Microb. Pathog.* **2009**, *47*, 118–127.
96. Dadashipour, M.; Yamazaki, M.; Momonoi, K.; Tamura, K.; Fuhshuku, K.I.; Kanase, Y.; Uchimura, E.; Kaiyun, G.; Asano, Y. *S*-selective hydroxynitrile lyase from a plant *Baliospermum montanum*: Molecular characterization of recombinant enzyme. *J. Biotechnol.* **2011**, *153*, 100–110.
97. Riveros-Rosas, H.; Julián-Sánchez, A.; Villalobos-Molina, R.; Pardo, J.P.; Piña, E. Diversity, taxonomy and evolution of medium-chain dehydrogenase/reductase superfamily. *Eur. J. Biochem.* **2003**, *270*, 3309–3334.
98. Lauble, H.; Miehlich, B.; Förster, S.; Wajant, H.; Effenberger, F. Crystal structure of hydroxynitrile lyase from *Sorghum bicolor* in complex with the inhibitor benzoic acid: A novel cyanogenic enzyme. *Biochemistry* **2002**, *41*, 12043–12050.
99. Wiedner, R.; Gruber-Khadjawi, M.; Schwab, H.; Steiner, K. Discovery of a novel *R*-selective

bacterial hydroxynitrile lyase from *Acidobacterium capsulatum*. *Comput. Struct. Biotechnol. J.* **2014**, *10*, 58–62.

100. Hussain, Z.; Wiedner, R.; Steiner, K.; Hajek, T.; Avi, M.; Hecher, B.; Sessitsch, A.; Schwab, H. Characterization of two bacterial hydroxynitrile lyases with high similarity to cupin superfamily proteins. *Appl. Environ. Microbiol.* **2012**, *78*, 2053–2055.
101. Hajnal, I.; Łyskowski, A.; Hanefeld, U.; Gruber, K.; Schwab, H.; Steiner, K. Biochemical and structural characterization of a novel bacterial manganese-dependent hydroxynitrile lyase. *FEBS J.* **2013**, *280*, 5815–5828.
102. Lanfranchi, E.; Pavkov-Keller, T.; Koehler, E.M.; Diepold, M.; Steiner, K.; Darnhofer, B.; Hartler, J.; Bergh, T. Van Den; Joosten, H.J.; Gruber-Khadjawi, M.; *et al.* Erratum: Enzyme discovery beyond homology: a unique hydroxynitrile lyase in the Bet v1 superfamily. *Sci. Rep.* **2017**, *7*, 46834.
103. Glieder, A.; Weis, R.; Skranc, W.; Poechlauer, P.; Dreveny, I.; Majer, S.; Wubbolts, M.; Schwab, H.; Gruber, K. Comprehensive Step-by-Step Engineering of an (*R*)-Hydroxynitrile Lyase for Large-Scale Asymmetric Synthesis. *Angew. Chemie - Int. Ed.* **2003**, *42*, 4815–4818.
104. Gruber, K.; Gartler, G.; Krammer, B.; Schwab, H.; Kratky, C. Reaction mechanism of hydroxynitrile lyases of the α/β-hydrolase superfamily: The three-dimensional structure of the transient enzyme-substrate complex certifies the crucial role of Lys236. *J. Biol. Chem.* **2004**, *279*, 20501–20510.
105. Seely, M.K.; Criddle, R.S.; Conn, E.E. The metabolism of aromatic compounds in higher plants - On the requirement of hydroxynitrile lyase for flavin. *J. Biol. Chem.* **1966**, *241*, 4457–4462.
106. Dreveny, I.; Andryushkova, A.S.; Glieder, A.; Gruber, K.; Kratky, C. Substrate binding in the FAD-dependent hydroxynitrile lyase from almond provides insight into the mechanism of cyanohydrin formation and explains the absence of dehydrogenation activity. *Biochemistry* **2009**, *48*, 3370–3377.
107. Jorns, M.S. Mechanism of catalysis by the flavoenzyme oxynitrilase. *J. Biol. Chem.* **1979**, *254*, 12145–12152.
108. Poelarends, G.J.; van Hylckama Vlieg, J.; Marchesi, J.R.; Freitas Dos Santos, L.M.; Janssen, D. Degradation of 1,2-Dibromoethane by *Mycobacterium sp.* Strain GP1. *J. Bacteriol.* **1999**, *181*, 2050–8.
109. van den Wijngaard, A.J.; Reuvekamp, P.T.; Janssen, D.B. Purification and characterization of haloalcohol dehalogenase. *J. Bacteriol.* **1991**, *173*, 124–129.
110. Van Den Wijngaard, A.J.; Janssen, D.B.; Witholt, B. Degradation of epichlorohydrin and halohydrins by bacterial cultures isolated from freshwater sediment. *Microbiology* **1989**, *135*, 2199–2208.
111. Castro, C.E.; Bartnicki, E.W. Biodehalogenation. Epoxidation of halohydrins, epoxide opening, and transhalogenation by a *Flavobacterium sp.* **1968**, *7*, 3213–3218.
112. Koopmeiners, J.; Diederich, C.; Solarczek, J.; Voß, H.; Mayer, J.; Blankenfeldt, W.; Schallmey, A. HheG, a halohydrin dehalogenase with activity on cyclic epoxides. *ACS Catal.* **2017**, *7*, 6877–6886.
113. Schallmey, A.; Schallmey, M. Recent advances on halohydrin dehalogenases - from enzyme identification to novel biocatalytic applications. *Appl. Microbiol. Biotechnol.* **2016**, *100*, 7827–7839.
114. Hasnaoui-Dijoux, G.; Elenkov, M.M.; Lutje Spelberg, J.H.; Hauer, B.; Janssen, D.B. Catalytic promiscuity of halohydrin dehalogenase and its application in enantioselective epoxide ring opening. *ChemBioChem* **2008**, *9*, 1048–1051.
115. Calderini, E.; Wessel, J.; Suess, P.; Schrepfer, P.; Wardenga, R.; Schallmey, A. Selective ring-opening of di-substituted epoxides catalysed by halohydrin dehalogenases. *ChemCatChem* **2019**, *11*, 2099–2106.
116. Elenkov, M.M.; Hauer, B.; Janssen, D.B. Enantioselective ring opening of epoxides with

cyanide catalysed by halohydrin dehalogenases: A new approach to non-racemic β-hydroxy nitriles. *Adv. Synth. Catal.* **2006**, *348*, 579–585.

117. Koopmeiners, J. *Characterization of novel halohydrin dehalogenases for application in fine chemical synthesis*; 2017; Doctoral thesis
118. Schallmey, M.; Jekel, P.; Tang, L.; Majerić Elenkov, M.; Höffken, H.W.; Hauer, B.; Janssen, D.B. A single point mutation enhances hydroxynitrile synthesis by halohydrin dehalogenase. *Enzyme Microb. Technol.* **2015**, *70*, 50–57.
119. Schallmey, M. *Novel halohydrin dehalogenases by protein engineering and database mining*; 2015; Doctoral thesis
120. De Jong, R.M.; Tiesinga, J.J.W.; Rozeboom, H.J.; Kalk, K.H.; Tang, L.; Janssen, D.B.; Dijkstra, B.W. Structure and mechanism of a bacterial haloalcohol dehalogenase: A new variation of the short-chain dehydrogenase/reductase fold without an NAD(P)H binding site. *EMBO J.* **2003**, *22*, 4933–4944.
121. Kavanagh, K.L.; Jörnvall, H.; Persson, B.; Oppermann, U. The SDR superfamily: Functional and structural diversity within a family of metabolic and regulatory enzymes. *Cell. Mol. Life Sci.* **2008**, *65*, 3895–3906.
122. Schallmey, M.; Koopmeiners, J.; Wells, E.; Wardenga, R.; Schallmey, A. Expanding the halohydrin dehalogenase enzyme family: Identification of novel enzymes by database mining. *Appl. Environ. Microbiol.* **2014**, *80*, 7303–7315.
123. Koopmeiners, J.; Halmschlag, B.; Schallmey, M.; Schallmey, A. Biochemical and biocatalytic characterization of 17 novel halohydrin dehalogenases. *Appl. Microbiol. Biotechnol.* **2016**, *100*, 7517–7527.
124. Xue, F.; Liu, Z.Q.; Wang, Y.J.; Zhu, H.Q.; Wan, N.W.; Zheng, Y.G. Efficient synthesis of (*S*)-epichlorohydrin in high yield by cascade biocatalysis with halohydrin dehalogenase and epoxide hydrolase mutants. *Catal. Commun.* **2015**, *72*, 147–149.
125. Wang, X.; Lin, H.; Zheng, Y.; Feng, J.; Yang, Z.; Tang, L. MDC-Analyzer-facilitated combinatorial strategy for improving the activity and stability of halohydrin dehalogenase from *Agrobacterium radiobacter* AD1. *J. Biotechnol.* **2015**, *206*, 1–7.
126. Schallmey, M.; Floor, R.J.; Hauer, B.; Breuer, M.; Jekel, P.A.; Wijma, H.J.; Dijkstra, B.W.; Janssen, D.B. Biocatalytic and structural properties of a highly engineered halohydrin dehalogenase. *ChemBioChem* **2013**.
127. Hietanen, A.; Kanerva, L.T. One-pot oxidation-hydrocyanation sequence coupled to lipase-catalyzed diastereoresolution in the chemoenzymatic synthesis of sugar cyanohydrin esters. *European J. Org. Chem.* **2012**, 2729–2737.
128. Hietanen, A.; Ekholm, F.S.; Leino, R.; Kanerva, L.T. Applying biocatalysis to the synthesis of diastereomerically enriched cyanohydrin mannosides. *European J. Org. Chem.* **2010**, 6974–6980.
129. Sakai, T.; Wang, K.; Ema, T. Lipase-catalyzed dynamic kinetic resolution giving optically active cyanohydrins: Use of silica-supported ammonium hydroxide and porous ceramic-immobilized lipase. *Tetrahedron* **2008**, *64*, 2178–2183.
130. Veum, L.; Kanerva, L.T.; Halling, P.J.; Maschmeyer, T.; Hanefeld, U. Optimisation of the enantioselective synthesis of cyanohydrin esters. *Adv. Synth. Catal.* **2005**, *347*, 1015–1021.
131. Veum, L.; Hanefeld, U. Enantioselective formation of mandelonitrile acetate: Investigation of a dynamic kinetic resolution II. *Tetrahedron: Asymmetry* **2004**, *15*, 3707–3709.
132. Purkarthofer, T.; Skranc, W.; Schuster, C.; Griengl, H. Potential and capabilities of hydroxynitrile lyases as biocatalysts in the chemical industry. *Appl. Microbiol. Biotechnol.* **2007**, *76*, 309–320.
133. Roos, J.; Stelzer, U.; Effenberger, F. Synthesis of (1*R*,*cis*,α*S*)-cypermethrine via lipase catalyzed kinetic resolution of racemic m-phenoxybenzaldehyde. *Tetrahedron: Asymmetry* **1998**, *9*, 1043–1049.
134. Adrio, J.L.; Demain, A.L. Microbial enzymes: tools for biotechnological processes. *Biomolecules* **2014**, *4*, 117–139.

135. Hidalgo, A.; Bornscheuer, U.T. Directed Evolution of Lipases and Esterases for Organic Synthesis. In *Biocatalysis in the Pharmaceutical and Biotechnology Industries*; Patel, R., Ed.; CRC Press, Taylor & Francis Group, Boca Raton, USA, 2006; pp. 159–179.
136. Hanefeld, U. Reagents for (ir)reversible enzymatic acylations. *Org. Biomol. Chem.* **2003**, *1*, 2405–15.
137. Valivety, R.H.; Halling, P.J.; Macrae, A.R. Water as a competitive inhibitor of lipase-catalysed esterification in organic media. *Biotechnol. Lett.* **1993**, *15*, 1133–1138.
138. Kim, J.E.; Han, J.J.; Yoon, J.H.; Rhee, J.S. Effect of salt hydrate pair on lipase-catalyzed regioselective monoacylation of sucrose. *Biotechnol. Bioeng.* **1998**, *57*, 121–125.
139. Kvittingen, L.; Sjursnes, B.; Anthonsen, T. Use of salt hydrates to buffer optimal water level during lipase catalysed synthesis in organic media: A practical procedure for organic chemists. *Tetrahedron* **1992**, *48*, 2793–2802.
140. Reis, P.; Holmberg, K.; Watzke, H.; Leser, M.E.; Miller, R. Lipases at interfaces: A review. *Adv. Colloid Interface Sci.* **2009**, *147–148*, 237–250.
141. Ericsson, D.J.; Kasrayan, A.; Johansson, P.; Bergfors, T.; Sandström, A.G.; Bäckvall, J.E.; Mowbray, S.L. X-ray structure of *Candida antarctica* lipase a shows a novel lid structure and a likely mode of interfacial activation. *J. Mol. Biol.* **2008**, *376*, 109–119.
142. Paiva, A.L.; Balcao, V.M.; Malcata, F.X. Kinetics and mechanisms of reactions catalyzed by immobilized lipases. *Enzyme Microb. Technol.* **2000**, *27*, 187–204.
143. Jing, Q.; Kazlauskas, R.J. Determination of absolute configuration of secondary alcohols using lipase-catalyzed kinetic resolutions. *Chirality* **2008**, *20*, 724–735.
144. Kazlauskas, R.J.; Weissfloch, A.N.E.; Rappaport, A.T.; Cuccia, L.A. A rule to predict which enantiomer of a secondary alcohol reacts faster in reactions catalyzed by cholesterol esterase, lipase from *Pseudomonas cepacia*, and lipase from *Candida rugosa*. *J. Org. Chem.* **1991**, *56*, 2656–2665.
145. Savile, C.K.; Kazlauskas, R.J. How substrate solvation contributes to the enantioselectivity of subtilisin toward secondary alcohols. *J. Am. Chem. Soc.* **2005**, *127*, 12228–12229.
146. Pozo, M.; Gotor, V. Double enantioselective enzymic synthesis of carbonates and urethanes. *Tetrahedron: Asymmetry* **1995**, *6*, 2797–2802.
147. Moberg, C.; Wingstrand, E. Enantioenriched acylated cyanohydrins: Synthesis and analysis. *Synlett* **2010**, 355–367.
148. Phillips, R.S. Temperature modulation of the stereochemistry of enzymatic catalysis: Prospects for exploitation. *Trends Biotechnol.* **1996**, *14*, 13–16.
149. Paravidino, M.; Hanefeld, U. Enzymatic acylation: assessing the greenness of different acyl donors. *Green Chem.* **2011**, *13*, 2651–2657.
150. Ortiz, C.; Ferreira, M.L.; Barbosa, O.; Dos Santos, J.C.S.; Rodrigues, R.C.; Berenguer-Murcia, Á.; Briand, L.E.; Fernandez-Lafuente, R. Novozym 435: The “perfect” lipase immobilized biocatalyst? *Catal. Sci. Technol.* **2019**, *9*, 2380–2420.
151. Gotor-Fernández, V.; Busto, E.; Gotor, V. *Candida antarctica* lipase B: An ideal biocatalyst for the preparation of nitrogenated organic compounds. *Adv. Synth. Catal.* **2006**, *348*, 797–812.
152. Anderson, E.M.; Larsson, K.M.; Kirk, O. One biocatalyst - many applications: The use of *Candida antarctica* B-lipase in organic synthesis. *Biocatal. Biotransformation* **1998**, *16*, 181–204.
153. Kirk, O.; Christensen, M.W. Lipases from *Candida antarctica*: Unique biocatalysts from a unique origin. *Org. Process Res. Dev.* **2002**, *6*, 446–451.
154. Yang, C.; Wang, F.; Lan, D.; Whiteley, C.; Yang, B.; Wang, Y. Effects of organic solvents on activity and conformation of recombinant *Candida antarctica* lipase A produced by *Pichia pastoris. Process Biochem.* **2012**, *47*, 533–537.
155. Widmann, M.; Juhl, P.B.; Pleiss, J. Structural classification by the lipase engineering database: A case study of *Candida antarctica* lipase A. *BMC Genomics* **2010**, *11*, 1–8.
156. Müller, J.; Fredrich, B.; Kohlmann, C.; Maksym, L.; Bornscheuer, U.T. A high-throughput

assay for the determination of acyltransferase activity of lipase CAL-A. *Eur. J. Lipid Sci. Technol.* **2014**, *116*, 232–236.
157. Brenneis, R.; Baeck, B. Esterification of fatty acids using *Candida antarctica* lipase A in water-abundant systems. *Biotechnol. Lett.* **2012**, *34*, 1459–1463.
158. Persson, M.; Costes, D.; Wehtje, E.; Adlercreutz, P. Effects of solvent, water activity and temperature on lipase and hydroxynitrile lyase enantioselectivity. *Enzyme Microb. Technol.* **2002**, *30*, 916–923.
159. Okrob, D.; Paravidino, M.; Orru, R.V.A.; Wiechert, W.; Hanefeld, U.; Pohl, M. Hydroxynitrile lyase from *Arabidopsis thaliana*: Identification of reaction parameters for enantiopure cyanohydrin synthesis by pure and immobilized catalyst. *Adv. Synth. Catal.* **2011**, *353*, 2399–2408.
160. Cabirol, F.L.; Hanefeld, U.; Sheldon, R.A. Immobilized hydroxynitrile lyases for enantioselective synthesis of cyanohydrins: Sol-gels and cross-linked enzyme aggregates. *Adv. Synth. Catal.* **2006**, *348*, 1645–1654.
161. Chmura, A.; Van Der Kraan, G.M.; Kielar, F.; Van Langen, L.M.; Van Rantwijk, F.; Sheldon, R.A. Cross-linked aggregates of the hydroxynitrile lyase from *Manihot esculenta:* Highly active and robust biocatalysts. *Adv. Synth. Catal.* **2006**, *348*, 1655–1661.
162. Shen, Z.L.; Zhou, W.J.; Liu, Y.T.; Ji, S.J.; Loh, T.P. One-pot chemoenzymatic syntheses of enantiomerically-enriched *O*-acetyl cyanohydrins from aldehydes in ionic liquid. *Green Chem.* **2008**, *10*, 283–28.
163. Veum, L.; Hanefeld, U. Enantioselective synthesis of aliphatic cyanohydrin acetates. *Synlett* **2005**, 2382–2384.
164. Veum, L.; Kuster, M.; Telalovic, S.; Hanefeld, U.; Maschmeyer, T. Enantioselective synthesis of protected cyanohydrins. *Eur. J. Org. Chem.* **2002**, 1516–1522.
165. Purkarthofer, T.; Skranc, W.; Weber, H.; Griengl, H.; Wubbolts, M.; Scholz, G.; Pöchlauer, P. One-pot chemoenzymatic synthesis of protected cyanohydrins. *Tetrahedron* **2004**, *60*, 735–739.
166. Baeza, A.; Najera, C.; Sansano, J.M.; Saa, J.M. Asymmetric synthesis of *O*-benzoyl cyanohydrins by reaction of aldehydes with benzoyl cyanide catalysed by BINOLAM-Ti(IV) complexes. *Tetrahedron: Asymmetry* **2005**, *16*, 2385–2389.
167. Roose, P.; Eller, K.; Henkes, E.; Rossbacher, R.; Höke, H. Amines, Aliphatic. In *Ullmann's Encyclopedia of Industrial Chemistry*; Elvers, B., Ed.; Wiley-VCH Verlag GmbH & Co, Weinheim, Germany, 2015.
168. Vogt, P.F.; Gerulis, J.J. Amines, Aromatic. In *Ullmann's Encyclopedia of Industrial Chemistry*; Elvers, B., Ed.; Wiley-VCH Verlag GmbH & Co, Weinheim, Germany, 2012.
169. Bagal, D.B.; Bhanage, B.M. Catalytic reduction of nitriles. *Sci. Synth.* **2018**, *6*, 375–400.
170. Legnani, L.; Bhawal, B.N.; Morandi, B. Recent developments in the direct synthesis of unprotected primary amines. *Synth.* **2017**, *49*, 776–789.
171. Saavedra, J.Z.; Resendez, A.; Rovira, A.; Eagon, S.; Haddenham, D.; Singaram, B. Reaction of $InCl_3$ with various reducing agents: $InCl_3$–$NaBH_4$-mediated reduction of aromatic and aliphatic nitriles to primary amines. *J. Org. Chem.* **2012**, *77*, 221–228.
172. Haddenham, D.; Pasumansky, L.; DeSoto, J.; Eagon, S.; Singaram, B. Reductions of aliphatic and aromatic nitriles to primary amines with diisopropylaminoborane. *J. Org. Chem.* **2009**, *74*, 1964–1970.
173. Baker, R.T.; Westcott, S.A. Hydroboration and Diboration of Imines. In *Modern Reduction Methods*; Anderson, P., Munslow, I.M., Eds.; Wiley-VCH Verlag GmbH & Co. KGaA, Weinheim, Germany, 2008; pp. 297–320.
174. Veum, L.; Pereira, S.R.M.; Van Der Waal, J.C.; Hanefeld, U. Catalytic hydrogenation of cyanohydrin esters as a novel approach to *N*-acylated β-amino alcohols - Reaction optimisation by a design of experiment approach. *European J. Org. Chem.* **2006**, 1664–1671.
175. Freifelder, M. A low pressure process for the reduction of nitriles. Use of rhodium catalyst.

J. Am. Chem. Soc. **1960**, *82*, 2386–2389.
176. Enthaler, S.; Junge, K.; Addis, D.; Erre, G.; Beller, M. A practical and benign synthesis of primary amines through ruthenium-catalyzed reduction of nitriles. *ChemSusChem* **2008**, *1*, 1006–1010.
177. Segobia, D.J.; Trasarti, A.F.; Apesteguía, C.R. Hydrogenation of nitriles to primary amines on metal-supported catalysts: Highly selective conversion of butyronitrile to n-butylamine. *Appl. Catal. A: Gen.* **2012**, *445–446*, 69–75.
178. Vilches-Herrera, M.; Werkmeister, S.; Junge, K.; Börner, A.; Beller, M. Selective catalytic transfer hydrogenation of nitriles to primary amines using Pd/C. *Catal. Sci. Technol.* **2014**, *4*, 629.
179. Schärringer, P.; Müller, T.E.; Lercher, J.A. Investigations into the mechanism of the liquid-phase hydrogenation of nitriles over Raney-Co catalysts. *J. Catal.* **2008**, *253*, 167–179.
180. Wietelmann, U.; Felderhoff, M.; Rittmeyer, P. Hydrides. In *Ullmann's Encyclopedia of Industrial Chemistry*; Elvers, B., Ed.; Wiley-VCH Verlag GmbH & Co, Weinheim, Germany, 2016.
181. Liu, S.; Yang, Y.; Zhen, X.; Li, J.; He, H.; Feng, J.; Whiting, A. Enhanced reduction of C–N multiple bonds using sodium borohydride and an amorphous nickel catalyst. *Org. Biomol. Chem.* **2012**, *10*, 663.
182. Wu, B.; Zhang, J.; Yang, M.; Yue, Y.; Ma, L.J.; Yu, X.Q. Raney Ni/KBH_4: An efficient and mild system for the reduction of nitriles to amines. *Arkivoc* **2008**, *2008*, 95–102.
183. Caddick, S.; Judd, D.B.; Lewis, A.K.D.K.; Reich, M.T.; Williams, M.R.V. A generic approach for the catalytic reduction of nitriles. *Tetrahedron* **2003**, *59*, 5417–5423.
184. Krupka, J.; Pasek, J. Nitrile hydrogenation on solid catalysts – New insights into the reaction mechanism. *Curr. Org. Chem.* **2012**, *16*, 988–1004.
185. Bagal, D.B.; Bhanage, B.M. Recent advances in transition metal-catalyzed hydrogenation of nitriles. *Adv. Synth. Catal.* **2015**, *357*, 883–900.
186. Lévay, K.; Hegedűs, L. Selective heterogeneous catalytic hydrogenation of nitriles to primary amines. *Period. Polytech. Chem. Eng.* **2018**, *62*, 476–488.
187. Braun, J.; Blessing, G.; Zobel, F. Katalytische Hydrierungen unter Druck bei Gegenwart von Nickelsalzen, VI.: Nitrile. *Berichte der Dtsch. Chem. Gesellschaft* **1923**, *36*, 1988–2001.
188. Greenfield, H. Catalytic hydrogenation of butyronitrile. *Ind. Eng. Chem. Prod. Res. Dev.* **1967**, *6*, 142–144.
189. Zhang, Y.; Bai, G.; Li, Y.; Yan, X.; Chen, L. Racemization of *R*-2-amino-1-butanol catalyzed by a fixed-bed Raney cobalt catalyst. *J. Mol. Catal. A Chem.* **2006**, *255*, 269–274.
190. Gomez, S.; Peters, J.A.; Maschmeyer, T. The reductive animation of aldehydes and ketones and the hydrogenation of nitriles: Mechanistic aspects and selectivity control. *Adv. Synth. Catal.* **2002**, *344*, 1037–1057.
191. Zhou, Z.; Li, M.; Xu, J.H.; Zhang, Z.J. A single mutation increases the activity and stability of *Pectobacterium carotovorum* nitrile reductase. *ChemBioChem* **2018**, *19*, 521–526.
192. Li, M.; Zhou, Z.; Zhang, Z.J.; Yu, H.L.; Xu, J.H. *Biochemical properties of a new nitrile reductase cloned from Pectobacterium carotovorum*; Elsevier B.V., 2016; Vol. 131.
193. Moeller, K.; Nguyen, G.S.; Hollmann, F.; Hanefeld, U. Expression and characterization of the nitrile reductase queF from *E. coli*. *Enzyme Microb. Technol.* **2013**, *52*, 129–133.
194. Wilding, B.; Winkler, M.; Petschacher, B.; Kratzer, R.; Glieder, A.; Klempier, N. Nitrile reductase from *Geobacillus kaustophilus*: A potential catalyst for a new nitrile biotransformation reaction. *Adv. Synth. Catal.* **2012**, *354*, 2191–2198.
195. Bar-Even, A.; Noor, E.; Savir, Y.; Liebermeister, W.; Davidi, D.; Tawfik, D.S.; Milo, R. The moderately efficient enzyme: Evolutionary and physicochemical trends shaping enzyme parameters. *Biochemistry* **2011**, *50*, 4402–4410.
196. Sheldon, R.A.; Pereira, P.C. Biocatalysis engineering: The big picture. *Chem. Soc. Rev.* **2017**, *46*, 2678–2691.
197. Newton, M.S.; Arcus, V.L.; Gerth, M.L.; Patrick, W.M. Enzyme evolution: innovation is easy,

optimization is complicated. *Curr. Opin. Struct. Biol.* **2018**, *48*, 110–116.
198. Reetz, M.T.; Bocola, M.; Carballeira, J.D.; Zha, D.; Vogel, A. Expanding the range of substrate acceptance of enzymes: Combinatorial active-site saturation test. *Angew. Chemie - Int. Ed.* **2005**, *44*, 4192–4196.
199. Reetz, M.T.; Brunner, B.; Schneider, T.; Schulz, F.; Clouthier, C.M.; Kayser, M.M. Directed evolution as a method to create enantioselective cyclohexanone monooxygenases for catalysis in Baeyer-Villiger reactions. *Angew. Chemie - Int. Ed.* **2004**, *43*, 4075–4078.
200. Chen, K.; Arnold, F.H. Tuning the activity of an enzyme for unusual environments: Sequential random mutagenesis of subtilisin E for catalysis in dimethylformamide. *Proc. Natl. Acad. Sci.* **1993**, *90*, 5618–5622.
201. Ma, S.K.; Gruber, J.; Davis, C.; Newman, L.; Gray, D.; Wang, A.; Grate, J.; Huisman, G.W.; Sheldon, R.A. A green-by-design biocatalytic process for atorvastatin intermediate. *Green Chem.* **2010**, *12*, 81–86.
202. Jennifer Kan, S.B.; Huang, X.; Gumulya, Y.; Chen, K.; Arnold, F.H. Genetically programmed chiral organoborane synthesis. *Nature* **2017**, *552*, 132–136.
203. Bloom, J.D.; Meyer, M.M.; Meinhold, P.; Otey, C.R.; MacMillan, D.; Arnold, F.H. Evolving strategies for enzyme engineering. *Curr. Opin. Struct. Biol.* **2005**, *15*, 447–452.
204. Tee, K.L.; Wong, T.S. Polishing the craft of genetic diversity creation in directed evolution. *Biotechnol. Adv.* **2013**, *31*, 1707–1721.
205. Wilson, D.S.; Keefe, A.D. Random mutagenesis by PCR. *Curr. Protoc. Mol. Biol.* **2001**, 1–9.
206. Wong, T.; Zhurina, D.; Schwaneberg, U. The diversity challenge in directed protein evolution. *Comb. Chem. High Throughput Screen.* **2006**, *9*, 271–288.
207. Park, S.; Morley, K.L.; Horsman, G.P.; Holmquist, M.; Hult, K.; Kazlauskas, R.J. Focusing mutations into the *P. fluorescens* esterase binding site increases enantioselectivity more effectively than distant mutations. *Chem. Biol.* **2005**, *12*, 45–54.
208. Davids, T.; Schmidt, M.; Böttcher, D.; Bornscheuer, U.T. Strategies for the discovery and engineering of enzymes for biocatalysis. *Curr. Opin. Chem. Biol.* **2013**, *17*, 215–220.
209. Reetz, M.T.; Carballeira, J.D. Iterative saturation mutagenesis (ISM) for rapid directed evolution of functional enzymes. *Nat. Protoc.* **2007**, *2*, 891–903.
210. Guo, C.; Chen, Y.; Zheng, Y.; Zhang, W.; Tao, Y.; Feng, J.; Tang, L. Exploring the enantioselective mechanism of halohydrin dehalogenase from *Agrobacterium radiobacter* AD1 by iterative saturation mutagenesis. *Appl. Environ. Microbiol.* **2015**, *81*, 2919–2926.
211. Calderini, E. *A chemo-enzymatic cascade for the production of enantiopure aminoalcohols*; 2019; Doctoral thesis.
212. Mayer, J. *Protein engineering of the halohydrin dehalogenase HheG*; 2017; Master thesis.
213. Malona, J.A.; Cariou, K.; Spencer, W.T.; Frontier, A.J. Total synthesis of (±)-rocaglamide via oxidation-initiated nazarov cyclization. *J. Org. Chem.* **2012**, *77*, 1891–1908.
214. Hanahan, D. Studies on transformation of *Escherichia coli* with plasmids. *J. Mol. Biol.* **1983**.
215. Rahman, M.T.; Uddin, M.S.; Sultana, R.; Moue, A.; Setu, M. Polymerase chain reaction (PCR): A short review. *Anwer Khan Mod. Med. Coll. J.* **2013**, *4*, 30–36.
216. Barnes, W.M. Polymerase Chain Reaction (PCR). In *Encyclopedia of Genetics*; Brenner, S., Miller, J.H., Eds.; Elsevier Science Inc., Amsterdam, The Netherlands, 2001; pp. 1499–1503.
217. Laemmli, U.K. Cleavage of structural proteins during the assembly of the head of bacteriophage T4. *Nature* **1970**, *227*, 680–685.
218. Hanefeld, U.; Straathof, A.J.J.; Heijnen, J.J. Study of the (*S*)-hydroxynitrile lyase from *Hevea brasiliensis*: Mechanistic implications. *Biochim. Biophys. Acta - Protein Struct. Mol. Enzymol.* **1999**, *1432*, 185–193.
219. Lowe, M.E. Assays for pancreatic triglyceride lipase and colipase. *Methods Mol. Biol.* **1999**, *109*, 59–70.
220. Chen, C.; Fujimoto, Y.; Girdaukas, G.; Sih, C.J. Quantitative analyses of biochemical kinetic resolutions of enantiomers. *J. Am. Chem. Soc* **1982**, *104*, 7294–7299.
221. Sakuth, M.; Mensing, T.; Schuler, J.; Heitmann, W.; Strehlke, G.; Mayer, D. Ethers,

Aliphatic. In *Ullmann's Encyclopedia of Industrial Chemistry*; Elvers, B., Ed.; Wiley-VCH Verlag GmbH & Co. KGaA, Weinheim, Germany, 2012; p. 440.
222. Halling, P.J. Salt hydrates for water activity control with biocatalysts in organic media. *Biotechnol. Tech.* **1992**, *6*, 271–276.
223. Yildirim, D.; Tükel, S.S.; Alagöz, D. Crosslinked enzyme aggregates of hydroxynitrile lyase partially purified from *Prunus dulcis* seeds and its application for the synthesis of enantiopure cyanohydrins. *Biotechnol. Prog.* **2014**, *30*, 818–827.
224. van Langen, L.M.; van Rantwijk, F.; Sheldon, R.A. Enzymatic hydrocyanation of a sterically hindered aldehyde. Optimization of a chemoenzymatic procedure for (*R*)-2-chloromandelic acid. *Org. Process Res. Dev.* **2003**, *7*, 828–831.
225. Adlercreutz, P. Immobilisation and application of lipases in organic media. *Chem. Soc. Rev.* **2013**, *42*, 6406–36.
226. Bastida, A.; Sabuquillo, P.; Armisen, P.; Fernández-Lafuente, R.; Huguet, J.; Guisán, J.M. A single step purification, immobilization, and hyperactivation of lipases via interfacial adsorption on strongly hydrophobic supports. *Biotechnol. Bioeng.* **1998**, *58*, 486–493.
227. Gossauer, A. Cyanohydrins: The Benzoin condensation. In *Structure and Reactivity of Biomolecules: An Introduction into Organic Chemistry*; Wiley-VCH Verlag GmbH & Co. KGaA, Weinheim, Germany, 2018; p. 316.
228. Paul, I.; Schladenhauffen, B. Process for chemical reactions involving cyanohydrins; 2005; Patent application publication number: US 2006/0111586 A1
229. Hickel, A.; Radke, C.J.; Blanch, H.W. Role of organic solvents on *Pa*-hydroxynitrile lyase interfacial activity and stability. *Biotechnol. Bioeng.* **2001**, *74*, 18–28.
230. Bauer, M.; Griengl, H.; Steiner, W. Parameters influencing stability and activity of a *S*-hydroxynitrile lyase from *Hevea brasiliensis* in two-phase systems. *Enzyme Microb. Technol.* **1999**, *24*, 514–522.
231. Hickel, A.; Radke, C.J.; Blanch, H.W. Hydroxynitrile lyase adsorption at liquid/liquid interfaces. *J. Mol. Catal. - B Enzym.* **1998**, *5*, 349–354.
232. Griengl, H.; Klempier, N.; Pöchlauer, P.; Schmidt, M.; Shi, N.; Zabelinskaja-Mackova, A.A. Enzyme catalysed formation of (*S*)-cyanohydrins derived from aldehydes and ketones in a biphasic solvent system. *Tetrahedron* **1998**, *54*, 14477–14486.
233. Bornscheuer, U.T.; Kazlauskas, R.J. *Hydrolases in Organic Synthesis: Regio- and Stereoselective Biotransformations;* Second Edition; Wiley-VCH Verlag GmbH & Co. KGaA, Weinheim, Germany, 2006.
234. Cahn, R.S.; Ingold, C.; Prelog, V. Specification of molecular chirality. *Angew. Chemie Int. Ed. English* **1966**, *5*, 385–415.
235. Jin, X.; Liu, B.; Ni, Z.; Wu, Q.; Lin, X. A novel control of enzymatic enantioselectivity through the racemic temperature influenced by reaction media. *Enzyme Microb. Technol.* **2011**, *48*, 454–457.
236. Domínguez De María, P.; Carboni-Oerlemans, C.; Tuin, B.; Bargeman, G.; Van Der Meer, A.; Van Gemert, R. Biotechnological applications of *Candida antarctica* lipase A: State-of-the-art. *J. Mol. Catal. B Enzym.* **2005**, *37*, 36–46.
237. Storz, T.; Gu, J.; Wilk, B.; Olsen, E. Regioselective lipase-catalyzed acylation of 41-desmethoxy-rapamycin without vinyl esters. *Tetrahedron Lett.* **2010**, *51*, 5511–5515.
238. Tamarez, M.; Morgan, B.; Wong, G.S.K.; Tong, W.; Bennett, F.; Lovey, R.; McCormick, J.L.; Zaks, A. Pilot-scale lipase-catalyzed regioselective acylation of ribavirin in anhydrous media in the synthesis of a novel prodrug intermediate. *Org. Process Res. Dev.* **2003**, *7*, 951–953.
239. Méndez-Sánchez, D.; López-Iglesias, M.; Gotor-Fernández, V. Hydrolases in organic chemistry. Recent achievements in the synthesis of pharmaceuticals. *Curr. Org. Chem.* **2016**, *20*, 1186–1203.
240. García, J.; Fernández, S.; Ferrero, M.; Sanghvi, Y.S.; Gotor, V. A mild, efficient and regioselective enzymatic procedure for 5'-*O*-benzoylation of 2'-deoxynucleosides.

Tetrahedron Lett. **2004**, *45*, 1709–1712.
241. Sakulsombat, M.; Vongvilai, P.; Ramström, O. *In situ* evaluation of lipase performances through dynamic asymmetric cyanohydrin resolution. *Org. Biomol. Chem.* **2012**, 1–6.
242. Chen, C.S.; Fujimoto, Y.; Girdaukas, G.; Sih, C.J. Quantitative analyses of biochemical kinetic resolutions of enantiomers. *J. Am. Chem. Soc.* **1982**, *104*, 7294–7299.
243. Willeman, W.F.; Straathof, A.J.J.; Heijnen, J.J. Reaction temperature optimization procedure for the synthesis of (*R*)-mandelonitrile by *Prunus amygdalus* hydroxynitrile lyase using a process model approach. *Enzyme Microb. Technol.* **2002**, *30*, 200–208.
244. Ueatrongchit, T.; Tamura, K.; Ohmiya, T.; H-Kittikun, A.; Asano, Y. Hydroxynitrile lyase from *Passiflora edulis*: Purification, characteristics and application in asymmetric synthesis of (*R*)-mandelonitrile. *Enzyme Microb. Technol.* **2010**, *46*, 456–465.
245. Willeman, W.F.; Hanefeld, U.; Straathof, A.J.J.; Heijnen, J.J. Estimation of kinetic parameters by progress curve analysis for the synthesis of (*R*)-mandelonitrile by *Prunus amygdalus* hydroxynitrile lyase. *Enzyme Microb. Technol.* **2000**, *27*, 423–433.
246. O'Neil, M.J.; Patricia E. Heckelman, A.S.; Budavari, S. *The Merck Index - An Encyclopedia of Chemicals Drugs and Biologicals*, Royal Society of Chemistry, London, UK, 2006.
247. Shakeri, M.; Engström, K.; Sandström, A.G.; Bäckvall, J.E. Highly enantioselective resolution of β-amino esters by *Candida antarctica* lipase a immobilized in mesocellular foam: Application to dynamic kinetic resolution. *ChemCatChem* **2010**, *2*, 534–538.
248. Ding, W.; Li, M.; Dai, R.; Deng, Y. Lipase-catalyzed synthesis of the chiral tetrahydroisoquinoline (*R*)-salsolinol. *Tetrahedron: Asymmetry* **2012**, *23*, 1376–1379.
249. Zamost, B.L.; Nielsen, H.K.; Starnes, R.L. Thermostable enzymes for industrial applications. *J. Ind. Microbiol.* **1991**, *8*, 71–81.
250. Müller, J.; Sowa, M.A.; Fredrich, B.; Brundiek, H.; Bornscheuer, U.T. Enhancing the acyltransferase activity of *Candida antarctica* lipase a by rational design. *ChemBioChem* **2015**, *16*, 1791–1796.
251. Bracco, P.; Torrelo, G.; Noordam, S.; de Jong, G.; Hanefeld, U. Immobilization of *Prunus amygdalus* hydroxynitrile lyase on Celite. *Catalysts* **2018**, *8*, 287.
252. Effenberger, F.; Ziegler, T.; Förster, S. Enzyme-catalyzed cyanohydrin synthesis in organic solvents. *Angew. Chemie Int. Ed. English* **1987**, *26*, 458–460.
253. Basso, A.; De Martin, L.; Ebert, C.; Gardossi, L.; Linda, P. Controlling the hydration of covalently immobilised penicillin G amidase in low-water medium: Properties and use of Celite R-640. *J. Mol. Catal. - B Enzym.* **2000**, *8*, 245–253.
254. Semba, H.; Dobashi, Y.; Matsui, T. Expression of hydroxynitrile lyase from *Manihot esculenta* in yeast and its application in (*S*)-mandelonitrile production using an immobilized enzyme reactor. *Biosci. Biotechnol. Biochem.* **2008**, *72*, 1457–1463.
255. Valivety, R.H.; J. Halling, P.; Macrae, A.R. Reaction rate with suspended lipase catalyst shows similar dependence on water activity in different organic solvents. *Biochim. Biophys. Acta.* **1992**, *1118*, 218–222.
256. Schmitke, J.L.; Wescott, C.R.; Klibanov, A.M. The mechanistic dissection of the plunge in enzymatic activity upon transition from water to anhydrous solvents. *J. Am. Chem. Soc.* **1996**, *118*, 3360–3365.
257. Wehtje, E.; Costes, D.; Adlercreutz, P. Enantioselectivity of lipases: Effects of water activity. *J. Mol. Catal. - B Enzym.* **1997**, *3*, 221–230.
258. Pepin, P.; Lortie, R. Influence of water activity on the enantioselective esterification of (*R,S*)-ibuprofen by *Candida antarctica* lipase B in solventless media. *Biotechnol. Bioeng.* **1999**, *63*, 502–505.
259. Bovara, R.; Carrea, G.; Ottolina, G.; Riva, S. Water activity does not influence the enantioselectivity. *Biotechnol. Lett.* **1993**, *15*, 169–174.
260. Carrea, G.; Riva, S. Properties and synthetic applications of enzymes in organic solvents. *Angew. Chem. Int. Ed. Engl.* **2000**, *39*, 2226–2254.
261. Xu, L.L.; Singh, B.K.; Conn, E.E. Purification and characterization of mandelonitrile lyase

from *Prunus lyonii*. *Arch. Biochem. Biophys.* **1986**, *250*, 322–328.
262. Jaenicke, L.; Preun, J. Chemical modification of hydroxynitrile lyase by selective reaction of an essential cysteine-SH group with α,β-unsaturated propiophenones as pseudo-substrates. *Eur. J. Biochem.* **1984**, *138*, 319–325.
263. Schaaf, P.; Bayer, T.; Koley, M.; Schnürch, M.; Bornscheuer, U.T.; Rudroff, F.; Mihovilovic, M.D. Biocompatible metal-assisted C–C cross-coupling combined with biocatalytic chiral reductions in a concurrent tandem cascade. *Chem. Commun.* **2018**, *54*, 12978–12981.
264. Srinivasamurthy, V.S.T.; Böttcher, D.; Bornscheuer, U.T. A multi-enzyme cascade reaction for the production of 6-hydroxyhexanoic acid. *Zeitschrift fur Naturforsch. - Sect. C J. Biosci.* **2019**, *74*, 71–76.
265. Dawood, A.W.H.; Bassut, J.; de Souza, R.O.M.A.; Bornscheuer, U.T. Combination of the Suzuki–Miyaura cross-coupling reaction with engineered transaminases. *Chem. - A Eur. J.* **2018**, *24*, 16009–16013.
266. Hartung, W.H. Catalytic reduction of nitriles and oximes. *J. Am. Chem. Soc.* **1928**, *50*, 3370–3374.
267. Rosenmund, K.W.; Schindler, H. Über die katalytische Reduktion von Mandelsäuren. *Arch. Pharm. (Weinheim).* **1928**, *432*, 281–283.
268. Hertzberg, R.; Dinér, P.; Moberg, C. Palladium-catalyzed C(sp3)–C(sp2) cross-couplings of *O*-(α-Bromoacyl) cyanohydrins with boronic acids: An entry to enantio-enriched *N*-acylated β-amino alcohols. *Synthesis (Stuttg).* **2016**, *48*, AcH.
269. Hertzberg, R.; Monreal Santiago, G.; Moberg, C. Synthesis of the β3-adrenergic receptor agonist Solabegron and analogous *N*-(2-ethylamino)-β-amino alcohols from *O*-acylated cyanohydrins – expanding the scope of minor enantiomer recycling. *J. Org. Chem.* **2015**, *80*, 2937–2941.
270. Banwell, M.G.; Jones, M.T.; Reekie, T.A.; Schwartz, B.D.; Tan, S.H.; White, L. V Raney cobalt – an underutilised reagent for the selective cleavage of C-X and N-O bonds. *Org. Biomol. Chem.* **2014**, *12*, 7433–7444.
271. Bhor, M.D.; Bhanushali, M.J.; Nandurkar, N.S.; Bhanage, B.M. Highly efficient chemoselective catalytic hydrogenation of diaryl substituted α,β-unsaturated nitriles/carbonyls using homogeneous $Pd(OAc)_2/PPh_3$ catalyst. *Catal. Commun.* **2007**, *8*, 2064–2068.
272. Volf, J.; Pasek, J. Hydrogenation of Nitriles. In *Studies in Surface Science and Catalysis: Catalytic Hydrogenation*; Cerveny, L., Ed.; Elsevier Science Publishers B.V., Amsterdam, The Netherlands, 1986; Vol. 27, pp. 105–144.
273. Greenfield, H. Hydrogenation of benzonitrile to dibenzylamine. *Ind. Eng. Chem. Prod. Res. Dev.* **1976**, *15*, 156–158.
274. Huang, Y.; Adeeva, V.; Sachtler, W.M.H. Stability of supported transition metal catalysts in the hydrogenation of nitriles. *Appl. Catal. A Gen.* **2000**, *196*, 73–85.
275. Fureby, A.M.; Virto, C.; Adlercreutz, P.; Mattiasson, B. Acyl group migrations in 2-monoolein. *Biocatal. Biotransformation* **1996**, *14*, 89–111.
276. Novi, R. *Hydrogenation of aliphatic nitriles over nickel catalysts modified by formaldehyde*; 2004; Doctoral thesis
277. Leemans, L.; van Langen, L.; Hollmann, F.; Schallmey, A. Bienzymatic cascade for the synthesis of an optically active *O*-benzoyl cyanohydrin. *Catalysts* **2019**, *9*, 522.
278. Hsiao, M.K.; Lo, W.T.; Wang, J.H.; Chen, H.L. Hydrogenation of hydrogen cyanide to methane and ammonia by a metal catalyst: Insight from first-principles calculations. *J. Phys. Chem. C* **2016**, *120*, 22946–22956.
279. Besson, P.; Thirion, P. Process for Manufacture of Methylamines; 1969; Patent number: US3468953
280. Rosano, G.L.; Ceccarelli, E.A. Recombinant protein expression in *Escherichia coli*: Advances and challenges. *Front. Microbiol.* **2014**, *5*, 1–17.
281. Steffens, D.L.; Williams, J.G.K. Efficient site-directed saturation mutagenesis using

degenerate oligonucleotides. *J. Biomol. Tech.* **2007**, *18*, 147–149.
282. Hutchison, C.A.; Phillips, S.; Edgell, M, H.; Gillam, S.; Jahnke, P.; Smith, M. Mutagenesis at a specific position in a DNA sequence. *J. Biol. Chem.* **1978**, *253*, 6551–6560.
283. Lundell, K.; Raijola, T.; Kanerva, L.T. Enantioselectivity of *Pseudomonas cepacia* and *Candida rugosa* lipases for the resolution of secondary alcohols: The effect of *Candida rugosa* isoenzymes. *Enzyme Microb. Technol.* **1998**, *22*, 86–93.
284. Nakagawa, Y.; Izumi, K.; Oikawa, N.; Sotomatsu, T.; Shigemura, M.; Fujita, T. Analysis and prediction of hydrophobicity parameters of substituted acetanilides, benzamides and related aromatic compounds. *Environ. Toxicol. Chem.* **1992**, *11*, 901–916.
285. Arnold, F.H. Design by directed evolution. *FASEB J.* **1997**, *11*, 125–131.
286. Wikmark, Y.; Svedendahl Humble, M.; Bäckvall, J.E. Combinatorial library based engineering of *Candida antarctica* lipase a for enantioselective transacylation of sec-alcohols in organic solvent. *Angew. Chemie - Int. Ed.* **2015**, *54*, 4284–4288.
287. Roberge, C.; Fleitz, F.; Pollard, D.; Devine, P. Asymmetric synthesis of cyanohydrin derived from pyridine aldehyde with cross-linked aggregates of hydroxynitrile lyases. *Tetrahedron Lett.* **2007**, *48*, 1473–1477.
288. Veum, L.; Hanefeld, U. Carrier enabled catalytic reaction cascades. *Chem. Commun.* **2006**, 825.
289. Jan, A.H.; Subileau, M.; Deyrieux, C.; Perrier, V.; Dubreucq, É. Elucidation of a key position for acyltransfer activity in *Candida parapsilosis* lipase/acyltransferase (*Cp*LIP2) and in *Pseudozyma antarctica* lipase A (CAL-A) by rational design. *Biochim. Biophys. Acta - Proteins Proteomics* **2016**, *1864*, 187–194.
290. Sehl, T.; Hailes, H.C.; Ward, J.M.; Wardenga, R.; Von Lieres, E.; Offermann, H.; Westphal, R.; Pohl, M.; Rother, D. Two steps in one pot: Enzyme cascade for the synthesis of nor(pseudo)ephedrine from inexpensive starting materials. *Angew. Chemie - Int. Ed.* **2013**, *52*, 6772–6775.
291. Subileau, M.; Jan, A.H.; Drone, J.; Rutyna, C.; Perrier, V.; Dubreucq, E. What makes a lipase a valuable acyltransferase in water abundant medium? *Catal. Sci. Technol.* **2017**, *7*, 2566–2578.
292. Brahma, A.; Musio, B.; Ismayilova, U.; Nikbin, N.; Kamptmann, S.B.; Siegert, P.; Jeromin, G.E.; Ley, S. V.; Pohl, M. An orthogonal biocatalytic approach for the safe generation and use of HCN in a multistep continuous preparation of chiral *O*-acetylcyanohydrins. *Synlett* **2016**, *27*, 262–266.
293. Hartung, W.H.; Simonoff, R. Hydrogenolysis of benzyl groups attached to oxygen, nitrogen, or sulfur. *Org. React.* **1953**, *7*, 267–275.
294. Baltzly, R.; Buck, J.S. Catalytic debenzylation. The effect of substitution on the strength of the *O*-benzyl and *N*-benzyl linkages. *J. Am. Chem. Soc.* **1943**, *65*, 1984–1992.
295. Chojecki, A.; Veprek-Heijman, M.; Müller, T.E.; Schärringer, P.; Veprek, S.; Lercher, J.A. Tailoring Raney-catalysts for the selective hydrogenation of butyronitrile to n-butylamine. *J. Catal.* **2007**, *245*, 237–248.
296. Verhaak, M.J.F.M.; van Dillen, A.J.; Geus, J.W. The selective hydrogenation of acetonitrile on supported nickel catalysts. *Catal. Letters* **1994**, *26*, 37–53.
297. Smith, H.A.; Bedoit, W.C.; Fuzek, J.F. The preparation and aging of Raney nickel catalysts. *J. Am. Chem. Soc.* **1949**, *71*, 3769–3771.
298. Augustine, R.L. Unsupported Metals. In *Heterogeneous Catalysis for the Synthetic Chemist*; Marcel Dekker Inc., New York, USA, 1996; pp. 241–248.
299. Koscielski, T.; Bonnier, J.M.; Damon, J.P.; Masson, J. Catalytic hydrogenation on Raney nickel catalyst modified by chromium hydroxide deposition. *Appl. Catal.* **1989**, *49*, 91–99.
300. Degischer, O.G.; Roessler, F. Modification of a Hydrogenation Catalyst; 2001; Patent application publication number: US 2001/0004672 A1.
301. Cioffi, E.A.; Willis, W.S.; Suib, S.L. Ultrasonically induced enhancement of isotope-exchange catalysts: Surface analysis of Raney nickel alloys. *Langmuir* **1988**, *4*, 697–702.

302. Schmidt, S.; Castiglione, K.; Kourist, R. Overcoming the incompatibility challenge in chemoenzymatic and multi-catalytic cascade reactions. *Chem. - A Eur. J.* **2018**, *24*, 1755–1768.
303. Sheldon, R. a. The E factor: fifteen years on. *Green Chem.* **2007**, *9*, 1273.
304. Phue, J.N.; Sang, J.L.; Trinh, L.; Shiloach, J. Modified *Escherichia coli* B (BL21), a superior producer of plasmid DNA compared with *Escherichia coli* K (DH5α). *Biotechnol. Bioeng.* **2008**, *101*, 831–836.

Appendix

List of tables

List of figures

List of abbreviations

Standard amino acid and nucleotide abbreviations have been used in this thesis.

ACN	Acetonitrile
AcOEt	Ethyl acetate
API	Active pharmaceutical ingredient
*At*HNL	Hydroxynitrile lyase from *Arabidopsis thaliana*
bp	Base pairs
CALA	Lipase A from Candida antarctica
CALB	Lipase B from Candida antarctica
CFE	Cell free extract
CRL	Lipase from *Candida rugosa*
DKR	Dynamic kinetic resolution
DMSO	Dimethyl sulfoxide
DpnI	Restriction enzyme from *Diplococcus pneumoniae* G41
DTT	Dithiothreitol
DWP	Deep-well plate
E. coli	*Escherichia coli*
e.e.	Enantiomeric excess
e.g.	*exempli gratia* (for example)
EDTA	Ethylenediaminetetraacetic acid
et al.	*et alii (and others)*
EV	Empty vector, negative control
FID	Flame ionization detector
G	Relative centrifugal force
GC	Gas chromatography
GC-MS	Gas chromatography- mass spectroscopy
*Hb*HNL	Hydroxynitrile lyase from *Hevea brasiliensis*
HHDH	Halohydrin dehalogenase
HheC	Halohydrin dehalogenase from *Agrobacterium radiobacter*
HheG	Halohydrin dehalogenase from *Ilumatobacter coccineus* YM16-304
HNL	Hydroxynitrile lyase
HPLC	High performance liquid chromatography

iPr_2O	Diisopropyl ether
*i*PrOH	Isopropanol
IPTG	Isopropyl β-D-1-thiogalactopyranoside
kan	Kanamycin
kb	Kilobase
k_{cat}	Turnover number
kDa	Kilodalton
k_M	Michaelis constant
KRED	Ketoreductase
LB	Luria broth
M	Marker
*Me*HNL	Hydroxynitrile lyase from *Manihot esculenta*
MeOH	Methanol
MOF	Metal-organic framework
MTP	Microtiterplate
NADH	Nicotinamide adenine dinucleotide
NADPH	Nicotinamide adenine dinucleotide phosphate
NPs	Nanoparticles
Nu^-	Nucleophile
OD_{600}	Optical density at λ = 600 nm
P	Insoluble pellet fraction
*Pa*HNL	Hydroxynitrile lyase from *Prunus amygdalus*
PBR	Packed-bed reactor
PCR	Polymerase chain reaction
PLE	Porcine liver esterase, from *sus domesticus*
PTFE	Polytetrafluoroethylene
S	Soluble protein fraction
SDS	Sodium dodecyl sulphate
SDS-PAGE	Sodium dodecyl sulphate polyacrylamide gel electrophoresis
SOC	Super optimal broth with Catabolite repression
SSM	Site-saturation mutagenesis
TAE	Tris base, acetic acid and EDTA
TB	Terrific broth
*t*BME	Methyl *tert*-butyl ether
*t*BuOH	*Tert*-butanol
TEMED	Tetramethylethylenediamine
THF	Tetrahydrofuran
T_m	Melting temperature
Tris	Tris(hydroxymethyl)aminomethane
UV	Ultraviolet
Vis	Visible
vs	Versus
WT	Wild-type
X^-	Halide

Supplementary material

Heterologous expression of *Me*HNL

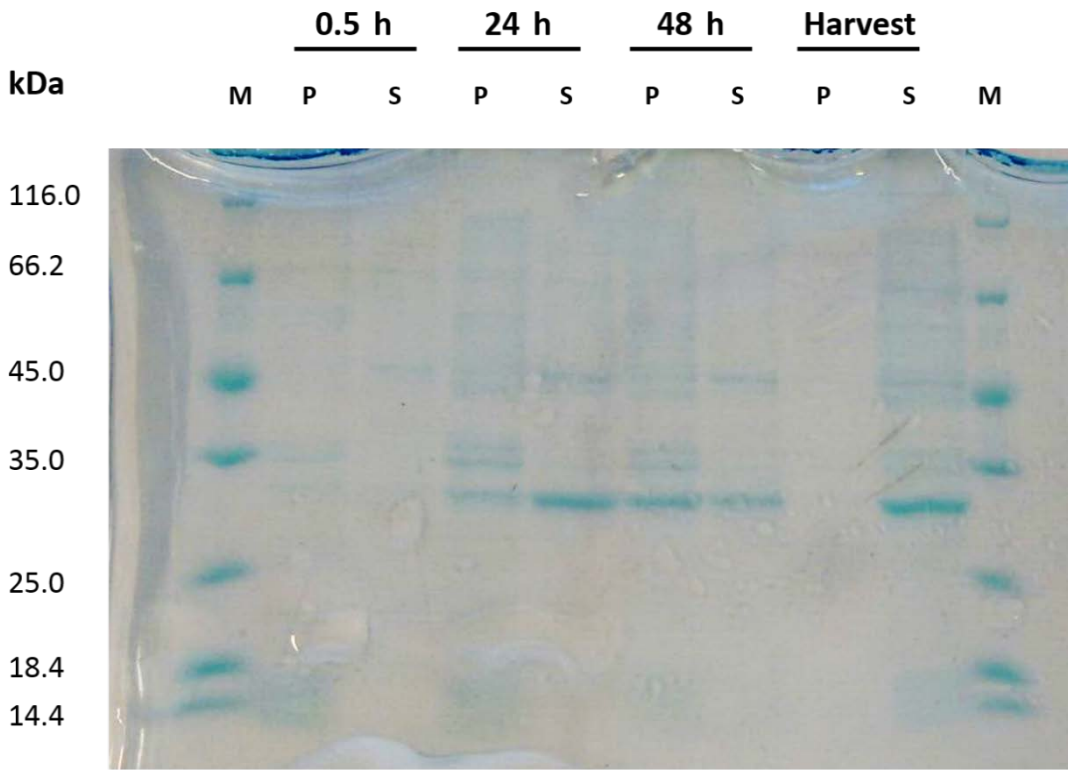

Figure S1. SDS-PAGE showing the progression of protein expression over time (0.5 h, 24 h and 48 h after induction) in the production of *Me*HNL in shake flasks using *E. coli.* K12 Top 10F' harboring the pSE420-MeHNL plasmid as described in section 2.2.2.1. The soluble protein fractions (S) were obtained after incubation of the cell pellets (OD_{600} = 2) with the cell lysis reagent B-PER (40 µL) and subsequent centrifugation to remove cell debris. The insoluble pellet fraction (P) after centrifugation was resuspended in 40 µL B-PER. The 'harvest' lanes correspond to a sample of the insoluble pellet fraction (P) and of the cell-free extract (S) after sonication of the culture. These samples were diluted with Milli-Q® water, as B-PER was not required. Both S and P samples were 4× diluted with Milli-Q® water and incubated with 33% (v/v) loading dye before loading 7 µL in each lane.

Chiral HPLC chromatograms

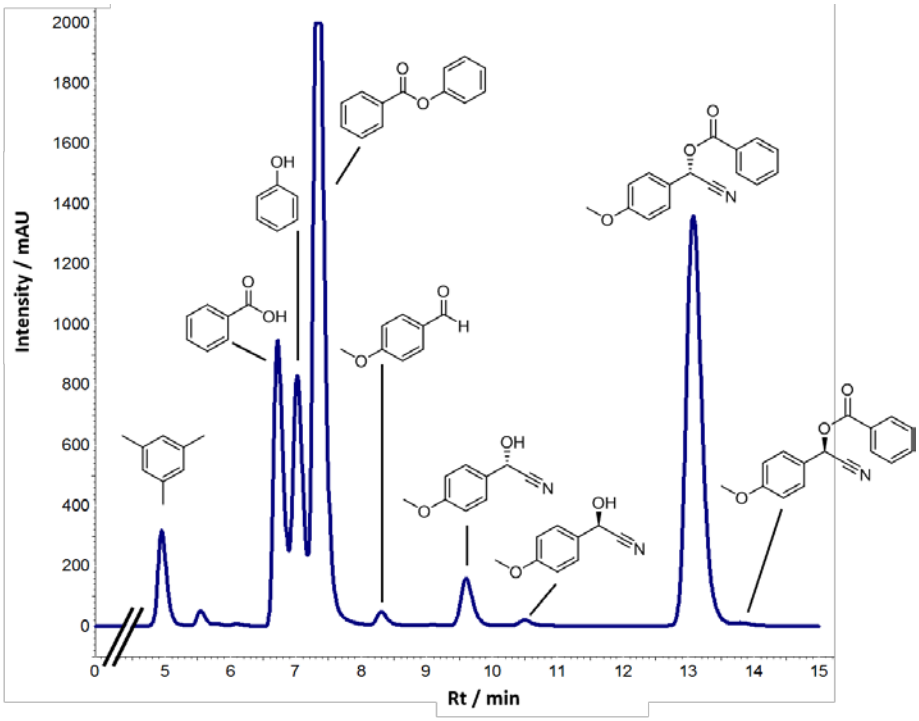

Figure S2. Chiral normal phase HPLC chromatogram from the preparative synthesis of (*S*)-4-methoxymandelonitrile benzoate catalyzed by *Me*HNL and CALA in *i*Pr$_2$O under optimized conditions as described in section 2.2.7.1.

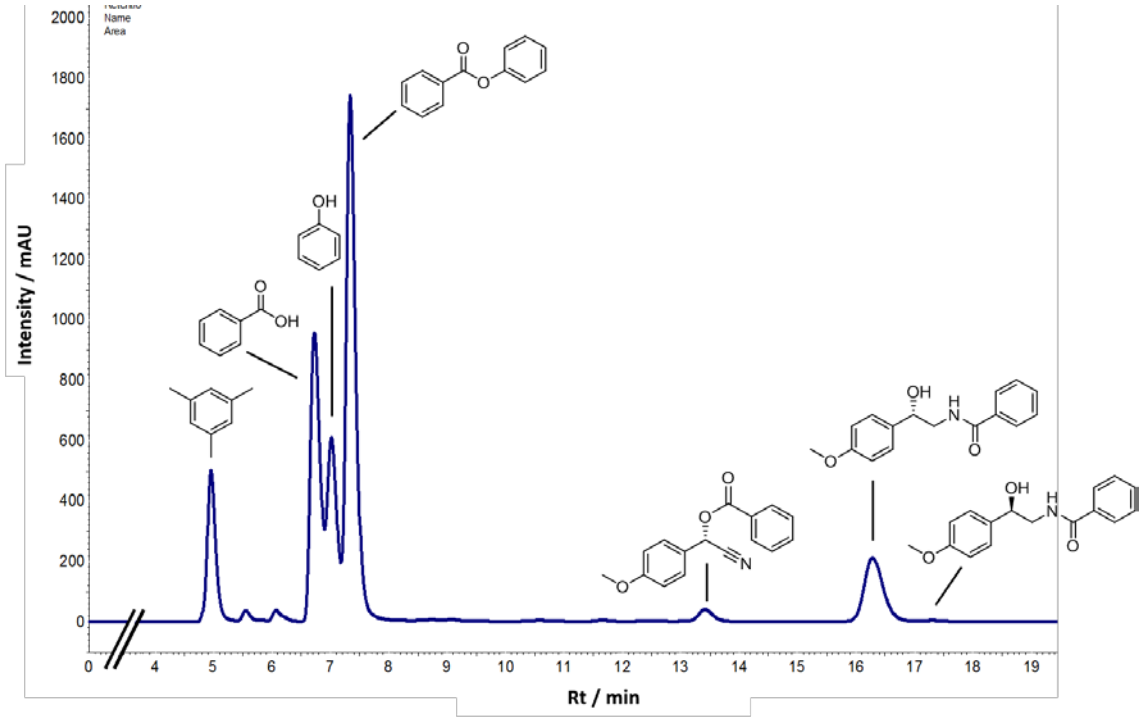

Figure S3. Chiral normal phase HPLC chromatogram from the preparative synthesis of (*S*)-tembamide *via* benzoylation of (*S*)-4-methoxymandelonitrile benzoate catalyzed by Raney Ni *i*Pr$_2$O under optimized conditions as described in section 2.2.7.2.

Identification of major side products in the catalytic hydrogenation of 4-methoxymandelonitrile benzoate

High resolution GC-MS

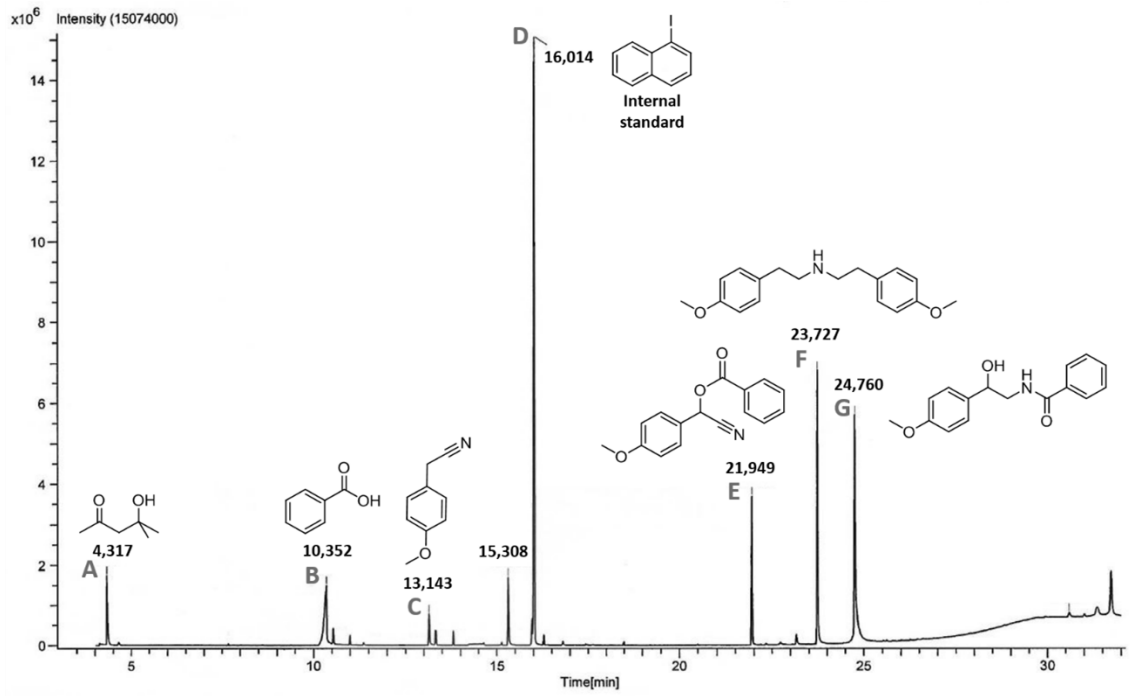

Figure S4. Gas chromatogram of the crude reaction mixture from the Raney Ni-catalyzed hydrogenation of (±)-4-methoxymandelonitrile benzoate at 100 °C under 5 bar of H_2. Compounds of peaks with retention times 4.317, 10.352, 13.143, 16.014, 21.949, 23.727 and 24.760 min were identified by comparison of their mass spectrum and database-listed spectra. Peak at 16.014 min corresponds to the internal standard and peak at 4.317 is likely diacetone alcohol, an impurity from acetone.

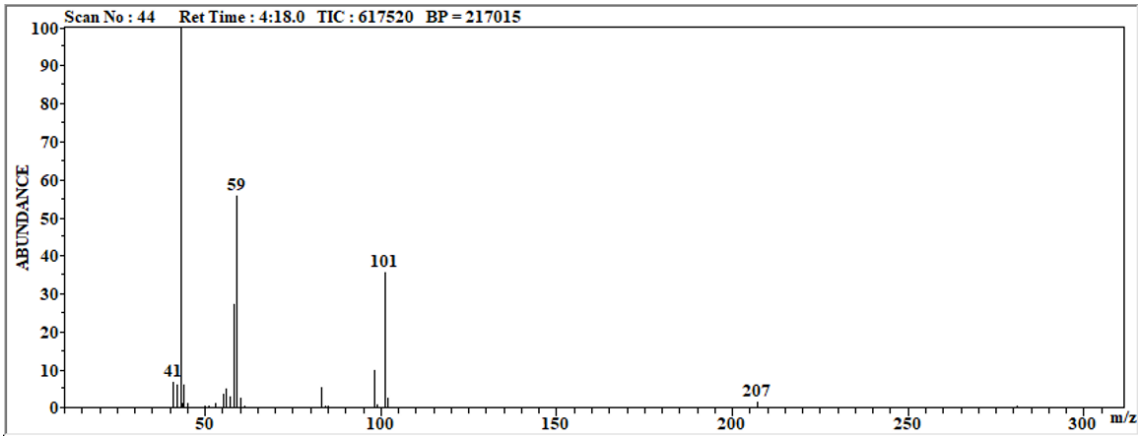

Figure S5. Mass spectrum of peak A from the GC chromatogram shown in Figure S4, identified as diacetone alcohol.

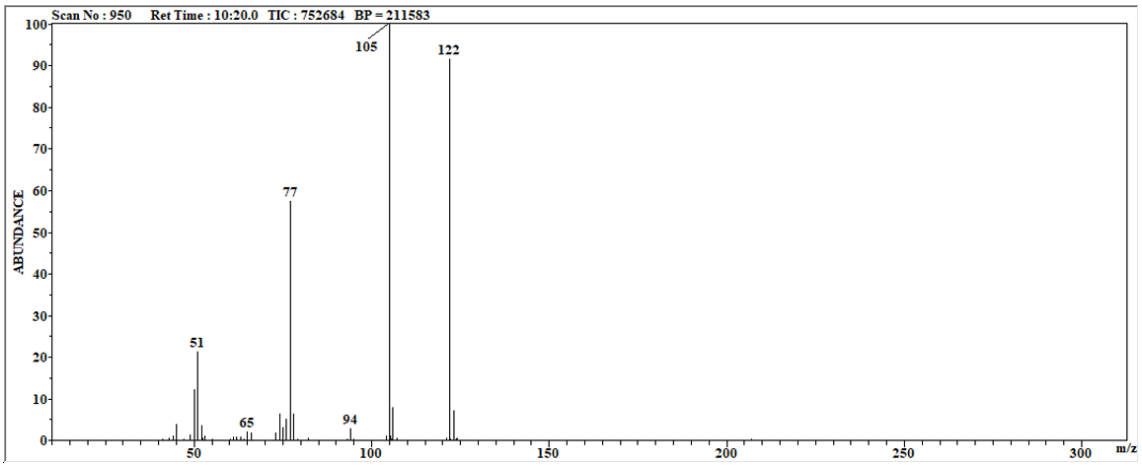

Figure S6. Mass spectrum of peak B from the GC chromatogram shown in Figure S4, identified as benzoic acid.

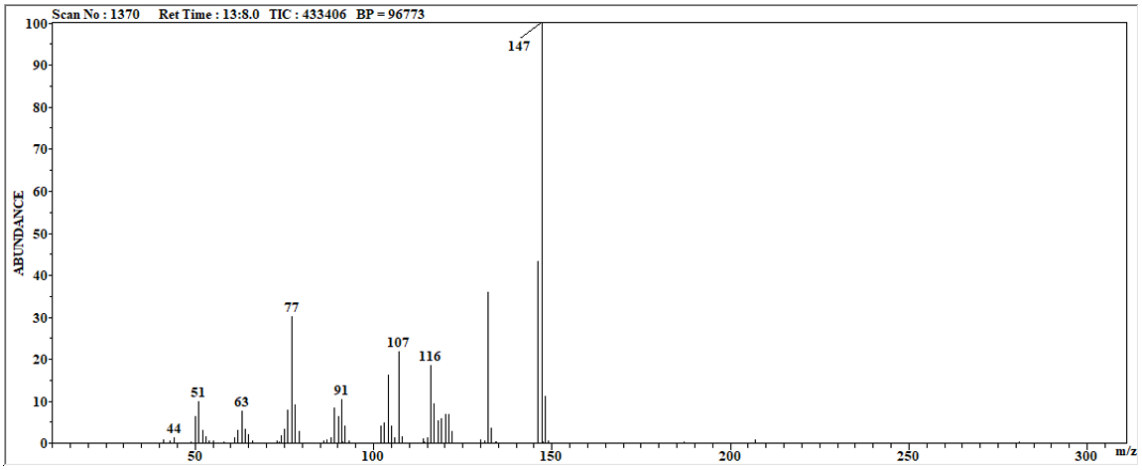

Figure S7. Mass spectrum of peak C from the GC chromatogram shown in Figure S4, identified as 4-methoxyphenylacetonitrile.

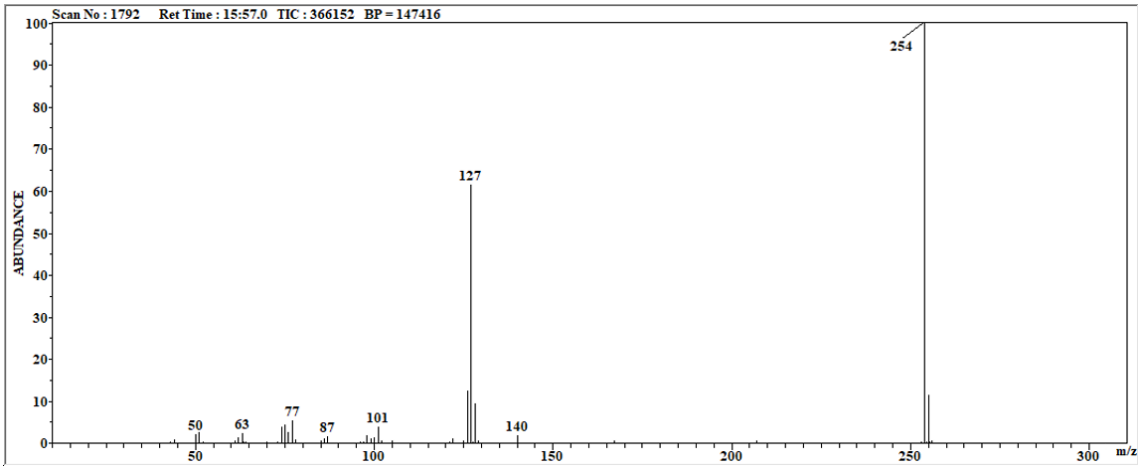

Figure S8. Mass spectrum of peak D from the GC chromatogram shown in Figure S4, which corresponds to 1-iodonaphthalene.

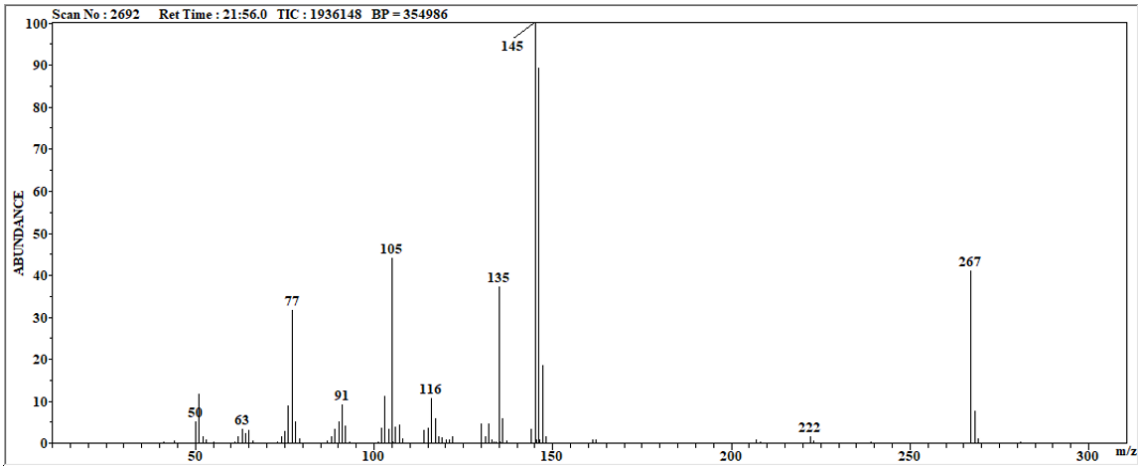

Figure S9. Mass spectrum of peak E from the GC chromatogram shown in Figure S4, identified as 4-methoxymandelonitrile benzoate.

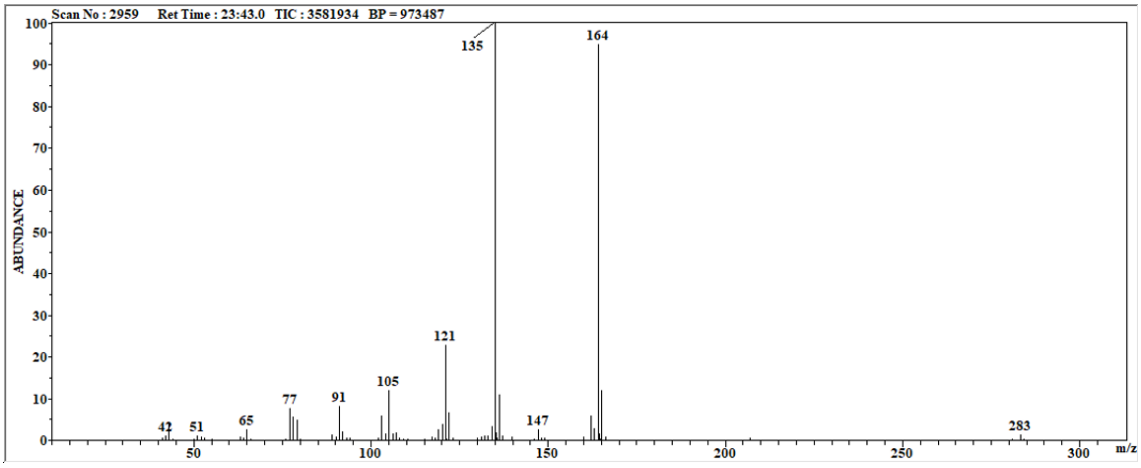

Figure S10. Mass spectrum of peak F from the GC chromatogram shown in Figure S4, identified as 4-methoxy-*N*-[2-(4-methoxyphenyl)ethyl] benzeneethanamine.

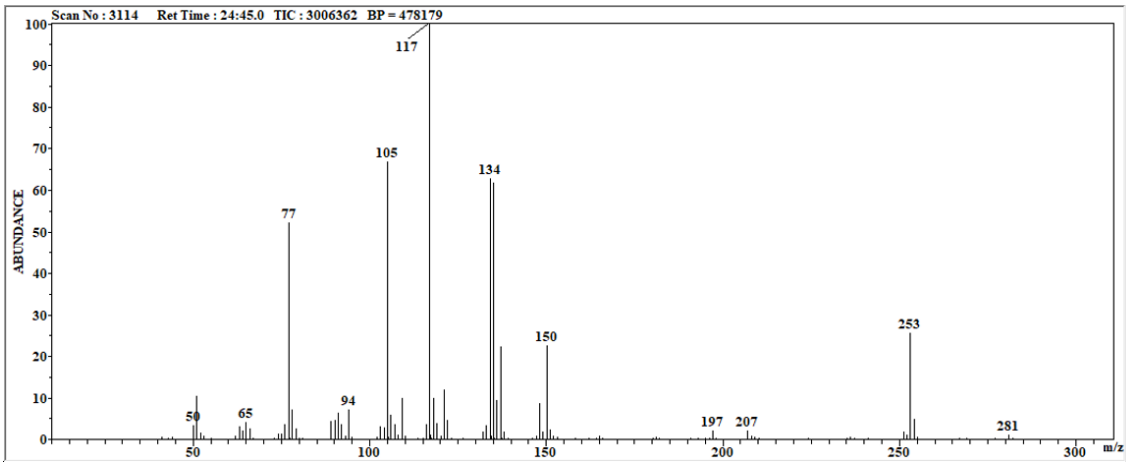

Figure S11. Mass spectrum of peak G from the GC chromatogram shown in Figure S4, identified as tembamide.

^{1}H NMR, ^{13}C NMR and DEPT-135 NMR

The ^{1}H NMR, ^{13}C NMR and DEPT-135 NMR analysis of one of the fractions from a column chromatography purification of (±)-tembamide synthetized *via* Raney Ni-catalyzed hydrogenation of 4-methoxymandelonitrile allowed for the elucidation of another side product. The major compounds in this fraction were identified as benzoic acid and *N*-(4-methoxyphenylethyl)benzamide. The peak shifts of benzoic acid in ^{1}H NMR and ^{13}C NMR were confirmed with NMR of commercial benzoic acid.

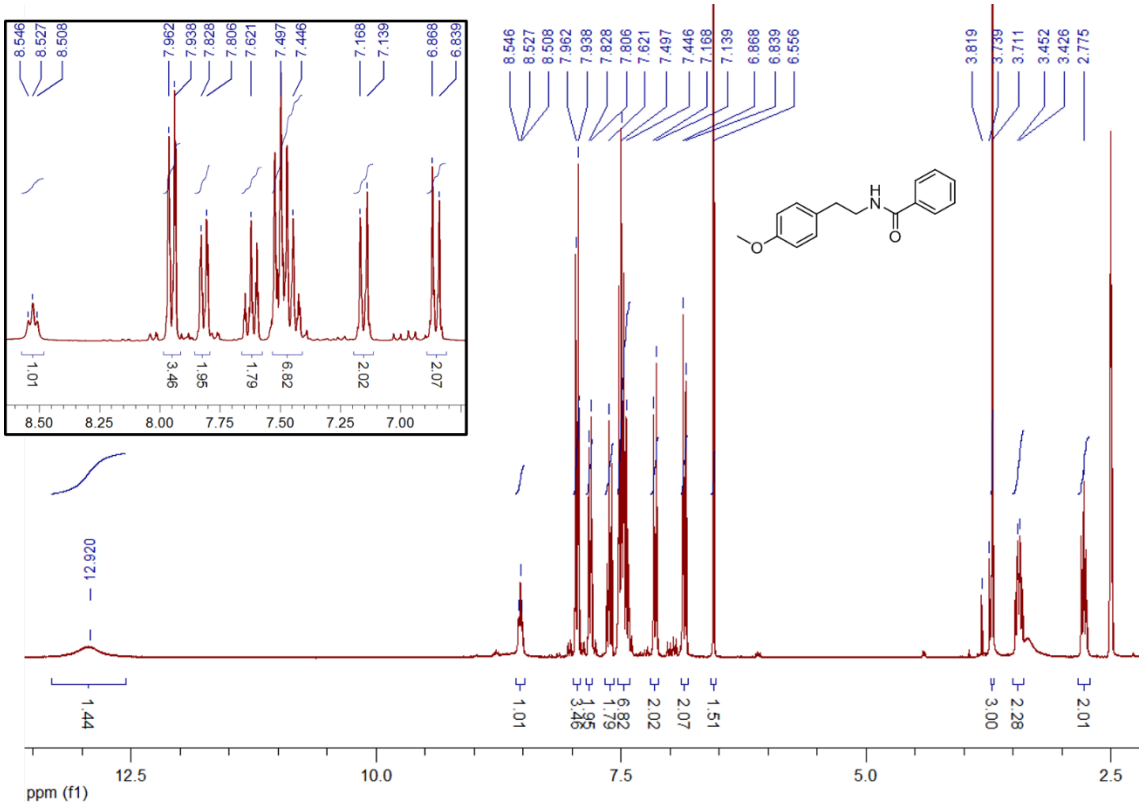

Figure S12. ^{1}H NMR spectrum of a column chromatography fraction containing side products from the Raney Ni-catalyzed hydrogenation of (±)-4-methoxymandelonitrile benzoate at 100 °C under 5 bar of H_2. Major components of the fraction identified as benzoic acid and *N*-(4-methoxyphenylethyl)benzamide.

Benzoic acid ^{1}H NMR (300 MHz, DMSO-d_6): δ [ppm] = 7.50 (2H, t, Ar-m), 7.62 (1H, t, Ar-p), 7.95 (2H, d, Ar-o), 12.92 (1H, s, COOH).

***N*-(4-methoxyphenylethyl)benzamide** ^{1}H NMR (300 MHz, DMSO-d_6): δ [ppm] = 2.780 (2H, t, Ar-CH_2), 3.44 (2H, m, N-CH_2)), 3.71 (3H, s, OCH_3), 6.85 (2H, d, Ar-m'), 7.15 (2H, d, Ar-o'), 7.45 (3H, m, Ar-p and Ar-m), 7.82 (2H, dd, Ar-o), 8.53 (1H, t, NH).

Due to the presence of benzoic acid, H_2O presents a broad peak that partially contributes to the integration of the CH_2 peak at δ = 3.44 ppm. The Ar-m signal from benzoic acid overlaps with the Ar-p and Ar-m signals from *N*-(4-methoxyphenylethyl)benzamide. The singlet at δ = 6.56 ppm belongs to a compound without aromatic protons, as confirmed by contrasting with other fractions from the column purification.

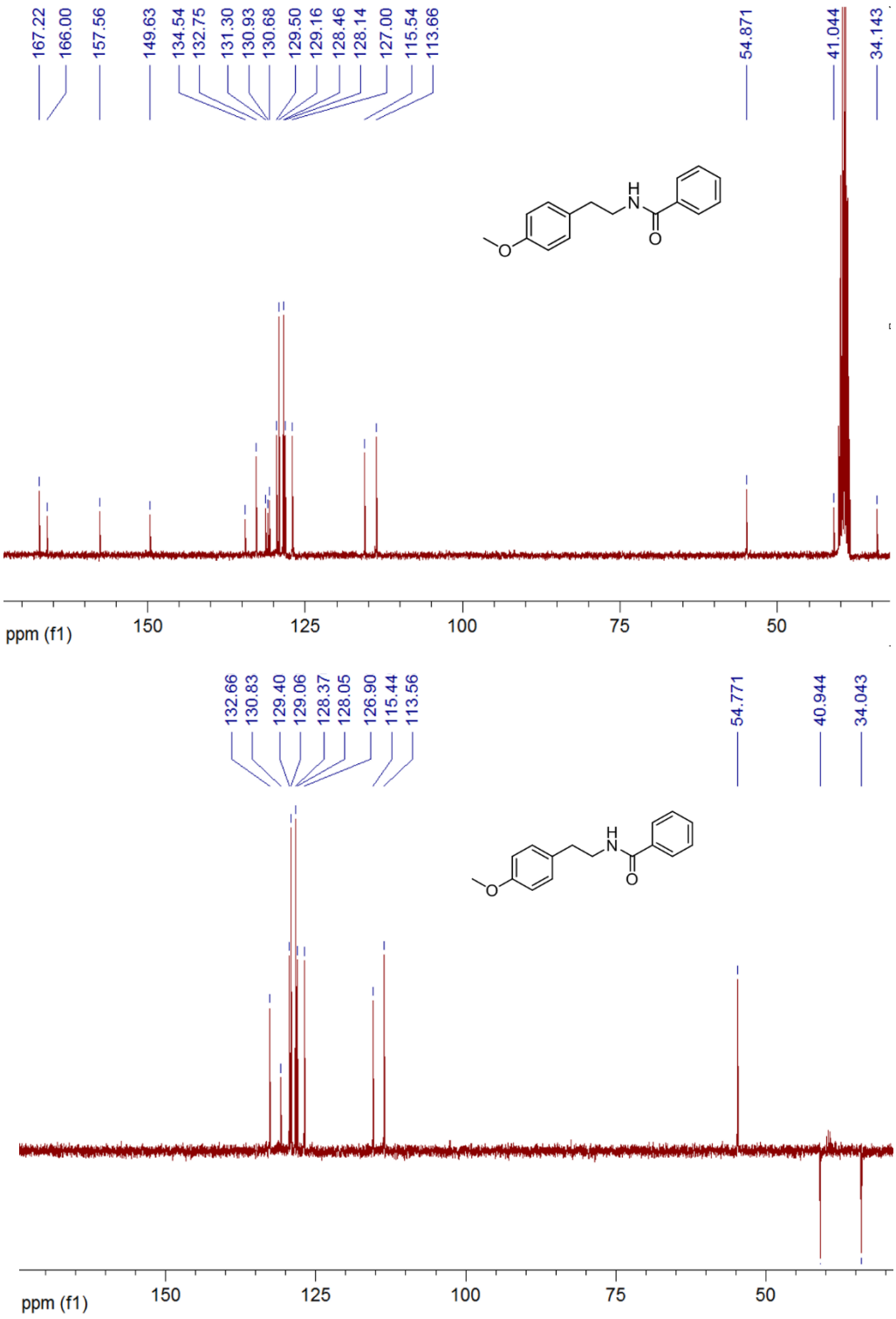

Figure S13. ^{13}C-NMR (top) and DEPT-135 (bottom) spectra of a column chromatography fraction containing side products from the Raney Ni-catalyzed hydrogenation of (±)-4-methoxymandelonitrile benzoate at 100 °C under 5 bar of H_2. Major components of the fraction identified as benzoic acid and *N*-(4-methoxyphenylethyl)benzamide.

Benzoic acid ^{13}C-NMR (300 MHz, DMSO-d_6): δ [ppm] = 128.5, 129.2, 130.7, 132.8, 167.2.

***N*-(4-methoxyphenylethyl)benzamide** ^{13}C-NMR (300 MHz, DMSO-d_6): δ [ppm] = 34.1, 41.0, 54.9, 115.5, 127.0, 128.1, 129.5, 130.9, 131.3, 134.5, 157.6, 166.0.

^{1}H NMR and ^{13}C NMR spectra of (*S*)-tembamide crystals obtained from the preparative chemo-enzymatic cascade synthesis starting from 4-anisaldehyde

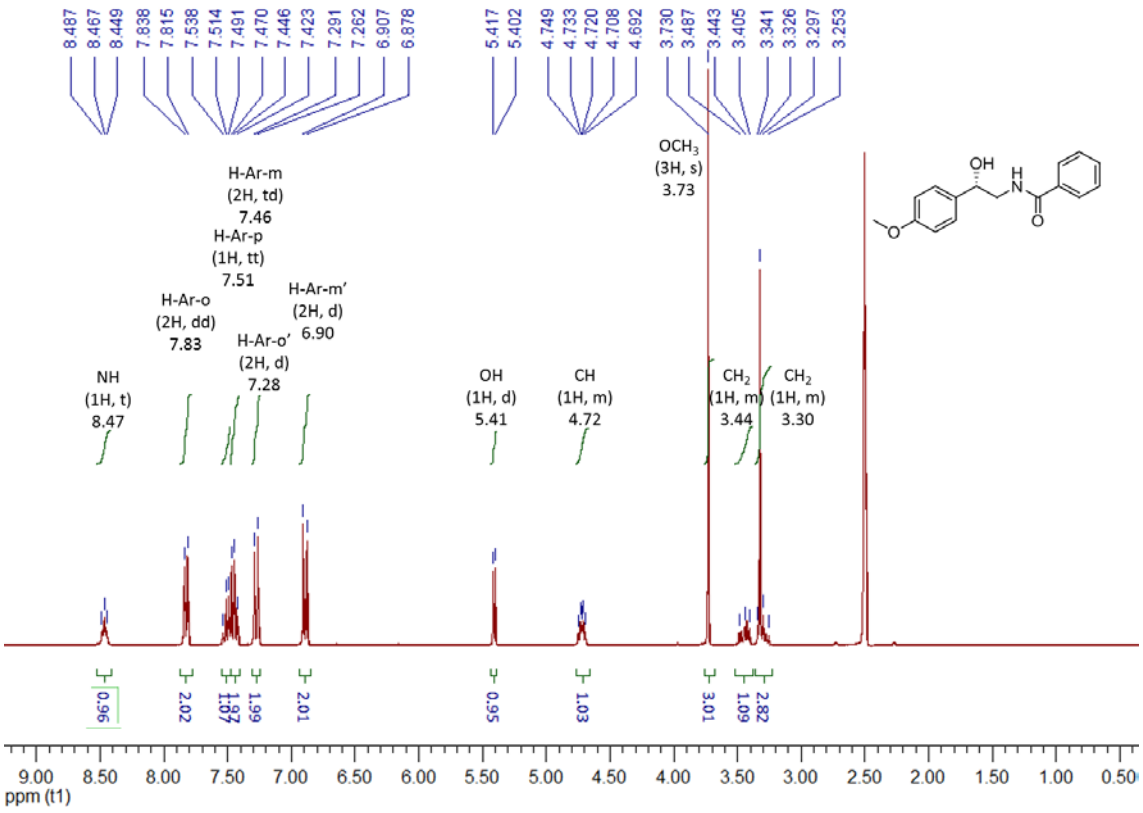

Figure S14. ^{1}H NMR spectrum of (*S*)-tembamide in DMSO-d_6. The signal at δ 3.30 ppm overlaps with the H_2O peak.

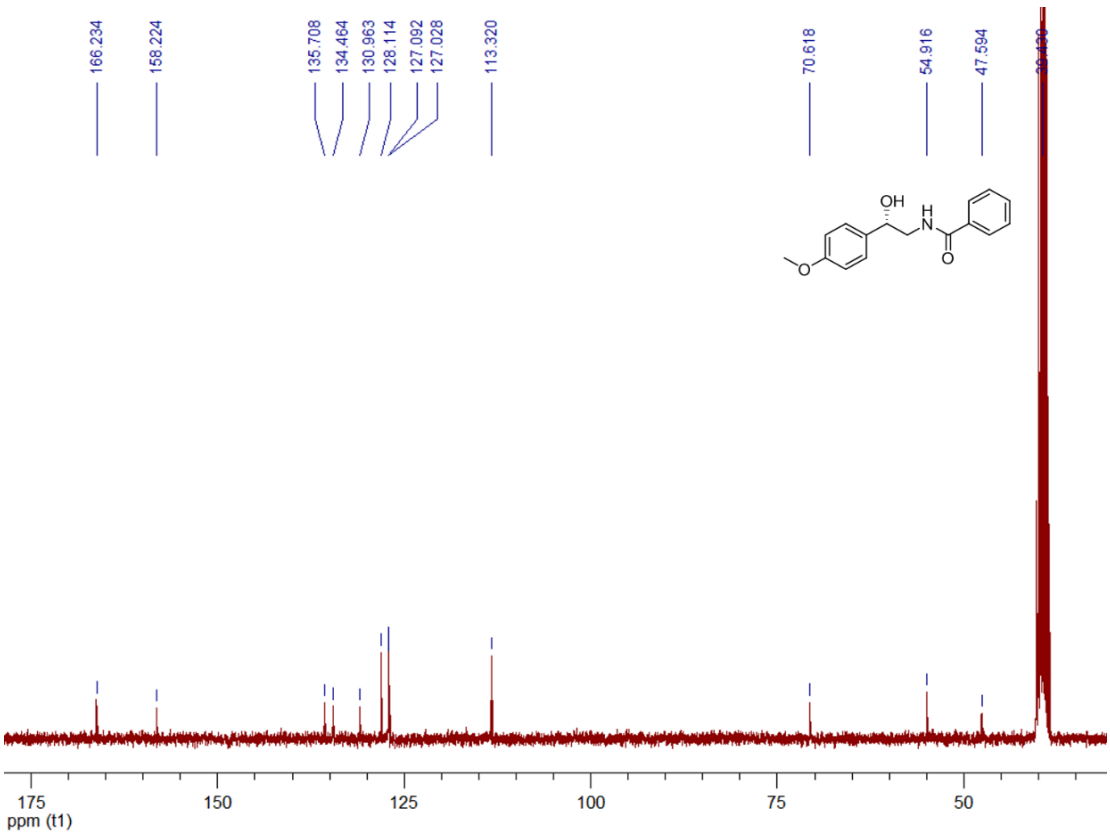

Figure S15. ^{13}C-NMR spectrum of (*S*)-tembamide in DMSO-d_6. δ [ppm] = 47.6, 54.9, 70.6, 113.3, 127.0, 127.1, 128.1, 130.9, 134.5, 135.7, 158.2, 166.2.

Acknowledgements

This project has received funding from the European Union's Horizon 2020 MSCA ITN-EID program under grant agreement No. 634200 and was in collaboration with Viazym B.V. and TU Delft.

First of all, I would like to sincerely thank my mentor, Anett Schallmey for taking me under her wing and taking the time and patience to guide me through this odyssey of becoming a doctor. Your dedication, knowledge and integrity have been and will continue to be a true inspiration to me.

A special thanks to my supervisor at Viazym, B.V., Luuk van Langen, for all the knowledge transfer and for welcoming me into the Viazym family. Your encouragement and wit have motivated me since the beginning of my PhD. Thank you also for contributing so much to improving my Dutch and my understanding of Dutch culture.

I would also like to thank Prof. Dr. Marc Walter for agreeing to review my thesis and to be a member of my oral defense evaluation committee. Thanks also to Prof. Dr. Dieter Jahn for agreeing to be the third member of my PhD evaluation committee.

I big thank too, to Frank Hollmann for hosting the first six months of my PhD and treating me just like any other member of his research group at TU Delft.

A special mention goes to Yvonne Göcke for her technical support with the HPLC at TU Braunschweig.

My PhD journey would not have been as enjoyable without all the friends and colleagues that I had the pleasure to meet:

Elisa, Raquel, Elia, Federica, Lisa, Juraj, Aline, Florian, Gaurav and Olha. It was a pleasure to belong to the Biocascades family with you. I would also like to thank all the members of the Biocascades project for their support and scientific input.

My lovely Delft family: Marine, Georg, Seb, Morten, Elena, Milja, Andrés, Caroline, Hanna, Wuyuan, Tiago, and many others.

My dear colleagues from TU Braunschweig: Jana, Hazel, Willem, Marcus, Jenny, Rita, Jhon Alex, Hauke, Patrick, Kathi, Nils.

I am sure that I have forgotten some names, but I hope you will forgive me.

Thanks to my friends for their emotional support, for sharing the good and the bad moments. Though we may be far apart, you are always right by my side.

Obrigada, Wesley, por me contagiar com sua alegria, por ter-me ensinado tantas coisas e por seu apoio incondicional.

Gracias a mis padres por todo su amor y el incalculable apoyo emocional y económico, por haber confiado siempre en mí...por prepararme para los fracasos. Si he llegado hasta aquí es, sin duda, gracias a ustedes.

Academic CV

Personal information

Name:	Laura Leemans Martin
Birth date:	8 February 1991
Place of birth:	Arrecife, Spain
Nationality:	Spanish

Employment history

Post-Doc in Biocatalysis – Novartis, Basel, Switzerland (January 2020 – present)

Internship as Doctoral Candidate – Novartis, Basel, Switzerland (January 2019 – June 2019)

PhD Biotechnology – Technical University of Braunschweig (2015 – June 2020)
Thesis title: Design and optimization of (chemo-)enzymatic processes for the synthesis of hydroxynitriles and their derivatives

Education history

MSc Applied Chemistry – Autonomous University of Madrid (2013 – 2014)
Master thesis: Bioorganometallic compounds based on 4-ferrocenylaniline and Pt (II) centers

BSc Chemistry – Autonomous University of Madrid (2009 – 2013)
Bachelor thesis: Synthesis of ferrocene derivatives functionalized with nitrogen moieties

Peer-reviewed publications:

Leemans, L.; Walter, M. D.; Hollmann, F.; Schallmey, A.; van Langen, L. "Novel multi-catalytic route for the synthesis of an *N*-acyl-β-amino alcohol" *Catalysts*, **2019**, 9, 822; **DOI:**10.3390/catal9100822

Leemans, L.; van Langen, L.; Hollmann, F.; Schallmey, A. "Bienzymatic Cascade for the Synthesis of an Optically Active *O*-benzoyl Cyanohydrin" *Catalysts*, **2019**, *9*, 522. **DOI:** 10.3390/catal9060522

Zhang, W.; Fernandez Fueyo, E.; Hollmann, F.; **Leemans Martin, L.**; Pesic, M.; Wardenga, R.; Höhne, M.; Schmidt, S. “Combining Photo-Organo Redox- and Enzyme Catalysis Facilitates Asymmetric C-H Bond Functionalization” *European Journal of Organic Chemistry,* **2019**, *10*, 80-84. **DOI:** 10.1002/ejoc.201801692

Gonzalez-Alfonso, J.; **Leemans, L**.; Poveda, A.; Jiménez-Barbero, J.; Peñalver, P.; Ballesteros Olmo, A.; Morales, J.; Plou, F. J. "Efficient α-glucosylation of epigallocatechin gallate catalyzed by cyclodextrin glucanotransferase from Thermoanaerobacter sp.” *Journal of Agricultural and Food Chemistry,* **2018**, *66* (28), 7402-7408. **DOI***:* 10.1021/acs.jafc.8b02143

Enriquez, A.; González-Vadillo, A.; Martinez-Montero, I.; Bruña, S.; **Leemans, L.**; Cuadrado, I. "Efficient Thiol–Yne “Click” Chemistry of Redox–Active Ethynylferrocene". *Organometallics,* **2014***, 33* (24), 7307–7317. **DOI:** 10.1021/om501110w

Additional research achievements:

Oral presentation: Leemans, L.; van Langen, L.; Schallmey, A.: Bi-enzymatic cascade to optically active *O*-acyl cyanohydrins. (Vortrag). Gordon Research Conference (GRC) on Biocatalysis, Biddeford, ME, US (2018). 30-minute presentation as result of poster prize.